Etude du mutant E255L de l'ATPase Ca2+ SERCA1a de lapin et de l'ATPase Ca2+ PfATP6 de Plasmodium falciparum

Delphine Cardi

UNIVERSITE PARIS XI

FACULTE DE MEDECINE PARIS SUD

THESE

Pour obtenir le grade de

DOCTEUR DE L'UNIVERSITE PARIS XI

Ecole Doctorale « Signalisations et réseaux intégratifs »

Présentée et soutenue publiquement par

Delphine CARDI

le 24 mars 2009

ETUDE DU MUTANT E255L DE L'ATPase Ca^{2+} SERCA1a DE LAPIN ET DE L'ATPase Ca^{2+} PfATP6 DE *Plasmodium falciparum*

Expression chez la levure *S. cerevisiae*, purification, characterisation et essai d'inhibition par un antipaludéen puissant, l'artemisinine.

Directeur de thèse: M. Marc le MAIRE

JURY

Mr Jean-Luc POPOT (Président du Jury)
Mr Anthony LEE (Rapporteur)
Mr Steven KARLISH (Rapporteur)
Mme Anne ROBERT (Examinateur)
Mme Christine JAXEL (Examinateur, co-responsable de thèse)
Mr Marc le MAIRE (Examinateur, directeur de thèse)

UNIVERSITE PARIS XI

FACULTE DE MEDECINE PARIS SUD

THESE

Pour obtenir le grade de

DOCTEUR DE L'UNIVERSITE PARIS XI

Ecole Doctorale « Signalisations et réseaux intégratifs »

Présentée et soutenue publiquement par

Delphine CARDI

ETUDE DU MUTANT E255L DE L'ATPase Ca^{2+} SERCA1a DE LAPIN ET DE L'ATPase Ca^{2+} PfATP6 DE *Plasmodium falciparum*

Expression chez la levure *S. cerevisiae*, purification, characterisation et essai d'inhibition par un antipaludéen puissant, l'artemisinine.

Directeur de thèse: M. Marc le MAIRE

JURY

Mr Jean-Luc POPOT (Président du Jury)
Mr Anthony LEE (Rapporteur)
Mr Steven KARLISH (Rapporteur)
Mme Anne ROBERT (Examinateur)
Mme Christine JAXEL (Examinateur, co-responsable de thèse)
Mr Marc le MAIRE (Examinateur, directeur de thèse)

Remerciements/Aknowledgments

François Jacob, prix Nobel de Physiologie/Médecine en 1965, disait: « *La recherche est un processus sans fin dont on ne peut jamais dire comment il évoluera. L'imprévisible est dans la nature même de la science.* »
En cette période d'importante réorganisation de la recherche en France, nos dirigeants, en souhaitant que la durée d'un projet soit le plus court possible, semblent cependant l'oublier! La thèse en est pourtant un parfait exemple puisque le(s) projet(s) développés au cours de ces trois années n'aboutissent que rarement à ce qui était prévu et il est courant que le doctorant conclut que le processus va être long pour répondre à la question initialement posée. Ma thèse n'a pas échappé à cette règle. Elle fut donc pour moi une intense période de questionnement, de réflexion, de doute, de remise en question, d'attentes impatientes, de débats. Heureusement, elle fut aussi ponctuée de moments de joie, de partage et de rencontres.
Une thèse n'est effectivement pas une aventure solitaire et je souhaite donc remercier toutes les personnes qui m'ont soutenues et qui ont contribué à ce travail.

First, I would like to express my deep and sincere gratitude to the referees, Anthony Lee and Steven Karlish, for their detailed review, constructive criticism and also their excellent advices during the preparation of this thesis.

Un grand merci également à Anne Robert d'avoir accepté de juger ce travail et surtout de m'avoir rendu plus appréhendable la chimie de l'artémisinine et toutes les controverses qui y sont liées. Je fus très touchée par votre implication, votre discours passionné et votre rigueur scientifique. De même, je souhaiterais remercier celui qui fut mon tuteur pendant ces trois années de thèse et qui a accepté de présider le jury de ma thèse, Jean-Luc Popot. Merci pour vos conseils avisés, merci de m'avoir rassuré dans les moments difficiles.

Je souhaiterais maintenant remercier les personnes qui ont permis à ce sujet de thèse de prendre vie et qui m'ont accompagnée pour le faire vivre. Il s'agit de mes deux directeurs de thèse, Christine Jaxel et Marc le Maire. Merci à vous deux pour la confiance, la liberté et le soutien que vous m'avez accordé pendant ces trois années.
Marc, je vous remercie de m'avoir fait bénéficier de votre expérience tant scientifique que diplomatique et d'avoir toujours essayé d'être présent malgré votre emploi de plus en plus chargé.
Christine, je te remercie d'avoir encadré ce travail de thèse, avec beaucoup de compétences (surtout en biologie moléculaire !), de rigueur, d'enthousiasme et de disponibilité. Je te suis également grandement reconnaissante de m'avoir fait prendre conscience au quotidien qu'il faut souvent forcer le destin pour avancer.

Cette thèse a fait naître une grande équipe de travail mais n'a pas été menée qu'à un seul endroit. En effet, j'ai pu bénéficier des compétences et des connaissances de plusieurs laboratoires et ce, en France, en Angletterre et au Danemark. C'est d'ailleurs pour que cette thèse soit compréhensible par tous les contributeurs de ce projet que j'ai décidé de la rédiger en anglais.

Thus, I would like to aknowledge Jesper Møller and Poul Nissen from the university of Aarhus (Denmark) and the member of their teams (especially Birte Nielsen, Claus Olesen and Anne-Marie Lund-Winter) for welcoming me in their labs in february 2008. Thank you for sharing with me your knowledge, your skills but also your danish culture in spite of your heavy schedule.

I also would like to thank Sanjeev Krishna and his team (especially Leyla Bustamante Rodriguez and Charles Woodrow) for sharing their experience in malaria with me and especially for their welcome at St georges's hospital in december 2006. It was very

enriching to work with you. Nevertheless, I still remains disappointed that frogs were so nervous that a french girl came to eat them that they could not produce good oocytes !

Beaucoup plus près de mon bureau (pas besoin de prendre l'avion, une seule porte à franchir !), j'ai eu la chance de beaucoup voyager dans l'univers des protéines membranaires et surtout sur la planète SERCA avec Philippe Champeil. Que ce soit sur le projet PfATP6 ou sur l'autre projet que j'ai eu à mener pendant ma thèse (les nanosomes, non rédigé dans ce manuscrit), chaque moment passé a été pour moi une découverte tant scientifique que philosophique. Philippe, j'ai énormément appris à tes côtés et je te suis très reconnaissante de tout le temps que tu m'as consacré.

Je profite de cette évocation du projet nanosomes pour remercier les équipes qui ont participer à ce projet. Merci beaucoup à Eric Doris, Aurélie Tarrade et Julien Ogier (CEA Saclay) pour la partie synthèse et Christine Ebel et Florence Manon pour la partie analyse (IBS, Grenoble). D'ailleurs, un grand merci à toi Christine de m'avoir accueilli dans ton laboratoire pour m'initier à l'ultracentrifugation analytique. J'en garde un excellent souvenir.

Quelle que soit le projet sur lequel j'ai travaillé, j'ai bénéficié du savoir-faire de Jean-Marc Verbavatz, de Maité Paternostre et de Manuel Garrigos et je leur en suis très reconnaissante car ils m'ont souvent permis de faire un grand pas en avant ! Merci à vous également pour votre disponibilité, vos conseils et votre gentillesse.

Je souhaite maintenant remercier tous les membres encore non cités de « the SERCA team » : Cédric, Agnès, Alex, Guillaume et surtout Bertrand et Estelle pour leur contribution à ce projet. Merci à vous tous pour les bons moments passés ensemble et pour votre soutien… surtout en chambre froide ! Je voudrais également faire un petit clin d'œil aux stagiaires Kahina, Laura et Aude. Merci les filles d'être venu avec votre bonne humeur au labo !

Je tiens maintenant à remercier toutes celles et ceux, non encore cités, qui ont contribué à mon épanouissement au laboratoire. Merci à tout le personnel administratif et notamment à Pascale pour son dévouement et sa bonne humeur. Merci à tous les chercheurs du SB^2SM pour leur écoute et leurs conseils (Béatrice, Ghada, Stéphane, Marcel, Alain…). Merci à tous les anciens et actuels doctorants et post-doctorants pour vos conseils, votre réconfort mais surtout pour tous les souvenirs qu'il va me rester des bonnes tranche de rire et des soirées que j'ai passé à vos côtés. Béa, Emmanuelle, Martin, Marie, Morgane, Karsten, Charlotte, Pierre, les Céline… Je vous souhaite à tous une grande réussite !

Cette thèse est l'aboutissement de mon rêve d'enfant. Je dois le fait que ce rêve est devenu réalité grâce à l'amour et au soutien incessant de ma famille. Maman, Papa, je ne vous remercierai jamais assez de tout ce que vous m'avez donné et de tous les lourds sacrifices que vous avez fait pour moi. Je vous remercie infiniment de m'avoir guidée comme vous l'avez fait et d'avoir toujours eu confiance en moi. Séverine, je n'oublierai jamais le temps que tu as passé à me faire réciter mes leçons alors que tu savais à peine lire ! Jean-Loïc, sans toi, je n'y serais pas arrivée! Je te remercie pour ton soutien quotidien et toute l'affection que tu m'as apportée tout au long de ces trois années et je te suis très reconnaissante d'avoir sacrifié plusieurs nuits pour m'aider à finir ce manuscrit.

L'attrait pour la nature et la biologie m'est venu de mes longues promenades en forêt, au bord de l'eau ou dans les champs avec mon grand père qui très tôt m'a appris à reconnaître les arbres, les champignons, les plantes, les poissons, les oiseaux et surtout à observer la nature pour mieux la comprendre et la préserver. Le jour où j'ai appris que j'étais retenue pour débuter cette thèse, j'étais dans sa chambre d'hôpital. Il s'en est allé un mois après. Papi Louis, je te dédie cette thèse. Merci de m'avoir tant donné.

Study of the mutant E255L of the rabbit Ca^{2+}-ATPase and of PfATP6, the Ca^{2+}-ATPase of *Plasmodium falciparum*

Heterologous expression in yeast (*S. cerevisiae*), purification, characterization and inhibition assays by artemisinin, a powerful antimalaria

Table of Contents

List of abbreviations

ACN	acetonitrile
ADP	adenosine diphosphate
AMPPCP	adenosine 5'-(β,γ–methylenetriphosphate)
ATP	adenosine triphosphate
BAD	Biotin Acceptor Domain
BCA	Bicinchoninic acid
BHQ	2,5-di-*tert*-butyl-*benzo*- hydroquinone
BSA	Bovine Serum Albumin
C12E8	octaethyleneglycol monododecylether
CAPS	3-[cyclohexylamino]-1-propanesulfonic acid
cDNA	complementary DNA
CMC	critic micellar concentration
CO	codon optimized
COS	acronym derived from the cells being **C**V-1 (simian) in **O**rigin, and carrying the **S**V40 (simian virus 40) genetic material
CPA	cyclopiazonic acid
DDM	dodecyl maltoside
ddNTP	dideoxynucleotide triphosphate
DHA	dihydroartemisinin
DMSO	dimethylsulfoxide
DNA	Deoxyribonucleic acid
DOPC	dioleoyl phosphatidyl choline
DOPS	dioleoyl phosphatidyl serine
DTT	dithiothreitol
EDTA	ethylenediamine tetraacetic acid
EGTA	[ethylene bis-(oxyethylenenitrilo)] tetraacetic acid
ER	endoplasmic reticulum
EYPC	egg yolk phosphatidyl choline
EYPS	egg yolk phosphatidyl serine
HEPES	N-2-hydroxy ethyl piperazine-N'-2-ethanesulfonic acid
IC_{50}	half maximal inhibitory concentration
IMAC	Immobilized Metal Affinity Chromatography
IP3	inositol triphosphate
LDH	lactate dehydrogenase
MALDI-TOF	Mass Absorption Laser Desorption Ionization-Time Of Light
MES	2-[N-morpholino]propanesulfonic acid
MOPS	3-[N-morpholino]propanesulnonic acid
MPD	2-methyl-2,4-pentanediol
mRNA	messenger RNA
MS	Mass Spectrometry
NADH	α-nicotinamid adenine dinucleotid acid
NTA	nitrilo triacetic acid
OD	optical density
PBS-(T)	Phosphate Buffer Saline (+Tween)
PCR	Polymerase Chain Reaction
PEG	polyethylene glycol
PEP	phohoenol pyruvate
Pi	inorganic phosphate
PK	pyruvate kinase
PMSF	phenyl methyl sulfonyl fluoride
PVDF	polyvinylidene difluoride
RNA	Ribonucleic acid

SDS	sodium dodecylsulfate
SDS-PAGE	Polyacrylamide Gel Electrophoresis (with SDS)
SEC	size exclusion chromatography
SERCA	Sarco/Endoplasmic Reticulum Ca2+-ATPase
SR	sarcoplasmic reticulum
t-BuOH	tertiobutanol
TCA	trichloroacetic acid
TES	2-([2-hydroxy-1,1-bis(hydroxymethyl)ethyl]amino)ethanesulfonic acid
TFA	trifluoroacetic acid
TG	thapsigargin
Tris	tris(hydroxymethyl)aminoethane
v/v	volume/volume
w/v	weight/volume
w/w	weight/weight
WT	wild type

CHAPTER I :

INTRODUCTION

Artemisinin combination therapies represent the most efficient treatment against the third more important infectious disease in the world: malaria. However, the mechanism of action of artemisinin drugs is still unclear. Many hypotheses based on morphological observations and chemical studies were formulated. One of them proposes that artemisinin would deregulate Ca^{2+} homeostasis of the parasites responsible for malaria (belonging of the genus *Plasmodium)* by inhibiting its single sarco/endoplasmic Ca^{2+}-ATPase, PfATP6. This protein being difficult to purify from parasite cultures, it is therefore necessary to develop a heterologous overexpression of this protein, followed by an efficient purification to characterize it and especially its potential interaction with artemisinin.

In the present introduction, I will therefore explain what are malaria and artemisinin, what are the different hypotheses about the mechanism of action of artemisinin, what is known about the Ca^{2+} homeostasis of *Plasmodium* parasites. Then I will present the family of the sarco/endoplasmic Ca^{2+}-ATPase. To finish, I will present some examples of heterologously expressed Ca^{2+}-ATPases and plasmodial proteins.

I.1 Why malaria is one of the most important infectious diseases of the world?

I.1.1 Generalities on malaria and history of its discovery

Malaria is one of the most common infectious diseases in the world. It is caused by protozoan parasites transmitted to human by female *Anopheles* mosquitoes. The symptoms characterizing this disease are due to the multiplication of parasites within human red blood cells. They consist in anemia, periodic fever, chills, nausea, flu-like illness, and in severe cases, coma and death. Malaria is widespread in tropical and subtropical regions, including parts of the Americas, Asia, and Africa (Fig. I.1-1). Each year, 500 million people suffer from this disease and between one and three millions die. Eighty percent of cases are located in Sub-Saharan Africa where they mainly concern young children and pregnant women (WHO, 2005). Malaria is a major public health problem commonly associated with poverty, but is also a cause of poverty and a major hindrance to economic development (www.malariasite.com).

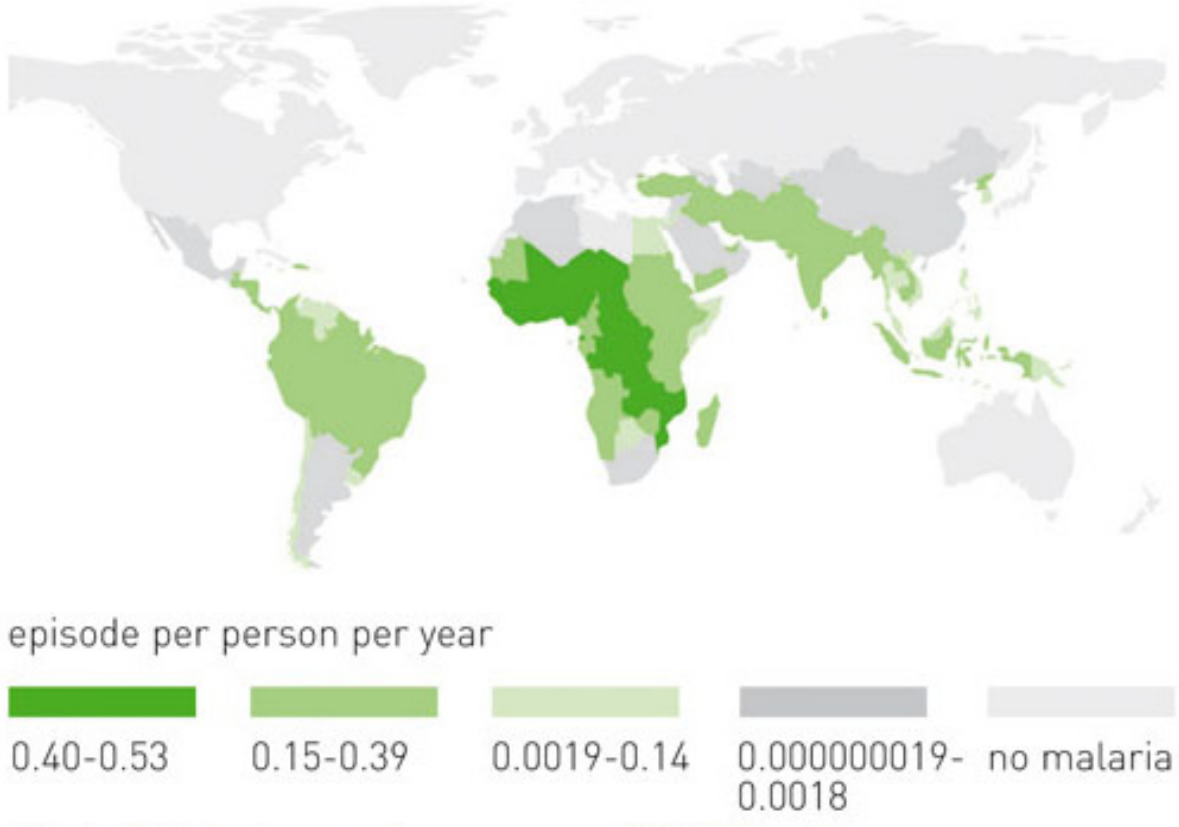

Figure I.1-1: global distribution of malaria (www.partec.com)

Malaria affects more than 2400 million people, over 40% of the world's population, in more than 100 countries

Malaria has infected humans for over 50,000 years, and may have been a human pathogen for the entire history of our species. References to the unique periodic fevers of malaria are found throughout recorded history, beginning in 2700 BC in China. The term malaria originates from Medieval Italian: *mala aria* — "bad air"; and the disease was formerly called ague or marsh fever due to its association with swamps.

The cause of the disease was discovered in 1880 by Charles Louis Alphonse Laveran, a French army doctor, at the military hospital of Constantine in Algeria. He observed parasites inside the red blood cells of people suffering from malaria and proposed that malaria was caused by this protozoan. It was the first time protozoa were identified as causing disease. For this and later discoveries, he was awarded the 1907 Nobel Prize for Physiology or Medicine. This protozoan was called *Plasmodium* by the Italian scientists Ettore Marchiafava and Angelo Celli. Although there were former evidences that mosquitoes were transmitting diseases to and from humans since the beginning of the 1880's, it was Britain's Sir Ronald Ross working in the Presidency General Hospital in Calcutta who finally proved in 1898 that malaria is transmitted by mosquitoes. Indeed, he showed that certain mosquito species transmitted malaria to birds and he isolated malaria parasites from the salivary glands of mosquitoes that had fed on infected birds. For this work, Sir Ronald Ross received the 1902 Nobel Prize for Medicine (http://en.wikipedia.org/wiki/History_of_malaria).

I.1.2 Parasites responsible for malaria and their life cycle with a focus on *Plasmodium falciparum*

More than 70 species of *Plasmodium* have been identified and some of them are met in mammals such as rodents (*P. berghei*, *P. chabaudi*) or monkeys (*P. cynomolgy*), in birds (*P. gallinaceum*) or in reptiles (*P. basilisci*). Five species are involved in human malaria: *P. ovale*, *P. malariae*, *P. vivax, P. knowlesi* and *P. falciparum*. The most serious forms of the disease are caused by *P. falciparum*, the major wide-spread parasite in intertropical areas, because it can lead to cerebral malaria. This group of human-pathogenic *Plasmodium* species is usually referred to as *malaria parasites*. *Plasmodia* species are members of the *Apicomplexa* family. The apicomplexa have many common morphological features such as an apicoplast, a non-photosynthetic plastid organelle acquired by an ancient endosymbiosis with an organism of the red algal lineage and probably involved in lipid metabolism (Waller et al., 2005), and a complex life cycle. For *Plasmodium falciparum*, this life cycle can be divided in four different stages. One occurs in the female mosquito, *Anopheles gambiae* and the three others in human: an exoerythrocytic, mainly in the liver, an erythrocytic phase and a sexual phase (Fig. I.1-2) in the blood stream.

When an infected mosquito takes a blood meal through human skin, sporozoites in the mosquito's saliva enter the bloodstream (8-15 parasites) and migrate to the liver thanks to brisk motility conferred by circum sporozoite protein (CSP). Within 30 minutes of being introduced into the human host, they infect hepatocytes, multiplying asexually and asymptomatically for a period of 6–15 days. Once in the liver, these organisms differentiate to yield thousands of merozoites (between 10000 and 30000) and they induce the death and the detachment of their host hepatocytes. Parasites, wrapped in the cell membrane of the infected host liver cells forming parasite-filled vesicles (merosomes) are then released into the bloodstream.

Anopheles gambiae

Homo sapiens

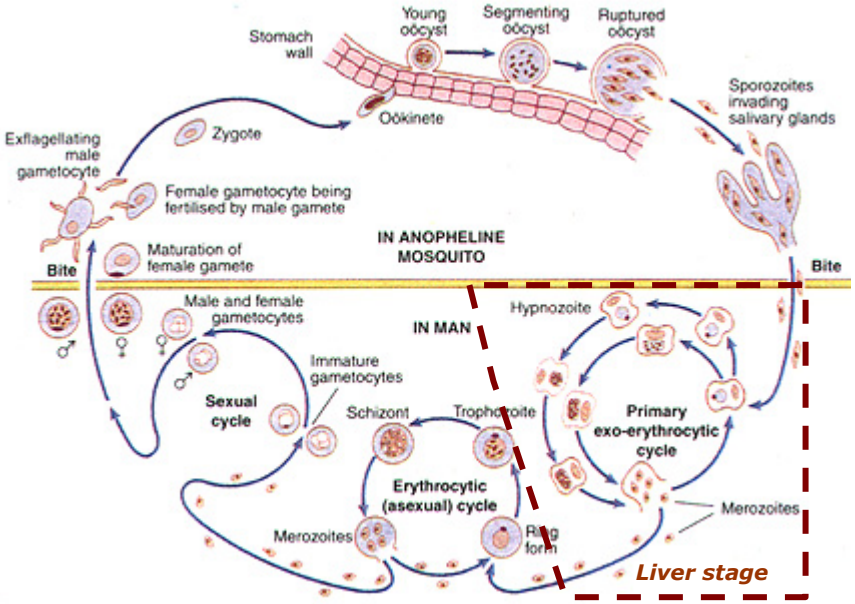

Figure I.1-2: Plasmodium life cycle (adapted from www. malariasite.com)

Plasmodium life cycle is divided in four different cycles: sporogony in the Anopheles Mosquito, a primary exo-erythrocytic cycle in the human liver where it penetrates inside hepatocyte[1], an erythrocytic cycle where it penetrates inside the red blood cells and a sexual cycle where it differentiates in gametocytes.

[1] In the case of P. vivax and P. ovale, some sporozoites do not immediately develop into exoerythrocytic-phase merozoites, but instead produce hypnozoites that remain dormant for periods ranging from several months (6–12 months is typical) to as long as three years. After a period of dormancy, they reactivate and produce merozoites. Hypnozoites are responsible for long incubation and late relapses in these two species of malaria.

At this stage, parasites protected by these hepatocyte-derived vesicles remain undetectable by the human immune system and infect red blood cells, thus beginning the erythrocytic stage of the life cycle. The merozoite (mero=separate) develops within the erythrocyte through ring, trophozoïte and schizont stages in 48h. During this stage, called erythrocytic schizogony, the parasite modifies its host cell in several ways

to enhance its survival. It first attaches to red cells via the erythrocyte binding antigen 175 and the merozoite surface protein 1, 2 with sialoglycoproteins as ligands, enters inside and induces the formation of a parasitophorous vacuole by the invagination of the erythrocyte membrane around the merozoite accompanied by the removal of its cell coat. When the merozoite invades the erythrocyte, it rounds up due to the degradation of the inner membrane complex and some microtubules. Thus, it becomes a trophozoïte (trophos=nourish). The parasitophorous vacuole membrane (PVM), surrounding now the parasite, mainly derives from the erythrocyte membrane and serves as an interface between the parasite and the host cell cytoplasm. Molecules such as nutrients must cross the PVM from the host cell to the parasite and other molecules such as metabolites and parasite-synthesized proteins must cross the PVM in the opposite direction. The trophozoite survives and develops intracellularly by ingesting host cell cytoplasm through a circular structure named the cytostome. The cytostome possesses a double-membrane, consisting of an outer membrane (parasite plasmalemma) and an inner membrane (PVM). Malaria parasites use host proteins and especially haemoglobin as a source of amino acids. However, they cannot degrade the hemoglobin heme byproduct and free heme is potentially toxic for the parasite. Therefore, during hemoglobin degradation, most of the liberated heme is detoxified by polymerization into hemozoin, also called the malaria pigment and stored within the food vacuoles. In addition, as pLDH (lactate dehydrogenase) and *Plasmodium* aldolase have been identified, it is likely that the parasite metabolic pathway goes through an anaerobic glycolysis. During this stage, the parasite divides in schizont (=split). At the end of this cycle, when schizonts are mature, the red blood cell ruptures. This leads to the release of 6-36 merozoites from each schizont coupled with certain factors and toxins which triggers a host immune reaction responsible for chills and fevers of the human host. The new merozoites will infect other erythrocytes or may turn into male and female gametocytes. If a mosquito takes a blood meal from an infected person, it potentially picks up gametocytes within the blood which will continue their development in its gut. The male and female gametes will fuse and form into a zygote prior to transform into an ookinete which will penetrate the gut wall and will become an oocyst. Finally, the oocyst will divide asexually into numerous sporozoites that reach the salivary gland of the mosquito. The sporogony in the mosquito takes about 10 - 20 days and thereafter the mosquito remains infective for 1 - 2 months. Consequently, when this infected mosquito bites another man, it will contaminate him with malaria because these sporozoites will be concomitantly inoculated into his blood stream. That will start a new cycle.

During its human stage, the parasite is relatively protected from attack by the body's immune system because it resides mainly within liver and blood cells. Inside these cells, it remains relatively invisible to immune watch-out but it can not survive the destruction of circulating infected blood cells that occurs in the spleen. However, *P. falciparum* parasite is protected because it displays adhesive proteins (PfEMP1, *Plasmodium falciparum* erythrocyte membrane protein 1) on the surface of the infected blood cells, causing the blood cells to stick to the endothelial cells of post-capillary venules or leading to the formation of *rosettes* with uninfected cells. It is thereby sequestered from passage through the general circulation and the spleen. One may think that with this strategy, the parasite will be destroyed because PfEMP1 proteins will be exposed to the immune system, but *P. falciparum* can synthesize about 60 different variations of this protein thus staying always one step ahead of the pursuing immune system (Sinou, 1998; Fujioka et al., 2002); www. malariasite.com).

I.1.3 Symptoms, prevention and treatments of malaria

I.1.3.1 Symptoms and diagnosis

Symptoms appear at the introerythrocytic stage of the parasite life cycle. The first manifestations of the disease are chills and fevers. As mentioned in the description of the parasite life cycle, waves of fever arise from simultaneous waves of merozoites escaping and infecting red blood. During its presence inside the erythrocyte, the parasite induces especially anemia and hemolysis (due to an immune response targeting all red blood cells) provoking bleeding and cardiovascular disorders, lactic acidosis and therefore acid-base disturbances, renal failure, hypoglycemia and jaundice. The infected human will thereby suffer from high grade fevers, headache, vertigo, altered behavior, weakness, cough and breathlessness, pallor. Besides, if parasites breach the blood brain barrier and attached to endothelial venules, they block these vessels, it results in cerebral malaria that can lead to coma and death.

Malaria can only be identified when the first symptoms occur and therefore when parasites infect the erythrocytes. First malaria is mainly identified from its typical symptoms: chills and repetitive fevers but the presence of the parasite is confirmed by blood analysis. However, to get a deeper diagnosis (e.g. determination of *Plasmodium* species), other methods are required like, from the less to the most sensitive, antigen detection test (based on the presence of Pf lactate dehydrogenase), microscopic examination of blood films and *Plasmodium* DNA detection by PCR (very expensive) (http://en.wikipedia.org/wiki/Malaria).

I.1.3.2 Prevention

Although some populations are resistant to malaria such as people suffering from sickle-cell anemia and thalassemias (blood disorders due to mutations of the gene encoding the beta-globin subunit of hemoglobin), or partially resistant like some people living in endemic area (they have longer incubation periods and less severe malaria), most humans living or travelling in endemic areas are susceptible to catch this disease. However, malaria transmission can be reduced by preventing mosquito bites with mosquito nets, air conditioning and insect repellents, or by mosquito control measures such as spraying insecticides inside houses and draining standing water where mosquitoes lay their eggs.

Some vaccines are under development but they are not currently available. Nevertheless, one of them (RTS,S/AS02A) seems to be very promising and GlaxoSmithKline announced that the vaccine could be submitted for regulatory approval in 2011 (The New York Times, December 13, 2008). Indeed, a proof of concept phase IIb trial in Mozambican children (1-4 years old) determined vaccine efficiencies against risk of clinical malaria of 35% and against severe malaria of 48% with only self-limited adverse effects (Sacarlal et al., 2008). Another study performed in Kenya and Tanzania on 9 months old babies showed an even higher efficiency of this vaccine candidate since 65% of these babies were protected against malaria (Collins et al., 2008). This pre-erythrocytic vaccine candidate consists in a formulation including the circumsporozoite protein fused to the hepatitis B surface antigen (HBsAg). This hybrid was significantly more potent than the circumsporozoite protein alone (Stoute et al., 1997).

Preventative drugs must therefore be taken continuously to reduce the risk of infection. These prophylactic drug treatments are often too expensive for most people living in endemic areas. They are therefore not taken permanently which favors parasite mutations that might lead to drug resistances.

I.1.3.3 Treatments

Many malaria treatments are currently available and they act at different stages of the parasite life cycle. Consequently, they can be used in prophylaxis, as a cure or for preventing relapse.

Tissue schizonticides act on primary tissue form of *Plasmodium* which after growth within the liver, initiate the erythrocytic stage. Blocking this stage prevents further development of the infection. Blood schizonticides act on the blood forms of the

parasite, the most destructive form of the human host. These are thereby the most important drugs in anti-malarial chemotherapy because they terminate clinical attacks of malaria. Gametocytocides destroy the sexual forms of the parasite in the blood and thereby prevent transmission of the infection to the mosquito. Sporontocides prevent the development of oocysts in the mosquito and thus ablate the transmission. Drugs used at these stages are presented in fig. I.1-3.

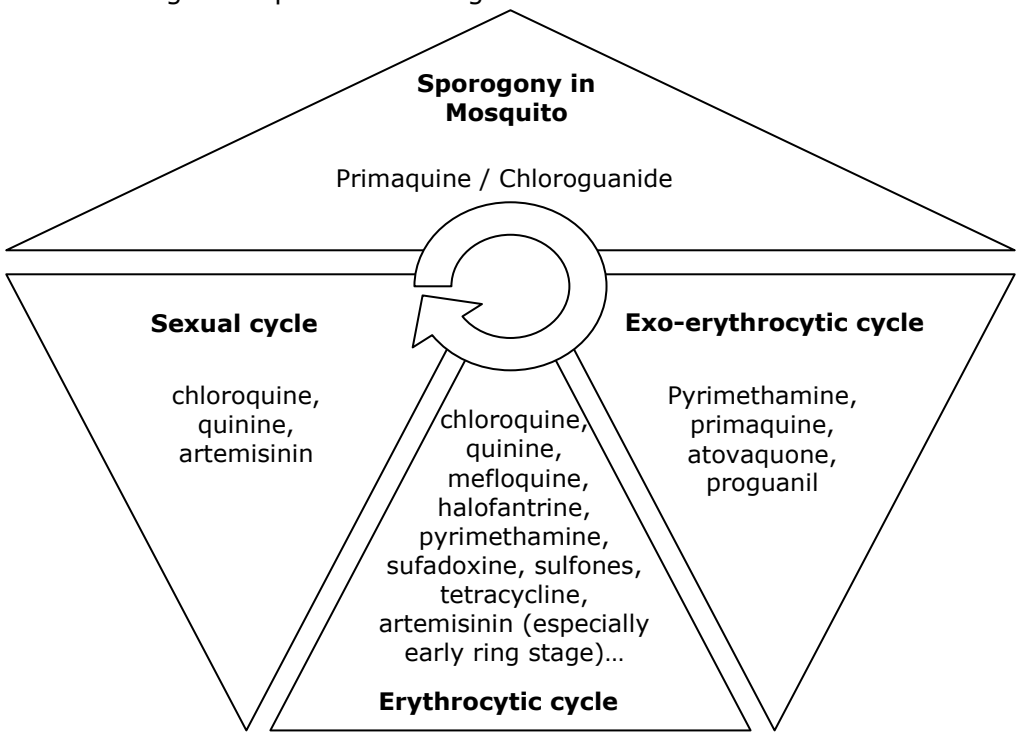

Figure I.1-3: Classification of anti-malarial drugs according to their place of action in the *Plasmodium* life cycle

Anti-malaria drugs can be classified according to their structure and their mechanism of action when the latter is known.

Aryl amino alcohols	Quinine (prevents hemozoïn formation), quinidine (cinchona alkaloids), mefloquine, halofantrine.
4-aminoquinolines	Chloroquine (prevents hemozoïn formation), amodiaquine.
8-aminoquinolines	Primaquine
Folate synthesis inhibitors	Type 1 – competitive inhibitors of dihydropteroate synthase - sulphones, sulphonamides Type 2 - inhibit dihydrofolate reductase (proguanil ; pyrimethamine
Antimicrobials	Tetracycline, doxycycline, clindamycin, azithromycin (inhibitors of protein biosynthesis) and fluoroquinolones (replication inhibitor)
Naphthoquinones	Atovaquone (inhibitor of parasite mitochondria)
Peroxides	Artemisinin (Qinghaosu) derivatives and analogues - artemether, arteether, artesunate, artelinic acid

Table I.1-1: Classification of anti-malarial drugs according to their chemical family and their mode of action.
(adapted from www.malariasite.com and completed with data obtained in http://www.phac-aspc.gc.ca/publicat/ccdr-rmtc/04vol30/30s1/index_f.html)

Many blood schizonticidal drugs are available but they present many differences in terms of anti-malarial activity, efficiency, toxicity and their cost. Table I.1-2 compares the most used ones according to these criteria.

The most efficient way to fight malaria is a combination of a blood schizonticide, a gametocytocide and a tissue schizonticide. In the case of non chloroquine resistant malaria, a combination of chloroquine and primaquine is thus required. But in case of severe malaria with chloroquine resistant parasite, the treatment of choice is an artemisinin combination therapy (ACT) as recommended by the World Health Organization (2006) based on artemisinin derivatives like artesunate/mefloquine or amodiaquine and artemether/lumefantrine.

In the next section, I will focus on this efficient class of antimalarial that represent artemisinin drugs.

	Chloroquine	**Pyrimethamine /Sulphadoxine**	**Quinine**	**Mefloquine**	**Artemisinin**
Efficacy	++++	++	+++	+++	+++++
Onset of action	Rapid	Slow	Rapid	Rapid	Fastest
Use	first choice for all cases	Only for uncomplicated, chloroquine resistant *P. falciparum*	Only for resistant *P. falciparum*	Only for uncomplicated, multi drug resistant *P. falciparum*	Reserved for drug resistant *P. falciparum*. However, it may be considered in life threatening complications of *P. falciparum* due to its rapid action
Use in severe *P. falciparum* malaria	Parenteral preparation can be used in areas with sensitive strains	Not useful in acute illness; can be co-prescribed with other parenteral antimalarials	Drug of choice for severe malaria; it was the only parenteral drug available for a long time until parenteral chloroquine and artemisinin arrived	Not to be used in acute illness; can be co-prescribed with artemisinin after acute phase is over.	Useful in severe malaria; may be more effective and better tolerated than quinine.
Toxicity	++	+++	+++	+++	+
Contra indications	Almost none, only advanced liver disease	Allergy to sulpha	Prior hypersensitive reactions	Epilepsy, psychosis, heart block, ß blocker use	None
Use in pregnancy	Yes	Only in 2nd trimester if warranted	Only if warranted, watch for hypoglycemia	Not in first trimester	Yes, if the situation demands
Cost	Cheapest	Cheap	Moderate	Expensive	Expensive
Resistance	++	++	+ (but rare)	+	Observations of lower sensitivity to Artemether[1], artesunate[2]

Table I.1-2 : Comparison between blood schizonticidal drugs (adapted from www.malariasite.com)

[1](Jambou et al., 2005); [2](Noedl et al., 2008)

I.2 The anti-malarial drug Artemisinin

I.2.1 Discovery, extraction and characterization of artemisinin

A plant named *Artemisia* has been used by Chinese herbalists for more than a thousand years in the treatment of many illnesses, such as skin diseases and malaria. The earliest record dates back to 200 BC (the "Fifty two Prescriptions" unearthed from the Mawangdui Han Dynasty Tombs). Its antimalarial application was first described in "The Handbook of Prescriptions for Emergencies", edited in the middle of fourth century by Ge Hong.

In the 1960s a research program (project 523) was set up by the Chinese army to find an adequate treatment for malaria. A list of nearly 200 traditional Chinese medicines for treating malaria were tested and in 1972, in the course of this research, Tu Youyou (Institute of Chinese Materia Medica, Academy of Chinese Traditional Medicine, Peking) extracted artemisinin (Qinghaosu in Chinese) from the leaves of *Artemisia annua* (sweet wormwood, fig. I.2-1, panel A) by low temperature ethyl ether extraction. This drug was the only one that was effective against malaria. It was even found that it cleared malaria parasites from infected patients faster than any other drug in history. The structure of artemisinin (fig. I.2-1, panel B) was then determined in 1979 (group, 1979) by the groups of Tu Youyou and Chou Wei-shan (Institute of Organic Chemistry, Academia Sinica, Shanghai). This drug is a sesquiterperne trioxane lactone and contains an endoperoxide bridge. This last particularity appeared to be too unstable to be a viable drug that is why this discovery was first welcome with skepticism.

A. 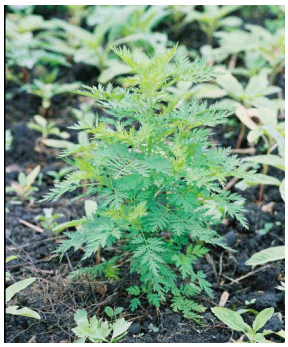

B. 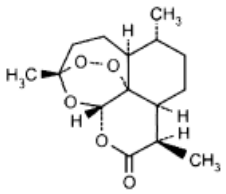

Figure I.2-1 : Artemisia annua and its anti-malaria component : artemisinin
Panel A. : photography of Artemisia annua. It is a common herb and has been found in many parts of the world
Panel B. : structure of artemisinin

To be studied and administered to patients, artemisinin has to be extracted from Artemisia plants. However, the amount of artemisinin that may be extracted from Artemisia plant varies widely, depending on plant material and growth conditions and yields remain low (generally range between 0.01% and 0.8% of the dry weight) (van Agtmael et al., 1999; Abdin et al., 2003; Wang et al., 2003). This factor represents a serious limitation to the commercialization of the drug. Fully synthetic synthesis was attempted but it remains too expensive (Schmid et al., 1983). However, metabolic and genetic engineering strategies have been developed in order to reduce this cost and to increase artemisinin production in plants and also to produce artemisinic acid, a precursor of artemisinin, in yeast and *E. coli* (Arsenault et al., 2008).

I.2.2 Development of artemisinin derivatives

Artemisinin has low solubility in water or oil, and thus can only be administered orally. This method of administration is practical; however, in patients with severe malaria oral administration is often impossible. In addition, artemisinin has a short half-life (<10min). To resolve these problems, several semi-synthetic artemisinin derivatives were developed by Chinese just after their discovery of artemisinin. Among these derivatives, dihydroartemisinin was the most efficient and has a longer half-life (~1h, (Krishna et al., 2004) but, because of stability problems, more stable derivatives of this drug were developed: arteether, artemether (oil-soluble) and artesunate (water-soluble)(fig. I.2-2). These derivatives have the advantages to have a longer and greater anti-malarial activity (Balint, 2001) because their metabolite, dihydroartemisin, is also active (see table I.2-1). Today, arteether has been discarded in favor of artemether and artesunate. New derivatives are currently being developed to improve solubility and pharmacokinetics (O'Neill, 2005) and one seems to be a good candidate, artemisone (fig. I.2-2) (Haynes et al., 2006) because it is 10 times more potent (Vivas et al., 2007) than artesunate *in vitro* and safe for humans (Nagelschmitz et al., 2008).

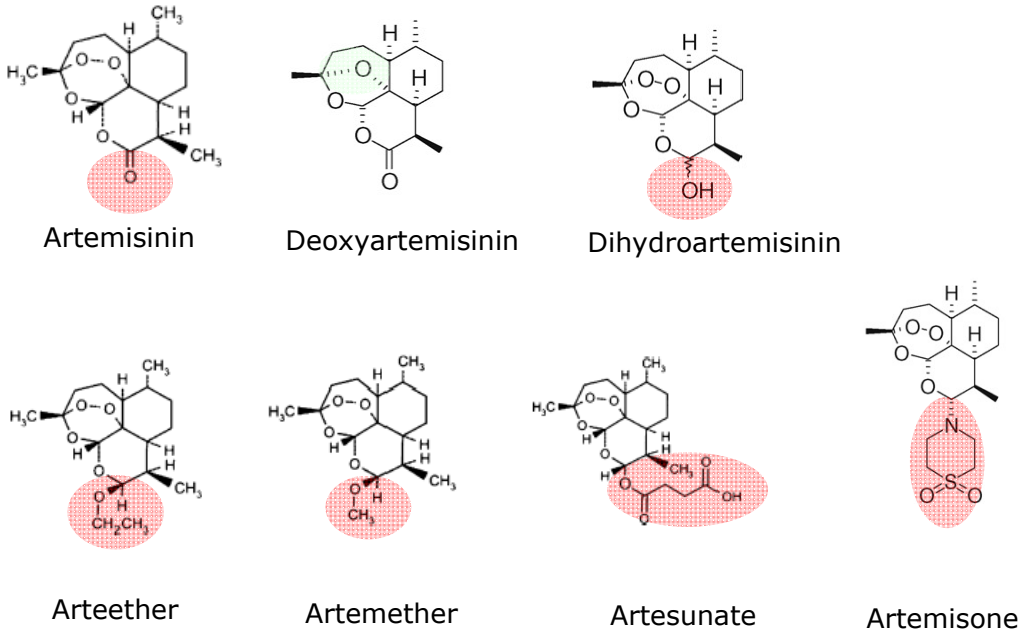

Figure I.2-2 : chemical structure of artemisinins

Artemisinin isolated in crystalline form in 1973 from Artemisia annua and derivatives dihydroartemisinin, artemether, artesunate and arteether were first prepared by Chinese scientists in the 1970s.
Artemisone, representative of a new class of artemisinin known as amino-artemisinins, is curative in clinical trials at one-third the dose regimen of artesunate and it is characterized by low toxicity.
Deoxyartemisinin, lacking the peroxidebridge, is biologically inert.
These structures were taken from (Golenser et al., 2006; Krishna et al., 2008)

	Artemisinin	Dihydroartemisinin	Artesunate	Artemether	Arteether
Administration method (in vivo)	Oral (tablets) suppository	Oral (tablets) suppository	Oral (tablets) Suppository Intravenous Intramuscular	Oral (capsules) intramuscular	Intramuscular
IC_{50} (in vitro)	10-100nM	0.36-7nM	1.7-2.2nM	0.6-6.6nM	1.7-3.5nM

Table I.2-1 : Artemisinins properties and efficiency

according to (Golenser et al., 2006)

Treatment with artemisinin drugs causes reduction of parasite burden below detectable levels without eliminating all parasites because of its very short half-life. To eliminate the last remaining parasites which could lead to a new infection and maybe to artemisinin resistant parasites, artemisinin which was first used in monotherapy is currently administered to patient only in combination with another anti-malarial drug (see section I.1). For this reason, efforts are carried out to develop combined salts and hybrid molecules.

For instance, MEFAS is a salt that contains two antimalarial functionalities: one quinolinic ring from mefloquine and one endoperoxide ring from artesunate (fig. I.2-3). MEFAS is active against chloroquine-resistant and chloroquine-sensitive *P. falciparum* parasites. The average inhibitory concentrations for both parasites at the IC_{50} were ~2.5nM. This IC_{50} value shows that MEFAS was two fold more potent than the mixtures of artesunate with mefloquine tested at different mass proportions. MEFAS is also able to cure mice infected with *P. berghei* parasites (de Pilla Varotti et al., 2008).

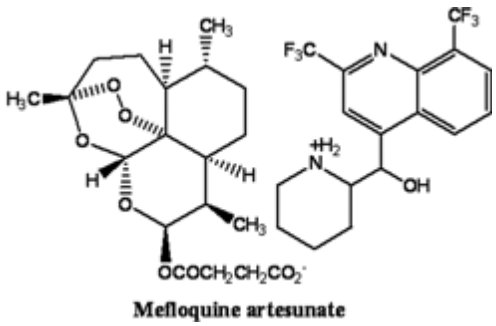

Figure I.2-3: Chemical structure of MEFAS

As a second example, chimeric molecules which combine two lethal pharmacophores for *Plasmodium* were developed (Dechy-Cabaret et al., 2004). Note that this hybrid molecule was first developed for chloroquine-resistant parasites. These hybrid molecules are called trioxaquine because they are composed of a trioxane motif (derived from artemisinin) designed to be a potential alkylating agent for the heme and/or proteins of the *Plasmodium* parasite, and an aminoquinoline moiety (derived from chloroquine) which has been selected to facilitate a good accumulation in the parasite and for the interaction with free heme (fig I.2-4).

These molecules are highly active both on chloroquine-sensitive and chloroquine-resistant strains (IC_{50}=3-30nM for trioxaquine R=R*=Phenyl (Basco et al., 2001) on respectively chloroquine sensitive and chloroquine-resistant strains and IC_{50}=5-20nM for trioxaquine R= $CH(CH_3)_2$, R*=CH_3 (Dechy-Cabaret et al., 2004) on respectively chloroquine sensitive and chloroquine-resistant strains. These new molecules are also efficient to cure infected mice. Among the 120 tested molecules (Cosledan et al., 2008), one is currently in clinical trial.

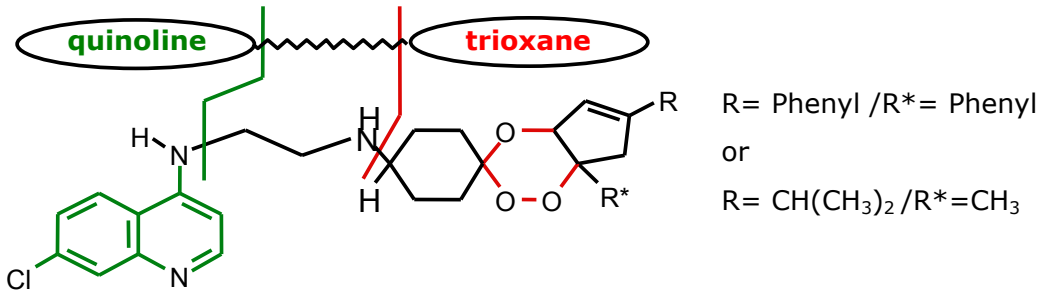

Figure I.2-4: Chemical structure of trioxaquines
R=Ph : (Basco et al., 2001)
R= $CH(CH_3)_2$: (Dechy-Cabaret et al., 2004)

I.2.3 Effects of artemisinin on *Plasmodium* and hypotheses regarding its mechanism of action

Clinical parasite resistance to artemisinin drugs has not yet been observed, although variations in sensitivity have been described (van Agtmael et al., 1999; Gordi et al., 2004; Jambou et al., 2005; Cojean et al., 2006). In order to avoid the emergence of resistance and/or to efficiently counteract, it is of major importance to know the mechanism of action of this drug. However, the mechanism of action of artemisinin is still unclear and controversed. Several hypotheses have been made from chemical and biological observations but a consensual picture has not yet been found.
In the following sections, I will present a summary of the main effects of artemisinin on *Plasmodium* observed by many groups in the world and the hypotheses derived from these results. Other effects of artemisinin have also been observed on cancer cells and viruses but I will not detail them.

I.2.3.1 Stage of action and morphological consequences on the parasite

Artemisinins exhibit a quick onset of action and high efficacy against the blood stages of *Plasmodium*, including the youngest stages (ring forms) (ter Kuile et al., 1993) and have been shown to reduce the number of gametocytes in the blood (Kumar et al., 1990; Kombila et al., 1997) due to their activity against both the precursors of the sexual stages and early gametocytes. Artemisinins also decrease the infectivity of the surviving gametocytes (Chen et al., 1994; Targett et al., 2001).

Interestingly, infected red blood cells are enriched in artemisinin compared to healthy erythrocytes (Gu et al., 1984; Vyas et al., 2002). Artemisinin seems therefore to specifically target the parasite.
Electron microscopic autoradiography performed on infected erythrocytes exposed *in vitro* to ^{3}H-dihydroartemisinin and ^{14}C-artemisinin shows that these drugs were located in food vacuoles and mitochondria. Besides, they induced ultrastructural changes in parasite mitochondria, rough endoplasmic reticulum, and nuclear envelope. Then, in addition to the earlier changes, nuclear membranes and, to a lesser extent, some plasma membranes formed myelin figures. In addition, there was a disappearance of ribosomes, and a destruction of food vacuole membranes. These changes may lead to the total disorganization of the parasites (Maeno et al., 1993).

Other studies show that, in the parasite, artemisinins are localized in the red blood cell tubovesicular membrane network which transports the drug into the parasite, in parasite membranes but not in parasite food vacuole membranes (Eckstein-Ludwig et al., 2003). However, these data can be criticized because they were obtained with fluorecent artemisinin and therefore with modified artemisinin. The structure of the molecule being bigger, its localization can be ordered by this supplemental group rather than artemisinin itself.
Its localization of artemisinin is therefore debated and especially since recent evidence showing that artemisinin derivatives cause early disruption of the parasite food vacuole and do not seem to affect the structure of the endoplasmic reticulum (Fidock et al., 2008).

I.2.3.2 Structure related action

Deoxyartemisinin (fig. I.2-2), a derivative in which a simple oxygen replaces the endoperoxide bridge is biogically inactive (Klayman, 1985). The endoperoxide bridge is therefore essential for antimalarial activity of artemisinin.
In vitro antimalarial activity was shown to be sensitive to steric effects (since replacement of the methyl at C3 of artemisinin by much larger group (phenylethyl) results in diminution in activity (Avery et al., 1996; Haynes et al., 2004; Krishna et al., 2004). However, enantiomers of trioxanes, structurally related to artemisinin, were equivalently efficient in killing parasites (O'Neill, 2005) suggesting an achiral target.

I.2.3.3 Reactivity via radical production occurring after reaction with iron

I.2.3.3.1 Proposed mechanism of activation

The treatment of infected erythrocytes by dihydroartemisinin causes the reduction of red blood cell antioxidants and glutathione (Ittarat et al., 2003). Thus, the capacity of artemisinin drugs to kill parasites was correlated to their ability to generate radicals through their endoperoxide bridge.

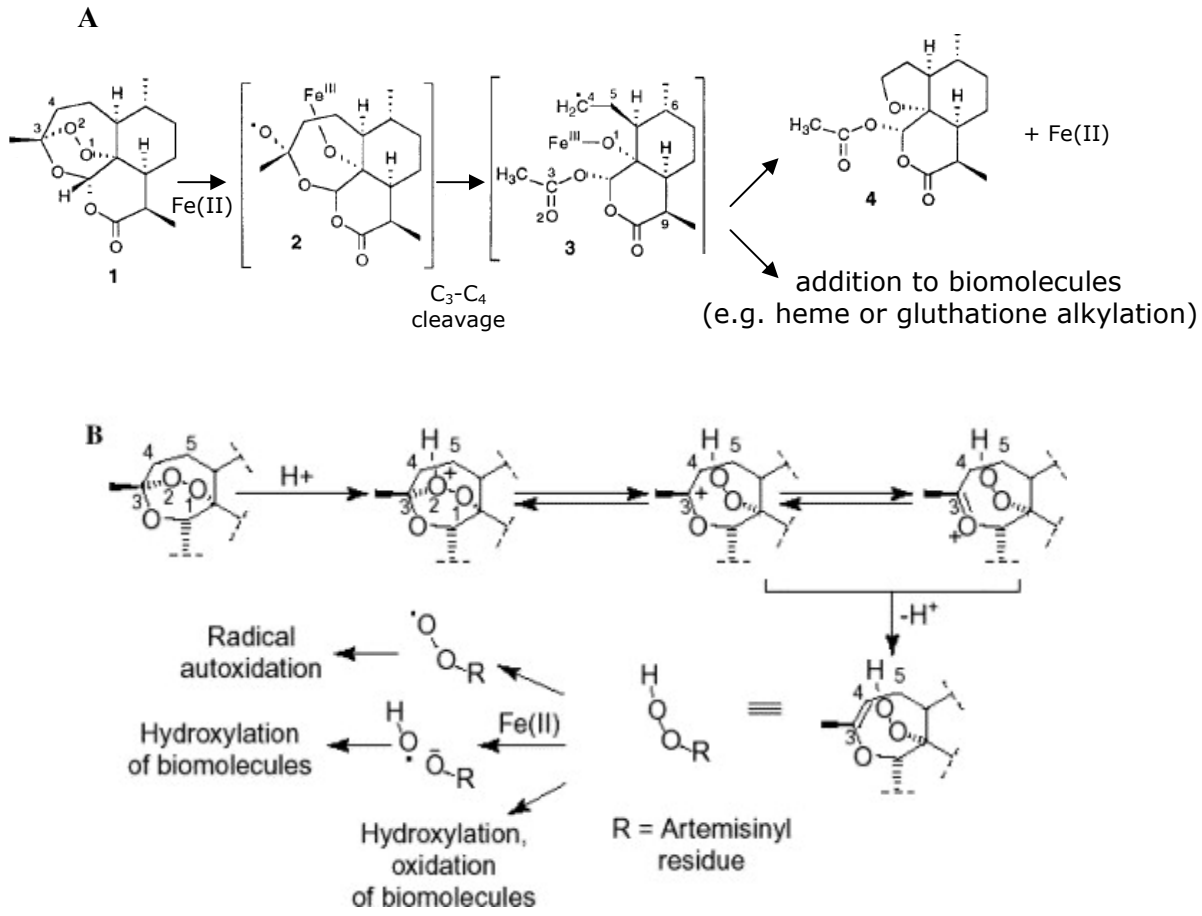

Figure I.2-5: Possible mechanisms of artemisinin peroxide bond opening.
(A) Proposed reductive scission of the peroxide bond and formation of carbon-centered radicals. Fe(II) can be, for instance, iron(II) in ferrous haem. Adapted from (Robert et al., 2006)
(B) Proposed ring opening of the peroxide bond to generate hydroperoxides, and subsequent decomposition pathways. The case using a proton is illustrated, but equally a metal ion [such as Fe(II)] might trigger ring-opening by complexation.
Reprinted from Golenser et al. (2006)

In presence of chelating agents of iron, the in vitro antimalarial activity of artemisinin drugs was antagonized (Meshnick et al., 1993). Thus, it was suggested that iron may catalyze the generation of radical species from artemisinin.

Based on these findings, two models of formation of free radicals derived from artemisinin and mediated by iron were proposed (fig. I.2-5). In the reductive scission model, the peroxide bridge is cleaved by divalent Fe^{2+} (fig. I.2-5 panel A) and alkoxyl radicals (**2**). These radicals quickly isomerize to produce the alkyl radicals (**3**) via a C-C

β-scission. In the open peroxide model, the peroxide ring is opened by protonation or by complex formation with Fe^{2+}, resulting in an open hydroxy- or metal-peroxide (fig. I.2-5 panel B). The oxygen atom which is not in the ring stabilizes the positive charge of the open peroxide, lowering the energy needed to open the ring. This mechanism of activation of artemisinin was recently disputed by Haynes (Haynes et al., 2007). As the energy necessary to cleave a C-O bond is higher (90kDa) than the one needed in the case of a O-O bond (35kDa), the first model is nevertheless more likely. Whatever the mechanism of generation of artemisinin radicals, they lead to highly reactive species and they can react with all molecules of their surrounding environment. However, some proteins, such as heme-binding proteins and proteases involved in hemoglobin degradation were mentioned as potential targets of these radicals (Meshnick et al., 1993; Olliaro et al., 2001; Haynes et al., 2004).

I.2.3.3.2 Potential origin of iron: heme, cytosolic iron, Fe-S proteins

The origin of the iron is intensively debated. It was suggested that it could be heme-iron (Robert et al., 2001) or cytosolic labile iron (Golenser et al., 2003). The first idea comes from the fact that the parasite uses hemoglobin as main source of amino-acids, the by-product of hemoglobin degradation being heme (heme-Fe(II)). Given heme is toxic for the parasite, it is then polymerized in a non toxic form: hemozoin, a polymer of hemin (heme-Fe(III)). The second idea has been proposed because the parasite would use cytosolic iron for its metabolic purposes (Scholl et al., 2005).

Heme–artemisinin adducts have been characterized by mass spectrometry in *P. falciparum* cultures treated with artemisinin (Meshnick et al., 1991).
Besides, the antimalarial efficiency of artemisinin and its derivatives has been found proportional to their binding to hemin (Cheng et al., 2002; Zhang et al., 2008). The efficiency of the artemisinin-type drugs in forming noncovalent complexes with Fe^{3+}-heme was comparable with that of quinine, indicating a possible similar target (Pashynska et al., 2004). Then, covalent binding to hemoglobin heme has been demonstrated *in vitro* (Kannan et al., 2005).
These results can nevertheless be explained by the fact that the samples were analyzed in a mass spectrometer. Indeed, the ionization process occurring during the analysis can lead to the formation of products that were not in the sample before its injection in this device.

The fact that heme and hemoglobin react with artemisinin seems to be consistant with the expected reactivity of artemisisin. Heme iron would activate artemisinin leading to

the alkylation of protoporphyrin IX. The reaction between heme and artemisinin is depicted in fig. I.2-6

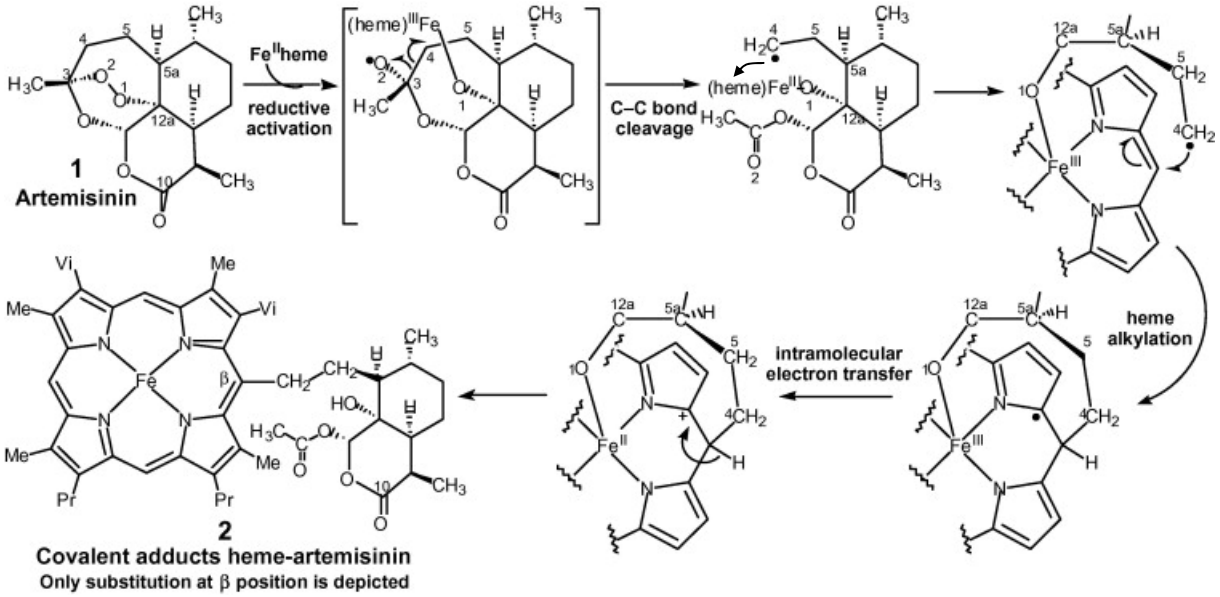

Figure I.2-6: Activation of artemisinin by FeII heme and subsequent reaction of alkylation of heme with activated artemisinin

The peroxide function, included within a 1,2,4-trioxane cycle, readily reacts with heme (the iron(II) complex of protoporphyrin-IX), a low-valent transition metal complexes. In vitro, the reductive homolysis of the O–O bond of artemisinin by iron(II) heme produces, after β-scission, a C_4-centred radical able to alkylate the protoporphyrin-IX ligand of heme on its meso positions, giving rise to covalent coupling products which have been identified by mass-spectrometry analysis.
Reprinted from (Accardo et al., 2007)

Moreover, Robert et al. (2005) found heme–artemisinin adducts in the spleen and urine of mice infected with *Plasmodium vinckei* and treated with artemisinin but not in non-infected mice. These results indicate that the alkylation of heme by this antimalarial drug also occurs *in vivo* and confirm the powerful alkylating ability of artemisinin in mammals, this effect being triggered by the presence of the parasite (Robert et al., 2005). These findings were disputed (Golenser et al., 2006) since the alkylation may have happened in spleen macrophages, which are loaded with lysing infected-and non-infected erythrocytes (Schwarzer et al., 1994).

The heme-dependent activation theory (heme as a byproduct of hemoglobin formation) has been criticized because it was not in agreement with biological aspects. Firstly, artemisinins kill the early stages (ring forms) of *P. falciparum*, which do not yet

metabolize hemoglobin and which therefore lack hemozoin (Eckstein-Ludwig et al., 2003). Secondly, artemisinins are also efficient on various species of *Babesia* that are hemozoin deficient (Kumar et al., 2003). Thirdly, artemisinins do not seem to be localized in the food vacuole where occurred hemoglobin digestion and therefore where hemin is sequestered (Olliaro et al., 2001; Eckstein-Ludwig et al., 2003). This argument is nevertheless debated because these localization where performed with the use of acridin-artemisinin, a dramatically different molecule compared to artemisinin.
The Fe^{2+}-dependent activation of artemisinin and its antimalarial activity was then shown to be independent of heme. Indeed, the use of a protease inhibitor to prevent the first step of hemoglobin degradation did not inhibit the activity of artemisinin (Eckstein-Ludwig et al., 2003). Further evidence that heme iron is not needed for the antimalarial effects of artemisinin was also demonstrated by changing the culture conditions of the parasite (Parapini et al., 2004). Artemisinin activity increased by 20–30% under an oxygen-rich atmosphere (20% instead of standard 1% O_2), and by 40–50% in the presence of carboxy-haemoglobin and 2% carbon monoxide. Although the authors postulated that these last conditions inhibit heme iron (II) reactivity, other showed that artemisinin can react with carboxyhemoglobin via heme-Fe(II) (Robert et al., 2006).

Other sources of iron were postulated. In addition to the cytosolic iron pool, there are also proteins that contain iron−sulfur-redox centers (e.g. ferredoxins, NADH dehydrogenase, hydrogenases, nitrogenase…). These proteins are known for their role in the oxidation-reduction reactions of mitochondrial electron transport but have also other roles such as catalysis and generation of radicals. With this type of protein, the same cleavage of artemisinin, as observed in the heme model is expected to occur (see fig. I.2-7) and would lead to a S-alkylation of a cysteine and a covalent bonding to artemisinin. This latter would therefore lead to irreversible damage of the redox center. If the inactivated redox center is, for example, a critical enzyme/functional protein, lethal consequences may of course result. Up to now, covalent adducts with artemisinin were only highlighted with small Fe-S molecules such as gluthatione (Wu, 2002). The interaction with iron-sulfur redox proteins are still awaited.

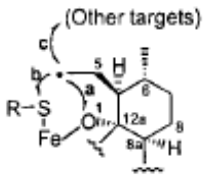

Figure I.2-7: Schematic representation of the possible reaction occurring between a Fe-S protein and artemisinin
This chemical reaction is of the same nature as the one occuring between heme and artemisinin (reprinted from Wu et al., 2002)

In this section, we saw that activated artemisinin could react intramolecularly with this activator if the latter is a macromolecule but we could also hypothesized that it could react intermolecularly if it is activated with all source of available iron(II) and alkylate other type of proteins.

I.2.3.4 Alkylation of some parasite proteins by artemisinin

We have seen in the pevious section that activated artemisinin can alkylate heme and probably Fe-S proteins. In order to identify artemisinin alkylated proteins, the group of S. Meshnick treated parasites with radiolabeled artemisinins and analyzed the protein content of *the parasite*-infected erythrocytes on autoradiograms of SDS-polyacrylamide gels (Asawamahasakda et al., 1994). They observed that six proteins (<25, 25, 50, 65, 200 and >200kDa) were radioactively labeled by these endoperoxides (fig. I.2-8). These proteins were not the most abundant proteins seen on Coomassie-stained gels and seem localized in the membrane fraction of the parasite lysate. In addition, they could conclude that these proteins were parasite proteins because no proteins were labeled when uninfected erythrocytes were treated with these drugs, nor when infected erythrocytes were treated with the inactive analog deoxyarteether.

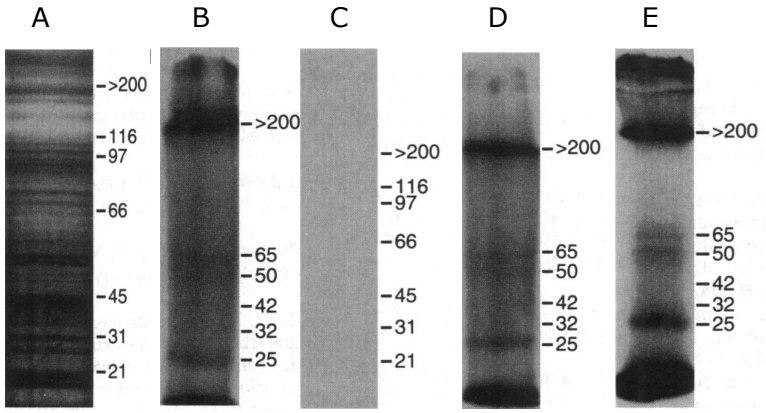

Figure I.2-8: SDS-PAGE autoradiograms of artemisins-treated parasites
Coomassie blue stained gel and autoradiograms of P. falciparum trophozoites lysates after treatment with [^{3}H]arteether (A and B respectively), autoradiograms of P. falciparum trophozoites lysates after treatment with [^{3}H]deoxyarteether (C), [^{3}H]dihydroartemisinin (D) and autoradiograms of the pellet of [^{3}H]dihydroartemisinin-treated lysed trophozoites obtained after centrifugation at 14,000 x g (E) (Asawamahasakda et al., 1994)

Up to now, only the 25kDa protein was identified. It is an orthologous protein to the Translationally Control Tumor Protein (TCTP) (Bhisutthibhan et al., 1998; Bhisutthibhan et al., 1999; Bhisutthibhan et al., 2001). This protein is located in both the cytoplasm and food vacuoles and limiting membranes. Like other TCTPs, the *P. falciparum* protein binds to calcium and if its function is conserved, it could act on the stabilization of microtubules. TCTP reacts with artemisinin *in situ* and *in vitro* in the presence of heme-Fe(II) and appears to bind to heme. However, the function of the malarial TCTP and the role of this reaction in the mechanism of action of artemisinin await elucidation. Interestingly, resistance in *P. yoelii* was correlated to a high expression level of parasite TCTP (Walker et al., 2000).

I.2.3.5 Artemisinin affects hemoglobin degradation proteins and hemozoïn formation

Hemoglobin degradation is carried out by different proteins among which there are a cysteine protease and a histidine-rich protein (HRPII). Pandey et al. showed that artemisinin could disrupt hemoglobin catabolism and heme detoxification system in malarial parasite (Pandey et al., 1999). They also observed, *in vitro*, a decrease of the proteolytic cleavage (~50%) of peptides by cysteine protease when the enzyme was pre-incubated with artemisinin (and it was even more obvious in presence of heme (~70%)). Cysteine proteases in *Plasmodium* are more generally involved in the

progression of intraerythrocytic life cycle, with roles in degradation of hemoglobin and erythrocyte cytoskeletal proteins, and erythrocyte rupture. It can also be noted that the activity of these enzyme are triggered (indirectly) by calcium release in the cytoplasm.

Kannan et al. observed that heme-artemisinin adducts could bind to *Plasmodium falciparum* histidine-rich protein II and that resulted in inhibition of heme polymerization and death of the malaria parasite (Kannan et al., 2002). PfHRP-II which is present in the parasite food vacuole contributes indeed to the initiation of heme polymerization and PfHRP-II–heme complex is thought to be a required step in the formation of hemozoin (Sullivan et al., 1996). However, it is interesting to note that these results could not be reproduced with peptides mimicking the sequence of the heme-binding site of HRP-II (Accardo et al., 2007). This suggests that the binding of heme-artemisinin adducts on PfHRPII does not only depend on the coordination ability of the iron center but probably also on the tertiary structure of the protein.

I.2.3.6 Effect of artemisinin on the parasite proteome

A large-scale quantitative proteomic approach examined protein expression changes in trophozoite stages of the malarial parasite *Plasmodium falciparum* after artemisinin treatment (Prieto et al., 2008). In drug treated parasites, more than 800 proteins were quantified. Under artemisinin treatment 41 proteins respectively were upregulated (>1.5) whereas 14 proteins were down-regulated (<0.5). More precisely, they observed that the vacuolar ATP synthase; subunits α and γ (PF13_0130) display down regulation when the parasite was treated with artemisinin. In addition, several processes show slight upregulation under artemisinin treatment. This upregulation affects mainly nucleotide and nucleic acid metabolism, transport and secretion as well as the expected response to drugs like *pfmdr1*, the multidrug resistance gene that was found to be upregulated under artemisinin treatment- this confirms the previous result showing that this gene contributes to antimalarial drug-resistance (Duraisingh et al., 2005).

Another proteomic study carried out by Sumalee Kamchonwongpaisan showed that artemisinin might affect parasite endocytosis of host proteins (Fidock et al., 2008). Interestingly, it has already been observed that artemisinin inhibited endocytosis of red blood cell cytoplasmic macromolecules by the parasite (Hoppe et al., 2004). Note, in addition, that changes in calcium levels may have a significant regulatory effect on endocytosis.

I.2.3.7 Artemisinins interfere with mitochondrial electron transport

The effect of artemisinin on *Plasmodium* mitochondria was first highlighted with *Plasmodium inui* infecting *Macaca assamensis* monkeys. It was observed that the artemisinin treatment resulted in parasite mitochondrial swelling (Jiang et al., 1985). Artemisinin has also been shown to have inhibitory effects on the oxygen consumption by both sexual and asexual stages of *P. falciparum* suggesting an inhibition of the respiratory chain (Krungkrai et al., 1999).

More recently, Li et al. (Li et al., 2005) suggested that artemisinin and its derivatives are in fact activated by, and interfere with, components of the electron transport chain of the parasite mitochondria. Remember that it was proposed that artemisinin could react with Fe-S proteins, proteins especially found in mitochondria electron transport chain (see section I.2.3.3.2). Yeast, such as *Saccharomyces cerevisiae*, in the presence of a non-fermentable carbon source, required mitochondrial activity for growth. Under this metabolism, yeast were shown to be inhibited by artemisinin (IC_{50} of 10 nM, a concentration comparable with that which is effective against *P. falciparum in vivo*) whereas under fermentative metabolism that does not require mitochondrial activity, they were not inhibited by artemisinin. In addition, the presence of artemisinin was shown to cause depolarization of the mitochondrial membrane. Although criticized (Krishna et al., 2008), genetic studies demonstrated that deletion of yeast genes NDE1 and NDI1, which encode NADH dehydrogenases in the mitochondrial electron transport chain, led to artemisinin resistance. A gene homologous to NDI1 was found in the *P. falciparum* database, suggesting that the mitochondria, which contain transition metals including iron, have a role in the activation of artemisinin. Thus, after activation, artemisinin may cause local production of reactive oxygen species and depolarization of the mitochondrial membrane (Li et al., 2005). This result would be worth verifying directly on *Plasmodium*.

Interestingly, it was also noticed that, at high artemisinin concentration, mammalian cells partially lose their mitochondria function (Fishwick et al., 1998; Reungpatthanaphong et al., 2002).

I.2.3.8 Artemisinins disrupt ion homeostasis

Acridine orange enters acidic compartments such as lysosomes and become protonated and sequestered. In these low pH conditions, the dye will emit orange light when exited by blue light. The dye acridine orange is accumulated in subcellular compartment of *Plasmodium* (probably acidocalcisome) and it is released in the cytosol, revealing an acidification of the cytosol, in presence of artemisinin (and also in presence of chloroquine, fig. I.2-9) (Gazarini et al., 2007).

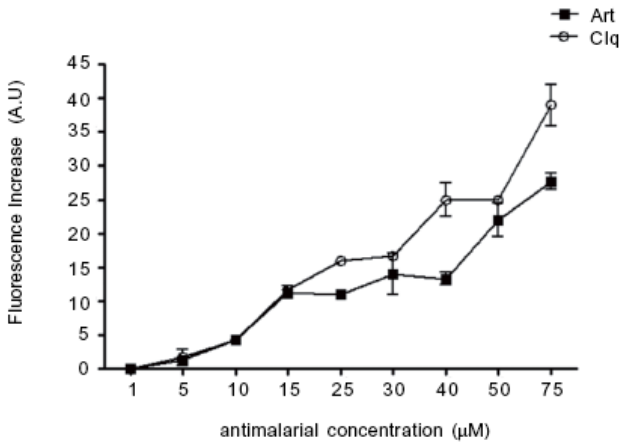

Figure I.2-9: Effect of artemisinin, Art (and chloroquine, Clq) on the acidification of the cytosol.

The acidification of the cytosol is proportional to the fluorescence of acridine orange. Data reprinted from (Gazarini et al., 2007)

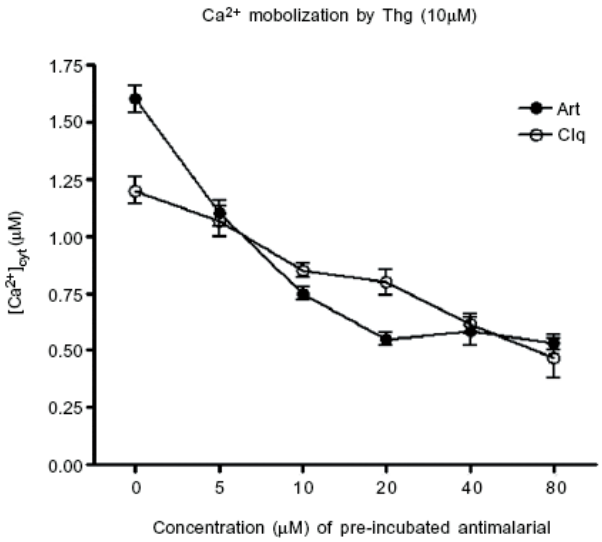

Figure I.2-10: Effect of artemisinin (and chloroquine) on calcium maintenance on endoplasmic reticulum in *Plasmodium chabaudii*.

The concentration of calcium measured through the use of sensitive dyes corresponds to the amount of calcium released in the cytosol by thapsigargin (inhibitor of the sarco/endoplasmic Ca^{2+}-ATPase) when the parasite was treated with different concentration of artemisinin (or chloroquine).
Reprinted from (Gazarini et al., 2007)

In addition of this disruption of H^+ homeostasis, the same authors observed that the Ca^{2+} concentration in the endoplasmic reticulum decreased when the parasite was treated with artemisinin (and also with chloroquine) (Gazarini et al., 2007). This decrease, observed in fact by the amount of calcium released in the cytosol when the sarco/endoplasmic Ca^{2+}-ATPase (SERCA, a protein responsible for the maintenance of cytosolic calcium ion concentrations) is inhibited by thapsigargin, was proportional to the amount of drug used (fig. 1.2-10). It can nevertheless be noted that, in both cases, the artemisinin concentrations necessary to observe an effect are higher (x100-1000) than those required to kill *Plasmodium* parasites.

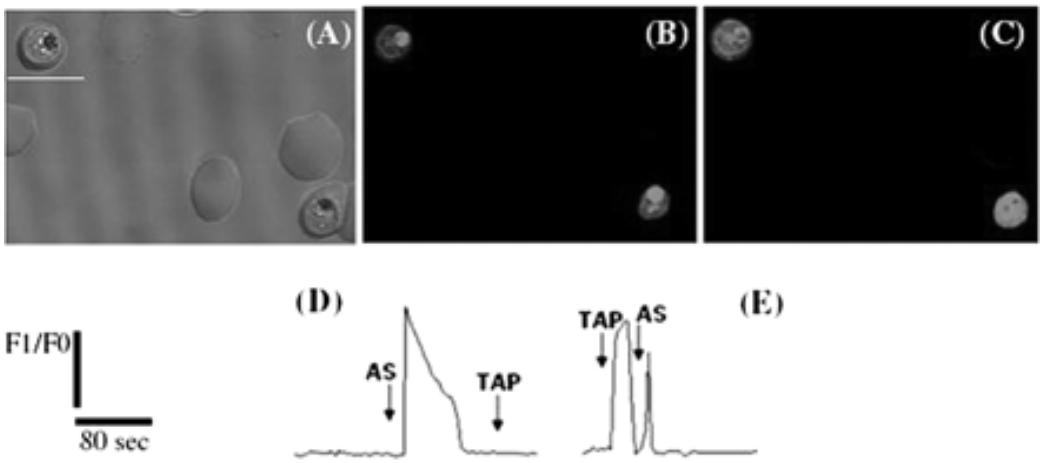

Figure I.2-11: Ca^{2+} mobilization by artesunate on infected red blood cells loaded with a calcium sensitive dye (Fluo-4 AM).

(A) Differential interference contrast image. (B) Basal fluorescence image. (C) Fluorescence image after artesunate (2.6nM) addition. (D) artesunate (increase of 1.3 ± 0.1 fluorescence arbitrary units) and thapsigargin action. (E) Thapsigargin (increase of 1.2 ± 0.1) and artesunate (increase of 0.7 ± 0.2) action.
Reprinted from of (de Pilla Varotti et al., 2008)

Other results showed that artesunate (2.6nM) exhibited intracellular action increasing cytoplasmic Ca^{2+}. This effect, although less intense, was also observed in the presence of thapsigargin (fig. 1.2-11), an inhibitor of SERCA, suggesting an intracellular target of artesunate distinct from SERCA (de Pilla Varotti et al., 2008).

Interestingly, artemisinin which also kills *Toxoplasma gondii* parasites, was shown to interfere with the calcium homeostasis of this other Apicomplexa (Nagamune et al., 2007; Nagamune et al., 2007). In this case, the authors presented results in favor of an interaction of artemisinin with *Toxoplasmi gondii* sarco-endoplasmic reticulum Ca^{2+}-ATPase.

I.2.3.9 Artemisinin inhibits PfATP6, the single sarco/endoplasmic Ca^{2+}-ATPase of *Plasmodium*

Artemisinin belongs to the same chemical family as thapsigargin (sesquiterpene lactone), a specific inhibitor of SERCA. Although these molecules are dramatically

different, this common feature was used as starting point to postulate another mechanism of action of artemisinin. It was thereby hypothesized that artemisinins specifically inhibit PfATP6, the only SERCA-type Ca^{2+}-ATPase in *P. falciparum* (Eckstein-Ludwig et al., 2003). SERCA is responsible for the maintenance of calcium ion concentrations, which is important for the generation of calcium-mediated signaling and the correct folding and post-translational processing of proteins. PfATP6 was therefore expressed in *Xenopus laevis* oocytes and the effect of antimalarial drugs was examined on oocyte membranes. In these conditions, artemisinin completely inhibited PfATP6 activity, with a half-maximal inhibition constant (K_i) of 150 nM. This inhibition was highly specific, such that even at 50 µM artemisinin, no other transporters, including the non-SERCA Ca^{2+}-ATPase PfATP4, were affected (fig. I.2-12). In addition, this inhibition was shown to depend on the presence of iron since in presence of an iron chelating agent (desferrioxamine), artemisinin was not anymore able to inhibit PfATP6 (fig. I.2-13). This was also correlated with parasite cultures since artemisinin was not able to kill the parasites in presence of this iron chelator (Eckstein-Ludwig et al., 2003). These results confirm that iron plays an important role in the mechanism of action of artemisinin.
In parallel to these results, *P. falciparum* cultures treated with fluorescent thapsigargin and artemisinin showed antagonism, indicating that both drugs have a common target. Besides, testing of several artemisinin derivatives, including dihydroartemisinin, showed a correlation between the concentration at which PfATP6 was inhibited by the drug in the *X. laevis* system, and the IC_{50} obtained in parasite cultures (Eckstein-Ludwig et al., 2003).

Based on these results, it was suggested that artemisinin binds to the same region in the protein that binds thapsigargin. Three-dimensional modeling of the PfATP6 amino acid sequence and subsequent docking simulation suggested that artemisinins bind to the protein by hydrophobic interactions while leaving the peroxide bonds exposed (not covered by the binding pocket) (Jung et al., 2005). This might allow cleavage of the peroxide bridge by iron to generate carbon-centered radicals (as discussed in section I.2.3.3), leading to enzyme inactivation and parasite death.

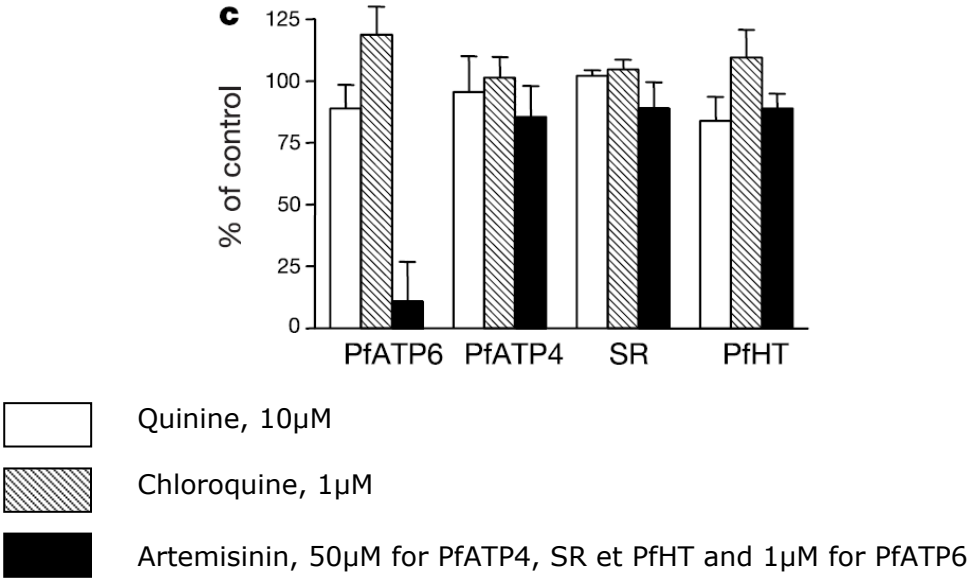

Fig. I.2-12 : Effects of antimalarial on two Ca^{2+}-ATPases of the parasite (PfATP6, PfATP4), mammalian SERCA (SR) and *P. falciparum* hexose transporter (PfHT)

PfATP6, PfATP4 and PfHT were expressed in Xenopus laevis oocytes
SR is the rabbit skeletal muscle endoplasmic reticulum containing more than 70% of SERCA
% of control corresponds to the ATPase activity measured in each case divided by the activity measured in presence of DMSO (the solvent in which the drugs were dissolved)
Reprinted from Eckstein-Ludwig et al., 2003

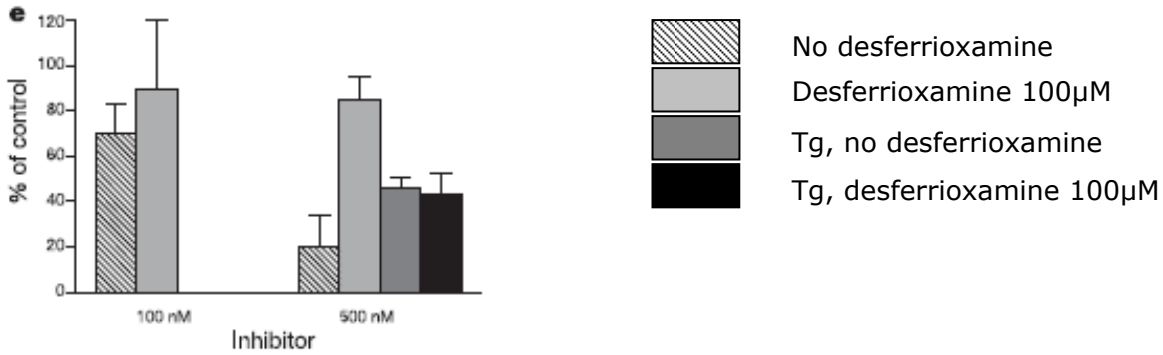

Figure I.2-13: Effect of iron removal on the inhibition capacity of artemisinin toward PfATP6 expressed in *Xenopus laevis* oocyte

ATPase activity ratios between the ATPase activity of PfATP6 measured either in presence of 100nM or 500nM of artemisinin (dissolved in DMSO) and the activity of PfATP6 measured in presence of DMSO. The ATPase activities were measured in absence and in presence of an iron chelator (desferrioxamine) and also in presence and in absence of thapsigargin (only in the case 500nM artemisinin).
Reprinted from Eckstein-Ludwig et al., 2003

Tg (thapsigargin) concentration is not mentioned by the authors

This theory was supported by the fact that a single amino acid mutation in the plasmodial SERCA modulates sensitivity to artemisinins *in vitro* (table I.2-2, Uhlemann et al., 2005). Mutation studies of PfATP6 expressed in *X. laevis* oocytes showed that Leu263, and additional residues, modulate sensitivity to artemisinin. Indeed, when this amino acid was replaced by the corresponding residue in *Plasmodium vivax* SERCA (Ala), *Plasmodium berghei* SERCA (Ser), the susceptibility of mutated PfATP6 for artemisinin was correlated with the concentration of artemisinin necessary to kill the parasite. In addition, the effect of artemisinin on PfATP6 was fully abrogated when L263 was replaced by the corresponding residue in mammalian SERCA1 and conversely, SERCA1 which is not inhibited by artemisinin, became sensitive to artemisinin when this amino acid (Glu 255) was replaced by a leucine (table I.2-2).
Position 263 (255 on mammalian SERCA) is on the L6/7 loop of the protein, at the apex of the thapsigargin-binding cleft formed by helixes M3 and M7 (Fig. I.2-13). This 'gatekeeper residue' and its surrounding area possibly regulate the conformation of the L6/7 loop of PfATP6 by forming electrostatic interactions between the residues in the helices. The authors postulated that changes in the conformation of the loop may prevent the noncovalent binding of artemisinin to the protein, resulting in resistance (Uhlemann et al., 2005).

Subsequent studies have revealed that mutations in PfATP6 (S769N) found in field isolates were associated with a lower *in vitro* sensitivity to artemether (Jambou et al., 2005). The authors suggested that this mutation prevents artemisinin derivatives from interfering with the conformational changes necessary for protein function. However, it is interesting to note that this cytosolic residue is not located in the predicted binding region of artemisinin.

In this section we saw that artemisinin seems to trigger a cascade of reactions that affect many vital functions of *Plasmodium* but the first targeted element(s) have not yet been identified. In the present thesis, we will focus on the effect of artemisinin on PfATP6 and it is therefore interesting to understand how calcium homeostasis is regulated and why the control of the cytosolic level of calcium is important for *Plasmodium*.

Sequence	Artemisinin K_i (nM)	IC_{50} (artesunate)
PfATP6		
Leu263 (wild type)	169 ± 31	4,4 ± 1,7 nM
L263A (*P. vivax*)	63 ± 12	
L263S (*P. berghei*)	530 ± 84	
L263E (mammalian)	>50,000	
L263D	>50,000	
L263K	>50,000	
L263Q	552 ± 143	
F264L	4,150 ± 1,850	
SERCA1		
E255L (*P. falciparum*)	314 ± 109	
Orthologs		
PvSERCA	7.7 ± 4.9	1,3 ± 0,3 nM
PbSERCA	5,660 ± 2,330	28 nM

Table I.2-2: Effect of artemisinin on mutated PfATP6 expressed in *X. leavis* oocyte (2[d] column) and comparison with the ability of artesunate to kill different *Plasmodium parasites* (3[d] column)

Adapted from Uhlemann et al., 2005

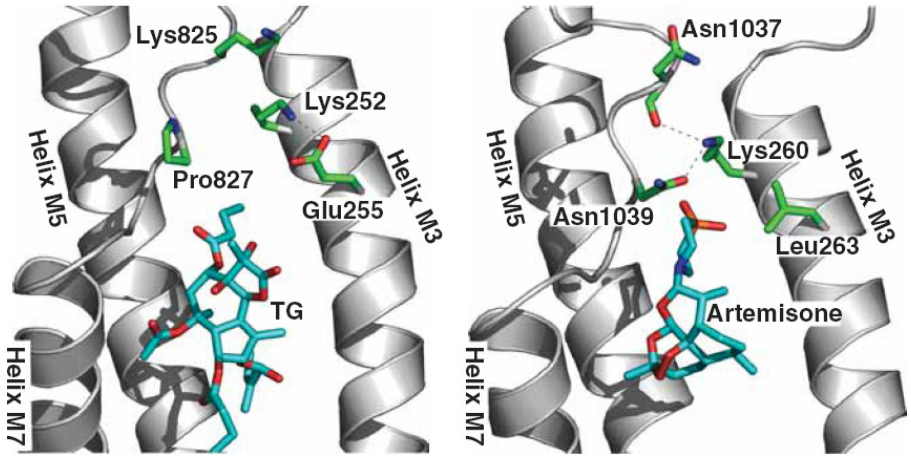

Figure I.2-13: Energy-minimized models of the rabbit SERCA1 thapsigargin binding site (left) and the corresponding region of a model of PfATP6 containing artemisone (right)

The structure of SERCA1a corresponds to the crystal structure 1IWO (PDB entry). Electrostatic interactions are predicted to exist between Lys 252 and Glu 255 on helix M3 in the mammalian SERCA1. In PfATP6, Lys 260 is predicted to bond to the L6/7 loop above helix M7.
Reprinted from Uhlemann et al., 2005

I.3 Calcium homeostasis and signaling in the malaria parasite

Calcium controls a number of vital processes in malaria parasite including protein secretion, motility and differentiation (Nagamune et al., 2008). Moreover, extracellular Ca^{2+} is essential for the invasion of the erythrocyte by the malaria merozoite, as well as for the maturation of the intracellular trophozoite (Wasserman et al., 1982).

Malaria-infected erythrocytes have a somewhat higher Ca^{2+} concentration than healthy erythrocytes. This higher Ca^{2+} concentration is, in fact, localized in the intracellular parasite and more precisely in the organelles (mitochondrion, endoplasmic reticulum, acidocalcisome) of the parasite (Leida et al., 1981; Tanabe et al., 1982; Adovelande et al., 1993). The concentration of free Ca^{2+} within the parasite cytosol is only two to four times higher than that in the host erythrocyte cytosol, evidence that the cytosolic Ca^{2+} concentration is strongly regulated. In early trophozoite-stage parasites, the Ca^{2+} concentration in the parasite cytosol is reportedly 40–44 nM, increasing to 110–125nM in the late trophozoite/schizont stage (Adovelande et al., 1993; Garcia et al., 1996). *P. falciparum* parasites freed from their host erythrocytes are able to accumulate $^{45}Ca^{2+}$ (Kramer et al., 1991). However, in freed parasites exposed to an increased extracellular Ca^{2+} concentration of 5 mM, it was reported no significant increase in the cytosolic Ca^{2+} concentration, consistent with the intracellular Ca^{2+} levels being tightly controlled (Kramer et al., 1991).

The pathways involved in the regulation of Ca^{2+} in the intracellular parasite are not yet completely known but many factors have already been characterized especially by genetic studies and the use of Ca^{2+} probes. These studies provided evidence for the presence of a number of discrete intracellular Ca^{2+} pools within the intracellular parasite (reviewed in (Garcia, 1999; Nagamune et al., 2008)).

Recent comparative genomic and phylogenetic analyses on a range of different plasmodial species and other Apicomplexa organisms (of the genus *Toxoplasma* and *Cryptosporidum*) helps to define calcium response pathways (Nagamune et al., 2006). Interestingly, exploring the genome of *Plasmodium* did not reveal any IP3 receptor nor ryanodin receptor Ca^{2+} channels no cyclic nucleotide-gated Ca^{2+} and voltage gated Ca^{2+} channel (Nagamune et al., 2006).

Thus, several P-type Ca^{2+}-ATPases, a single Ca^{2+}/H^{+} exchanger and other calcium binding proteins were identified in the malaria parasite.

I.3.1 Calcium binding proteins

P-type ATPases
A Ca^{2+}-ATPase orthologous to the yeast PMR1 found in the Golgi, PfATP4, was identified in the plasma membrane in asexual stages of malaria (Dyer et al., 1996). This Ca^{2+}-ATPase, heterogously expressed in *Xenopus laevis* oocytes, was shown to be sensitive to vanadate and CPA but not to the specific inhibitor of sarcoplasmic reticulum calcium ATPases (SERCA), thapsigargin (Krishna et al., 2001).

However, other studies suggested the presence of an endoplasmic reticulum Ca^{2+} pump since the parasite's endoplasmic reticulum was reportedly discharged by SERCA-type inhibitors: thapsigargin and BHQ (2,5-di-(*tert*-butyl)-1,4-hydroquinone) (Garcia et al., 1996; Passos et al., 1997). SERCA pumps are responsible for refilling calcium in the ER store, which represents the most readily mobilizable source of calcium for signaling. Further studies reported that thapsigargin caused an increase in cytosolic calcium at doses as low as 2µM but with a maximum effect at 25µM (fig. I.3-1). According to Eckstein-Ludwig et al., thapsigargin was able to kill parasites with an IC_{50} value of 2.6µM (Eckstein-Ludwig et al., 2003). Both values are much higher than the concentration required to kill mammalian cells and to inhibit mammalian SERCAs (<1nM) (Sagara et al., 1991). For the group of Celia Garcia, it was not surprising that SERCAs of species so different from mammals require much higher doses of the inhibitor but for Eckstein-Ludwig et al., this could be explained by the fact that multiple membranes need to be crossed in parasites (such as the erythrocyte membrane and the parasitophorous membrane), compared to mammalian cells.

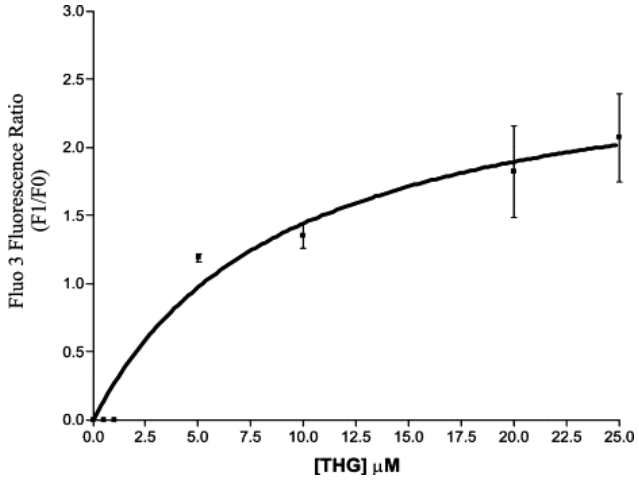

Figure I.3-1: Dose–response curve of the effect of thapsigargin (THG) on [Ca^{2+}] mobilization on *Plasmodium falciparum* parasites
in medium with 1 mM [Ca^{2+}] at different concentrations of THG. Trophozoite stage parasites were loaded with Fluo-3/AM, and exposed to −500 nM, 1, 5, 10, 20 and 25 µM of THG. The Fluo-3 fluorescence ratio (F1/F0) intensity (n=10) was plotted as a function of THG concentration (from (Varotti et al., 2003)).

Thereafter, a gene showing similarities with SERCA-type protein was identified and cloned (Kimura et al., 1993). This enzyme, named PfATP6, was found to have important similarities with the rabbit SERCA, despite the phylogenetic distance between these organisms. As mentioned in the previous section, this protein was expressed in *Xenopus laevis* oocytes and its sensitivity to thapsigargin was confirmed (Eckstein-Ludwig et al., 2003).

Three other putative Ca^{2+}-ATPase which seem to belong to the Golgi-ER-type family were also identified. Two of them contain putative signal peptides which indicates that they are within the secretory system but no specific information is available about their subcellular localization and functions (Nagamune et al., 2006).

Ca^{2+}/H^{+} exchanger

A Ca^{2+}/H^{+} exchanger was identified and was found to be similar to proteins found in the plant vacuole and yeast but not in metazoan animal cells (Nagamune et al., 2006).

EF-Hand containing proteins

These proteins contain helix-loop-helix structure (EF-Hand) that contains acidic residues that bind calcium.

A membrane associated EF-hand Ca^{2+}-binding protein*, Pfs40,* has been cloned and purified from the sexual stage of *P. falciparum* (Rawlings et al., 1992), and may be involved in intracellular Ca^{2+} storage.

Among this large family of Ca^{2+} binding proteins, calmodulin, a protein involved in a variety of signaling events, is present in *Plasmodium* and has been cloned (Robson et al., 1991). The importance of calmodulin in regulating Ca^{2+}-dependent processes in malaria parasites is supported by *in vitro* experiments with *P. falciparum* in which calmodulin inhibitors, inhibited invasion of red blood cells as well as maturation of schizonts (Matsumoto et al., 1987; Tanabe et al., 1989). Calmodulin is located at the apical region of both free and intraerythrocytic merozoites and it is this region that attaches to the erythrocyte at the first step in invasion.

Other calmodulin-like genes were identified and three of them resemble centrin and centrin-like proteins. Centrin is a constituent of the microtubular organizing centers.

A large number of Ca^{2+} dependent kinases (but no calmodulin dependent kinases) containing a serine/threonine kinase domain and four EF-hand domains were identified in *Plasmodium falciparum*. These proteins are involved in the cellular signal transmission but the exact roles of these kinases and of the proteins phosphorylated by these enzymes in *Plasmodium* are not yet known. The diversity of these calcium response proteins implies that many cellular processes are controlled by calcium-responsive conformational changes (i.e., EF-hand-containing proteins) or by phosphorylation cascades (calcium-dependent Serine/Threonine kinases). Note that these proteins share common sequences with their plant orthologous (Nagamune et al., 2006).

I.3.2 Calcium storage compartments

Endoplasmic reticulum

Endoplasmic reticulum is an important Ca^{2+} storage compartment. As mentioned above, one single SERCA-type ATPase (PfATP6) was identified.

Acidocalcisome

Acidocalcisome, found in *Trypanosoma, Plasmodium* and other apicomplexans is an electron dense acidic organelle which contains a matrix of pyrophosphates with bound calcium and other cations (Na^+, Zn^{2+} and Mg^{2+}). This organelle is also present in a diverse range of organisms from bacteria to man (Docampo et al., 2005). Acidocalcisome was reported to constitute the main calcium storage compartment in different stages of *Plasmodium* (Marchesini et al., 2000). This acidic Ca^{2+} storage organelle is acidified by the combined action of a V-type H^+-ATPase and a H^+-PPase

(reviewed in (Docampo et al., 2001)). This acidification seems to be coupled with a transient cation release. Although acidocalcisome would contain a low free Ca^{2+} concentration (whereas it is possible that it accumulates Ca^{2+} in the millimolar range), this compartment could have a role as a source of releasable Ca^{2+}. This nevertheless remains to be demonstrated.

Both the endoplasmic reticulum and acidic intracellular Ca^{2+} pools within the parasite are reported to be mobilized in response to inositol 1,4,5-trisphosphate (IP_3), and this is inhibited by heparin, an IP_3 receptor antagonist (Passos et al., 1998). It has been reported that the hormone melatonin triggers the IP_3 cascade within the parasite, and this has been implicated as playing a role in the maintenance of synchrony of *Plasmodium* infections *in vivo* (Hotta et al., 2000). However, as mentioned above, the genome analysis of the parasite does not identify an IP_3 receptor Ca^{2+} channel (Nagamune et al., 2006).

Mitochondrion

A study with *P. berghei* has demonstrated the uptake of Ca^{2+} into the parasite mitochondria (Uyemura et al., 2000) and another study has confirmed that the malaria parasite mitochondrion senses cytosolic Ca^{2+} fluctuations (Gazarini et al., 2004).
They have demonstrated that Ca^{2+} increases, as elicited by treatment of parasites with sarco-endoplasmic reticulum Ca^{2+} ATPase inhibitors or the hormone melatonin, induce rapid and reversible increases of the Ca^{2+} concentration in the mitochondria of both human and murine parasites. In addition, pre-treatment of parasites with a mitochondrial uncoupler, suppresses mitochondrial Ca^{2+} accumulation. Thus, mitochondria of malaria parasites are able to reversibly accumulate part of the Ca^{2+} released in the cytoplasm by pharmacological and physiological agents. This suggests that this organelle participates in the maintenance of Ca^{2+} homeostasis of *Plasmodia*.

The food vacuole, another important compartment of *Plasmodium* contains only moderate amounts of Ca^{2+}, disfavoring a role as a major intracellular calcium store (400nM compared to 100nM in the cystosol)(Rohrbach et al., 2005).

I.3.3 Conclusion

Although some calcium-binding proteins are missing compared to plants and animals, Ca^{2+} homeostasis seems to be tightly regulated by *Plasmodium* and Ca^{2+} signaling pathway seems to regulate many functions of the parasite development. It is interesting to note that many calcium binding proteins found in *Plasmodium* are reminiscent of plant-like genotype and this seems ancestral to the acquired secondary endosymbiont (Nagamune et al., 2006).

Factors maintaining calcium homeostasis are therefore valid targets for drug intervention. Besides, as seen in the previous section, two anti-malarial drugs, artemisinin and chloroquine, have already been shown to affect calcium homeostasis (Gazarini et al., 2007).

I.4 SERCAs, proteins of the family of the P-type ATPases

I.4.1 Generalities about the family of the P-type ATPases

Some ATPases have the particularity to form a phosphorylated intermediate during their enzyme cycle. For this reason, they were called P-type ATPases. They are phosphorylated on an aspartate residue belonging to a highly conserved sequence: DKTG. P-type ATPases are located in the plasma membrane of cells or in the membranes of intracellular organelles. Mediated by ATP hydrolysis, these pumps transport cations (Ca^{2+}, Na^{+}, K^{+}, H^{+} , Cu^{2+}, Zn^{2+}, Cd^{2+}) from the cytoplasm to the outside of the cell or to the lumen of an organelle against their gradient of concentration. It was also proposed that some P-type ATPase could transport phospholipids (Paulusma et al., 2005). During their pumping, they adopt two main conformations: E1 that corresponds to a high affinity state for one of the transported elements and E2 that corresponds to a low affinity state for this element. For this reason, these enzymes are also called E1/E2 ATPases.

The family of P-type ATPases gathers many homologous and orthologous proteins that are present in prokaryote and eukaryote cells (Moller et al., 1996).
They are composed of a polypeptide chain of 70 to 150 kDa (Kuhlbrandt, 2004) which manages the ATP hydrolysis and the cation transport. Some of these proteins have a single subunit while others are composed of several subunits. For instance, the Na^{+}/K^{+} ATPase is composed of two subunits α and β. The α-subunit is homologous to single-subunit P-type ATPases and the β-subunit is required for routeing of the α-subunit and for occlusion of K^{+} ions (Lutsenko et al., 1993; Geering, 2001; Kaplan, 2002).

In 1998, Palmgren and Axelsen, aligned the sequences of 159 P-type ATPases and proposed a phylogenetic classification (Fig. I.4-1) (Palmgren et al., 1998). According to this classification, SERCAs belong to the type IIA-ATPases (proteins located in the reticulum) involved in calcium transport.

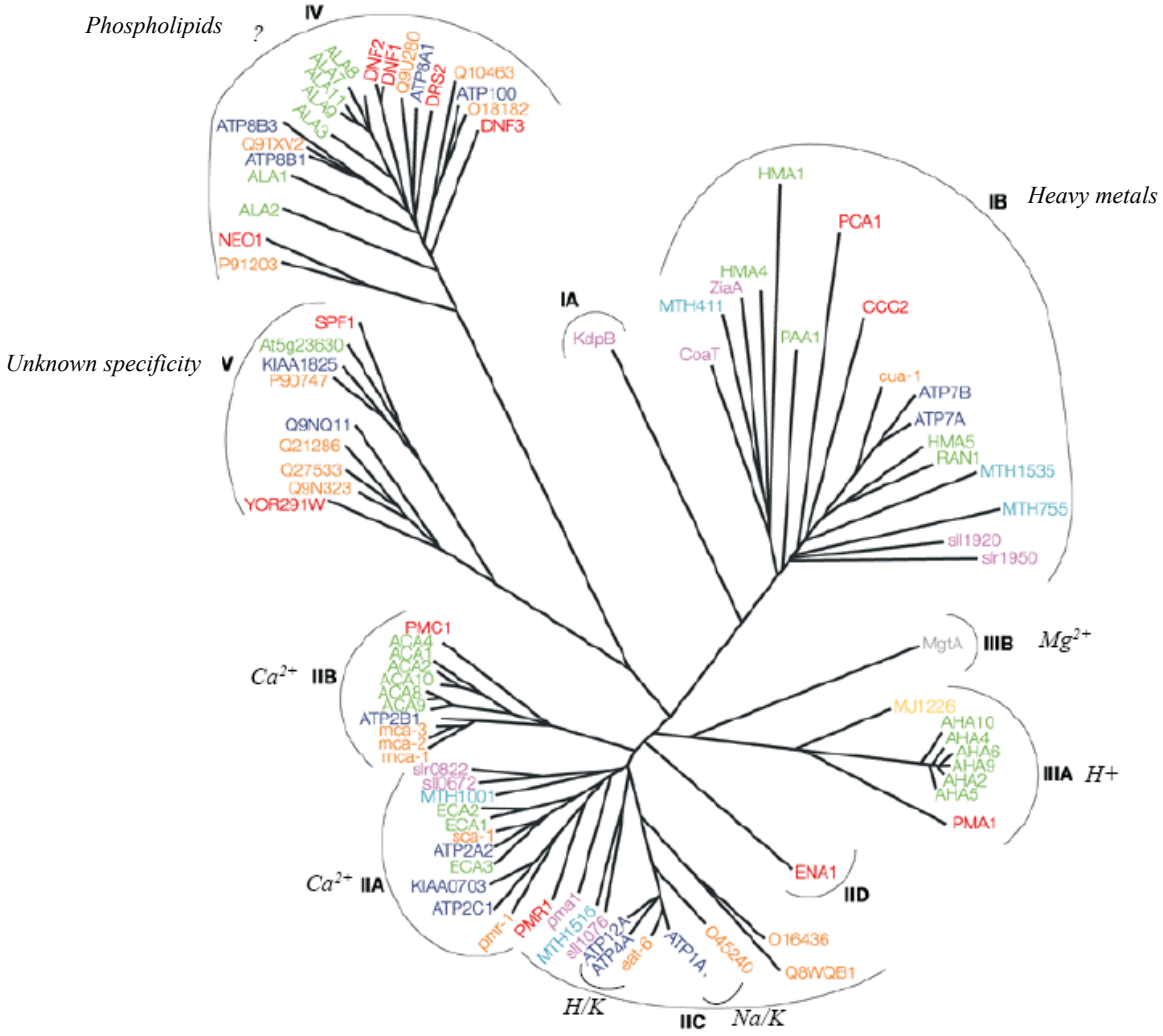

Figure I.4-1: Phylogenetic tree of 159 P-type ATPases (from Palmgren & Axelsen, 1998 et Kuhlbrandt, 2004)

The transport specificity of each group is given in italic. The question mark indicates that the specificity is still controversial. The name of each branch corresponds to the protein name, the gene locus or the accession number of the DNA sequence.
Colours are related to the different species (green, Arabidopsis thaliana; orange, Caenorhabditis elegans; grey : Escherichia coli; dark blue : Homo sapiens; light blue: Methanobacterium thermoautotrophicum; yellow, Methanococcus jannaschii; purple, Synechocystis PCC6803; and red,Saccharomyces cerevisiae
Today, more than 300 P-type ATPases are known (www.patbase.kvl.dk/)

Type I ATPases are involved in the transport of transition metals.
Type II (A and B) ATPases are involved in calcium transport, A corresponding to SERCA and B to plasma membrane ATPases.
Type II C ATPases are close to Type II A according to the gene evolution. The presence of a regulative sub-unit "β" in addition to the main unit "α" characterizes these ATPases (Kaplan, 2002).
Type III ATPases are plasma membrane H^+-ATPases of microorganisms and plants and their sequence are close to the one of type IIB ATPases (Moller et al., 1996).
Type IV and V ATPases are almost unknown but are exclusively present in eukaryotes. It was suggested that type IV ATPases transport lipids such as phosphatidylserine, phosphatidylethanolamine and phosphatidylcholine (Paulusma et al., 2005).

I.4.2 The SERCA family

Early in the sixties, Hasselbach and Makinose highlighted the active transport of $^{45}Ca^{2+}$ inside sarcoplasmic reticulum (SR) vesicules by a membrane ATPase (Hasselbach et al., 1963). This mechanism was thereafter assigned to the sarco/endoplasmic Ca^{2+}-ATPase (SERCA). This pump was shown to transfer of calcium from the cytosol of the muscle cell to the lumen of the SR during muscle relaxation.

Then several isoforms were identified in other cell types, all related to calcium sequestration in reticulum vesicles.

The SERCA family is coded by three different genes: ATP2A1, ATP2A2 and ATP2A3. All are present in mammal cells but in other organism such as *Plasmodium*, only one gene may be present. In mammals, during mRNA maturation, it has been noticed that the transcripts of these three genes are submitted to different splicing that lead to the formation of different proteins from the same gene. This mRNA splicing will differ from the localization of the mRNA and the gene involved (see table I.4-1).

gene	Isoform	Length (amino acids)	Localization of the mRNA
ATP2A1	SERCA1a	994	Fast-twitch skeletal muscle (adult)
	SERCA1b	1001	Fast-twitch skeletal muscle (neonatal)
ATP2A2	SERCA2a	997	Smooth muscle (skeletal and cardiac)
	SERCA2b	1042	Everywhere
	SERCA2c	999	Epithelial, mesenchymatous and hematopoietic cells
ATP2A3	SERCA3a	999	All tested tissues except fast-twitch skeletal muscle
	SERCA3b	1043	Endothelial cells, kidney and pancreas
	SERCA3c	1029	kidney and pancreas
	SERCA3d	1044	All tested tissues and even skeletal and cardiac muscles
	SERCA3e	1052	Lung and pancreas
	SERCA3f	1033	All tested tissues and even skeletal and cardiac muscles

Table I.4-1: The human SERCA family

I.4.3 Presentation of SERCA1a

SERCA1a is the most abundant isoform and represents 70-80% of the membrane protein content of the rabbit SR. Due to the relatively easy extraction of the SR, this protein was extensively studied and today it is both structurally and functionally the best characterized member of the P-type (or E1/E2-type) ion translocating ATPases.

The Ca^{2+}-ATPase of muscle sarcoplasmic reticulum runs as long as ATP and Ca^{2+} are present in the cytoplasm, and establishes a ~10^4-fold concentration gradient across the membrane. To transport calcium, SERCA1a goes through several intermediates and requires Mg^{2+}, H_20, H^+ and of course ATP and Ca^{2+}.

SERCA1a is composed of 994 amino acids and has a molecular weight of ~110kDa.

From functional and structural studies e.g. (le Maire et al., 1976; Juul et al., 1995; Palmgren et al., 1998; Toyoshima et al., 2000; Toyoshima et al., 2002; Wuytack et al., 2002; Moller et al., 2005), the enzymatic properties, the general organization of the molecule, the identification of important residues (nucleotide binding site, calcium binding site…) and the structure of many intermediates (see table I.4-2) have been elucidated, giving a nice but still incomplete functional and structural picture of its enzyme cycle.

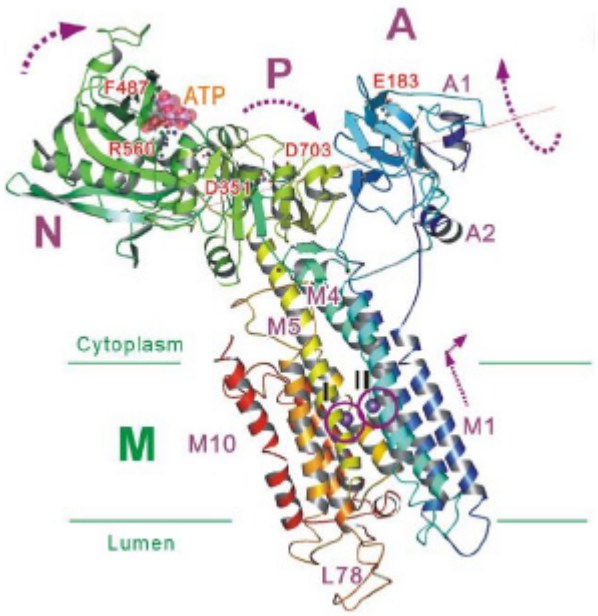

Figure I.4-2: Representation of the cristallographic structure of SERCA1a in the E1·2Ca^{2+}(Toyoshima, 2008)

Colours change gradually from the aminoacids terminus (blue) to the carboxy terminus (red). Purple spheres (numbered and circled) represent bound Ca^{2+}
Three cytoplasmic domains (A, N and P), the α-helices in the A-domain (A1–A3) and those in the transmembrane domain (M1–M10) are indicated. Docked ATP is shown in transparent space fill. Several key residues—E183 (A), F487 and R560 (N, ATP binding), D351 (phosphorylation site), D627 and D703 (P) are shown in ball-and stick.
Axis of rotation (or tilt) of the A-domain is indicated with thin orange line. PDB accession code is 1SU4 (E1·2Ca^{2+})

Its primary structure was identified in 1985 (MacLennan et al., 1985) and its first conformational organization was reviewed in detail by Moller, (Moller et al., 1996) from results of biochemical studies. In 2000, Toyoshima solved its first three dimensional structure by crystallographic studies (Toyoshima et al., 2000). Since, more than 20 crystal structures have been reported from 3 laboratories for this ATPase in 9 different states.

Thus, SERCA1a consists of 3 cytoplasmic domains (A, actuator; N, nucleotide binding; P, phosphorylation), 10 transmembrane (M1– M10) helices and small luminal loops (fig. I.4-2, I.4-3).

The A-domain is connected to the M1–M3 helices with rather long linkers. It works as the actuator of the transmembrane gating mechanism that regulates Ca^{2+} binding and release (fig. I.4-2). Crystal structures show that the linkers are flexible (Takahashi et al., 2007) yet the mutagenesis studies demonstrate that the length of the A-domain–M1 linker, at least, is critically important in gating of the ion pathway. The A-domain contains one of the signature sequences ^{181}TGES motif (fig. I.4-3) (Moller et al., 1996), which plays an important role in processing of aspartylphosphate (Clausen et al., 2004).

The P-domain contains the phosphorylation residue Asp351 and Mg^{2+} co-ordinating residue Asp703 (fig. I.4-3). The P-domain is relatively compacted and has a flat top surface to allow a large rotation of the A-domain on it (fig. I.4-2 and I.4-4) (Toyoshima et al., 2007).

The N-domain, a long insertion between two parts of the P-domain, contains the residues (e.g. Phe487) for adenosine binding and those (e.g. Arg560) critical for bridging ATP and the P-domain (fig. I.4-3) (Sorensen et al., 2004; Toyoshima et al., 2004).

These three domains are well separated in the $E1{\cdot}2Ca^{2+}$ crystal structure but gather to form a compact headpiece in the other states (fig. I.4-2)

The transmembrane domain is composed of 10 α-helices and some of them (M2–M5) have long cytoplasmic extensions (fig. I.4-2). In particular, M5 is 60 Å long and extends from the luminal surface of the membrane to the end of the P-domain, working as the spine of the molecule. M4–M6 and M8 contain the residues directly co-ordinating two Ca^{2+} (fig. I.4-3).

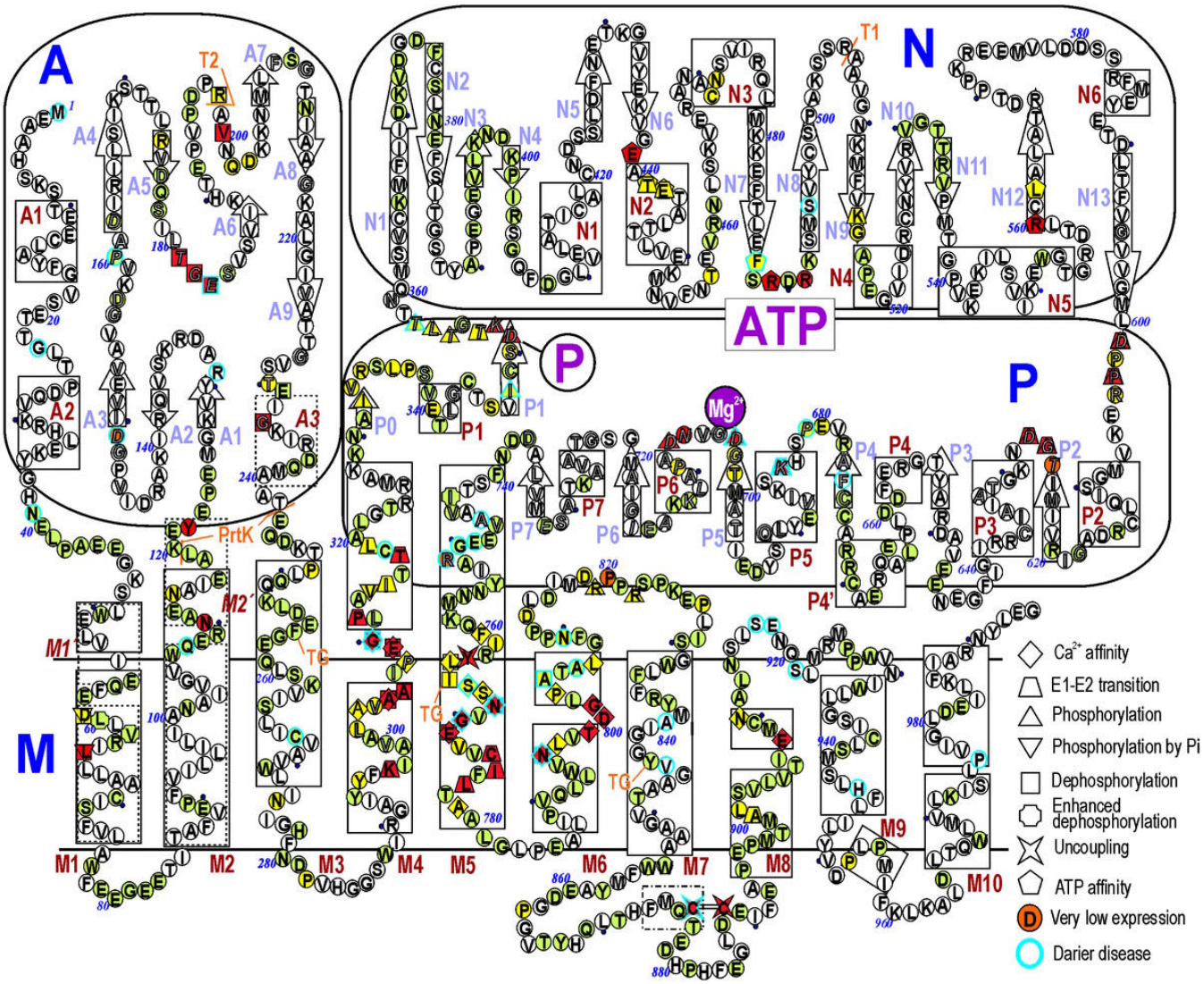

Figure I.4-3 : Two-dimensional diagram of the structure, the amino acid sequence, and the results of mutation experiments of SERCA1a. (from (Toyoshima et al., 2004))

Secondary structure elements corresponding to the Ca^{2+}-bound form are indicated such as boxes indicate helices and arrows, β-strands. The elements that change in E2(TG) (i.e., M1', M2', and A3) are shown in dotted lines and are identified by italic letters. T1 and T2 are trypsin digestion sites and PrtK, major proteinase K digestion sites. Conserved residues of the P-type ATPases are shown in different fonts (from green to red, red corresponding to highly conserved residues). Those conserved in 135 out of 159 sequences are shown in open italic letters; those conserved in only 90 sequences are in normal open letters.

Calcium binding site. It is well established that SERCA1 has two high affinity transmembrane Ca^{2+}-binding sites. Site I, the binding site for the first Ca^{2+}, is located in a space surrounded by M5, M6 and M8 helices (fig. I.4-3 and I.4-4). Site II is nearly 'on' the M4 helix, with residue Glu309 which will be mainly involved. Both sites have 7 co-ordinations (fig. I.4-4).

The Ca^{2+}-binding sites and phosphorylation site communicate with each other because they are mechanically connected through M5 because its cytoplasmic end is integrated into the P-domain near the phosphorylation site and is hydrogen bonded to the M4 helix forming a short β-strand (Toyoshima et al., 2002).

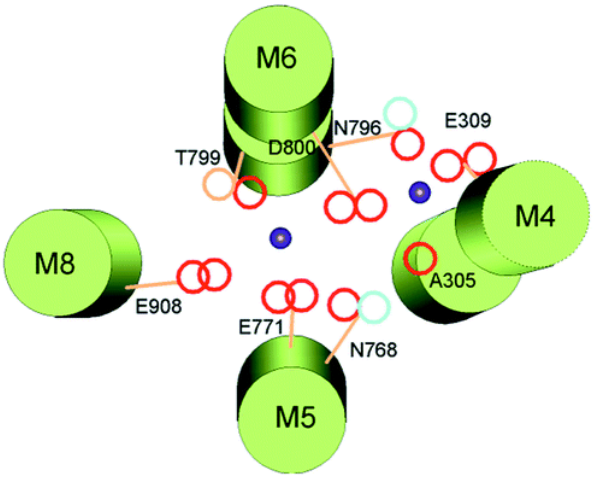

Figure I.4-4: Diagram for the arrangement of transmembrane helices M4, M5, M6, and M8, and of the amino acids participating in Ca^{2+} binding (from(Zhang et al., 2000)).

The arrangement is based on high-resolution X-ray crystallography of the enzyme with bound Ca^{2+} (Toyoshima et al., 2000). The transmembrane helices are viewed from the cytoplasmic side roughly normal to the membrane. Note that M4 and M6 helices are unwound around E309 and D800 and two Ca^{2+} (blue spheres) are virtually at the same level. Oxygen atoms are shown as red circles, and nitrogen atoms as blue circles. Alkyl group of T799 is represented by an orange circle.

I.4.3.1 Description of the enzyme cycle

The enzyme cycle of SERCA1a is a succession of many intermediates. Nine different states of SERCA1a have already been characterized structurally (see table I.4-2). From these states, the entire reaction can be described essentially with 4 principal structures depicted in Fig. I.4-5. This was recently reviewed by Toyohima (Toyoshima, 2008). Note that although exact analogs of E1P have not yet been determined, its domain

organization seems to be very similar to the crystal structures of E1·AMPPCP (analog of E1·ATP) and E1·AlF_4^-·ADP (analog of E1~P·ADP) (Sorensen et al., 2004).

A.

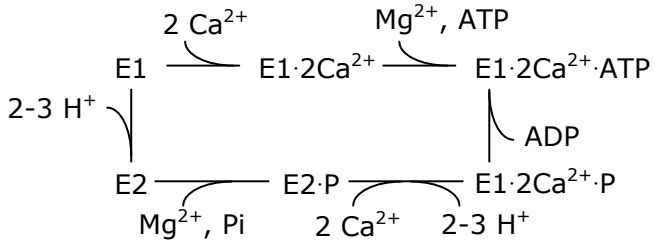

B.

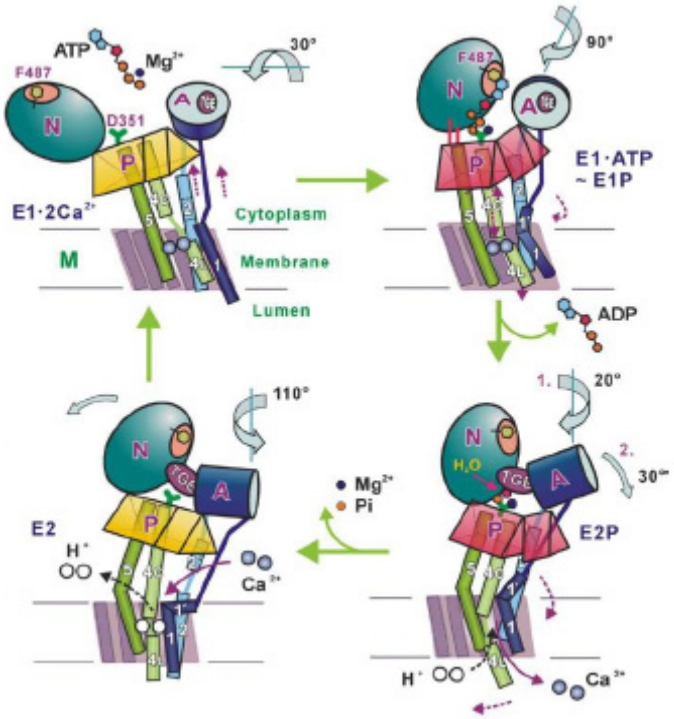

Figure I.4-5 : Enzyme cycle of SERCA1a

A. Schematical view of the enzyme cycle of SERCA1a
B. Cartoon illustrating the structural changes of the Ca^{2+}-ATPase during the reaction cycle.
According to the classical E1/E2 theory, in E1, transmembrane Ca^{2+}-binding sites have high affinity and face the cytoplasm, and in E2, they have low affinity and face the lumen of SR (or extracellular side).
The transfer of bound Ca^{2+} takes place between two phosphorylated intermediates, E1P and E2P, in exchange of H^+ from the luminal side. This was highlighted with low passive permeability protoliposomes to H^+, because SR vesicles are permeable to H^+ (Cornelius et al., 1991).

PDB entry	Description	State	References
1SU4	Crystal structure of calcium ATPase with two bound calcium ions	E1 Ca2	Toyoshima et al., 2000
1VFP	Crystal structure of the SR Ca^{2+}-ATPase with bound AMPPCP	~E1 Ca2 ATP	Toyoshima et al., 2004
1T5S	Structure of the (SR) Ca^{2+}-ATPase Ca_2-E1-AMPPCP form	~E1 Ca2 ATP	Sorensen et al., 2004
1T5T	Structure of the (SR) Ca^{2+}-ATPase Ca_2-E1-ADP:AlF_4^- form	~E1 Ca2 ADP+P	Sorensen et al., 2004
2ZBD	Crystal Structure of the SR Calcium Pump with Bound Aluminium Fluoride, ADP and Calcium	~E1 Ca2 ADP+P	Toyoshima et al., 2004
3BA6	Structure of the Ca_2E1P phosphoenzyme intermediate of the SERCA Ca^{2+}-ATPase	E1 Ca2 P	Olesen et al., 2007
2C88	Crystal structure of (SR) Calcium-ATPase E2(TG):AMPPCP FORM	E2 Tg : AMPPCP	Jensen et al., 2006
1WPG	Crystal structure of the SR Ca^{2+}-ATPase with MGF4	E2 Pi	Toyoshima et al., 2004
1XP5	Structure Of The (SR) Ca^{2+}-ATPase E2-AlF_4^- Form	E2 Ca2 P	Olesen et al., 2004
3B9R	SERCA Ca^{2+}-ATPase E2 aluminium fluoride complex without thapsigargin	E2	Olesen et al., 2007
3B9B	Structure of the E2 beryllium fluoride complex of the SERCA Ca^{2+}-ATPase	E2	Olesen et al., 2007
2ZBE	Calcium pump crystal structure with bound BeF_3 in the absence of calcium and TG	E2P	Toyoshima et al., 2007
1IWO	Crystal structure of the SR Ca^{2+}-ATPase in the absence of Ca2+	E2 Tg	Toyoshima et al., 2002
2AGV	Crystal structure of the SR Ca^{2+}-ATPase with BHQ and TG	E2 Tg BHQ	Obara, K. et al., 2005
2EAS	Crystal structure of the SR Ca^{2+}-ATPase with bound CPA	E2 CPA	Takahashi et al., 2007
2EAT	Crystal structure of the SR Ca^{2+}-ATPase with bound CPA and TG	E2 CPA Tg	Takahashi et al., 2007
2EAU	Crystal structure of the SR Ca^{2+}-ATPase with bound CPA in the presence of curcumin	E2 CPA curcumin	Takahashi et al., 2007
2O9J	Crystal structure of calcium ATPase with bound magnesium fluoride and cyclopiazonic acid	E2 CPA « Pi »	Moncoq et al., 2007
2OA0	Crystal structure of Calcium ATPase with bound ADP and cyclopiazonic acid	E2 CPA ADP	Moncoq et al., 2007
2ZBF	Calcium pump crystal structure with bound BeF_3 and TG in the absence of calcium	E2P +Tg	Toyoshima et al., 2007
2ZBG	Calcium pump crystal structure with bound AlF_4 and TG in the absence of calcium	E2 Tg « Pi »	Toyoshima et al., 2007

Table I.4-2: Crystal structure of SERCA1a in different states

AMPPCP is a non hydrolysable analog of ATP
$E2AlF_4$ and $E2MgF_4$ mimic the transition state in which the enzyme is during its dephosphorylation still in presence of « Pi » because AlF_4^- and MgF_4^- are analogs of Pi

E2→E1→E1·2Ca^{2+}: binding of Ca^{2+}

The E2 state, that is the state subsequent to the release of Ca^{2+} into the lumen and the hydrolysis of aspartylphosphate, is considered to be the ground state of the enzyme.

In E2 state, thermal agitation opens the cytosolic part of the protein and releases bound protons into the cytoplasm (Tadini-Buoninsegni et al., 2006). The released protons are dissipated away through the SR membrane and, at pH 7, placing most of the ATPase molecules into the E1 state (Inesi et al., 2008). In this state, the carboxyl groups in the Ca^{2+} binding cavity are not protonated and, therefore, have high affinity to Ca^{2+}. In addition, a reorganization of the protein occurs (mainly on M4, M5 and P) so that the two binding sites become properly formed. Two Ca^{2+} subsequently enter the high affinity sites. Glu309, on M4, may be one of the gating residues but the entrance pathway and the necessary calcium ion dehydration is not well understood. Ca^{2+} binding induces an opening of the headpiece by bringing the P-domain apart from the A-domain. In this configuration, ATP will be able to be delivered to the phosphorylation site.

The way the two Ca^{2+} bind to the ATPase remains also to be clarified. It was first proposed that the Ca^{2+} binding is sequential: the binding of the first Ca^{2+} would induce a conformation change of the enzyme allowing the second Ca^{2+} to bind with a higher affinity (Inesi et al., 1980). This hypothesis was emphasized by calcium dissociation experiments; however, the observed cooperativeness can be interpreted differently: it could be explained by the fact that both sites are independent and equivalent but present on only one of the two forms, E1 or E2 (Tanford et al., 1985). If, on the one hand, E1 and E2 are in equilibrium and on the other hand, only E1 is able to bind Ca^{2+}, the binding of Ca^{2+} on E1 will allow the increase of the ratio E1/E2 and thereby increase the apparent affinity of the second Ca^{2+} to bind the enzyme. Besides, it has been shown that the dissociation of only one Ca^{2+} is sufficient for the Ca^{2+}-ATPase to loose its reactivity toward the ATP.

E1·2Ca^{2+}→E1P transition: formation of the occluded state

The phosphorylation induces an occlusion of the two binding sites of calcium (Dupont, 1980). In presence of MgATP, occluding state is brief but this occluding state can be stabilized with AlF_4^--ADP (Troullier et al., 1992).

ATP binds near the hinge between the P-and N-domains and crosslinks them, so that the γ-phosphate of ATP and a Mg^{2+} bind to the P-domain to bend it in two directions. M1 moves until its top occupies the space aroung Glu309 and thereby fixes the conformation of the Glu 309 side chain. Thus, this putative cytoplasmic gate of the calcium binding sites is now closed and two Ca^{2+} are occluded in the transmemebrane binding sites. Phosphoryl transfer from the γ-phosphate to Asp351 fixes the N-domain

in a highly inclined position so that a mechanical couple is formed between the N- and A-domains in preparation for the next main event, a 90° rotation of the A-domain in the E1P–E2P transition.
The E1P state is a high energy intermediate and is qualified of "ADP sensitive" because it can make an ATP from one ADP.

E1P→E2P transition: release of Ca^{2+} into the lumen of SR
Phosphoryl transfer to Asp351 triggers the opening of the N- and P domain interface. The A domains rotates and causes the inclination of the P domain and thereby the rearrangement of transmembrane helices loosening the calcium binding sites. Luminal gates open (Olesen et al., 2007) and bound calcium are released.
This intermediate is "ADP insensitive" but can react with water to hydrolyze the acylphosphate bond E2P->E2 (formation ofE2P is possible in presence of Pi, Mg^{2+} but no calcium).

E2P→E2 transition: hydrolysis of aspartylphosphate and closing of the luminal gate
E2P is "ADP insensitive" but can react with water. Thus, when a water molecule is introduced in the phosphorylation site (on Glu183) it causes the hydrolysis of the acylphosphate bound. This induces a rotation of the A domain and the release of the Pi and Mg^{2+}. The P domain is relaxes and a rearrangement of M1, M2 occurs so that the luminal gate is closed, placing the ATPase in E2.

I.4.3.2 Some functional properties of the Ca^{2+}-ATPase

To study SERCA1a under the best conditions, it was necessary to investigate its behavior, related either by its ATPase activity or its Ca^{2+} transport rate, in different conditions of pH, calcium concentration, detergents and in presence of inhibitors.
Thus, it was shown that the Ca^{2+}-ATPase had a pronounced requirement for Mg^{2+} and potassium chloride, and the optimal levels were respectively 5mM and 100mM (MacLennan, 1970). At high ATP concentration (5mM), it exhibited an optimal ATPase activity at pH 7.5 (fig. I.4-6 panel A) and in presence of 1-10µM of Ca^{2+} (fig. I.4-6 panel B). In the case of vesicular calcium, higher Ca^{2+} concentrations produce inhibition of activity whereas, in presence of solubilizing concentration of detergent ($C_{12}E_8$), the Ca^{2+}-ATPase is somewhat stimulated in presence of 1-100µM of Ca^{2+}. In addition, it is less inhibited by higher concentration of Ca^{2+} compared to the vesicular ATPase (Moller et al., 1980).

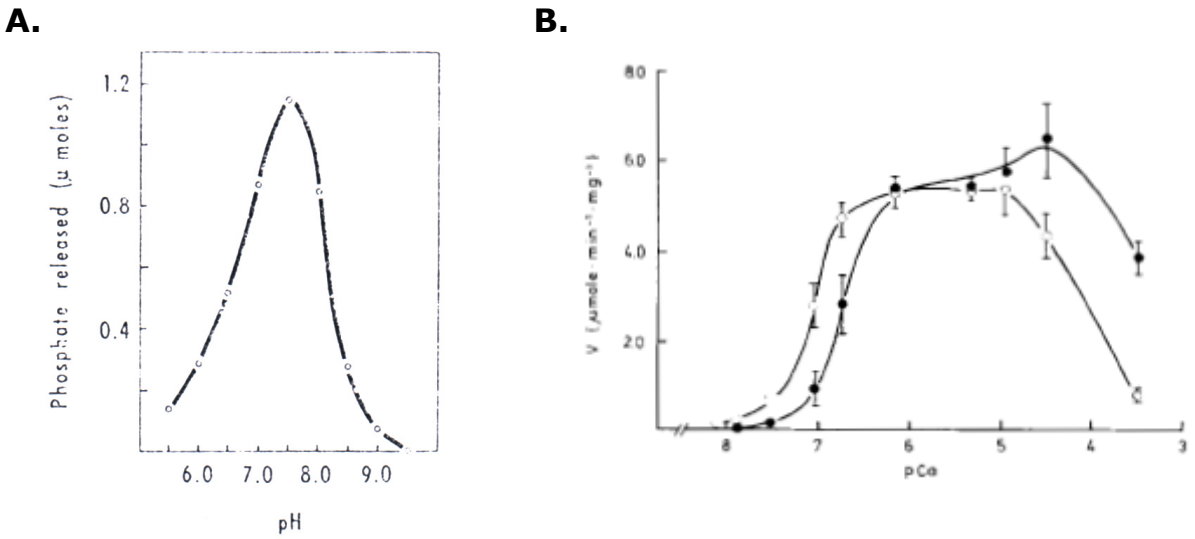

Figure I.4-6: Effect of pH and pCa on ATPase activity of SERCA1a

A. Effect of pH on ATPase activity of SERCA1a (10µg) in 50mM Tris-Cl (adjusted to the points indicated), 100mM KCl, 5mM $MgCl_2$, 50µM $CaCl_2$ and 10 mM ATP at 37°C. (MacLennan, 1970)
B. Effect of pCa on ATPase activity of vesicular (o) and $C_{12}E_8$-solubilized monomer (•) of ATPase. Enzyme activity was measured at 20°C and pH 7.5 in presence of 5 mM ATP, 1 mM free Mg^{2+}, various concentrations of free Ca^{2+}, and 0.5 mg/mL for the $C_{12}E_8$ detergent-solubilized ATPase (Moller et al., 1980).

As shown with the Ca^{2+} dependence of SERCA1a, detergent influences the ATPase activity of the enzyme. Detergents are nevertheless important elements to consider when studying a membrane protein because they allow its solubilization and thereby its purification. Thus, the properties of detergents required to substitute the lipid environment of sarcoplasmic reticulum Ca^{2+}- ATPase with retention of good functional properties were determined by the use of a large number of diverse detergents and delipidated enzyme. Detergents having an intermediate chain length (~C_{12}) and a polyoxyethylene glycol (e.g. $C_{12}E_8$) or carbohydrate polar group (DDM) were optimal for Ca^{2+}-ATPase function and stabilization, while detergents with short alkyl chain (C_8) or bulky head groups and many zwitterionic detergents led to rapid inactivation (table I.4-3). Long chain detergents cause protein aggregation and, despite their resemblance to natural lipids, are inferior in their activity-retaining properties (Lund et al., 1989). Besides, with heterologously expressed SERCA1a in yeast, Lenoir et al. observed that DDM was more efficient than $C_{12}E_8$ to solubilize yeast light membranes and to stabilize the Ca^{2+}-ATPase during the purification step (Lenoir et al., 2002).
In addition, under optimal conditions, stability of solubilized Ca^{2+}-ATPase was shown to depend on the presence of residual lipid in the preparation (Lund et al., 1989). Indeed,

during the development of their purification procedure, Miras et al. observed that the addition of phospholipids could improve the ATPase activity of SERCA expressed in Sf9 cells, measured in $C_{12}E_8$ (fig. I.4-7) and also that this effect depended on the type of added phospholipids (Miras et al., 2001).

Detergent	CMC (mM)	$k_{T0\ (min^{-1})}$	V_0 (µmol/mg/min)
$C_{12}E_8$	0.1	0.08	5.6
Triton X-100	0.2-0.9	0.11	2
octylglucoside	19-25	1.1	0.27
dodecylmaltoside	0.18	0.07	1.6
cholate	10		<0.1
Tween20	0.06	0.015	5.8

Table I.4-3: Inactivation of lipid-depleted Ca^{2+}-ATPase at pH 7.5 and 20°C by different detergent during enzyme turnover (TO)

CMC values were taken from (le Maire et al., 2000)
k_{TO} is the inactivation rate constant and V_0 the initial velocity after addition of 5mM MgATP to the solubilized Ca^{2+}-ATPase. Some detergents (cholate, Tween 20…) are inefficient solubilizers but in these experiments, the enzyme was initially solubilized and delipidated in C12E8, then a large excess of the detergents listed in the table was added before the measurements (Lund et al., 1989).

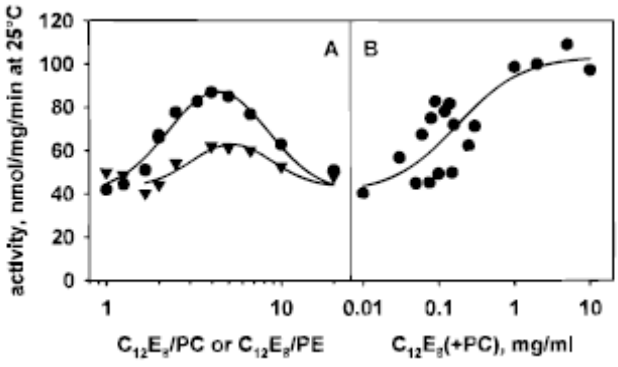

Figure I.4-7: Effect of $C_{12}E_8$ and phospholipids on the calcium dependent ATPase activity of SERCA1a-expressing membrane (Miras et al., 2001)

A. Varying phopholipid concentration in the presence of 1mg/mL $C_{12}E_8$.
• Phosphatidylcholine; ▾Phosphatidylethanolamine
B. Increasing $C_{12}E_8$ concentration while maintaining the $C_{12}E_8$ to phosphatidylcholine ratio equal to 3.5 (w/w)

The functional properties of the different SERCA isoforms are not equivalent. For instance, the optimal pH of activation of SERCA3a is more basic than the other and SERCA2b has a slower turnover (Lytton et al., 1992). Moreover, SERCA3 isoforms do not have a phospholamban recognition sites, like PfATP6, the single SERCA of *Plasmodium falciparum* (Kimura et al., 1993). Phospholamban is a 52 amino acid membrane protein that regulates the Ca^{2+} pump. This protein inhibits SERCA but when phosphorylated, this inhibition ability is lost.

I.4.3.3 Effect of different drugs on the Ca^{2+}-ATPase

	Tg	CPA		BHQ
formula	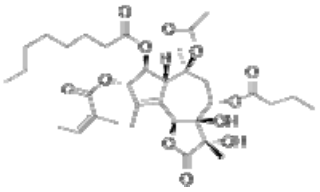	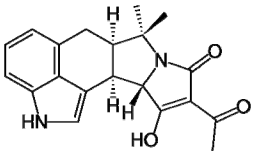		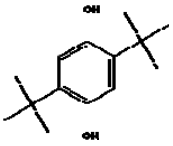
residues of SERCA1a interacting with the inhibitor	F256 (M3) I765 (M5) Y843 (M7) (Toyoshima et al., 2000)	L93 (M2) **N101** (M2) **G257** (M3) E309 (M4) **P312** (M4) (Takahashi et al., 2007)	G56, L61, V62 (M1) **N101**, A102 (M2) L311, P312 (M4) **G 257** (M3) (Moncoq et al., 2007)	D59 (M1) P308 (M4) (Obara et al., 2005)
Inhibition properties	Ki=0.1nM (Sagara et al., 1991)	6nmol/mg of SR (in presence of 0.5µM ATP) 50 nmol/mg of SR (in presence of 5mM ATP) (Seidler et al., 1989)		Ki=0.4µM (Wictome et al., 1992)

Table I.4-4: Inhibition of SERCA1a by Tg, CPA and BHQ

The Ca^{2+}-ATPase can be bloked in its E2 state and forms a dead-end complex in presence of sesquiterpene lactones such as thapsigargin (Tg) extracted from *Thapsia garganica* (Rasmussen et al., 1978); cyclopiazonic acid (CPA), a mycotoxin of *Aspergillus* and *Penicillium ;* and an hydroxy containing compound, 2,5-di-tert-butyl-1,4-benzohydroquinone (BHQ).

Tg binds with a 1:1 stoechiometry to the Ca^{2+}-ATPase. This property turned out to be very useful for stabilization of ATPase crystals obtained in the absence of Ca^{2+} (see table I.4-4), thereby permitting diffraction studies.

Tg binds mainly F256 and prevents a displacement concomitant with the E2 to E1-2Ca^{2+} transition (Toyoshima et al., 2002). CPA inhibits the calcium pump maybe by blocking the calcium access channel and immobilizing a subset of transmembrane helices (Moncoq et al., 2007). BHQ binds to a neighboring but distinct site relative to Tg and CPA in the ATPase molecule. The inhibitory mechanism is similar to that of Tg but with a weaker stabilization.

All these studies were lead with native SERCA1a extracted from rabbit SR but also from heterologously expressed native and mutated SERCA1a.

I.4.4 Heterologous expression and purification of SERCA1a and its mutants

The heterologous expression of SERCA1a was attempted in all the expression system available. However, some of them did not lead to a successful expression (e.g. *E. coli*, Fuentes et al., unpublished results).

The first reported system that led to the expression of SERCA1a was the use of mammalian cells (COS-1) (Maruyama et al., 1988). This system allows phosphorylation experiments and Ca^{2+}-transport measurements. Thus, it was successfully used to study the first mutants of SERCA1a (Clarke et al., 1989). This system is very convenient for the expression of mammalian proteins such as SERCA1a but has the drawbacks to lead to low expression yields (table I.4-5) and require complex and expensive culture media. Moreover, these cells have long doubling time (48h) and their culture is delicate.

Then, the expression of SERCA1a was attempted in the insect cells (Sf9) transfected with a recombinant baculovirus (Skerjanc et al., 1993). This system gave higher expression of Ca^{2+}-ATPase but the Ca^{2+}-ATPases represented a lower proportion of the total membrane protein (see table I.4-5). However, the authors were able to solubilize and purify the wild-type Ca^{2+}-ATPase and one of its mutant (E309Q) in presence of $C_{12}E_8$ and phospholipids thanks to the use of an antibody (see table I.4-5). This expression method was also used by Miras et *al.* who changed the composition of the culture medium and manage to obtain a higher proportion of Ca^{2+}-ATPase (see table I.4-5) but only 30% of the expressed protein was active (Miras et al., 2001). They were also able to solubilize

and purify the Ca^{2+}-ATPase with Red120 based on the ability of this component to mimic the triple negative charge of ATP and therefore to interact with the ATP binding site of SERCA1a. The expression in insect cells leads to a rather high amount of expressed Ca^{2+}-ATPase but shares the same disadvantages as the mammalian cells.

In parallel, a cheaper system that also has the advantages to grow faster (doubling time ~2h) and at high cell density was used: the yeast *Saccharomyces cerevisiae.* This eukaryotic organism, contrary to bacteria, has the machinery to carry out post translational modifications of proteins (such as phosphorylation, addition of fatty acids and glycosylation). However, for the expression of mammalian membrane proteins, it may be interesting to note that the membrane composition of yeast is different from mammalian cells since it contains ergosterol instead of cholesterol. The combination of this organism and the use of an inducible vector (that allows the separation of the growth phase and the expression phase to avoid a potential toxicity of the expressed proteins against the host) resulted in a successful expression of SERCA1a (table I.4-5) (Centeno et al., 1994). Thereafter, the yeast strain was genetically modified to improve the expression level of the heterologous protein. The resultant yeast had thereby the ability to synthesize a higher amount of transcription activators during the expression phase. Moreover, the use of another inducible vector made possible the culture of yeast in rich medium and therefore at higher cell densities. Thus, the cell density was ten times higher and higher amounts of SERCA1a were obtained (25mg/L of culture in the crude extract). The highest active fraction corresponded to the light membranes. For this reason, only this fraction was kept for subsequent purification (1/5 of the total expressed SERCA1a) (table I.4-5). As this protein was fused to a His-tag, this purification was possible by immobilized metal affinity chromatography with Ni-NTA resin and 1mg of purified proteins was recovered from one liter of culture with a purity of about 50% (table I.4-5). This purity was slightly increased to 70% by the use of a second step of purification with reactive Red120 chromatography but the amount of lost proteins was high (more than 70%) (Lenoir et al., 2002). The same expression strategy was then applied but the protein was fused to a cleavable tag after the C-terminus of SERCA1a, a thrombin cleavage site linked to a biotin acceptor domain (BAD). These modifications were performed to improve the yield of purification by increasing the interaction between the resin and the protein of interest. This fused protein was expressed in the same proportions as the His-tagged Ca^{2+}-ATPase (table I.4-5) and a protein with higher specific activity was obtained after affinity chromatography based on avidin-biotin interaction and elution by thrombin cleavage (Jidenko et al., 2006). Coupled to a second step of purification (size exclusion chromatography), especially to remove the main contaminant (the thrombin used to release the protein from the resin), this procedure allowed the recovery of a protein that could be successfully crystallized (Jidenko et al.,

2005). This last method was then successfully used for the crystallization of SERCA1a mutants (Marchand et al., 2008).

Other expression systems are available such as *Xenopus laevis* oocytes or *in vitro* expression systems. This latter has not been yet attempted for SERCA1a. However, *Xenopus laevis* oocytes were used to express the SERCA of *Plasmodium falciparum*, PfATP6 (Eckstein-Ludwig et al., 2003) and a mutant of SERCA1a (E255L). This system presents the advantage that *X. laevis* oocytes are cells which are easy to handle (~1mm) but each cell has to be injected by hand. This is very delicate and not appropriate for high-scale expression. This system was nevertheless convenient for measuring a transport across the plasma membrane when the expressed proteins were located in the plasma membrane e.g. (Geering et al., 1989).

With the exemple of SERCA1 proteins, we have seen that heterologous membrane protein expression and purification are difficult steps to develop. In a next section, we will see that when these proteins are derived from *Plasmodium* parasites, it is even more difficult.

ATPase	Expression		Solubilization	Purification			References
	host	yield		system	yield	purity	
SERCA1a	COS-1	5% of MP 5µg/10 plates					Maruyama and MacLennan 1988
	Sf9	1-2% of MP 3mg/L		Antibodies (+PL)	375 µg/L	<30%	Skerjanc et al., 1993
		6% of MP but only 1/3 was active 6mg/L	$C_{12}E_8$ (+PL)	Red 120 (+PL)	2 mg/L	26%	Miras et al., 2001
	S.cerevisiae	0.3% of PM 1mg/L	$C_{12}E_8$ (+PL)	Antibodies (+PL)	?	?	Centeno et al., 1994
SERCA1a-6His N^{al}		3-6% of PM 0.5mg/L	$C_{12}E_8$				(Reis et al., 1999)
SERCA1a-6His C^{al}		2% of PM[a] 5.5mg/L	DDM	Ni-NTA (+PL)	1mg/L	50-60%	Lenoir et al., 2002
SERCA1a-BAD		1-3% of PM[a] 5mg/L	DDM	avidin-agarose	0.3-0.5 mg/L	60%	Jidenko et al., 2006

Table I.4-5: Summary of some expression and purification assays of SERCA1a
MP: membrane proteins; PL: phospholipids
6His N^{al} (or C^{al}): addition of a 6 His N-terminal (or C-terminal) tag to the protein
BAD: addition of a biotinylated acceptor domain to the C-terminus of the protein
[a] light membranes only
Values are given in mg of SERCA1a per liter of culture

I.4.5 PfATP6, the single SERCA of *Plasmodium falciparum*

As seen in the previous sections (I.2 and I.3), *Plasmodium falciparum* has a single SERCA, PfATP6. The gene coding for PfATP6 was cloned for the first time by Kimura et al. in 1993. It is a 139 kDa protein composed of 1228 amino acids. PfATP6 has a 40% overall homology with rabbit SERCA1a (see alignment in Appendix 1). This protein conserves sequences and residues that are important for the function and/or structure of a sarco/endoplasmic reticulum Ca^{2+}-ATPase, such as high affinity Ca^{2+}-binding sites, nucleotide binding site, phosphorylation site, thapsigargin binding sites. It is also predicted that it contains 10 transmembrane helices as its orthologous protein SERCA1a. However, PfATP6 contains about 200 additional amino acids in its cytosolic region and lacks the sequence that binds to phospholamban, a protein that regulates the activity of the rabbit SERCA. This protein was found to be highly polymorphic (Dahlstrom et al., 2008).

In the previous sections, we saw that this protein was expressed in *Xenopus laevis* oocytes to study its potential interaction with the anti-malarial drug, artemisinin (Eckstein-Ludwig et al., 2003). In this work, the authors also included some data about the functional characterization of this expressed PfATP6. Thus, they described how this Ca^{2+}-ATPase behaves at different concentrations of Ca^{2+} and they showed (fig. I.4-8) that, in their conditions of measurement, it exhibited an optimal activity at 48µM free calcium. A similar Ca^{2+}-dependency to SERCA1a could also be observed.

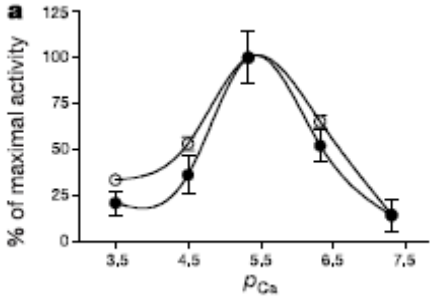

Figure I.4-8: Ca^{2+}-dependency of PfATP6 activity (filled circles) compared with SERCA1a (SR) activity (open circles) is shown in a percentage of maximal ATPase activity at the indicated $[Ca^{2+}]_{free}$ values (from(Eckstein-Ludwig et al., 2003))

At this optimal Ca^{2+} concentration, the ATPase activity of PfATP6 was shown to be inhibited in presence of a P-type ATPase inhibitor, vanadate; in presence of two SERCA-type inhibitors (thapsigargin and cyclopiazonic acid) but not in presence of ouabaïn (a specific Na^+/K^+ ATPase inhibitor)(fig. I.4-9).

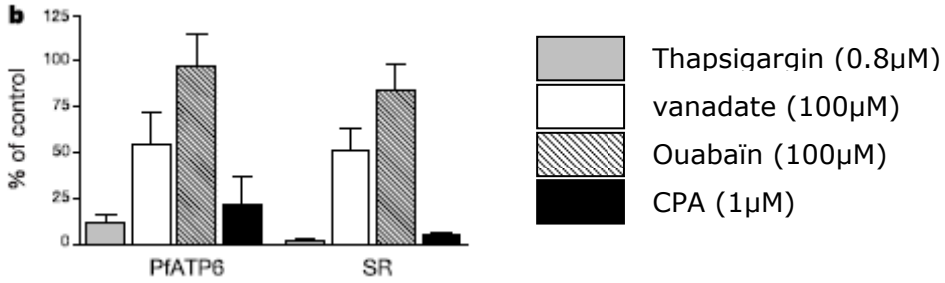

Figure I.4-9: Inhibition potency of PfATP6 activity compared with SERCA1a from ((Eckstein-Ludwig et al., 2003).

All these date are in favor of a common behavior of this parasite protein with the mammalian sarco/endoplasmic reticulum Ca^{2+}-ATPase although it probably needs a higher concentration of SERCA-type inhibitor to be fully inhibited (compare PfATP6 and SR in fig. I.4-9). These results were obtained in a system (*X. laevis* oocyte membranes) where many constituents may interfere with ATPase assays. It would therefore be interesting to perform this characterization with a pure protein.

I.5 Heterologous Expression of plasmodial proteins

The full sequence of the genome of *Plasmodium falciparum* 3D7 was published in 2002 (Gardner et al., 2002). It revealed that the sequence of the genome of *P. falciparum* contained 80% of A+T which is rather high compared for instance to the yeast genome which contains only 60% of A+T. *Plasmodium* is called an AT-rich organism. This difference in nucleotide content can generate a difference between the codon usage of these organisms. Thus, if a plasmodial protein has to be heterologously expressed in yeast, it is unlikely to be expressed or it will be poorly expressed. Indeed, when expressing proteins in a host with a different codon usage than the native organism, a number of problems have been encounted: i) lack of expression, ii) expression of protein that is non-functional or insoluble, iii) expression of a protein that is truncated owing to proteolysis or premature termination of translation (Kurland et al., 1996).

One solution consists in a synonymous codon replacement of the plasmodial gene toward optimal codon for the expression in yeast. This solution is often used in the case of plasmodial proteins and has allowed to carry out high throughput expression experiments (especially with *E. coli* as host cell). Many different expression systems were used to express plasmodial proteins and some of them did not require a codon optimized gene. It was true for *Xenopus laevis* oocytes and in most cases for *E. coli*.

Recently, two high throughput expression studies were performed (Mehlin et al., 2006; Vedadi et al., 2007) and the more recent one which started with 1000 proteins even led to the crystal structure of 36 plasmodial proteins from the 97 which crystallized by combining the use of native genes and optimized genes (Vedadi et al., 2007). However, these studies are more adapted to soluble proteins than to membrane proteins. Up to now, only few membrane proteins of *Plasmodium* parasites were expressed and purified (see table I.5-1) and only one has a resolved crystallographic structure (*P. falciparum* aquaporin) (Hedfalk et al., 2008; Newby et al., 2008). The expression and purification of plasmodial membrane proteins are therefore challenging.

Among the successful expressions, only two led to the purification of the proteins. Both studies were based on the use of the yeast *Pichia pastoris* as host and a codon optimized version of the genes to express (Table I.5-1). After these expressions, one protein was successfully reconstituted in proteoliposomes (Tan et al., 2006) and the other was crystallized (Hedfalk et al., 2008). This method seems therefore to be efficient.

It is nevertheless necessary to be cautious when using synonymous codon replacement because such operation can change the protein structure and function. Indeed, indication of the fact that protein structure depends on DNA sequence were recently highlighted

(Komar et al., 1999; Kimchi-Sarfaty et al., 2007). In the translation of the domain boundaries, ribosomal progression slows as the ribosome encounters clusters of infrequently used codons that preferentially encode a subset of amino acids. If this pause in the translation is not respected, it can lead to a misfolded protein. It is therefore important to keep this in mind when designing a codon optimized gene. It is recommended that synonymous substitutions with codons having usage frequencies match as nearly as possible to the native expression system (Angov et al., 2008).

Expression			Solubilization	Purification			References
host	protein	yield		system	yield	purity	
Xenopus laevis	PfATP4	value not mentioned					(Krishna et al., 2001)
	PfATP6	value not mentioned					(Eckstein-Ludwig et al., 2003)
	PfHT	Value not mentioned					(Ionita et al., 2007)
	PfCRT	Value not mentioned					(Nessler et al., 2004)
Pichia pastoris	*PfMDR1 + His tag et BAD*	1-3% of plasma membrane proteins					(Amoah et al., 2007)
	PfCRT + His tag		1% DDM	IMAC	200µg from 3g of wet cells	~60% (according to their gel)	(Tan et al., 2006)
	PfAQP+ His tag	64mg/ L of culture	1.5% DDM (w/v)	IMAC + SEC	18mg/ L of culture	100% (yield 28%)	(Hedfalk et al., 2008)
Saccharomyces cerevisiae	PfCRT	value not mentioned					(Zhang et al., 2002)
Mammalian cells	PfMDR1	value not mentioned					(van Es et al., 1994)
	PfCRT	Value not mentioned					(Reeves et al., 2006)

Table I.5-1: Heterologous expression of membrane proteins of *Plasmodium falciparum*

I.6 Project plan

In the section dealing with the possible mechanism of action of artemisinins (I.2), we have seen that artemisinin seems to inhibit the single sarco/endoplasmic Ca^{2+}-ATPase of *Plasmodium falciparum*, PfATP6 when heterologously expressed in *X. laevis* oocytes (Eckstein-Ludwig et al., 2003). Moreover, the sensitivity of this protein to artemisinin seems to be modulated by one amino acid: Leu 263. This interesting result was corroborated by the fact that the mammalian sarco/endoplasmic Ca^{2+}-ATPase SERCA1a, insensitive to artemisinin in its native form becomes sensitive when Glu 255 (the equivalent residue of Leu 263) was mutated in a leucine (Uhlemann et al., 2005). This last result was the starting point of my PhD project in december 2005. Indeed, our group had just developed a method to heterologously overexpress native and mutated SERCA1a, in yeast, and purify it (Jidenko et al., 2006) for valuable functional and structural characterization (Jidenko et al., 2005). My objective was thereby to use this method to express and purify SERCA1a E255L in order to functionally and structurally study the interaction between this mutant and artemisinin. However, ATPase activities assays revealed no inhibition of this mutant with artemisinin. These results will be presented in the section III.1 of this thesis. Consequently, we found of major importance to see if purified PfATP6 could be inhibited or not by artemisinin. Our objective changed and consisted therefore in trying to overexpress and to purify this plasmodial protein following the same method developed for SERCA1a in order to functionally characterize it, to check if it was sensitive to artemisinin and to try to obtain its crystallographic structure. In addition to the first aim of this project (interaction PfATP6-artemisinin), it seemed also interesting to study a parasite SERCA in order to compare the differences with mammalian SERCA1a.

To fulfill this new objective, the expression and purification protocols initially developed for SERCA1a had to be modified and adapted for PfATP6. This work will be presented in the section III.2.1 and III.2.2. Once this protocol was optimized, purified PfATP6 was characterized by ATPase assays and mass spectrometry, and some efforts were carried out to reconstitute it in proteoliposomes and to obtain suitable crystallization conditions. This will be described in the sections III.2.3 to III.2.6. All the experimental procedure supporting this work will be described in the next section (II).

CHAPTER II :

MATERIALS AND METHODS

The following sections give an overview of the methods used in the present thesis. For a detailed description of some experimental procedures employed, the reader is referred to the enclosed papers (articles I and II).

I.7 Mutagenesis and cloning of the genes of interest in a shuttle vector

The heterologous expression of SERCA1a was successful when performed in the yeast *S. cerevisiae* transformed with the vector pYeDP60-SERCA1a-BAD. Therefore, the gene coding for SERCA1a-E255L was generated from directed mutagenesis of this vector. As for the genes coding for PfATP6, they were inserted in this vector after removing the gene coding for SERCA1a. Two different genes of PfATP6 were available, one corresponding to the wild type cDNA (EMBL: X71765, Kimura et al., 1993) and another whose codons were optimized for the expression in yeast.
Although the expression is carried out in yeast, for vector preparations, it is convenient to have shuttle vectors. These vectors can be transformed in yeast and also in bacteria. The vector we used here has this property. It is a cloning vector in *E. coli* and an expression vector in *S. cerevisiae*. Its description is presented in article I.

I.7.1 Constructions of plasmids

I.7.1.1 Cloning strategies

The strategies used to prepare the mutated plasmid for the expression of SERCA1a-E255L and those developed for the cloning of the genes coding for PfATP6 were detailed in the Materials and Methods section of article II.
Nevertheless, for easiest understanding of these strategies, they were drawn and detailed in Fig. II-1.

The mutation E255L was carried out by directed mutagenenis of pYeDP60-S1a-BAD.

A modified pYeDP60-S1a-BAD vector was prepared in order to insert the genes of PfATP6 after EcoRI and BamHI digestions. This vector was modified by directed mutagenesis to remove an unsuitable BamHI restriction site (internal site at +3313 in 3’ of the region encoding BAD) by substitution of a C to a A.

A

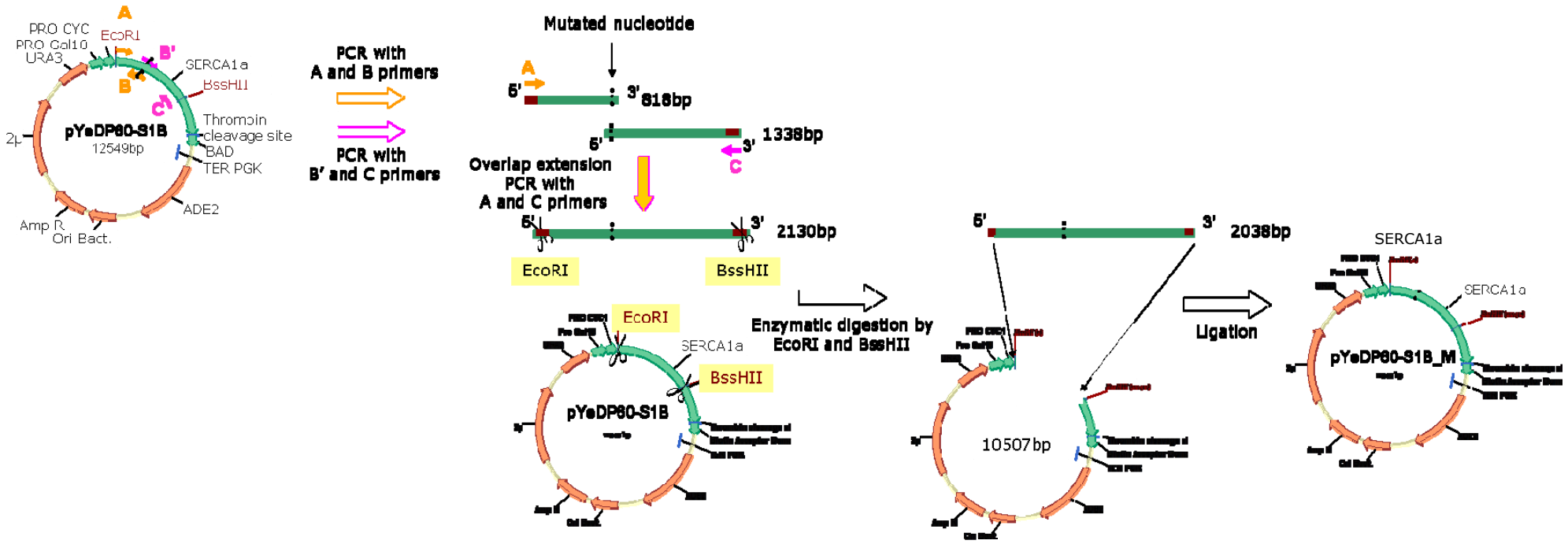

Figure II-1 : Cloning strategies

A. Directed mutagenesis of Serca1a to prepare the vector coding for SERCA1a E255L (pYeDP60-S1B_M)
B. Sub-cloning of Pfatp6 (wild type and codon optimized) in pYeDP60 to prepare the vectors coding for PfATP6 (next page)

B

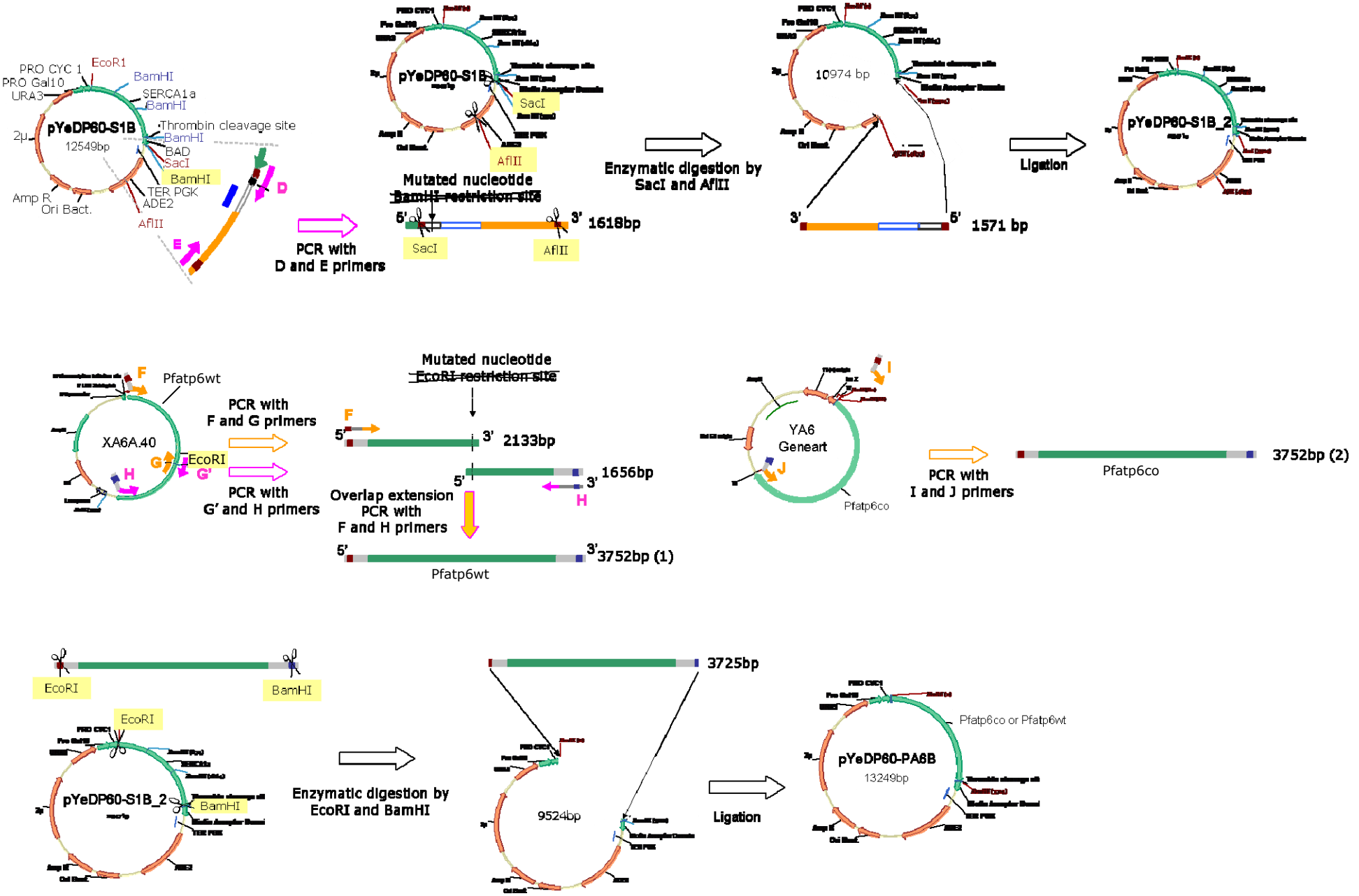
PRO CYC 1
EcoR1
PRO Gal10
BamHI
URA3
SERCA1a
BamHI
pYeDP60-S1B
12549bp
2μ
Thrombin cleavage site
BamHI
BAD
SacI
BamHI
TER PGK
ADE2
Amp R
Ori Bact.
AflII
D
E
PCR with
D and E primers
pYeDP60-S1B
SacI
AflII
Mutated nucleotide
BamHI restriction site
5'
3'
1618bp
SacI
AflII
Enzymatic digestion by
SacI and AflII
10974 bp
3'
5'
1571 bp
Ligation
pYeDP60-S1B_2
F
Pfatp6wt
XA6A.40
G
EcoRI
G'
H
PCR with
F and G primers
PCR with
G' and H primers
Mutated nucleotide
EcoRI restriction site
F
5'
3'
2133bp
5'
3'
1656bp
H
Overlap extension
PCR with
F and H primers
5'
3'
3752bp (1)
Pfatp6wt
YA6
Geneart
I
J
Pfatp6co
PCR with
I and J primers
3752bp (2)
Pfatp6co
EcoRI
BamHI
EcoRI
pYeDP60-S1B_2
BamHI
Enzymatic digestion by
EcoRI and BamHI
3725bp
9524bp
Ligation
Pfatp6co or Pfatp6wt
pYeDP60-PA6B
13249bp

To modify this vector, a 1618 pb fragment was PCR amplified from pYeDP60-SERCA1a-BAD with two primers, one, (5') G ACC TAA GAG CTC GGT ACC CGG ATC **A**GC GGG GGA TCT CCC ATG (3'), complementary to a region containing a SacI restriction site (internal site at +3304 in 3' of BAD, underlined) and mutated inside a BamHI restriction site, on the position 3318 from a C to a A (in bold) and another one, (5')GCGCTTGCTAGAGTTCCGGACTCCGTTCAA CTTAAGGCGAAG (3') complementary to a region containing a AflII restriction site (internal site at +4875 in a region coding for ADE2, underlined). The resulting mutated DNA fragment was digested by SacI and AflII, gel-purified, inserted into electroeluted digested pYeDP60-SERCA1a-BAD, transformed into *Escherichia coli* JM109, and the recombinant plasmid was colony-purified. The resultant construct, pYeDP60-Serca1a-BAD_2, was then checked by DNA sequencing.

The wild type gene of PfATP6 was mutated and PCR amplified from the plasmid XA6A.40 (Pfatp6wt) to remove an EcoRI restriction site located in the middle of the sequence and to add proper 5' and 3' sequences for further ligation with the vector. The codon optimized gene of PfATP6 was PCR amplified from the plasmid YA6-Geneart (Pfatp6co) during which proper 5' and 3' sequences were also introduced for further ligation with the vector.

I.7.1.2 Methods used

I.7.1.2.1 PCR and overlap extension PCR

PCR were carried out in a volume of 50µL with 0.1, 1 or 10ng of template DNA, 1.25U of *PfuTurbo*® DNA polymerase (STRATAGENE®, *Pyrococcus furiosus* derived polymerase), 200µM of an equimolar mix of dNTP, 0.25µM of forward and reverse oligonucleotide primers and 1X of enzyme buffer provided by the manufacturer.
Sometimes, it was necessary to increase the amount of polymerase up to 12.5U to obtain the desired PCR fragments and a suitable amount of them.
Then, PCR amplification of DNA occurred by repeated cycles of three temperature-dependent steps: denaturation of the double-stranded DNA template; annealing of oligonucleotide primers to the single-stranded DNA template; and extension of each primer in the 5' to 3' direction by DNA polymerase, duplicating the DNA fragment between the primers. With each cycle of denaturing, annealing, and synthesis, the specific DNA fragment was amplified exponentially. These reactions were performed with DNA thermal cycler 480 (PERKIN ELMER) and the conditions are detailed in Table II-1 Panel A. However, in spite of many trials, we were unable to amplify the cDNA of Pfatp6 genes with *PfuTurbo*® DNA polymerase. As *Plasmodium* genes are known to be difficult to amplify (as mentioned in I.5) because of their AT rich content, we tried a polymerase

with a better processivity: *Phusion® High fidelity polymerase (FINNZYMES).* The processivity of a DNA polymerase reflects its ability to remain bound to the template during DNA synthesis. Most thermostable polymerases extend a few bases before falling off of the primed template and are not inherently processive. Due to this dissociative nature, even a small fragment requires numerous binding events to complete elongation. Consequently, longer extension times and increased enzyme concentrations are required.
For the *Phusion®* polymerase, a *Pyrococcus* derived polymerase was fused to a double-strand DNA binding protein. Thanks to this additional domain, this modified polymerase remains bound to the DNA 10 times longer during the extension phase, helping the amplification of long and difficult templates such as Pfatp6.
The reaction mix was the same as the one previously described but with 1U of *Phusion®* polymerase. As this polymerase is faster than *Pfu® Turbo*, thermocycling conditions were adjusted. In parallel, we used another thermocycler with faster heating and cooling phases (Mastercycler gradient, Eppendorf). The thermocycling conditions are described in Table II-1 Panel B.

A.		Denaturation	Annealing	Extension
temperature (°C)		94	$Tm_{primers}$-5 *	72
time (**min**)	cycle 1	5	2	**
	cycles 2-30	1	1	
	cycle 31	2	1	10 ***
B.				
temperature (°C)		98	$Tm_{primers}$-5 *	72
time (**s**)	cycle 1	30	/	/
	cycles 2-31	5	10	**
	cycle 32	/	/	5

Table II-1: Thermocycling conditions of PCR used with *PfuTurbo®* (A) and *Phusion®* (B) DNA polymerase
** The annealing temperature is recommended to be in the range of 50 and 70°C. Primers were designed according to this requirement. Usually, the first annealing temperature tested was $Tm_{primers}$ -5°C but sometimes it was necessary to screen several temperatures to find the best one.*
*** The extension time depends both on the DNA polymerase used and on the length of the DNA fragment to be amplified. Usually, at its optimum temperature, PfuTurbo® DNA polymerase will polymerize a thousand bases per minute and Phusion® High fidelity polymerase will polymerize a thousand bases in 15-30s.*
**** Final elongation: This single step is performed for 10 minutes to ensure that any remaining single-stranded DNA is fully extended.*

Overlap extension PCR were carried out to insert mutations at specific points in DNA sequences (directed mutagenesis). It consists in joining two mutated DNA fragments generated by PCR that share a common sequence around the mutated region (Figure II-1). The amount of DNA template necessary for a successful amplification can vary between 10^8 and 10^{10} molecules for the bigger fragment. For the smaller fragment, the amount is calculated by multiplying the amount of copies used for the bigger fragment with the ratio between the size of the bigger fragment and the size of the smaller one. Except for this point, the reaction mix is identical to a normal PCR but contrary to a normal PCR, primers were added after the first cycle. Within this first step, the common region will interact as the binding of primers to a template DNA and the polymerase will add nucleotides to the remaining single stranded DNA (the uncommon sequence). Thermocycling conditions are presented in Table II-2 and they were independent of the polymerase used.

Remark: the use of fragments purified by electroelution with Electroelution G-capsules (G-Biosciences) after agarose gel electrophoresis gave better results (recovery of the predicted fragment without unexpected ones and higher amount obtained).

A.		Denaturation	Annealing	Extension
temperature (°C)		94	$Tm_{primers}$-5 *	72
time (**min**)	cycle 1	2	2	10
	addition of primers			
	cycle 2	2	2	**
	cycles 3-33	2	2	
	cycle 34	2	1	10 ***

Table II-2 : Thermocycling conditions for overlap extension PCR
** Same remarks as in Table II.1. For the first cycle, the annealing temperature corresponds to the melting temperature of the common region of the template fragments minus 5°C. However, as with normal primers, this optimal temperature may be optimized.*
*** and *** Same remarks as in Table II.1.*

In both cases (PCR and overlap extension PCR), to check whether the PCR product corresponds to the anticipated DNA fragment, agarose gel electrophoresis was used for size separation of the DNA content. The size of PCR products was determined by comparison with a molecular weight marker.

I.7.1.2.2 Cloning, bacteria transformation by $CaCl_2$ method, sequencing.

Enzymatic digestion and ligation of DNA

As ligation and transformation are low efficient steps, a large amount of DNA is often recommended to increase their yield. Consequently, it may be useful to firstly concentrate the PCR fragments by ethanol precipitation. Prior to this treatment, a desalting has to be done to remove contaminant salts, nucleotides and primers. A gel filtration was therefore performed with G100 Sephadex resin which retains molecules smaller than 100kDa. Equilibrated resin in TE' buffer (10mM Tris-Cl pH8, 0.1mM EDTA) was prepared in pouring 850µL of resin suspension into a filter tube (Spin module, Q-biogene) and centrifuging it for 3min at $1000g_{av}$ (rotor AM19, JOUAN MR22i). Several PCR solutions were then pooled, 200µL were transferred onto the resin and centrifuged for 8min at $1000g_{av}$. This last step can be repeated up to 5 times if a larger volume has to be purified.

The resulting purified DNA fragments were then precipitated with 0.8M ammonium acetate and 66% cold ethanol at -20°C. After 30min, the sample was centrifuged 30 min at $18500g_{av}$ and 4°C and the pellet was rinsed twice with 1mL of 70% ethanol to remove salts. 200µL of 100% ethanol was then added to the pellet before drying it and dissolving it in the appropriate volume of water.

Enzymatic digestions were performed following the instructions (enzyme concentration, enzyme buffer, incubation temperature, digestion time) provided by the manufacturer (New England Biolabs) from 5-10µg of purified DNA. Digestion efficiency was controlled by agarose gel electrophoresis. If the expected sizes were obtained, digested DNA fragments were purified by electroelution after agarose gel electrophoresis to remove restriction enzymes and undesired DNA fragments and salts.

To insert DNA fragments into plasmids, 50ng of vectors were mixed with three times more insert (in number of molecules) in presence of 400U of T4 DNA ligase (New England Biolabs) and 1X ligase buffer. The ligation was carried out overnight at 16°C.

Preparation of competent bacteria

Bacteria *E. coli* JM 109 were made competent to take up plasmid DNA by incubating the cells in calcium chloride. The advantage of using this strain resides in the fact that it provides minimized recombination and aids in plasmid stability. Moreover, it carries a genotype which prevents cleavage of heterologous DNA by an endogenous endonuclease. This results in high quality plasmid DNA preparation. After an overnight pre-culture of *E. coli* JM 109 in LB medium (Luria Bertani: 1% Bacto Tryptone, 0.5% Yeast extract, 1% NaCl, pH 7) at 37°C and 200 rpm, 100mL of fresh LB medium were inoculated with this pre-culture in order to have 5.10^8 cells/mL (OD_{600nm} = 0.05). When the culture was in exponential phase (OD_{600nm}= 0.4-0.6), bacteria were centrifuged 5 min at 4°C and 2000

g_{av} (rotor JA-12, Beckmann-Coulter). The pellet was resuspended in 15mL of cold buffer A (50mM $CaCl_2$, Tris-Cl 10mM pH8), kept on ice for 20min and centrifuged 5 min at 4°C and 2000 g_{av} (rotor JA-12, Beckmann-Coulter). The pellet was resuspended in 1.5mL of buffer A and kept on ice for 1h.
These competent bacteria were either used directly after their preparation or stored at -80°C for later uses. In this latter case, 20% glycerol (v/v) was added into the solution of competent cells and the resulting solution was fast frozen in liquid nitrogen. Before use, they were thawed slowly on ice to avoid cell damages.

Transformation of competent bacteria with plasmid DNA
Ligation products (90µL) were mixed with 10µL of cold buffer B (500mM $CaCl_2$, 50mM Tris-Cl pH8) and 100µL of competent cells. The samples were kept on ice for 1h. Then, a heat-shock was performed at 42°C for 2min in a water bath and 800µL of LB medium at 37°C were added to the bacteria. After 40 min of incubation at 37°C, the suspensions were transferred onto agar plates containing LB medium and 100mg/L ampicillin. Ampicillin is a β-lactam antibiotic that binds to and inhibits a number of enzymes in the bacterial membrane that are involved in the synthesis of the Gram negative cell wall. As *E. coli* are Gram- bacteria, they cannot grow in presence of ampicillin unless they have the ampicillin resistant gene which codes for β-lactamase (catalyzer of the hydrolysis of the β-lactam ring of ampicillin). The transformed plasmids, derived from the shuttle vector pYeDP60, contain this gene. Thereby, only the resistant bacteria will contain the plasmids of interest.

Plasmid DNA screening by bacterial colony PCR
In order to check if the insert was properly ligated to the vector, a colony PCR can be performed using an insert specific primer and a vector specific primer, both chosen to detect the good construct.
These reactions were carried out in 50µL by adding a small amount of cells to a mix containing 1.25U of *PfuTurbo*® DNA polymerase (STRATAGENE®), 200µM of an equimolar mix of dNTP, 0.25µM of forward and reverse primers and 1X of *Pfu* buffer provided with the enzyme. The results really depend on the amount of cells used. I noticed that it was better to use very low amount of cells.
The same conditions as those used for a classical PCR were then applied. Note that no further treatment was required. Indeed, during the first 5 min at 94°C cells were broken and the initial denaturation of DNA occurred as in a classical PCR.
Once positive clones are detected, plasmid DNA can be extracted for further analyses after growing each colony in liquid culture.

Isolation of plasmid DNA and enzyme digestion

Plasmid DNA were purified from transformed bacteria using either QIAprep®Miniprep (QIAGEN) or Wizard® Plus Minipreps DNA Purification system (PROMEGA) according to the protocol provided by the manufacturer.

The size of the recovered DNA can be directly checked after separation by agarose gel electrophoresis. Moreover, the presence of the insert and its size can be determined after the digestion of the plasmid with restriction enzyme(s) that excises the insert before separation by agarose gel electrophoresis. This also gives evidence that the restriction sites were not damaged during all the steps of the preparation of the plasmids.

If these tests are positive, it remains to verify that the nucleotide sequence corresponds to what was expected (the absence of undesired mutation and in some cases the presence of the induced mutations).

DNA Sequencing

DNA sequencing of plasmid DNA or PCR products was performed using the "Big Dye Terminator v1.1 Cycle sequencing kit" (Applied Biosystems) based on the chain termination method developed by Frederick Sanger (Sanger et al., 1977). This technique consists in a sequence-specific termination of a DNA synthesis reaction using a unique primer, normal and modified nucleotide substrates, dideoxynucleotides (ddNTP), without hydroxyl group in 3'. When such a nucleotide is recruited during the elongation, the reaction is immediately stopped. Here, each type of ddNTP is coupled with a different fluorescent dye. In the case of plasmid DNA purified after replication in bacteria, the DNA was amplified from a 20µL mix containing ~100ng of plasmid DNA, 0.25µM of primer, 40mM Tris-HCl pH9, 1mM $MgCl_2$ and 2µL of Big Dye Terminator (BDT) solution provided by the manufacturer after one cycle of 5min at 96°C and 30 cycles of 30 s of denaturation at 96°C, 15s of annealing at Tm_{primer}-5°C, and 4 min of elongation at 60°C. PCR products were then purified by ethanol precipitation and resuspended in 20µL of Hi-Di™ Formamide buffer (Applied Biosystems). After denaturing the DNA fragments by heating the samples 2 min at 95°C and quickly cooling them 2min on ice, they were separated by capillary electrophoresis in an automatic sequencing apparatus, ABI PRISM® 310 Genetic Analyser (Applied Biosystems), available at SIMOPRO, CEA-Saclay. This device detects automatically the type of fluorophore going out of the gel via a laser system and generates the electrophoregram of each analyzed sample.

In the case of PCR fragments, PCR products were gel-purified by electroelution with QuickPick electroelution capsules, after removal of enzymes by gel filtration on Sephadex G100. Then, the same protocol as described above was followed except that 200ng of DNA and 3µL of BDT solution were used.

I.7.2 Yeast transformation

I.7.2.1 Description of the yeast strain used

The strain of *Saccharomyces cerevisiae* used was W303.1b Gal4-2 (*a, leu2, his3, trp1::TRP1-*P_{GAL10}*-GAL4, ura3, ade2-1, can*^{r}*, cir*$^+$). It was provided by Denis Pompon and then modified by insertion of the Gal4 gene (Lenoir et al., 2002). This phenotype means that the mating-type of the strain is *a*. It is auxotrophous for two amino acids: leucine (*leu2*) and histidine (*his3)*; two nitrogene bases: uracile *(ura3)* and adenine *(ade2-1)*. These nutrients will have to be brought either by complementation or in the culture medium for a proper growth of this strain. It is sensitive to canavanine (*can*^{r}) and contains a plasmid 2µ (*cir*+).

The native W303.1b strain has a low constitutive expression level of GAL4p transactivation factor (1-3 copies of molecules/cell). GAL4p is a transcription factor which interacts with nucleotide sequences of GAL1 and GAL10 promoters to control the transcription. In presence of glucose, GAL4p is inactivated by a repressor and the transcription cannot occur. When this repressor is released in presence of galactose, the transcription is induced. To increase the number of this transactivator in presence of galactose, and therefore the expression of genes placed under the control of GAL1 and GAL10 promoters (like in pYeDP60 derived plasmids), this strain was genetically modified according to results obtained by Schultz at al. (Schultz et al., 1987). GAL4 gene coding for GAL4p was therefore inserted under the control of a GAL10 promoter in the locus of TRP1 (*trp1::TRP1-*P_{GAL10}*-GAL4,* TRP1 and GAL4 are functional*)*. Thereby, in absence of glucose and in presence of galactose: Gal4p will be activated, the amount of Gal4p copies will increase and the expression of genes under control of GAL1 or GAL10 promoters will be enhanced.

I.7.2.2 Yeast transformation by LiAc method

During my PhD, I used different protocols of yeast transformation. I present here the last one I used which was also, according to me, the more convenient. It was adapted from a protocol developed by Chen et al. (Chen et al., 1992) using the LiAc/single stranded DNA/ PEG method.

After an overnight culture of yeast at 28°C and 200rpm in YPD medium (1% bactopeptone, 1% yeast extract, 1% glucose) supplemented with 20µg/mL adenine, 5.10^7 cells, in stationary phase, are pelleted 5min at 4°C and 3000g_{av} (rotor AM 2.19, Jouan MR22i centrifuge). The pellet was gently resuspended on ice in cold mix containing 90µL of 1S buffer (0.1M LiAc, 40% PEG 4000, 100mM DTT), 5µL of denatured single stranded carrier DNA (10mg/mL) and about 1µg of plasmid DNA.

Yeasts were then heat-shocked at 45°C for 45min in a water-bath to help DNA to enter into the competent cells and transferred onto S6A agar plates (0.1% bactocasaminoacids, 0.7% yeast nitrogen base, 1.5% agar, 1% glucose and 20µg/mL adenine) and incubated at 28°C for 48h. This minimum medium is deprived of uracile. As *S. cerevisiae* W303.1b Gal4-2 is auxotrophous for uracile, only those transformed with vectors derived from pYeDP60 will have the ability to grow on this minimum medium since this plasmid will complement the *ura3* genotype of this yeast.

I.7.2.3 Yeast colony PCR

To check the plasmid DNA inserted into *S. cerevisae*, colony PCR may be carried out without first purifying the DNA.
Contrary to bacteria, a pre-treatment of cells has to be done in order to permeabilize the yeast cell wall. Therefore, I used Whole cell yeast PCR kit (Q-Biogene) which provides an enzyme mix to permeabilize the yeast cell wall and that is compatible with the next PCR reaction mix. I followed the protocol provided by the manufacturer. Briefly, a small amount of colony was pipetted and added into 5µL of lysis solution (lyticase- hydrolyze poly(beta-1,3-glucose) of the yeast cell wall; sorbitol; potassium phosphate). The solution was incubated at 37°C for 90 min and at 95°C for 10 minutes to lyse cells. Then, 2µL of the resulting cell suspension were used directly in the PCR reaction (same conditions as bacterial colony PCR).

I.8 Expression, purification and reconstitution of Ca^{2+}-ATPases

I.8.1 Selection of individual yeast clones

Before large scale expression, it is important to select the clone which gives the highest expression of the protein of interest. Several clones are therefore tested through a small scale expression under minimal medium. This protocol is described in article I and in supplemental data of article II. Briefly, yeast clones were grown on minimal medium (0.1% bactocasamino acids, 0.7% yeast nitrogen base, 2% glucose (w/v), 20µg/mL adenine) at 28°C and 200rpm during 24 h. Then pelleted yeasts were resuspended in 5 mL of minimum medium with 2 % galactose instead of glucose to induce expression. These cultures were incubated at 28°C during 18 h with shaking.
Then, pelleted yeasts were resuspended in cooled 2 % TCA, broken with glass beads and the precipitated cellular extract was collected. Precipitated content was then resuspended in 100 µL of 50mM Tris-Cl pH 7.5. These samples were finally analyzed by Western blotting in order to choose the best expressing clones.

I.8.2 Growth of yeast cells and large scale expression in Fernbach flasks and using a fermentor.

I.8.2.1 Expression in Fernbach flasks

This protocol is described for one Fernbach flask (500mL) and depicted in Fig. II-2. If several Fernbach flasks were used, the volumes were adjusted according to their numbers. These flasks were baffled to allow a best aeration of the medium (Bruno Coltrinari, glass master) and therefore a best oxygenation of yeasts during their culture.
A colony streaked onto a minimum medium storage plate was toothpicked into 5 mL minimum medium put in an Erlenmeyer and grown at 28°C for 24 h with shaking (200 rpm). 10 mL of fresh minimal medium were then inoculated with 2 ml of this preculture and incubated at 28°C, 200rpm for 48h until reaching the stationary phase (48h). In the meantime, Fernbach flasks filled with 500mL of YPGE-2X (glucose 1 %, yeast extract 2 %, bactopeptone 2 %, ethanol 2.7 %), were heated at 28°C and stirred at 130 rpm to be oxygenated and at a good temperature for yeast. Once the preculture reached its stationary phase, it was poured in this Fernbach flask and the whole was incubated at 130rpm, 28°C for 36h. At the end of the growth phase, when glucose was completely consumed and ethanol remained the only substrate, the Ca^{2+}-ATPase expression is induced by addition of 2% galactose and performed at 18°C for 13h. Lowering the temperature favors the Ca^{2+}-ATPase storage in the light membranes (Lenoir et al., 2002). A second addition of galactose was then carried out and the culture was incubated for 6 more hours. This second induction was shown to induce a significant increase of

the Ca^{2+}-ATPase expression level (Lenoir et al., 2002). The evolution of the culture was followed by measuring the turbidity of the solution. That was performed by measuring the absorbance of the solution at 600nm.

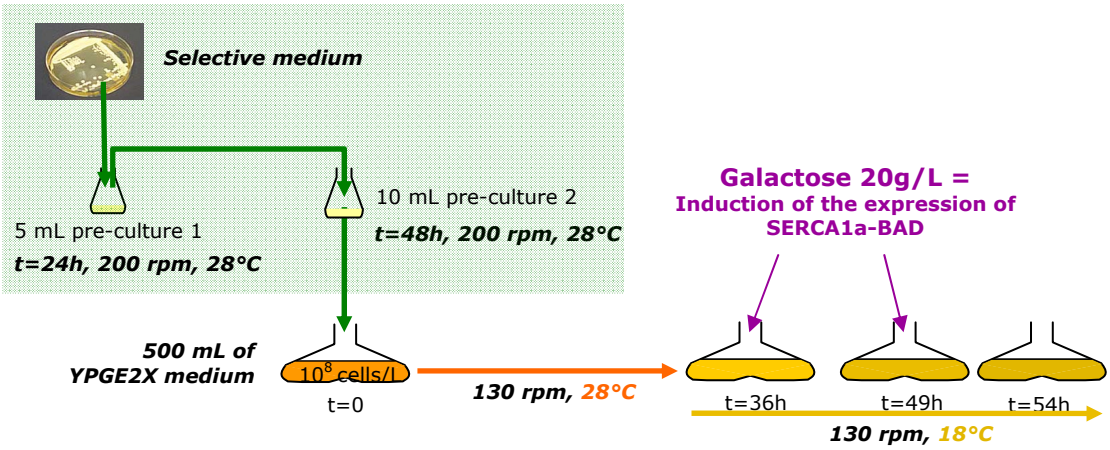

Fig II-2 : Schematic view of the yeast culture in Fernbach flasks

I.8.2.2 Expression in Fermentor

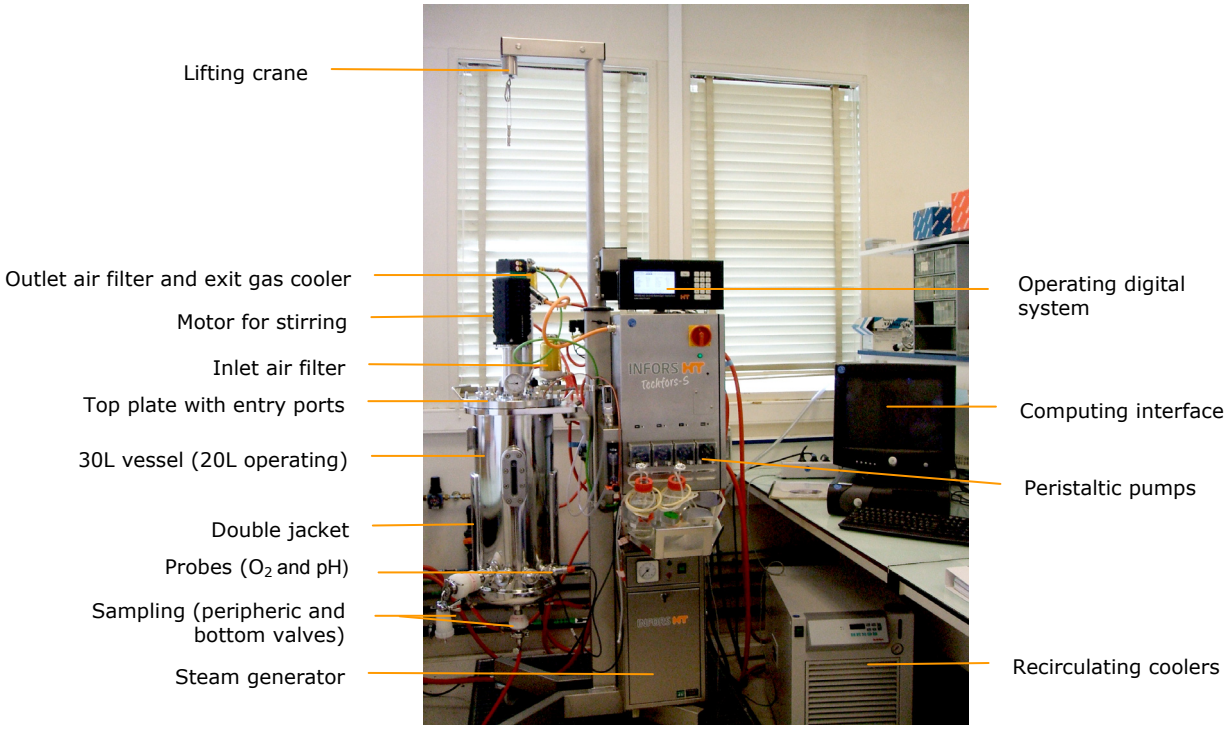

Figure II-3: Presentation of the 30L-fermentor and its installation
Techfor-S (INFORS) is composed of a vessel that can be filled with 6 to 20L of culture, a control station which measures and regulates the pH, the % of dissolved oxygen, the temperature and the foam level. It is connected to a stream generator to allow in-place sterilization and to a recirculating cooler to allow culture at low temperature.
The pH is measured via a gel-filled potentiometric probe and regulated through the addition of base and acid solutions with peristaltic pumps.
The percentage of dissolved oxygen is measured via a polarimetric probe and regulated through the addition of air and the stirring rate.
The temperature is measured via a temperature probe and regulated by the circulation of heated or cold water in the double jacket.
The foam level is measured with a conductive probe and regulated through the addition of antifoaming agent with peristaltic pumps.
The addition of galactose, necessary to trigger the induction of the expression, was performed with peristaltic pumps activated by the control station according to the desired time set-point.

As some characterization methods required a large amount of proteins (such as crystallization), we thought about a way to carry out higher culture volumes which could also lead to an increase of the yield (in terms of yeast and protein amount). We therefore decided to buy a 30-liters fermentor (working volumes: 6-20L) because of its large vessel and its control station which measures and regulates the pH, the % of dissolved oxygen, the temperature and the foam level (Fig. II-3). The purchasing and the set up of this instrument in addition to the scale up of the culture and its improvement represented an important part of my PhD work. This work, performed together with Cédric Montigny, was carried out until a valuable protocol was obtained for SERCA1a. This protocol, first developed for 6L culture, is detailed in article I. Then, I applied it to PfATP6 and I increased the culture volume to 20L. The final protocol is described in article II. The development of these protocols will be presented in section III.2.1.

I.8.3 Yeast recovery and preparation of light membrane fractions.

These protocols are detailed in article I. Yeast were harvested at the end of the culture by centrifugation and were weakened by an osmotic shock with 0.1M potassium chloride. Weakened yeast were then broken with glass beads because it is the most efficient mechanical way to break yeast cell wall. As each type of cell membrane (plasma membrane, mitochondrial membrane, reticulum…) has a different density, membrane fractions were separated by differential centrifugation.

During my PhD, the original protocol underwent some modifications in order to deal with higher amount of cells. The first modification consisted in using liners to inwardly cover centrifuge bottles during yeast harvesting. By this way, the pellet of yeast (~200g/liner) was easily resuspended by hand kneading instead of strongly agitating the centrifuge bottle for a long time. When low volumes of yeast were treated, the cell lysate was separated from the glass beads by pumping it with pipetting aids but in addition to the fact that it was long and boring, they were not efficient enough to recover all the crude extract. To gain in efficiency, a vaccum pump connected to a filtering flask was therefore used. The last modification concerned the step of ultracentrifugation leading to the recovery of light membranes. This step was previously performed in 45Ti rotor (45 min, 40krpm, 4°C) that can be filled with 6 tubes of 60mL (maximum volume 360mL). To centrifuge a bigger volume, it was replaced by type 19 rotor with which 1.2L of crude extract could be treated. However, with this rotor, to be in the same centrifugation conditions as with 45 Ti, it was necessary to reduce the rotation rate to 17.5krpm and to increase the running time to 5h.

The amount of the protein of interest was estimated by Western blot analysis using the appropriate antibody.

I.8.4 Washing of light membranes and solubilization of membrane proteins

The solubilization process of biological membranes is presented in Fig. II-4.

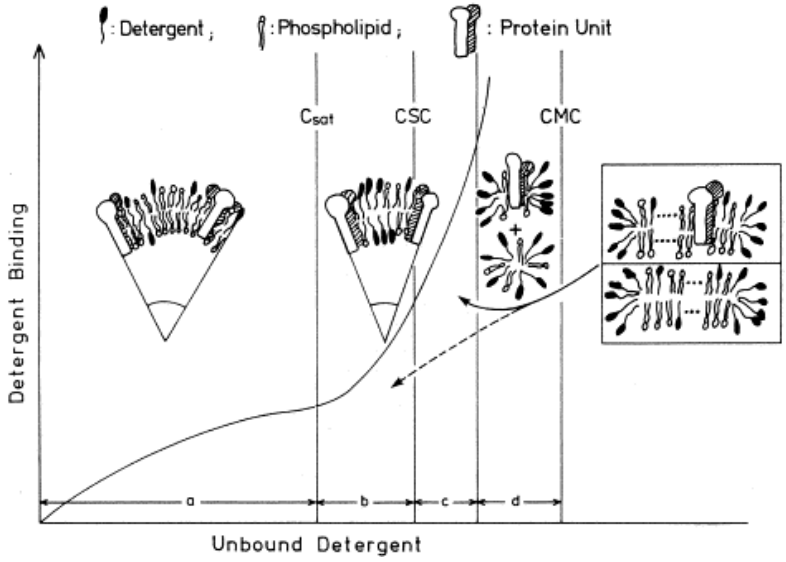

Figure II-4 : Model for the various phases leading to solubilization of protein-containing membranes as a function of free detergent concentration.

*In phase a, detergent is noncooperatively taken up by the lipid phase; in phase b, above Csat detergent molecules cooperatively interact in the membrane, producing fragmentation as membrane sheets; in phase c, at csc (*the critical solubilization concentration*), lipid and protein units (monomers, protomers, or oligomers) start to become solubilized as small membrane sheets or bilayer-containing complexes, sealed at the edges by micellar detergent structures (see inset). In phase d, mixed lipid/detergent micelles and detergent-solubilized protein units, covered by any remaining lipid and detergent, are formed. Above the cmc (the critic micellar concentration), detergents organized as micelles and together with mixed micelles, pure detergent micelles are found in solution.*
Data were taken from Kragh-Hansen et al. (Kragh-Hansen et al., 1993)

During my PhD, I used different solubilization methods.
For light membrane expressing SERCA1a E255L, the same protocol as developed for native SERCA1a was used. Briefly, light membranes were solubilized with DDM (6 mg/mL) at a protein concentration of 2mg/mL. The mixture was incubated for 2h at room temperature and under gentle stirring to complete the solubilization. The non-solubilized material was pelleted by centrifugation at 120,000 g for 45 min at 4°C (45 Ti rotor, Beckman) and the solubilized fraction was recovered in the supernatant.

Regarding PfATP6, solubilization conditions were modified and I added a washing step of the light membranes prior to detergent treatment in order to remove contaminant and

soluble biotinylated proteins (Acetyl-CoA Carboxylase, Pyruvate Carboxyase and Arc1p). The reasons will be explained in III.2.2. Since this protocol has been described in the supplemental part of article II, I will give here only a brief summary.

Light membranes were washed twice by diluting the membranes at 10 mg/mL (total protein concentration) in a buffer containing 0.5 M KCl. Light membranes were then pelleted by ultracentrifugation and the supernatants containing soluble proteins were discarded.

Washed membranes were then solubilized with DDM (30 mg/mL) at a protein concentration of 10 mg/ml and using a Potter homogenizer. As previously described for SERCA1a E255L, non-solubilized material was pelleted by centrifugation at 120,000 g (45 Ti rotor, Beckman) for 45 min at 4°C. The supernatant corresponding to the solubilized fraction was conserved for the next steps and for Western-blot analysis.

I.8.5 Purification by affinity chromatography through streptavidin-biotin interactions

All the purification steps (unless otherwise specified) were performed at 4°C

For SERCA1a E255L the initial protocol developed in the lab (Jidenko et al., 2006) was followed but using streptavidin Sepharose™ High Performance resin instead of Softlink™ Soft Release Avidin resin. The general principle of this purification based on the interaction between (strept)avidin and biotin is depicted in Fig. II-5.

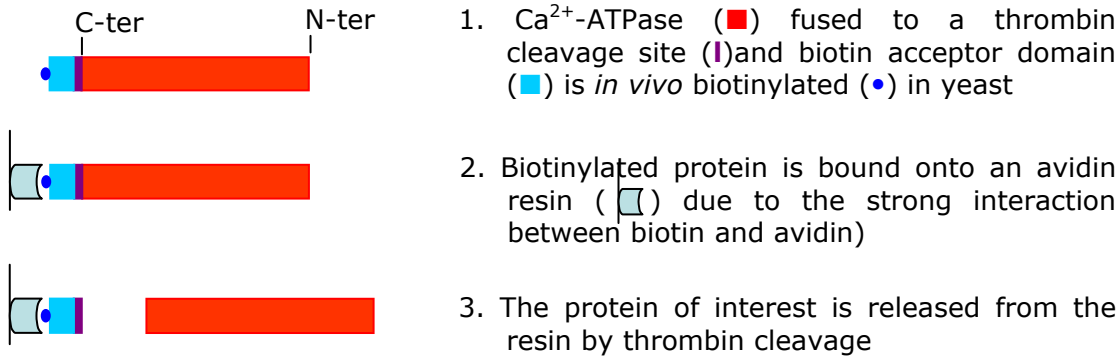

Figure II-5: Schematic description of the purification of the Ca^{2+}-ATPase by affinity chromatography through avidin-biotin interactions

The supernatant of the solubilization step was mixed with streptavidin Sepharose™ High Performance resin equilibrated with solubilization buffer in a 1.5:1 ratio (1.5mg of Ca^{2+}-

ATPase contained in the light membranes before solubilization in 1 mL of resin) and gently stirred overnight, at 4°C. The suspension was then put into a 11x100 mm column (BioSepra, MA, USA) connected to a peristaltic pump set at 1.5mL/min. The flow-through was loaded a second time on the resin. The resin was washed first with 10 column volumes (CV) of high salt buffer (50 mM Tris pH 7, 1 M NaCl, 20 % (w/v) glycerol, 1 mM $CaCl_2$, 0.05 % (w/v) DDM) and then with 10 CV of low salt buffer (50 mM Tris pH 7, 150 mM NaCl, 20 % glycerol, 2.5 mM $CaCl_2$, 0.05 % DDM) at a flow rate of 1 mL/min. The resin was then mixed with 1CV of low salt buffer and thrombin (25 units/mL of resin) was added and the mixture was gently stirred at room temperature for 30 min. The same amount of thrombin was added again and after 30 min, 2.5 mM PMSF were added in order to stop the thrombin cleavage. The column was placed in cold room. The proteins were eluted at 0.5mL/min from the column by adding low salt buffer 1CV at a time.

This initial procedure was progressively modified in order to improve the experimental conditions (decrease of the time of handling) and to optimize the purification of PfATP6. The adjustment of this protocol constituted a major part of my PhD work. The optimization will be described in III.2.2. The common modification of this protocol for PfATP6 and SERCA1a was to use a batch-procedure instead of columns.
The final protocols for PfATP6 and SERCA1a are respectively described in article II and article I.

I.8.6 Purification and buffer exchange by size exclusion chromatography

This step was carried out to prepare samples for MALDI-TOF analysis and crystallization assays. It aimed at removing thrombin which remained after affinity chromatography and exchanging the sample buffer to one that is compatible with these techniques. More details will be brought with the description of these experiments.
The size exclusion chromatography was performed by HPLC with a column TSK-gel $G3000SW_{XL}$ (0.78cm x 30cm, TosoHaas) mounted on a GOLD system apparatus (Beckman). It allows the separation of molecules according to their Stokes radius and therefore their size. The column was equilibrated with elution buffer (at least 2-3 column volumes ~20mL) at a flow rate between 0.3 and 1mL/min. Elution buffers will be described later in the MALDI-TOF and crystallization assays sections. The sample was loaded into a 500µL injection loop. Sample elution was monitored at 280nm and the fractions of interest were collected manually following the UV absorbance chromatogram.

I.8.7 Protein reconstitution in proteoliposomes

I.8.7.1 Lipid vesicles preparation

I.8.7.1.1 DOPC vesicles preparation by dialysis

This method consists in forming unilamellar vesicles by preparing mixed micelles of detergent and lipids (DOPC) and slowly removing the detergent by dialysis. To increase the dialysis efficiency, a resin of polystyrene beads that binds detergents was added to the dialysis buffer (Bio-Beads SM2, Biorad). By this way, during detergent removal and until no detergent remains in the lipid solution, the detergent concentration inside the dialysis tubing is maintained higher than the detergent concentration in the dialysis buffer. The dialysis is thereby never stopped.

DOPC was solubilized in chloroform at 40mg/mL and chloroform was vacuum evaporated at 37°C in a rotating evaporator until a dry film of lipids was formed and no chloroform could be smelled. Then, lipids were slowly solubilized at 15mg/mL in a cholate solution containing DTT to prevent their oxidation (30mM Tris-HCl pH 7.1, 400mM sucrose, 1mM $MgCl_2$, 1mM NaN_3, 1% sodium cholate (w/v), 5mM DTT) by gentle mixing. The resultant solution was composed of mixed micelles saturated with lipids. 6mL of this mixture were then enclosed into a 25-30 cm strips of dialysis tubing (cut-off 12-14kDa, pore size 2.4nm, 1cm wide, Visking) and the bag was transferred into a test tube filled with dialysis buffer 1 (100mM NaH_2PO_4, 1mM $MgCl_2$, 1mM NaN_3, 5mM DTT, adjuted to pH 7.1 with NaOH) and 6mL of Bio-beads resin. This test tube was rotated at 10-12 rpm at 7°C for 5h. Afterwards, the dialysis buffer was replaced by a fresh one (without removing Bio-beads resin) and the incubation was continued for 5 more hours. At the end of the incubation period, the dialysis buffer was removed and replaced by dialysis buffer 2 (dialysis buffer 1 without DTT). After 10 h of incubation, dialysis buffer was removed and fresh dialysis buffer 2 was added. Ten hours later, the solution of lipids was collected from the dialysis tubing.

I.8.7.1.2 Phospholipid vesicles preparation by extrusion and size determination by dynamic light scattering

Phospholipids (DOPC or EYPC) were solubilized in chloroform at 10mg/mL and chloroform was vacuum evaporated at 37°C in a rotating evaporator until a dry film of lipids was formed and no chloroform could be smelled. These lipids were then resuspended in N_2 saturated Milli-Q water at 10mg/mL by mixing with a vortex. Once the solution was homogenous, it was lyophilized to remove remaining traces of chloroform (Freeze dryer ALPHA 1-2/LD plus, CHRIST). Lyophilized lipids were then resuspended at 10mg/mL in phosphate buffer (50mM KPi pH 7, 30µM $CaCl_2$, 1mM $MgCl_2$ – unless otherwise specified)

and vesicles were extruded 5 times through a 400nm polycarbonate filter and once through a 100nm polycarbonate filter to form calibrated unilamellar vesicles.

The size of the liposomes was checked by dynamic light scattering (DLS) with Zetasizer Nano ZS (Malvern). This technique gives the size distribution profile of small particles in solution. It is based on two main facts: light that hits small particles scatters in all directions; small molecules in solutions are undergoing Brownian motion. Consequently, when using a monochromatic and coherent light source as a laser, a time-dependent fluctuation of the interferences formed by the particles and the scattered intensity can be recorded. Based on physical equations, the software calculates the hydrodynamic particle size from these fluctuations.

DLS measures were performed with 0.1 mg/mL of lipids to be in the correct range of analysis.

I.8.7.2 Titration of the vesicles with detergent

Liposomes were diluted at 3-5 mg/mL and exposed to increasing concentrations of detergent. This resulted in an initial swelling of the liposomes that can be followed by determining the turbidity of the suspension. The turbidity was monitored by measuring the optical density of the suspension at 540nm after each addition of detergent (Fig. II-6).

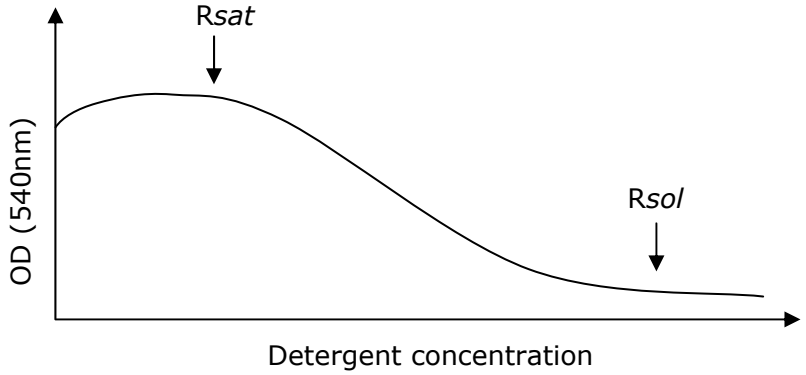

Fig II-6: Schematic follow-up of the solubilization of preformed liposomes by spectrophotometry

During this process, the detergent partition into the lipid bilayer liposomes until they saturate the liposomes (Rsat). At this stage, detergent addition to preformed liposomes does not disrupt the liposomes and induces slight changes in turbidity. Then, gradual solubilization of detergent saturated liposomes into small lipid-detergent mixed micelles occurs. Finally, liposomes are completely solubilized into lipid-detergent mixed micelles and the solution becomes optically transparent (Rsol)

I.8.7.3 Protein reconstitution in proteoliposomes

A first method consists in mixing detergent-solubilized membrane proteins and detergent-treated liposomes, and then slowly removing detergent by adsorption on polystyrene beads (Bio-beads) (Fig. II-7).
Thus, solubilized (and purified) Ca2+-ATPase was combined with detergent destabilized liposomes at 3-5mg lipids/mL. After mixing, the protein/lipid ratio is 1:60 (w/w) and the preparation contains a variable amount of detergent, as explained above. The reconstitution medium also contains 20% glycerol and 30µM free calcium (unless otherwise specified). Proteoliposomes were then formed at room temperature and gentle mixing by slowly removing detergent with Bio-beads (80mg/mL for 2h). These Bio-beads are then replaced by fresh ones for 1h and again twice but here with 120mg/mL of fresh Bio-beads.
For specific activity calculation, we assumed that all of the protein used was reconstituted into the proteoliposomes.

Another reconstitution method was also used where proteins were not inserted in pre-formed and detergent destabilized liposomes. In that case, phospholipids were solubilized by the detergent brought with the solubilized membrane protein and then, the detergent is slowly removed to allow the insertion of membrane proteins into the lipids. This method does not lead to calibrated, unilamellar and tight sealed proteoliposomes but proteins are nevertheless inserted into membrane networks that mimic a more native environment than detergent. The protocol is described in article II.

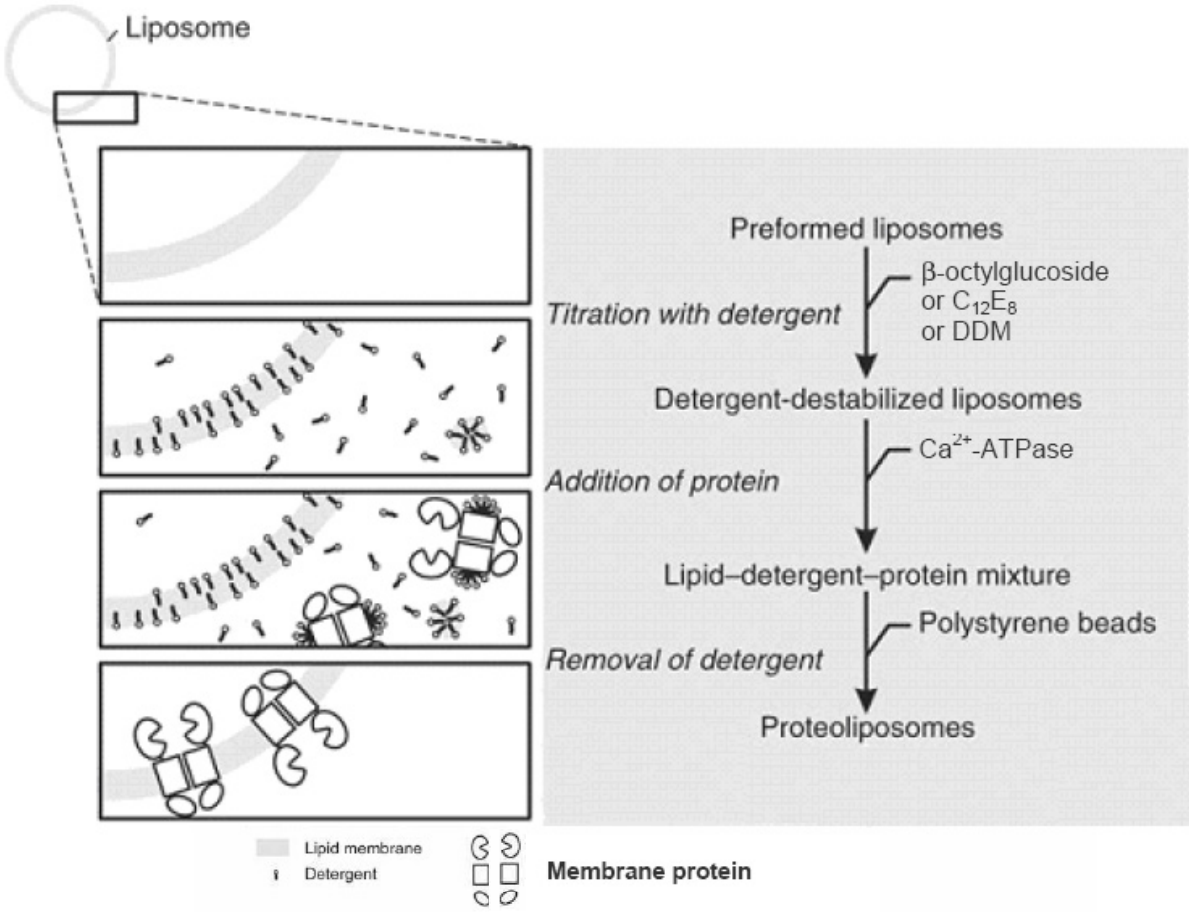

Figure II-7: proteoliposomes formation (adapted from (Geertsma et al., 2008))

Liposomes are detergent-destabilized by titration with detergent and mixed with the detergent-solubilized protein complex. Subsequent controlled removal of the detergent by polystyrene beads (Bio-beads) results in the formation of sealed proteoliposomes.

I.8.8 Protein relipidation

Briefly, phospholipids dissolved in chloroform were dried under a stream of nitrogen to form a thin film. They were then added to concentrated PfATP6 at a final concentration of 1mg/mL and a lipid to protein ratio of 3:1 (w/w). The solution was saturated with N_2 to avoid lipid oxidation. After 15 min of incubation at 18°C, detergent was removed with Bio-beads (Bio-Beads/detergent ratio of 200:1 (w/w)) by incubating the whole solution (saturated with N_2) at 18°C for 3h under gentle stirring. Biobeads were then removed and the suspension was kept at 4°C.

I.9 Biochemical analyses

I.9.1 Estimation of total membrane protein concentration

Estimation of the membrane protein concentration was performed by bicinchoninic acid (BCA) assay because this method remains accurate in presence of SDS necessary to completely remove and denature the membranous parts of proteins.

This method adapted from (Smith et al., 1985) relies on the reduction, in alkaline medium, of Cu^{2+} in Cu^{1+} by peptide bonds and the subsequent formation of a purple complex between cuprous ions and BCA that exhibits a strong linear absorbance at 562 nm with increasing protein concentrations. The unknown protein concentrations were determined from a reference curve obtained by using a concentration range of BSA samples.

The complete protocol is detailed in article I.

I.9.2 SDS-PAGE and western-blot analyses

Protein fractions were analyzed after electrophoresis in denaturing conditions (SDS-PAGE) by Coomassie blue staining or by detection after transfer onto PVDF membrane (Western-blotting). These protocols were described in detail in article I and in supporting information of article II. Table II-3 refers all the molecules used to reveal the targeted proteins from the western-blots.

Primary antibody or avidin peroxidase				Secondary antibody	
Detected proteins	Name (supplier)	Target	Dilution and incubation time	Name	Dilution and incubation time
Biotinylated proteins	avidin peroxidase (SIGMA)	biotin	1/50000 in PBS-T 75min	/	/
SERCA1a	79B, polyclonal antibody (A-M Lompré, INSERM, PARIS)	Mainly the actuator domain	1/20000 in PBS-T + milk 60min	anti guinea-pig	1/10000 in PBS-T + milk 60min
	IIH11, monoclonal antibody (SIGMA)	amino acids unknown	1/2500 in PBS-T + milk 60min	anti-mouse	1/2000 in PBS-T + milk 60min
PfATP6	2006, polyclonal antibody (ordered at Bethylgroup, provided by Sanjeev Krishna, St Georges' Hosptital)	amino acids 574-588	1/20000 in PBS-T + milk 60min	anti-goat	1/10000 in PBS-T + milk 60min
	2004 (ordered at Bethylgroup, provided by Sanjeev Krishna, St Georges' Hosptital)	amino acids 128-145	1/4000 in PBS-T + milk 60min		

Table II-3 : Conditions of incubation of avidin peroxidase and antibodies for protein detection on western-blot

The secondary antibodies were coupled to horseradish peroxidase for protein detection by chemilumiscence (ECL™, Enhanced Chemiluminescence, Amersham). The emitted light was either detected by autoradiography or with a cooled CCD camera (G:BOX HR16, Syngene).
PBS-T+milk: 90mM K_2HPO_4, 10mM KH_2PO_4, 100mM NaCl, 0.2% (v/v) Tween 20 + 5% (w/v) dry skimmed milk.

I.9.3 ATPase activity measurement

During its enzyme cycle, the Ca^{2+}-ATPase hydrolyzes ATP to ADP in presence of calcium. The follow-up of this hydrolysis was carried out by a spectrophotometric method based on the use of a coupled enzyme assay (Fig II-8 panel A). This system allows the correlation of the hydrolysis of one molecule of ATP with the oxidation of one molecule of NADH while regenerating the molecule of hydrolyzed ATP. This avoids ATP depletion and an accumulation of ADP which could inhibit the enzyme. NADH disappearance was measured by following the decrease of the absorbance at 340nm. The slope determined from the graphic Absorbance(340nm)=f(t) led to the ATP hydrolysis rate (Fig II-8 panels B and C). The specific activity is then deduced from the amount of enzyme used for the assay.

These measurements were carried out in 2mL of assay buffer. I mostly used the following assay buffer: 50mM Tes-Tris pH 7.5, 0.1M KCl, 6mM $MgCl_2$. When another buffer was used, it will be specified. Into this buffer were added the reagents required for the coupled enzyme assay (1mM phosphoenol pyruvate (PEP), 0.3mM NADH, 0.1mg/mL lactate dehydrogenase and pyruvate kinase). As the enzymes studied here are calcium-dependent and membrane proteins, it is essential to add some calcium to the assay medium and some detergent. The amount of calcium added to the assay depends on the desired final concentration. Except for the determination of the calcium dependence of PfATP6, the final concentration used was 125µM. The detergent added will be mainly $C_{12}E_8$ (0.2-1mg/mL) but it was sometimes supplemented with phospholipids (see III.2.4).

Two different ways were used to trigger the reaction. In most cases, 5mM ATP were added to the medium and the reaction was started by the sample addition but sometimes, the sample was first added to the medium and the reaction was started by addition of 5mM ATP. The way to proceed will be specified.

The reaction was then stopped by addition of EGTA (750µM) in order to determine the calcium independent activity. Thus, to determine the calcium dependent activity of the enzyme, this slope was deducted from the slope obtained before EGTA addition.

To measure the ATPase activity of the Ca^{2+}-ATPase according to different calcium concentrations, the concentration of free calcium was modulated either by adding some EGTA or by adding Ca^{2+}. The amounts to add were determined with the software Maxchelator which takes into account the concentration of Mg^{2+}, ATP, EGTA and Ca^{2+}, the pH, the ionic strength, and the temperature of the assay medium (http://www.stanford.edu/~cpatton/webmaxc/webmaxcS.htm).

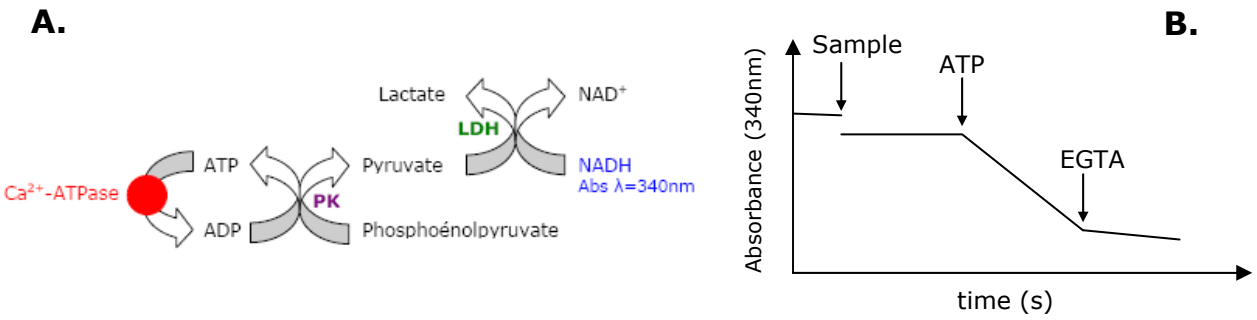

C. According to Beer-Lambert law : $Abs_{340nm} = \varepsilon_{340nm}.l.C$

So, $\Delta Abs_{340nm} / \Delta t = \varepsilon_{NADH,\ 340nm}.l.\ \Delta[NADH] / \Delta t$

i.e. $\Delta[ATP]/\ \Delta t = \Delta[NADH] /\Delta t = \Delta Abs_{340nm}/(\varepsilon_{NADH,\ 340nm}.l.\ \Delta t)$

SA = $|\Delta[ATP]|/(\Delta t .[SERCA]) = |\Delta Abs_{340nm}| / (l.\ \varepsilon_{NADH,\ 340nm}.\ [SERCA].\ \Delta t)$

Figure II-8: Determination of the specific activity of a Ca^{2+}-ATPase by a spectrophotometric measure using a coupled enzyme assay

A. *Schematic representation of a coupled enzyme assay (PK, pyruvate kinase ; LDH lactate dehydrogenase).* ***B.*** *Schematic view of the signal obtained by spectrophotometric measure.* ***C.*** *Relationship between the slopes of the graphic Abs(340nm)=f(t) and the specific activity of the Ca^{2+}- ATPase (l: cuvette length = 1 here, C: concentration of the molecule absorbing at 340nm, ε_{340nm}: molar absorptivity of this substance at 340nm=6.2.10^{-3} $M^{-1}.cm^{-1}$, SA: specific activity (in µmol of ATP.mg^{-1} of Ca^{2+}-ATPase.min^{-1}).*

I.9.3.1 Calcium uptake measurement

Calcium uptake measurements were carried out by measuring the increase of the calcium content accumulated (using $^{45}Ca^{2+}$) inside proteoliposomes during enzyme turnover. Proteoliposomes adsorb on nitrocellulose membrane and thus can be separated from the reaction medium. Thereby, counting the radioactivity bound on nitrocellulose filters and comparing it to standards lead to the amount of calcium accumulated into the proteoliposomes.

Experimentally, vesicles were diluted in reaction buffer (30mM imidazole pH 7.1, 150mM NaCl, 1mM $MgCl_2$, 1mM NaN_3 with 330µM of $^{45}Ca^{2+}$ and 0.3mM EGTA or 50 mM Tes-tris pH 7.5, 100mM KCl, 1mM $MgCl_2$, with 330µM of $^{45}Ca^{2+}$ and 0.3mM EGTA). The reaction was initiated by addition of 5mM MgATP and was carried out at 30°C. Aliquots (200µL) of the reaction solution were taken during the reaction and filtered on nitrocellulose filters (0.45µM, Whatman). Filters with retained proteoliposomes were then washed three times to remove unspecific $^{45}Ca^{2+}$ binding and were added to counting vials. The radioactivity was determined by scintillation counting.

I.9.3.2 Concentration determination by radioactive counting

Samples were placed in translucent plastic and dissolved or suspended with scintillation liquid, composed of a solvent and a fluorescent molecule. Beta particles emitted from the sample transfer energy to the solvent molecules, which in turn transfer their energy to the fluorescent molecules and these dissipate the energy by emitting light. In this way, each beta emission results in a pulse of light. The vials were loaded into a liquid scintillation counter (LS 5801, Beckman) to be analyzed. The resultant signals were given in counts per minute (cpm).

I.9.4 Molecular weight determination by MALDI-TOF mass spectrometry

MALDI-TOF mass spectrometry (MS) consists in a matrix laser desorption ionization process of molecules which are then separated according to their velocity in a Time–of-Flight analyzer. This velocity depends on their m/z ratio (mass/charge). Thus, if the charge of the molecule is known, it is therefore possible to obtain its accurate mass with this technique. It requires that samples are in suitable conditions to be submitted to MALDI-TOF (low salt, detergent and lipid concentrations, and compatible buffer).

I.9.4.1 Sample preparation

Prior to analyze the samples by mass spectrometry, they were purified and/or delipididated by size exclusion chromatography and prepared in a buffer that was formerly successfully used to analyze SERCA1a by MALDI-TOF MS (Lenoir et al., 2004).
Affinity purified proteins were concentrated and 300µL were applied at 1mL/min to the gel-filtration column equilibrated with the elution buffer (50mM MOPS-Tris pH6.8; NaCl 50mM; DDM 0.4mg/mL). The fraction corresponding to the protein of interest was collected and concentrated on centricon YM-100 (to avoid the concentration of DDM in the sample) until a suitable concentration was obtained (0.25-10mg/mL). The concentration was determined by measuring the optical density of the sample at 280nm.

I.9.4.2 MS analysis of protein sample by MALDI-TOF

For this purpose, a matrix solution is mixed with the protein sample. This solution is spotted onto a MALDI plate (a metal plate designed for this purpose). The solvents vaporize, leaving only the recrystallized matrix associated with the molecules spread throughout the crystals (e.g. protein). The matrix and the analyte are said to be co-crystallized in a MALDI spot. The laser is then fired at the crystals in the MALDI spot. The

matrix absorbs the laser energy and is ionized. In turn, it transfers part of its charge to the proteins which become protonated while still protecting them from the disruptive energy of the laser. The resultant quasimolecular ion, $[M+H]^+$ is then accelerated by an electric field and a time-of-flight (TOF) analyzer measures the time it takes for this ion to reach the detector. As in this case, the charge is known (+1), the mass of the ion can be directly deducted from its velocity. If it is a light ion, it will reach faster the detector.

A matrix consists of crystallized molecules, which are acidic to act as a proton source to help ionization of the analyte, and functionalized with polar groups to be used in aqueous solution. It must have a fairly low molecular weight to allow easy vaporization and a strong optical absorption in the UV to rapidly and efficiently absorb the laser irradiation. Here, we chose to work with 3,5-dimethoxy-4-hydroxycinnamic acid (sinapinic acid) because it is compatible with the detection of peptides, proteins and lipids. It was diluted in 30% acetonitrile (ACN) and 0.3% trifluoroacetic acid (TFA). The organic solvent (ACN) allows hydrophobic molecules to dissolve into the solution, while the water allows the solubilization of water-soluble (hydrophilic) molecules. TFA allows the acidification of the solution to help the formation of protonated molecules.

MALDI-TOF MS can detect low molecular weight proteins with a high accuracy (error <0.1% for protein <20kDa) but it is more difficult with bigger protein (<1% for proteins higher than 100kDa). Moreover, membrane proteins are maintained in solution with detergents that can prevent a co-crystallization of the matrix with the protein. It is thereby important to use a small amount of detergent.

This step was performed with Christophe MARCHAND at IBBMC (University Paris-Sud XI, Orsay).
Matrix (sinapinic acid) was dissolved in 30% acetonitrile and 0.3% trifluoroacetic acid in order to obtain a saturated solution. It was then vortexed for 60s and centrifuged briefly.
1µL of HPLC-purified proteins was mixed with 1-19µL of saturated matrix in 30% acetonitrile and 0.3% trifluoroacetic acid. 1µL of the resulting mixture was placed on the sample target, which was subsequently dried at room temperature under a hood. The sample target was then inserted into the mass spectrometer (Voyager DE-STR, Applied Biosystems) to be analyzed. Spectra were acquired in linear mode using delayed extraction, with an accelerating voltage of 25kV.
External calibration was performed with the single charged peaks of the monomer (67kDa) and the dimer (134kDa) of BSA.

I.10 Crystallization

Resolving the structure of a protein by X-ray crystallography involves the production of high quality crystals. This requires a highly pure protein sample and the determination of crystallization conditions.

I.10.1 Sample preparation

Prior to submit PfATP6 to crystallization assays, the purity of the sample was increased by removing the remaining contaminants after affinity chromatography (especially thrombin used during the elution step) by size exclusion chromatography. In addition, this step allows buffer exchange to place the protein in suitable conditions for crystallization.

For this purpose, affinity purified proteins were concentrated and 300µL were applied at 0.3-1mL/min to the gel-filtration column equilibrated with the elution buffer containing 0.5 mg/mL of $C_{12}E_8$. Different elution buffers were used according to the assays. They will be indicated in section III.2.6. The fraction corresponding to the protein of interest was collected and concentrated on Centricon YM-30 until a suitable concentration was obtained (5-20mg/mL). The protein concentration was determined by measuring the optical density of the sample at 280nm. From this value and from the concentration factor of the sample, the detergent concentration was calculated (Fig. II-9). For this purpose, we assumed that PfATP6 binds the same amount of $C_{12}E_8$ as SERCA1a and that 0.05mg/mL (=CMC) of $C_{12}E_8$ are monomers. In most cases, DOPC was added to the sample such as the ratio $C_{12}E_8$/DOPC reaches 3:1 (w/w). Then calcium concentration was adjusted and inhibitors or substrate analogs were added. The sample was left overnight at 4°C and then centrifuged at 125000g_{av} (rotor TLA100, Beckman Coulter) for 15 min to remove aggregated proteins before setting crystallization plates.

<table>
<tr><td colspan="2">$[C_{12}E_8]= [C_{12}E_8]_{\text{bound to the protein}}+[C_{12}E_8]_{\text{free micelles}}+[C_{12}E_8]_{\text{monomers}}$
$[C_{12}E_8]_{\text{monomers}}$ can be neglected so it was not taken into account</td></tr>
<tr><td>2mg of SERCA1a bind 1mg of $C_{12}E_8$ (Møller and le Maire, 1993):
$[C_{12}E_8]_{\text{bound to the protein}} = 0.5 \times [\text{protein}]$</td><td>0.05mg/mL (=CMC) of $C_{12}E_8$ are monomers
$[C_{12}E_8]_{\text{free}} = ([C_{12}E_8]_{\text{in solution}}-[C_{12}E_8]_{\text{monomer}}) \times f$
$= (0.5-0.05) \times f$
$= 0.45 \times f$ (f, concentration factor)</td></tr>
<tr><td colspan="2">$[C_{12}E_8]= 0.5 \times [\text{protein}]+ 0.45 \times f$</td></tr>
</table>

Figure II-9: Determination of the concentration of $C_{12}E_8$ in solution after SEC-HPLC and sample concentration

These equations were based on results obtained with SERCA1a. In order to verify if they can be applied to PfATP6, it would have been interesting to prepare a sample with an elution buffer containing radioactive $C_{12}E_8$.

I.10.2 Principle of protein crystallization

Among the different existing crystallization methods, the most commonly used was applied here: vapor diffusion. It was carried out by hanging-drops or sitting-drops (Fig. II-10). To grow crystals with these techniques, the protein solution (5-20mg/mL) is placed either on a siliconized glass cover slide (hanging-drop) or in the drop chamber (sitting-drop) and is mixed with an aqueous buffered solution with precipitant in a 1:1 ratio such that the reagents of the resulting drop have half their original concentration. In the case of hanging-drops, the cover slide is then inverted over a reservoir containing the crystallisation solution and sealed with immersion oil. In the case of sitting-drops, wells are sealed with an adhesive.

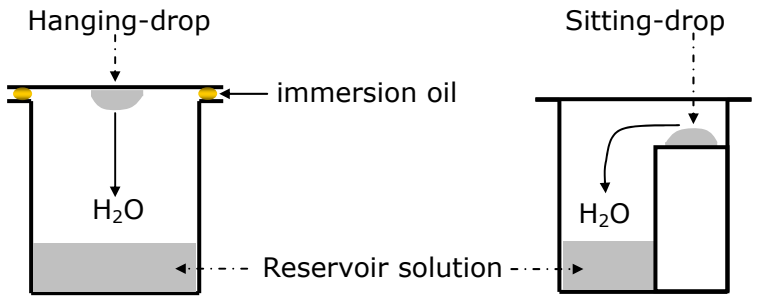

Figure II-10 : Schematic illustration of experimental devices used for crystallization by vapor diffusion

Since the reagents in the reservoir solution have double the concentration to those in the drop, water evaporates from the drop gradually up to a similar chemical potential of both compartments. This involves a progressive decrease of the protein solubility and a concomitant increase of the concentration of crystallizing agents and proteins in the drop. When the supersaturated state is reached and especially the nucleation area of the phase diagram, protein crystals may form (fig II-11). When the protein concentration reaches the nucleation region, nuclei are formed. This state of supersaturation can lead to protein precipitation but if the protein concentration decreases as nuclei form, the metastable phase can be reached in the phase diagram. In this region, it is likely that organized objects in which contact between molecules are regular, crystals will grow from the nuclei and already formed protein crystals can continue to grow, but no additional nucleation takes place. Cessation of crystal growth is thought to occur when the molecules reach exchange equilibrium between the solution and crystal phases and/or the concentration is depleted such that the undersaturated region is reached.

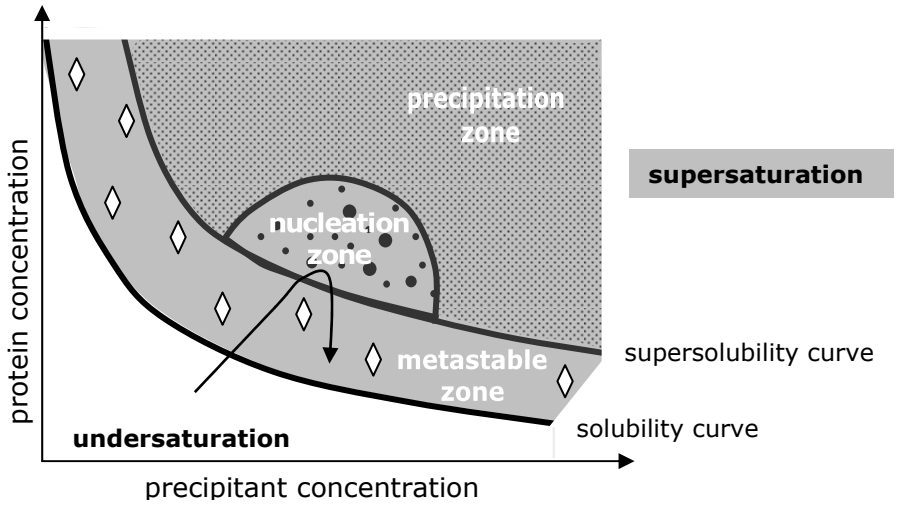

Figure II-11: Schematic illustration of a protein crystallization phase diagram (adapted from (Chayen, 2004))

A crystallization phase diagram is composed of four areas: an area of very high supersaturation, where the protein will precipitate; an area of moderate supersaturation, where spontaneous nucleation will take place; an area of lower supersaturation just below the nucleation zone, where crystals are stable and may grow, but no further nucleation will take place; and an undersaturated area where the protein is fully dissolved and will never crystallize.

The solubility curve is defined as the concentration of protein in the solute that is in equilibrium with crystals. The supersolubility curve is defined as the line separating conditions under which spontaneous nucleation (or phase separation or precipitation) occurs from those under which the crystallization solution remains clear.

The arrow indicates the route to reach the metastable zone through vapor diffusion crystallization.

In order to reach a supersaturation state which will lead to nucleation and crystal growth, multiple physicochemical and biochemical parameters must be taken into account and adjusted: nature and concentration of the precipitant (PEG, ammonium sulphate), ionic strength and nature of salt ($MgSO_4$, LiCl, KCl…), pH, temperature, pressure, sample ageing and degradation, the presence of inhibitors, or ligands. With membrane proteins, it is also important to consider the nature and concentration of detergent and lipids that solubilize and stabilize the protein. This involves that many conditions often need to be tested before finding those leading to crystals.

I.10.3 Crystallization assays

They were performed either in Denmark in Poul Nissen's lab, in France at iBiTec-S (CEA Saclay) and IBBMC (University Paris XI, Orsay).

To test as many conditions as possible, initial crystallization screening were carried out using liquid dispensing automates. These robots (Mosquito crystallization robot in the Danish lab (Molecular Dimensions Ltd), and Cartesian Microsys (Genomic solution) at IBBMC), are able to set up low volume crystallization drops (50nL to 1µL) in plates filled with reservoir solutions.

Here, 96 well plates were used, reservoirs were filled with 100µL or 150µL of crystallizing solution, and volumes of 140nL (Mosquito) or 100nL (Cartesian) were used for both the protein and the precipitant.

Some trials were also carried out by hanging-drop with 24 well plates filled by hand. In this case, the reservoir contained 400µL of crystallization solution, and drops were prepared by mixing 0.5µL of protein solution with 0.5µL of crystallization solution.

Crystallization solutions were either prepared with a robot (2T5 Liquid handler, GILSON) or by hand and sometimes were supplied in a commercial kit.

Screens used for crystallization attempts of PfATP6 were either developed by Poul Nissen's lab for the crystallization of purified SERCA1a (table II-4) or supplied with commercial kit (MbClass I, Qiagen).

Glycerol (0 or 10%) or Sucrose (10%)	
PEG 2000 or 6000	0, 8, 10, 12, 16%
Salts ($MgSO_4$, $MgCl_2$ KCl, LiCl, NaCl, $NaOCH_3COOH$)	200mM
MPD 6% or t-BuOH 3%	

Table II-4: Composition of crystallization screens developed in Poul Nissen's lab for purified SERCA1a.

The mix of all these components led to three screens of 48 conditions either without glycerol/sucrose, with 10% glycerol or 10% sucrose (respectively SERCA1a screen 1, 2 and 3)

Once prepared, crystallization plates were stored at 19°C. Evolution of the drops was followed everyday for the first week and then each week and finally more episodically by looking at their aspects with a stereomicroscope.

CHAPTER III :

RESULTS AND DISCUSSION

As mentioned in introduction, Krishna and colleagues studied the ATPase activity of PfATP6 and SERCA1a E255L after heterologous expression in *Xenopus laevis* oocytes (Eckstein-Ludwig et al., 2003; Uhlemann et al., 2005). On microsome preparation, the inhibitory potency of artemisinin and some of its derivatives on the ATPase activity of these two proteins was strongly correlated with their IC_{50} values in cultured chloroquine sensitive parasites. However, the complex environment that represents these membranes may interfere with the ATPase activity measurements and it was therefore interesting to be able to measure these activities and to check the effect of artemisinin drugs on pure proteins.

In this section, I will present the expression, purification and characterization of the mutant SERCA1a E255L and of PfATP6 in order to study a potential inhibition effect of these enzymes by artemisinin drugs. This work has led to a submitted publication (article II).

The procedures of expression and purification were based on the ones developed by Marie Jidenko (Jidenko et al., 2005; Jidenko et al., 2006). It consists in expressing, in yeast, the protein of interest fused to a biotin acceptor domain (BAD) to further purify it by affinity chromatography with streptavidin resin.

This chapter aims at adding supplemental data to the results described in this article.

I.11 Study of the mutant SERCA1a E255L: expression, purification and effect of artemisinin drugs

I.11.1 Expression of SERCA1a E255L BAD in *S. cerevisiae*

The mutant, SERCA1a E255L, was generated by directed mutagenesis of the gene coding for SERCA1a inserted in the vector pYeDP60-S1B as described in the Materials and Methods section of article II, supplemental information. The resultant vector was then transformed in yeast and positive clones were tested to select the one which gives the best expression of the mutant.

Three clones were picked up and submitted to an expression assay on minimal medium (see Materials and Methods of article I and supplemental information of article II). According to the expression levels of these three clones (Fig III.1-1), the second one appeared to give the highest yield. This variation of the expression efficiency may depend on the amount of plasmid copies inserted by yeast. It was shown that yeast transformed with this vector contained between 5 and 20 plasmids (Pompon et al., 1996) because such plasmids autonomously replicate in yeast at a medium copy number.

The second clone was thereby chosen for larger expressions in rich medium. After the culture in Fernbach flasks (see Materials and Methods), 35 mg of yeasts by liter of culture (wet weight) were recovered, which is comparable to the mass usually recovered when expressing native SERCA1a.

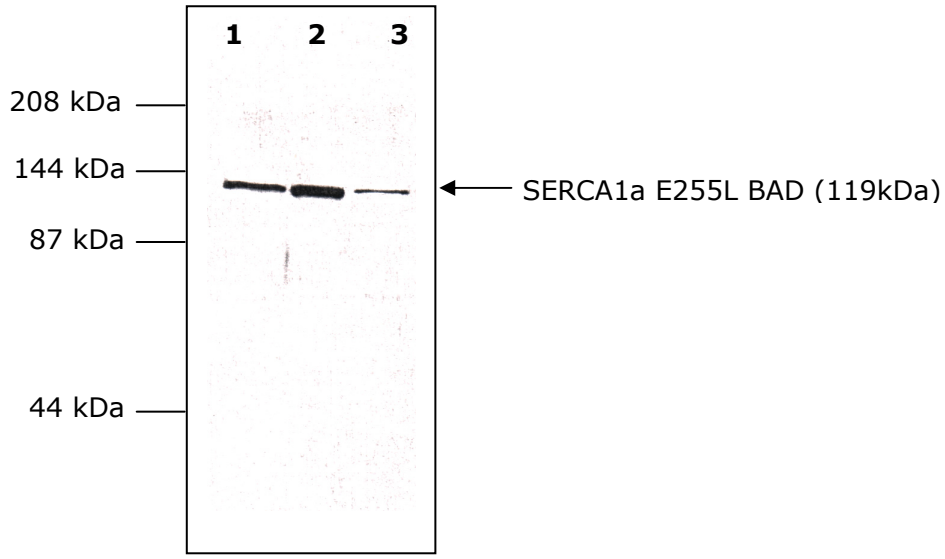

Figure III.1-1: Expression assay of SERCA1a E255L BAD from three yeast clones

Western-blot analysis with anti-SERCA1a antibodies
1,2,3 : ~ 10µg of total proteins

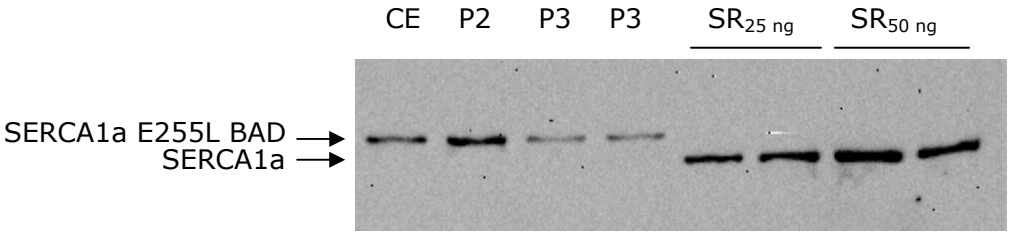

Figure III.1-2: Expression of SERCA1a E255L BAD in yeast (clone 2) in Fernbach

Western-blot analysis with anti SERCA1a antibodies (79b)
CE, P2, P3: 4, 2, 1µg of total proteins of these fractions were loaded
SR_{25ng} and SR_{50ng} : 25ng and 50ng of SR proteins
CE: crude extract; P2: heavy membranes; P3: light membranes

	CE	P2	P3
Total protein amount (mg)	2500 *3000*	800 *600*	325 *500*
Ca^{2+}-ATPase amount (mg)	12.5 *30*	10 *20*	1.6 *5*
% of Ca^{2+}-ATPase compared to total proteins	0.5% *1%*	1.25% *3%*	0.5% *1%*

Table III.1-1: Amount of expressed SERCA1a E255L BAD for one liter of culture

Average of three cultures in Fernbach
In grey are the values obtained for SERCA1a (Jidenko et al., 2006)

Then, yeasts were broken with glass beads, and membrane fractions were isolated by differential centrifugation as described in Article I. The Ca^{2+}-ATPase content of each fraction is presented in fig III.1-2 and in table III.1-1. The amounts of expressed Ca^{2+}-ATPase were determined by comparison with rabbit sarcoplasmic reticulum (SR) which contains more than 80% of SERCA1a. Consequently, the amounts of Ca^{2+}-ATPase given here are amounts equivalent to SR and not absolute values.

According to the amount of mutant contained in the crude extract (CE), it was half expressed compared to SERCA1a (table III.1-1). Although the expression level was lower, the percentage of Ca^{2+}-ATPases contained in heavy membranes (P2) was still threefold superior to the one contained in light membranes (P3). The same phenomena were also observed with other mutants (Marchand et al., 2008). Despite this higher level of Ca^{2+}-ATPases in the P2, Thierry Menguy previously showed that P3 contained more active Ca^{2+}-ATPases than P2, with SERCA1a without tag (Menguy et al., 1998) and Marie Jidenko confirmed it with the use of BAD (Jidenko et al., 2006). Therefore, only the P3 fraction was kept to further purify SERCA1a E255L.

I.11.2 Purification of SERCA1a E55L by affinity chromatography

From P3 fraction (i.e. 2L of cultures), membranes were solubilized and SERCA1a E255L was purified as described in Materials and Methods. The content of the different fractions recovered after each stage of the procedure is presented in Figure III.1-3. The solubilized amount of SERCA1a E255L was here very low (~10%, compare lane TF and SF in Figure III.1-3, panel B) but this value was highly variable in the three experiments I have performed (10%, 70% and 40%). The 10% result may be related to the fact that, in this preparation, DDM was added as a solid powder to the protein solution and not pre-dissolved in the solubilization buffer.

The solubilized SERCA1a E255L was then successfully bound onto the resin (Fig. III.1-3, Panels A1 and B, Lane R) and most of the other proteins, which are not biotinylated, were not retained by the resin and were eliminated with the flow through (Panel A1, Lane FT). Only the biotinylated ones were bound onto the resin but they were not cleaved by thrombin whereas SERCA1a E255L was cleaved (compare lanes R and R2). The thrombin cleavage was only partial since 60% of SERCA1a E255L BAD remained uncleaved (Panels A1 and B lane R2). Marie Jidenko, in her PhD thesis, explained that when she tried to increase the amount of thrombin to improve this cleavage, she observed undesired cleavages and therefore a decrease of the purity of the resultant eluted fraction. For this reason, I did not try to use more thrombin. This incomplete cleavage may be due to a bad accessibility to the thrombin cleavage site. The eluted SERCA1a E255L (Panels A2 and B, lanes E1, E2 and E3) has a high purity of about 70% and is concentrated at about 30 $\mu g.mL^{-1}$ in the first elution fraction (E1). 300µg of SERCA1a E255L were recovered from these two liters of culture.

Although the amount of resin loaded onto these gels were not exactly the same (it is difficult to precisely pipet a given amount of resin), it is clear that part of cleaved mutant was not recovered during the elution step (Panels A1 and B, Lane R*). This was also observed by M. Jidenko with wild type SERCA1a. This may be due to cleaved Ca^{2+}-ATPases still in interaction with uncleaved ones because hydrophobic interactions between these proteins may be higher than interactions with DDM.

This purification led to the recovery of 8% of SERCA1a E255L relatively to the amount contained in P3 before solubilization.

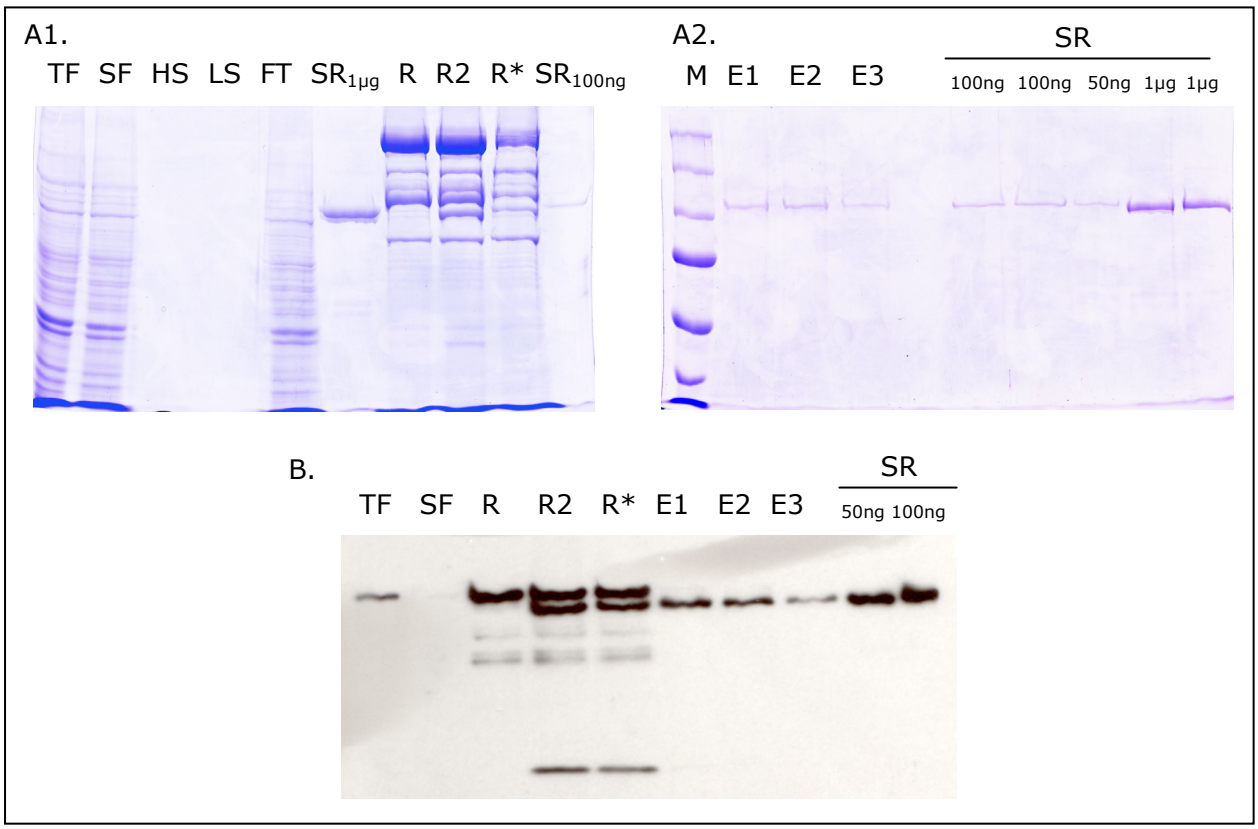

Figure III.1-3: Purification of SERCA1a E255L by affinity chromatography

A1. and A2. Coomassie blue stained gels
10µL of each fraction
SR_{50ng}, SR_{100ng} and $SR_{1µg}$: 50ng, 100ng and 1µg of SR proteins

B. Western-blot analysis with anti SERCA antibodies
SR_{50ng} and SR_{100ng} : 50ng and 100ng of SR proteins

TF: total fraction corresponds to P3 fractions diluted at 2mg/mL in solubilization buffer
SF: solubilized fraction
HS: fraction obtained after high salt wash
LS: fraction obtained after low salt wash
FT: flow through fraction
R : resin after washing
R2 : resin after the two additions of thrombin
R: resin after elution*
E1, E2, E3 : elution fractions
M: molecular mass markers (250, 150, 100, 75, 50 and 37 kDa)

I.11.3 Functional characterization of the mutant and evaluation of the effect of artemisinin

To verify if purified SERCA1a-E255L was a functional mutant and if it was sensitive to artemisinin, its ATPase activity was measured either in detergent ($C_{12}E_8$) or in a mix of lipids (DOPC) and detergent ($C_{12}E_8$). These results are presented and discussed in article II. As these results were different from those obtained by Uhlemann et al. (2005), I checked by DNA sequencing that yeasts were transformed with a mutated plasmid and not with a native one. To this aim, a yeast colony PCR was performed and from the resulting PCR product, a sequencing PCR was carried out (see Materials and Methods). After the analysis of the electrophoregram of this sample, I found the mutated codon in the sequence confirming that I did measure the activity of SERCA1a E255L and not wild type SERCA1a (fig. III.1-4).

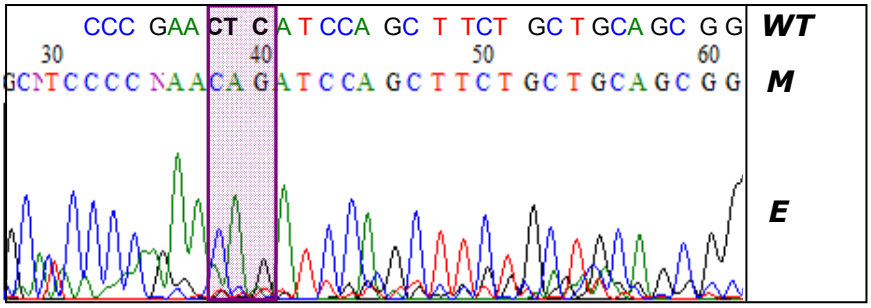

Figure III.1-4: Sequence analysis of Serca1a contained in the plasmid extracted from transformed yeast

*Electrophoregram (**E**) of the complementary region of Serca1a between the codons 253 and 268 (**M**),and comparison with the sequence of the wild type sequence of Serca1a (**WT**). The codon 255 was highlighted by a purple rectangle.*

Consequently, I suspected a problem with the quality of artemisinin I had. So, I went to S. Krishna's lab to measure these activities with their drugs and in their buffers conditions (40mM HEPES pH7.2, 100mM KCl, 4mM ATP, 4mM $MgCl_2$, 100µM Ca^{2+} (from $CaCO_3$)). Of course, it was necessary, in the case of purified E255L to add 1mg/mL $C_{12}E_8$ (while the experiments performed with oocytes were performed on oocyte microsomes supplemented with calcium ionophore) to the reaction solution. These further assays confirmed the fact that this purified mutant was not inhibited by artemisinin (data not shown).

Recently Krishna's group presented evidence that SERCA1a was sensitive to mefloquine, another anti-malarial drugs often used in combination with artemisinin (Toovey et al., 2008). I therefore checked if the mutant was also inhibited by (+)-mefloquine and I measured an inhibition of 51% of its specific activity at 30°C in Tes-Tris pH 7.5, 100mM KCl, 5mM ATP, 6mM $MgCl_2$, 125µM Ca^{2+} (from $CaCl_2$), 1mg/mL $C_{12}E_8$. This inhibition level is similar to the one measured on rabbit SERCA1a. Consequently, mefloquine does not seem to interact with Glu 255.

I.12 Study of PfATP6: expression, purification and effect of artemisinin drugs

As mutated and purified SERCA1a was not sensitive to artemisinin, we decided to study the plasmodial protein, PfATP6, in order to find out if in our conditions, PfATP6 was inhibited by artemisinin. Expressing and purifying a mutant of SERCA1a E255L needed simple adjustments of the protocol but regarding an orthologous protein, we faced the necessity of much more optimizations. Most of the work on PfATP6 is described in article II. This section aims at describing the points of the method that was adjusted for a proper expression and purification of PfATP6.

I.12.1 Expression of PfATP6

S. Krishna gave us two different cDNA of Pfatp6, the wild type one and another with optimized codons for the expression in *Saccharomyces cerevisiae*. Both genes were inserted into the plasmid pYeDP60-BAD after removing the gene of Serca1a. These sub-clonings took almost nine months because of the difficulty to amplify plasmodial genes which are AT rich together with the sequence of the biotin acceptor domain which is GC rich. Several cloning strategies, different polymerases and thermocyclers had to be tried to successfully insert these genes and we were even up to three persons (Christine Jaxel, Estelle Marchal and I) to perform these tests. The final strategies are presented in Materials and Methods and in article II, supporting information.
Once the vectors were ready, expression assays were attempted.

I.12.1.1 Expression assays

After the selection of yeast clones transformed with plasmids containing the wild type sequence (WT) and the codon optimized sequence (CO), two colonies of each were picked up and expression assays were performed as described in article II (supplemental information). In order to verify the expression of PfATP6 in yeast, western-blot analyses had to be performed. For this purpose, Sanjeev Krishna provided us anti-PfATP6 antibodies but as his group had only used them in immuno-fluorescence, we did not know the conditions to detect PfATP6 on a Western-blot (dilution, incubation time and buffer). Consequently, I chose to firstly use a detection method that I already knew and with which I could know if PfATP6 was expressed or not: avidin peroxidase. This method has also the advantage to answer two questions: is the protein expressed? Is it biotinylated? The results are presented in Fig. III.2-1.
The analysis showed that only the codon optimized gene was able to be expressed and biotinylated. Both clones "CO" expressed the protein almost at the same level but I chose to kept clone 1. With this method of detection, no signal was obtained with the clones

transformed with wild type gene. Thus, I could not conclude if this sequence led to a non-biotinylated protein or if this sequence was not expressed at all.

In order to confirm that the biotinylated protein between pyruvate carboxylase and acetyl CoA carboxylase was PfATP6, I developed the procedure to reveal Western-blots with the polyclonal anti-PfATP6 antibodies provided by Sanjeev Krishna. These antibodies were generated in goat from a peptide sequence located in the A-domain (position 128-145) and another targeting the N-domain (position 574-588). After some trials, I found the proper conditions which are described in Materials and Methods and in article II. Both antibodies were working (data not shown) but as the second one gave a better signal with a lower amount, thereafter, I have exclusively used it.

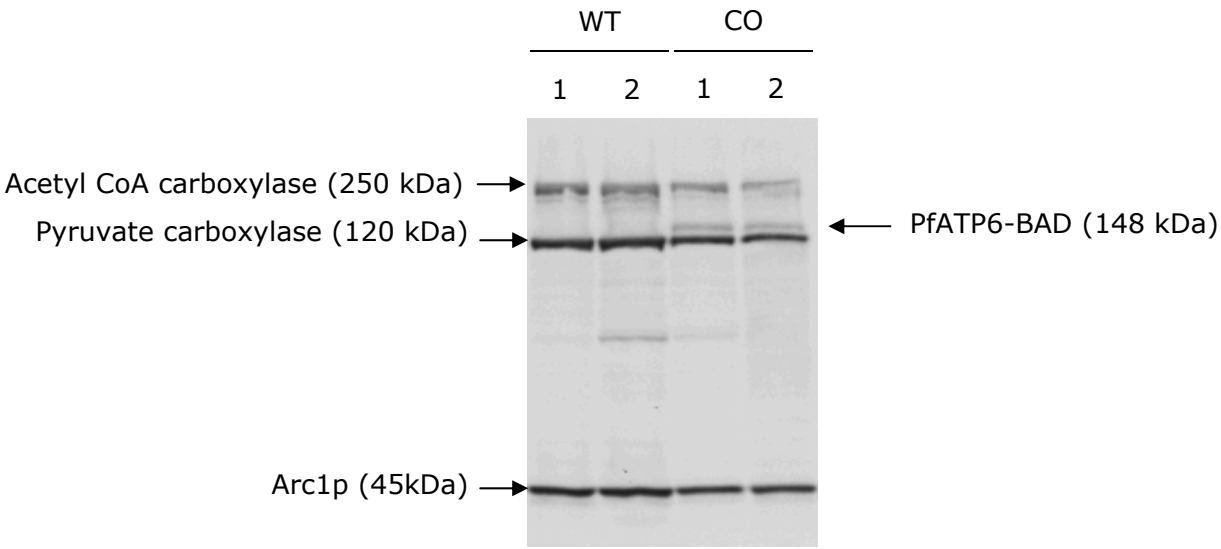

Figure III.2-1: Expression assays of PfATP6-BAD on minimal medium and analysis of the biotinylated proteins.

*Western-blot analysis with avidin peroxidase of the protein content of yeast expressing PfATP6-BAD from its wild type (**WT**) or codon optimized (**CO**) cDNA.*
Two clones of each type of yeast were grown onto minimum medium for overexpression of PfATP6-BAD. Yeast cells were then broken with glass beads and protein were recovered by TCA precipitation.
~10µg of total proteins were loaded in each case.

In order to be sure that yeast could not express WT Pfatp6, I tested different yeast clones. Yeasts were transformed with different ligation products of pYeDP60-Pfatp6wt-bad prepared from bacteria and two clones of each transformant were submitted to expression assays. As a control, the yeast clone containing the codon optimized sequence of Pfatp6 (clone 1) was also submitted to this assay. At the end of yeast cultures, low cell densities were reached (between 0.04 for clone 3.1 and 0.9 for clone 3.2) whatever the

culture. Consequently, for each clone, all the culture volume was used to recover its protein content by TCA precipitation. The results of the Western-blot analysis, revealed with anti-PfATP6 antibodies, are presented in Fig. III.2-2. Although after 2 min of signal acquisition, PfATP6-BAD was only detected from the codon optimized condition (panel A), after a longer acquisition time (14min, panel B), a signal was also visible in the wild-type conditions. Most of the signal was below 100kDa but one band was at the expected size of PfATP6-BAD (148kDa). The bands below 100kDa do not seem to be due to aspecific detection of the antibodies since they are not present in the codon optimized lane. Two hypotheses could explain this result: PfATP6-BAD was expressed from the wild-type sequence but was extensively degraded or partial PfATP6 proteins were generated after premature stop of the transcription. Due to the AT rich content of *P. falciparum* genes, their expression in *S. cerevisiae* can result in mRNAs that are truncated after AT-rich sequences. These AT-rich sequences resemble *S. cerevisiae* sequences that encode the positioning and efficiency elements in the 3' untranslated regions of yeast RNAs that are responsible for specifying the site of polyadenylation. Thus, mRNAs from *P. falciparum* genes expressed in yeast are often prematurely truncated and unable to synthesize full-length proteins (Sibley et al., 1997; Lacount et al., 2009).

In the CO sequence of Pfatp6, these regions were removed when possible (see alignment of CO Pfatp6 and WT Pfatp6 in appendix 2). In appendix 3 is presented the relatively high similarity between the usage codon tables of *P. falciparum* and *S. cerevisiae* which cannot explain why Pfatp6 wt did not express at a high level in yeast.

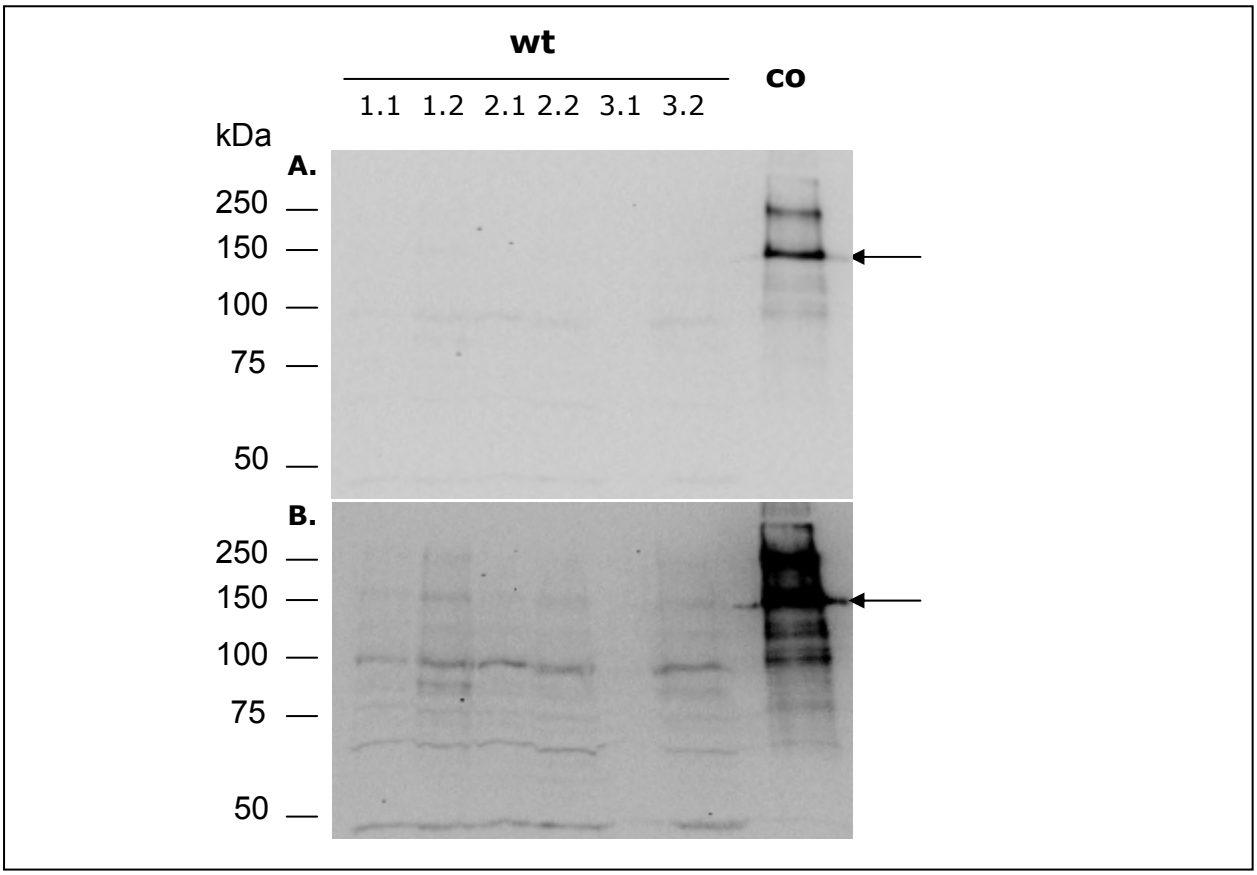

Figure III.2-2: Expression assay of PfATP6-BAD on minimal medium from wild type cDNA of Pfatp6 (wt) and comparison with codon optimized sequence (co)

*Western blot analysis with anti PfATP6 antibodies of the level of expression of PfATP6-BAD after 2 min of signal acquisition (**A.**) and 14 min (**B.**)*
1.1 corresponds to clone 1 of the yeasts transformed with the ligation product pYeDP60-Pfatp6wt number 1. For 3.1, lower amounts of yeast were harvested.
10µL of each protein solution after TCA extraction were loaded, corresponding respectively to 2, 10, 3, 10, 0.5, 10 and 10 µg of proteins for each sample (corresponding to the expected amount of proteins according to the amount of yeast obtained).
The arrows indicate the band corresponding to PfATP6-BAD (148kDa)

I.12.1.2 Effect of the temperature in the expression of PfATP6

In the protocol of large expression in Fernbach, heterologous protein production is triggered after a growth phase of yeasts of 36 hours. As the growth and the expression phases are separated, it is possible to change, from the induction, the yeast environment to obtain the best conditions for protein expression. According to this idea, G. Lenoir *et al*. showed that SERCA1a was more abundant in light membrane fraction (P3) when temperature was decreased to 18°C during the expression phase (Lenoir et al., 2002). I therefore wanted to verify if it was similar with PfATP6.

For this purpose, two expressions of PfATP6-BAD were performed in parallel: one with an expression phase at the same temperature as the growth phase, 28°C, and another with an expression phase at 18°C. The expression kinetic was followed by taking an aliquot of the culture every two hours to measure its optical density at 600nm and to further analyze the protein content by Western-blot after TCA precipitation (as described in Materials and Methods, Article I and supporting information of Article II). By comparison, the expression of SERCA1a performed at 18°C was analyzed in the same way. Contrary to what could be expected, the growth curves, presented in fig. III.2-3, show that yeast grew almost with the same rate whatever the induction temperature and the expressed protein. It seems that, in all cases, the change of substrate and/or the protein expression slowed down the yeast growth.

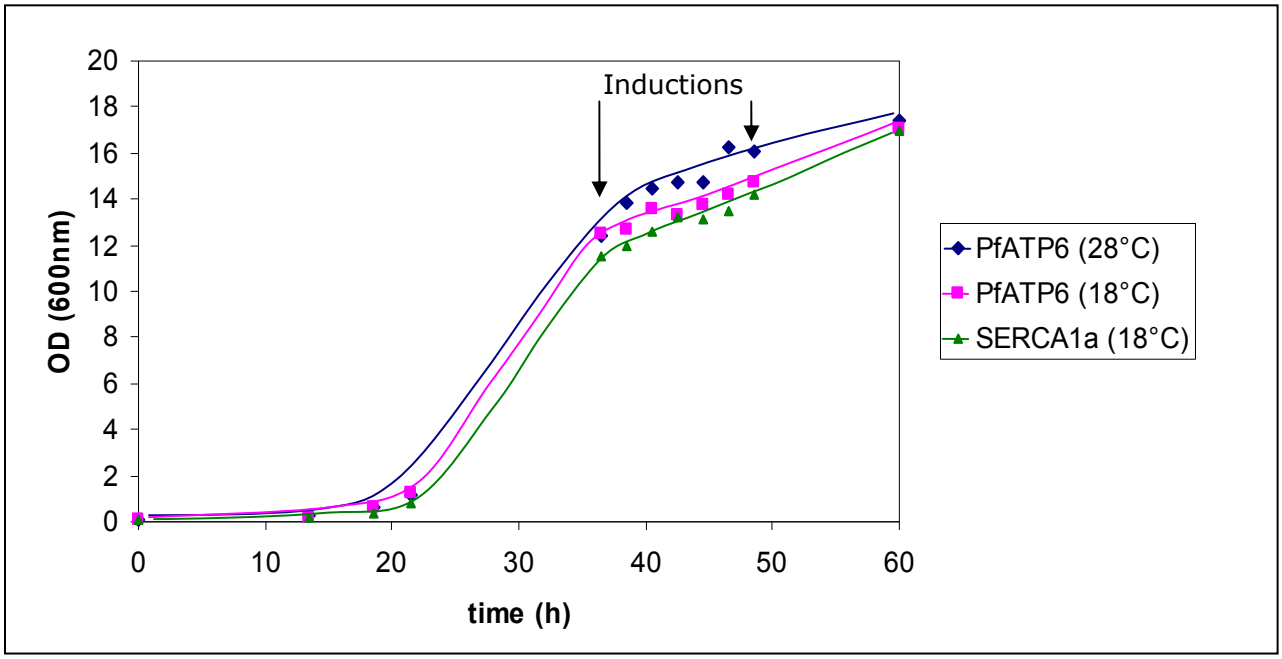

Figure III.2-3: Comparison of yeast growth as a function of the induction temperature (18°C or 28°C) and the expressed protein (PfATP6 or SERCA1a)

Under these conditions, the protein expression level, estimated by Western-blot analysis, is presented in fig. III.2-4. From these data, it can be noted that the level of SERCA1a-BAD increased exponentially during the expression phase, whereas, the level of PfATP6-BAD reached quickly (in 6-8h) an amount from which it did not really increased afterwards, whatever the induction temperature. However, the level of expression of PfATP6-BAD was lower when the temperature of the medium during the expression phase was lowered to 18°C.

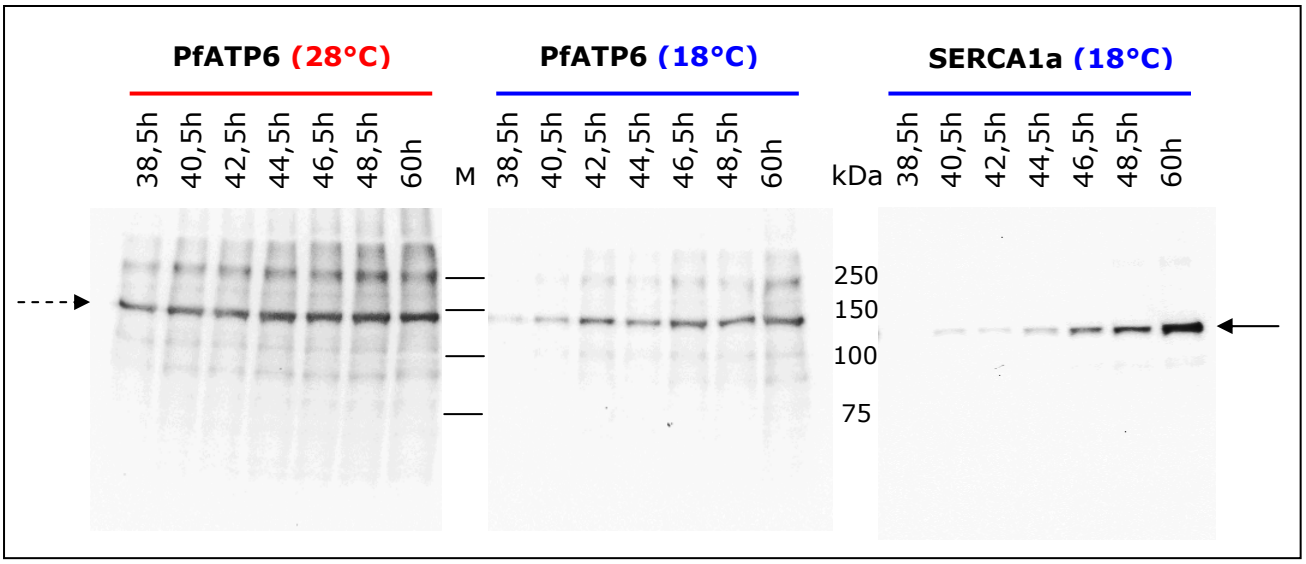

Figure III.2-4: Protein expression kinetic of PfATP6 at two different induction temperatures (28°C and 18°C) and SERCA1a at 18°C.

Western-blot analysis with anti-PfATP6 and anti-SERCA1a antibodies of the protein content of aliquots of the cultures.
PfATP6 samples belong to the same PVDF membrane whereas SERCA1a aliquots were transferred on another one.
The protein content of 4 mL of culture was TCA-precipitated and 1/1000 of each sample was loaded.
M corresponds to the molecular mass marker

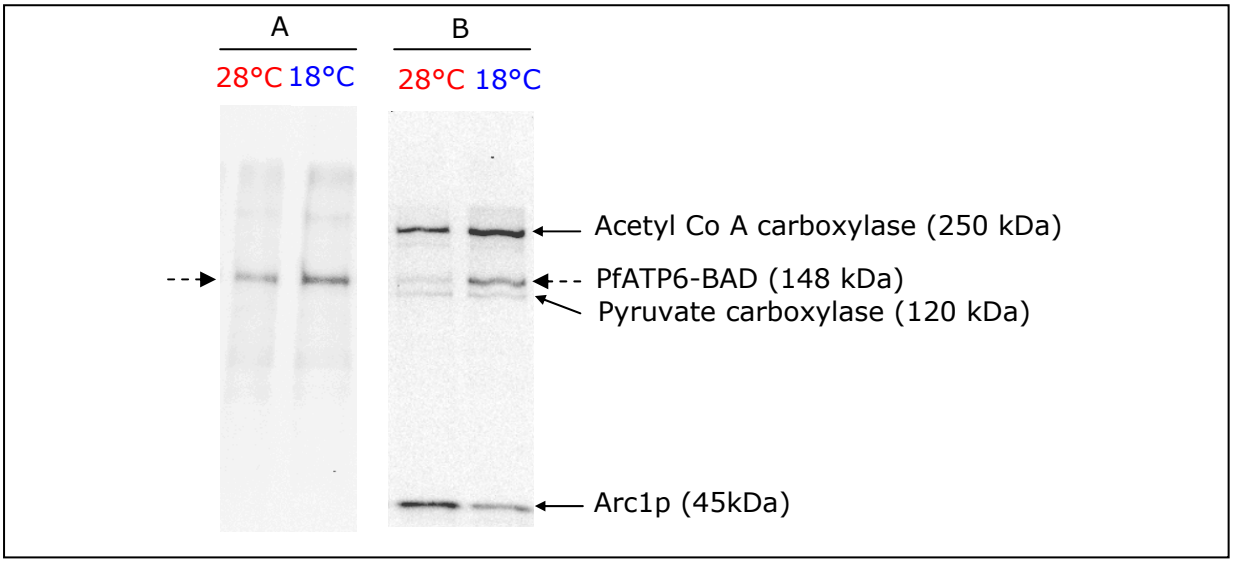

Figure III.2-5: Comparison of the amount of PfATP6-BAD in P3 as a function of the induction temperature.

Western-blot analyses with anti PfATP6 (A) or avidin peroxidase (B) of the light membrane fractions of yeast (P3). P3 were recovered after differential centrifugation of the crude extract obtained from cell breaking of yeasts grown at 28°C or 18°C during the expression phase of PfATP6-BAD.
3µg of total proteins were loaded into each lane.

The same results were obtained with SERCA1a-BAD (Lenoir et al., 2002) but although the general level of protein of interest was lower at 18°C, this amount was higher in the fraction of interest (light membrane fraction, P3). To see if the same phenomenon was observed with PfATP6, Western-blot analyses of the P3 fractions of PfATP6-BAD expressed at 28°C and 18°C were performed (Fig III.2-5). Whatever the detection mode (anti-PfATP6 antibodies or avidin peroxidase), more PfATP6-BAD were contained in P3 obtained after expression at 18°C. We therefore decided to keep this decrease of temperature in the expression protocol.

I.12.1.3 Improvement of the expression level of PfATP6 by using a fermentor

The procedure to heterologously express proteins in yeast via the plasmid pYeDP60, developed by Pompon et al. (1996), was applied in our lab with the use of 500mL Fernbach flasks. These flasks, filled with medium and inoculated with yeasts, were heated and shaked in incubators during the culture. Although it is easy to handle these flasks, problems of reproducibility between the cultures and the need of larger volumes led us to develop a more adapted method. In addition, except the temperature and the shaking rate, no other parameter can be controlled with the Fernbach method whereas it might be interesting to play with other factors to increase the level of expressed proteins. Because all these elements, we have considered the use of a 20L fermentor. Furthermore a protocol had already been described for cultures of 15L of yeasts transformed with pYeDP60 (Pompon et al. 1996). A fermentor is a closed vessel that can be filled with culture medium in which plunged probes, stirrers and addition nozzles to control the culture (description in Materials and Methods).
As PfATP6 was a new expressed protein, I did not have enough experience to deal with this protein first. In consequence, I decided to work first on the expression of SERCA1a to scale up the production procedure from the Fernbach flasks to a 20L fermentor and then to apply it to PfATP6.

I.12.1.3.1 Development of the method with SERCA1a

Before doing the culture scale up, it was necessary to determine the main parameters which govern the yeast culture in Fernbach flasks (500mL) to be able to reproduce them with the fermentor. Consequently, I measured the pH, the percentage of dissolved oxygen and the cell density of the culture performed in Fernbach after the inoculation of the medium with 10mL of a saturated culture in minimum medium (1/50 of the volume

of the medium contained in the flask). The cell density is given by the light scattering of the medium and obtained by measuring its optical density at 600nm. The main conditions are described in Fig. III.2-6 and the results are presented in the Fig. III.2-7. As described in Article I, it can be seen that during the culture, yeasts went through several states. These states come from the different metabolisms they employ to grow. It is indeed well-known that yeast can grow under fermentative or respiration metabolism and are facultative aerobic cells. First, they grew on a medium rich in glucose and consumed a lot of oxygen. During this stage, they used glucose as a substrate through an aerobic fermentation during which they produced ethanol and the growth rate was maximal. Once glucose was depleted of the medium, the growth rate decreased. Thereafter, yeast used ethanol they produced by fermentation and ethanol contained in the initial medium to grow and switched to a respiration metabolism until the induction. However, the medium was almost deprived from oxygen 6 hours before the induction leading to a new decrease of the growth rate. At the induction, the temperature was lowered to 18°C and high concentration of galactose (2%) was added to trigger protein expression. The yeast growth rate accelerated and the amount of oxygen in the medium first increased meaning that yeasts were using galactose as a substrate under an anaerobic fermentation and then decreased suggesting a switch to an aerobic fermentation.

Once these parameters were recorded, cultures were performed in the 20L fermentor but filled only with 6L in order to save some medium and therefore to spare some money. The first culture was carried out by following the parameters described by Pompon et al. (1996) and the second one was an improvement trial of SERCA1a-BAD expression. The culture conditions are described in Fig.III.2-6 and the measured parameters (pH, % of dissolved oxygen and OD_{600nm}) are presented in Fig III.2-7. Total protein concentration and the level of expressed SERCA1a-BAD in each condition are presented in Fig III.2-8.

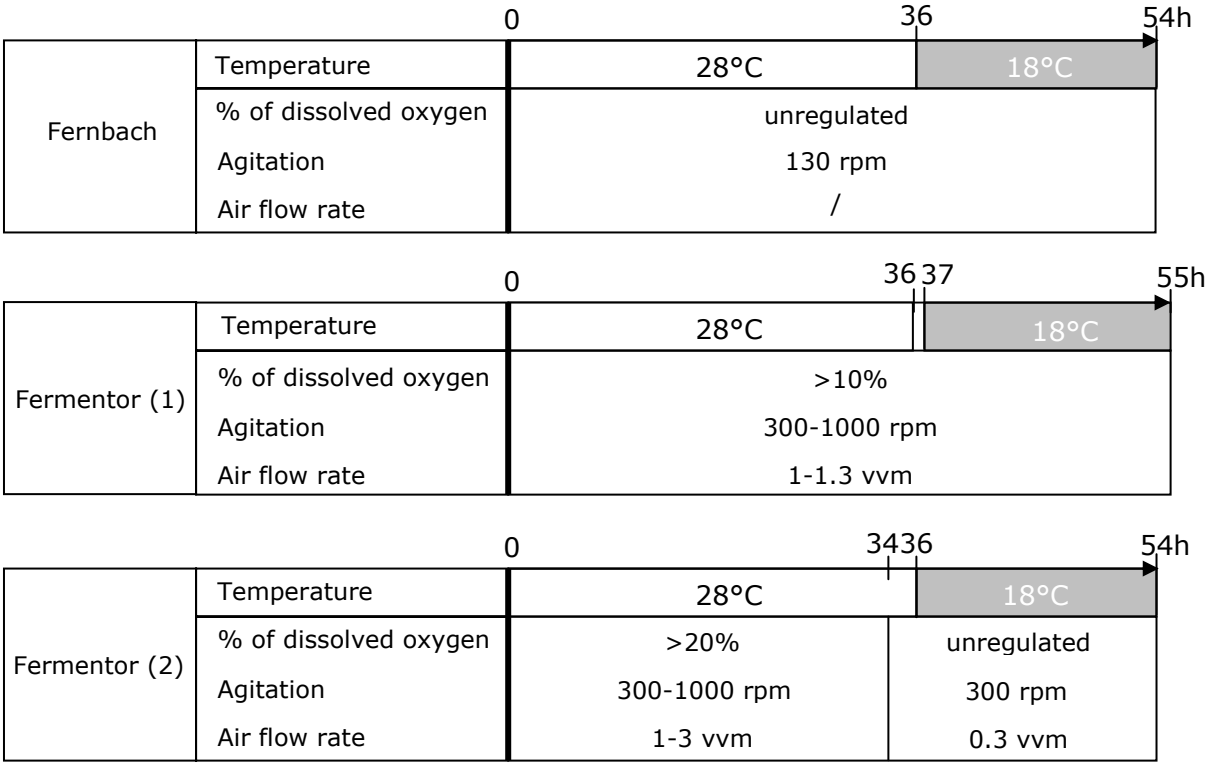

Figure III.2-6: Culture parameters set up in 500mL Fernbach flasks and in fermentor filled with 6L of medium for the expression of SERCA1a-BAD

Periods in grey correspond to the expression phase: the induction, corresponding to the addition of 2% of galactose was triggered after 36h of culture and thirteen hours later, the induction was maintained by adding again 2% galactose to the medium. The culture was stopped 5 hours later.
vvm and rpm corresponds respectively to volume of air per volume of medium per minute and rotations per minute.
In fermentor (1), the induction was delayed of one hour because of a problem with the peristaltic pump.

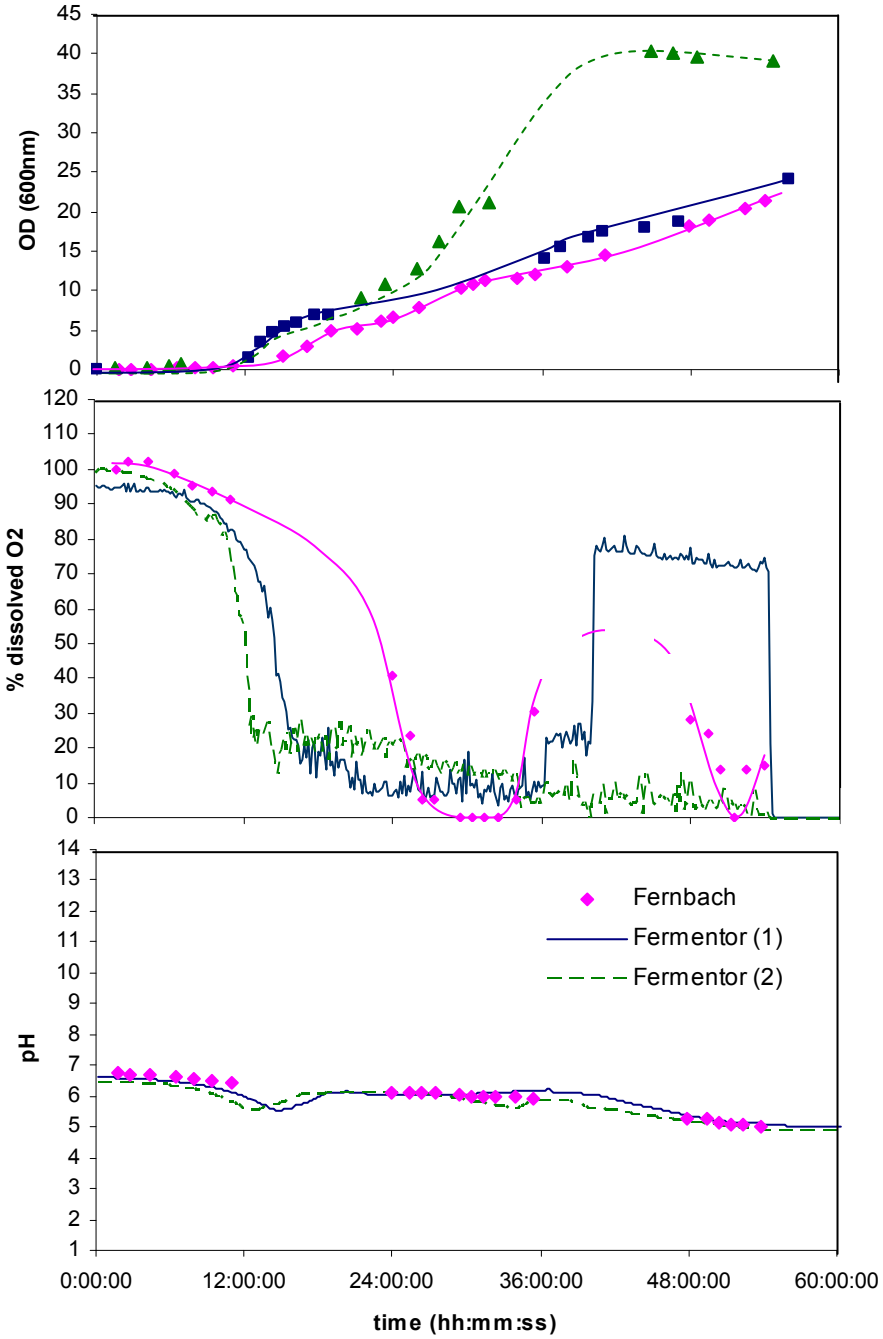

Figure III.2-7: Follow-up of the measured parameters (OD_{600nm}, pH and percentage of dissolved oxygen) during yeast cultures in Fernbach flasks or in fermentor filled with 6L of medium for the expression of SERCA1a-BAD

The curves following the increase of the optical density at 600nm (OD_{600nm}) and also the one following the % of dissolved oxygen measured in Fernbach flasks were extrapolated from the measured values but the real profile might be different.

Fermentor (1) was inoculated with 120mL (1/50 of total volume) of saturated culture of yeast grew in minimum medium and was programmed as described in Fig. III.2-6. Under these conditions yeast grew faster than in Fernbach flasks and the oxygen level decreased faster. Despite this faster start, yeasts then grew almost at the same rate as in Fernbach. Although some measurements are missing in the follow-up of the culture in Fernbach, it can be noted that the pH measured in fermentor followed the same profile as in Fernbach. It can be noted that the change in metabolism is correlated with a change in the pH evolution. In addition, after the induction, the level of dissolved oxygen increased while the regulation parameters did not change. These data argue in favor of a common behavior with the culture in Fernbach and this was verified with the level of expressed SERCA1a-BAD (Fig. III.2-8, compare Fernbach and fermentor 1). With fermentor (1), the level of total proteins and total expressed SERCA1a-BAD was a little higher than in Fernbach flasks but the ratio between the amount of SERCA1a-BAD in P2 and P3 was a little more in favor of P2 compared to the ratio obtained after a culture in Fernbach. Despite this statement, the amount of SERCA1a-BAD in P3 was not dramatically lower since 80% of the usual amount was obtained (4 mg/L of culture here *vs* 5 from a culture in Fernbach).

Since this first trial reproduced almost exactly the culture in Fernbach, I modified some parameters to try to increase the expression of SERCA1a-BAD and especially in P3. To do so, the fermentor was inoculated with a yeast culture in exponential phase (OD_{600nm}=0.6) rather than in stationary phase as suggested in the procedure described by Pompon (Pompon et al., 1996) and the setpoint of dissolved oxygen was turned to 20% (instead of 10%). This resulted in a high increase of the cell density especially when yeasts grew through a respiration metabolism. Then, in order to prepare yeast to store SERCA1a-BAD in its light membranes, the growth was slowed down by stopping the regulation of the percentage of dissolved oxygen and maintaining an air flow rate just sufficient to bring the oxygen necessary to the biosynthesis of unsaturated fatty acids and ergosterol (Bardi et al., 1998). Indeed, when yeast is in anaerobiosis, its growth is slowed down and an extended reticulum network is synthesized (Damsky, 1976). The strategy consisting in decreasing the temperature to increase the amount of SERCA1a-BAD in P3 is also based on the fact that when the yeast growth is slowed down, membranes are synthesized to prepare the future cell division. Under these conditions, as the amount of recovered yeasts was higher (~60mg/L of culture *vs* 40) the amount of expressed SERCA1a-BAD by liter of culture was also higher. In addition, the difference between the amount of SERCA1a-BAD contained in P2 and P3 was reduced and the level of SERCA1a-BAD in P3 was multiplied by 5 compared to the one recovered after the culture in Fernbach.

In conclusion, the modifications brought to the initial protocol allowed a general increase of the expression of SERCA1a-BAD and also an enrichment of this fusion protein in the light membrane fractions. Although these conditions of culture could still be improved, we judged that this new protocol was good enough to apply it to the expression of PfATP6-BAD.

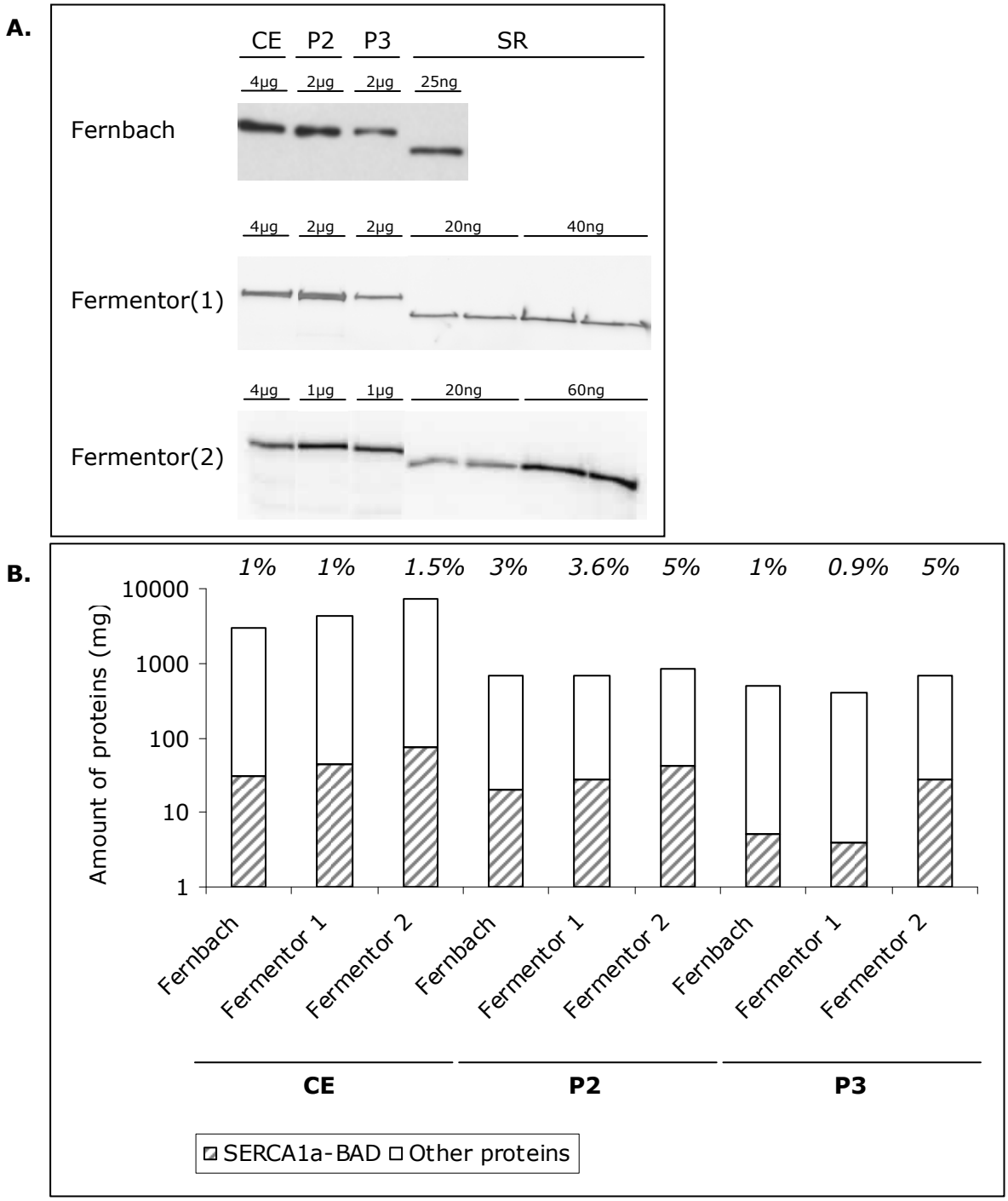

Figure III.2-8 : Comparison of the expression level of SERCA1a-BAD after yeast culture in Fernbach flasks and in fermentor.

A. *Western blot analysis with anti-SERCA1a antibodies of the protein content of the crude extract.*

B. *Graphical view of the SERCA1a content in the different conditions.*

The values of total protein concentration were obtained from bicinchonic acid method and the concentration of SERCA1a-BAD was determined from quantification of the western blot presented in panel A. Values correspond to 1L of culture.

The values on top of the histogram correspond to the percentage (w/w) of SERCA1a-BAD compared to the total amount of proteins contained in each fraction.

I.12.1.3.2 Application of the method to PfATP6

The last expression protocol of SERCA1a developed in fermentor allowed the recovery of about five times more Ca^{2+}-ATPase than usually obtained in Fernbach flask. The aim was therefore to use this last protocol to express PfATP6.

The first expression of PfATP6 in fermentor was set up in 6L culture medium with the same program as SERCA1a. Briefly, it was planned that yeast culture reached an OD_{600nm} of 30 before stopping oxygen regulation and waiting for two hours before decreasing the medium temperature to 18°C and triggering the induction by adding galactose. However, the preculture grew very slowly and instead of inoculating the fermentor with a preculture at OD_{600nm}=0.6, it was only at 0.1. As it induced a delay of the culture of 13 hours, induction time was deferred but I forgot to change the time of stopping oxygen regulation (Fig. III.2-9) which explains why for 4 hours (between 34 and 38h of culture), almost no oxygen was dissolved in the medium (fig.III.2-10, panel B). This trouble induced a deep modification of the initial procedure but did not alter the yeast growth. Moreover, despite these unexpected events, the amount of PfATP6-BAD contained in the membrane fraction of interest (P3) obtained by liter of culture, was increased by a factor higher than 2 compared to what was obtained in Fernbach (fig.III.2-13). This can be explained by higher yeast density (50g/L of culture compared to 30 in Fernbach flasks) and an enrichment of the light membranes content with PfATP6-BAD (PfATP6 represents here 1.8% of the total protein content vs 0.8% in Fernbach).

Although the oxygen regulation stop and the induction were concomitant, a higher amount of PfATP6-BAD contained in P3 was obtained. In consequence, I set up a culture of 20L and I decided to remove the interval between these two steps. This culture should allow the recovery of enough PfATP6 from one expression to purify it for functional and structural characterization experiments. Two cultures (20L_1 and 20L_2) were set up with these new parameters and except a small delay of the preculture in the first case, no problems occurred (fig.III.2-9) leading to a normal yeast growth. However, in both cases, half the amount of PfATP6-BAD was recovered compared to the culture of 6L (fig. III.2-13). This difference could be assigned to the lack of a time period without oxygen during the respiration phase of yeasts. Although I do not understand why, I set up a new 20L fermentor (20L_3) and I added an hour between the oxygen regulation stop and the induction to the process. Again, the culture was deferred for two hours while four hours would have been more appropriate since the preculture was delayed for four hours. This slightly reduced the yeast density but did not affect the overexpression of PfATP6. Indeed, the amount of PfATP6-BAD was improved to be even better than with the 6L fermentor. This confirmed that the adaptation period is crucial to recover more proteins of interest in the light membrane fraction.

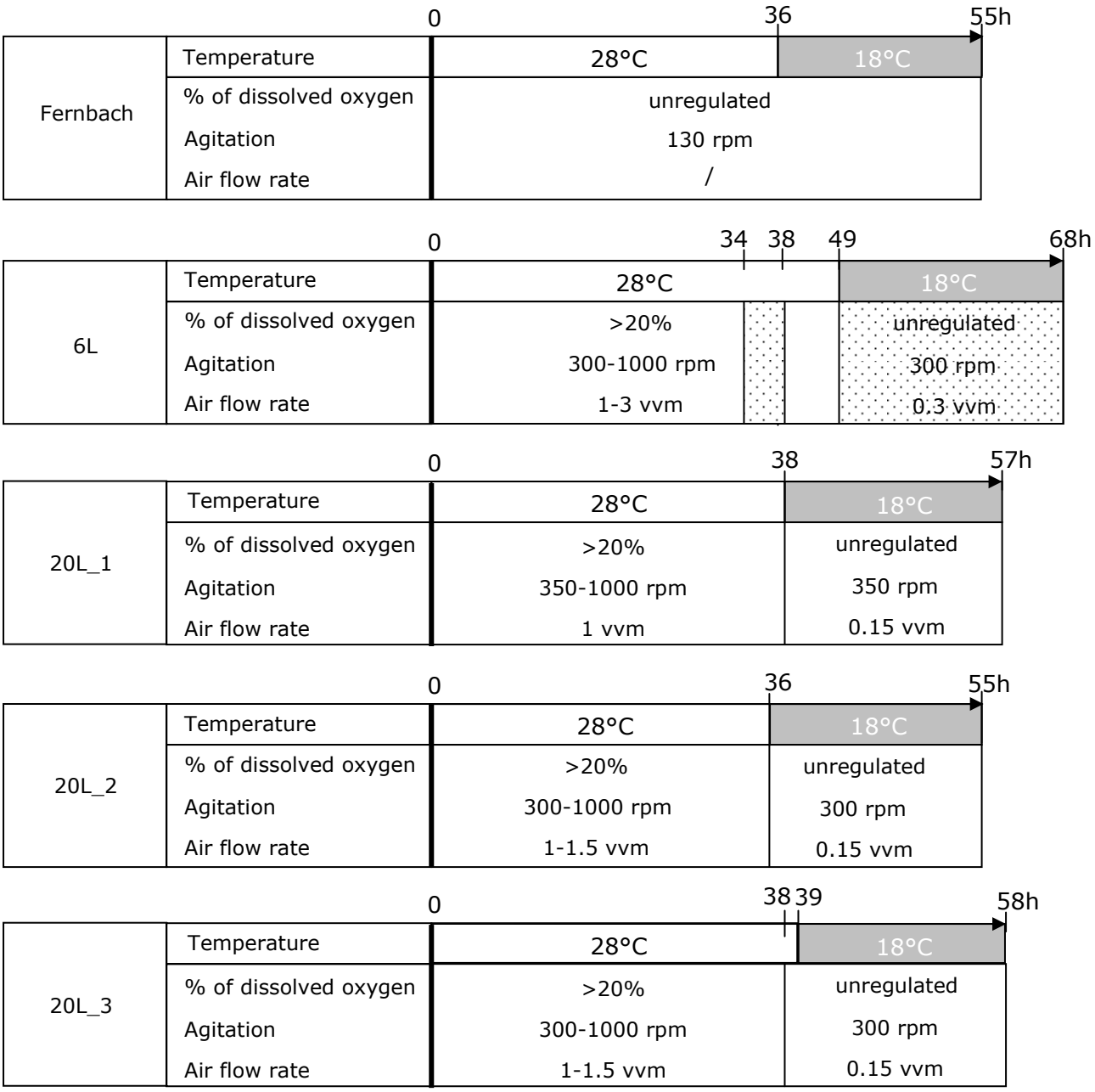

Figure III.2-9: Culture parameters set up in 500mL Fernbach flasks and in fermentors filled with 6L or 20L of medium for the expression of PfATP6-BAD

During the culture in fermentor, the percentage of dissolved oxygen is maintained over 20% by regulating the agitation and the air flow rate in the ranges mentioned in each case.
vvm and rpm corresponds respectively to volume of air per volume of medium per minute and rotations per minute.
The induction, corresponding to the addition of 2% of galactose, was triggered when the temperature of the medium decreased to 18°C first and when OD_{600nm} ~ 30. Thirteen hours after, the induction was maintained by adding again 2% galactose to the medium. The culture was then stopped after 6 hours.
The cultures did not last the same time because it was adjusted in function of the yeast growth. The aim was to induce the expression of PfATP6-BAD nearly at the same OD_{600nm}.

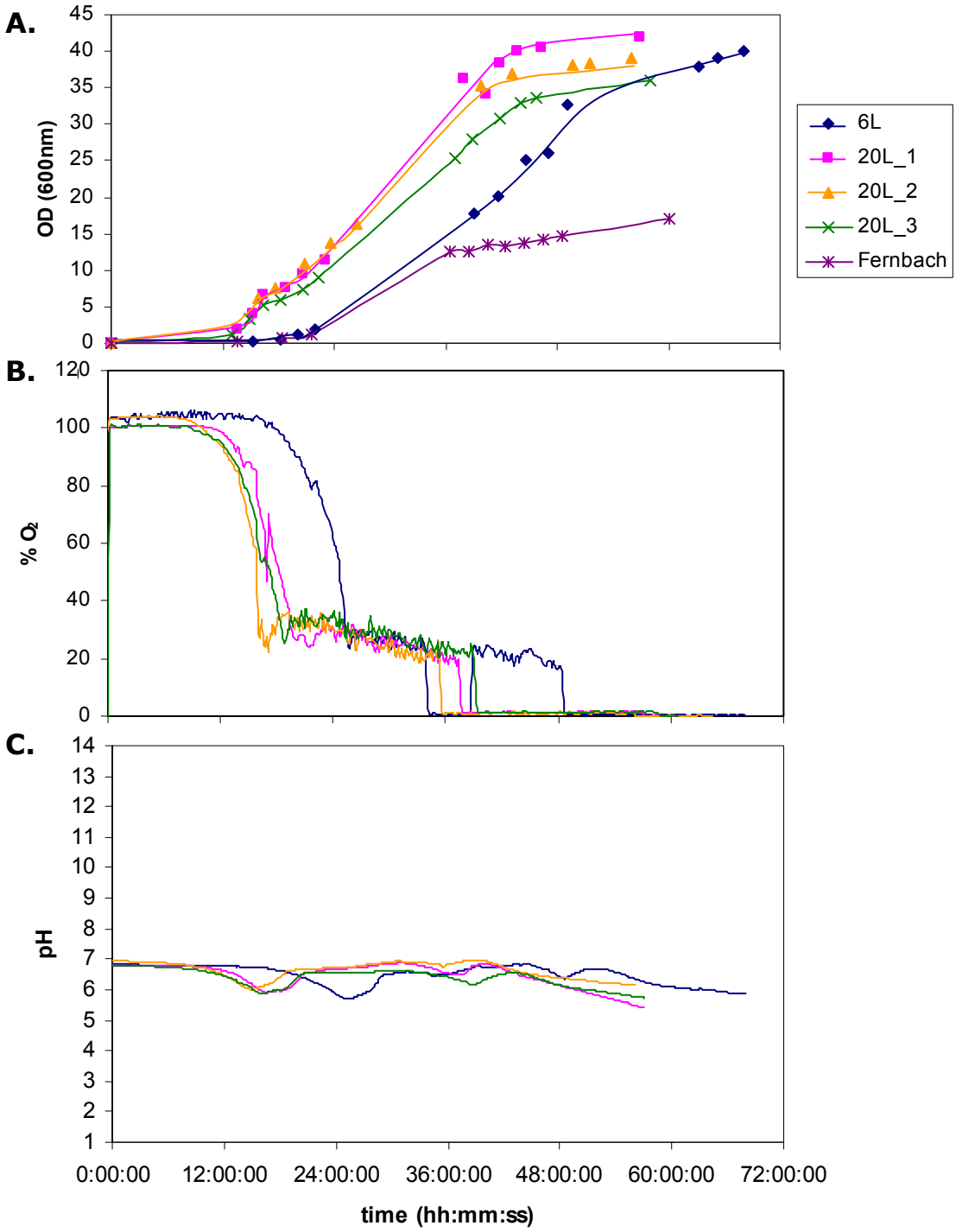

Figure III.2-10: Follow-up of the measured parameters (OD_{600nm}, *panel A*; percentage of dissolved oxygen, *panel B* and pH, *panel C*) during yeast cultures in Fernbach flasks and fermentor filled with 6L or 20L of medium

For OD_{600nm}, curves were extrapolated from the measured values but the real profile might be different.

In general, when comparing the yeast culture parameters (fig III.2-10), slight differences can be seen but the pH and the dissolved oxygen followed almost the same evolution.

Total PfATP6-BAD amounts are important values to know and were easy to obtain by western blot analysis as soon as purified and quantified PfATP6 was available. However, it was also interesting to know the amount of biotinylated PfATP6-BAD since it corresponds to the real fraction of interest (the one which can be purified by streptavidin-Sepharose chromatography). This was more difficult to determine because no commercial biotinylated marker was adapted for quantification. Proteins have to be biotinylated to bind streptavidin resin. Hence, one solution I found was to quantify the amount of PfATP6-BAD bound on streptavidin resin to have a home-made calibrant of biotinylated PfATP6-BAD. To do that, an aliquot of the resin and dilutions of purified and quantified PfATP6 were loaded onto a gel. Concentration of biotinylated PfATP6-BAD contained in this aliquot was determined after quantification on Coomassie blue staining gel. From this quantified resin, it was then possible to determine the amount of biotinylated PfATP6-BAD contained in a sample by western blot analysis with avidin peroxidase. Moreover, if the same quantification is performed, but this time, after Western blot analysis with anti-PfAT6 antibodies, it is even possible to determine the biotinylation percentage of this sample as shown on fig. III.2-11.
This method has a limit to consider. Resin solutions are difficult to pipet. It is therefore very important to carefully homogenize the solution before preparing the dilutions and loading the samples onto the gels to avoid an important error on the subsequent quantification.
I took into account this source of errors and I applied these methods for each sample of P3 to calculate its amount of biotinylated PfATP6-BAD. These results presented in fig. III.2-12 and III.2-13, showed that the amount of biotinylated PfATP6-BAD was almost identical whatever the culture in fermentor. About 50% of PfATP6-BAD were biotinylated but this ratio reached only 30% when more PfATP6-BAD were produced. This suggests that the biotinylation is less effective when too many proteins are produced. Two hypotheses could explain this observation: a lack of biotin or a difficulty to add biotin at a misfolded protein. I did not have time to investigate this point but it could be interesting to supplement the medium with biotin to see if it would improve the biotinylation level. Another idea would be to overexpress biotin ligase via another plasmid inserted in yeast.

Light membranes represent the main fraction of interest but I evaluated the distribution of PfATP6-BAD in the different cell fractions (fig III.2-14), after the culture “20L_3”, to see where the major part of this protein was located in yeast. In one liter of culture it

was possible to produce about 140 mg of PfATP6 (2% of total proteins) but about 30% of this amount were lost during the different steps of membrane preparation. Sixty percent of the remaining proteins (85 mg) were located in the heavy membranes and represented 5% of the proteins of this fraction. Nevertheless, 6% (8 mg) were contained in the light membranes and represented 2% of the proteins of this fraction.

These results show that most of the expressed proteins go to the heavy membranes instead of the light membranes. It could therefore be worth increasing the time of oxygen deprivation before induction to increase the light membranes network in yeast which would store the overexpressed proteins.

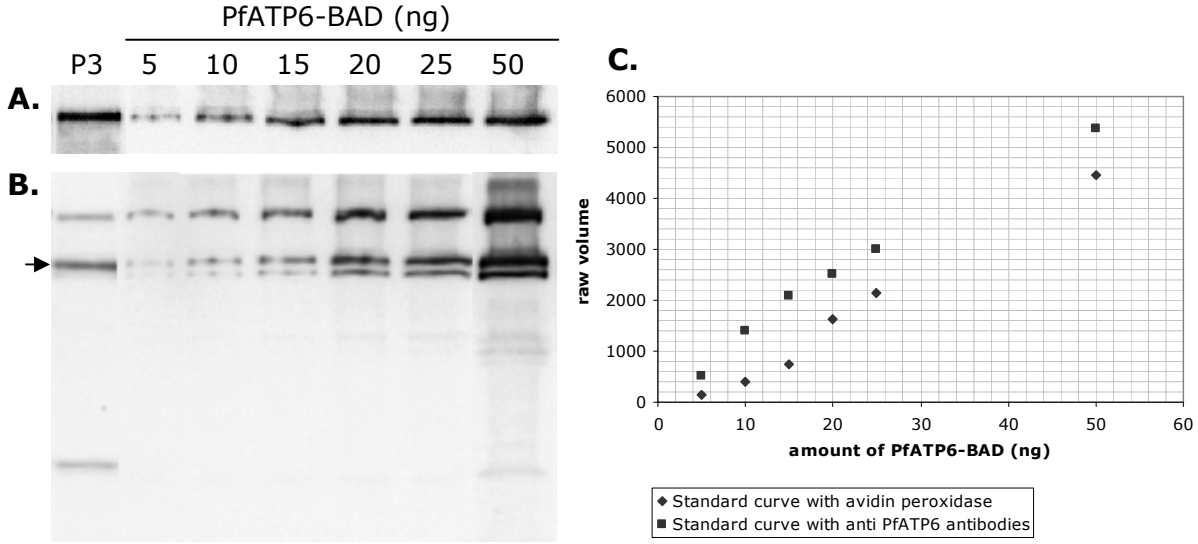

$$\frac{\text{Amount of biotinylated PfATP6-BAD}}{\text{Amount of total PfATP6-BAD}} \times 100$$

D.

Detection method	Raw volume of P3	Amount of PfATP6-BAD (ng)	Biotinylation percentage
Avidin peroxidase	1500	18	**36%**
Anti PfATP6 antibodies	5400	50	

Figure III.2-11: Methods of determination of the biotinylation percentage of PfATP6-BAD

A. Western blot analysis of a range of PfATP6-BAD amounts with anti-PfATP6 antibodies

B. Western blot analysis with avidin peroxidase
P3: 3µg of total proteins loaded (6L fermentor)
Range of PfATP6-BAD: known amounts of PfATP6-BAD bound on streptavidin Sepharose resin.

C. Standard curves of the amount of PfATP6 after densitometry analysis of A. and B.

D. Determination of the amount of PfATP6-BAD and biotinylated PfATP6-BAD from densitometry analysis of A. and B. and the standard curves obtained in C.

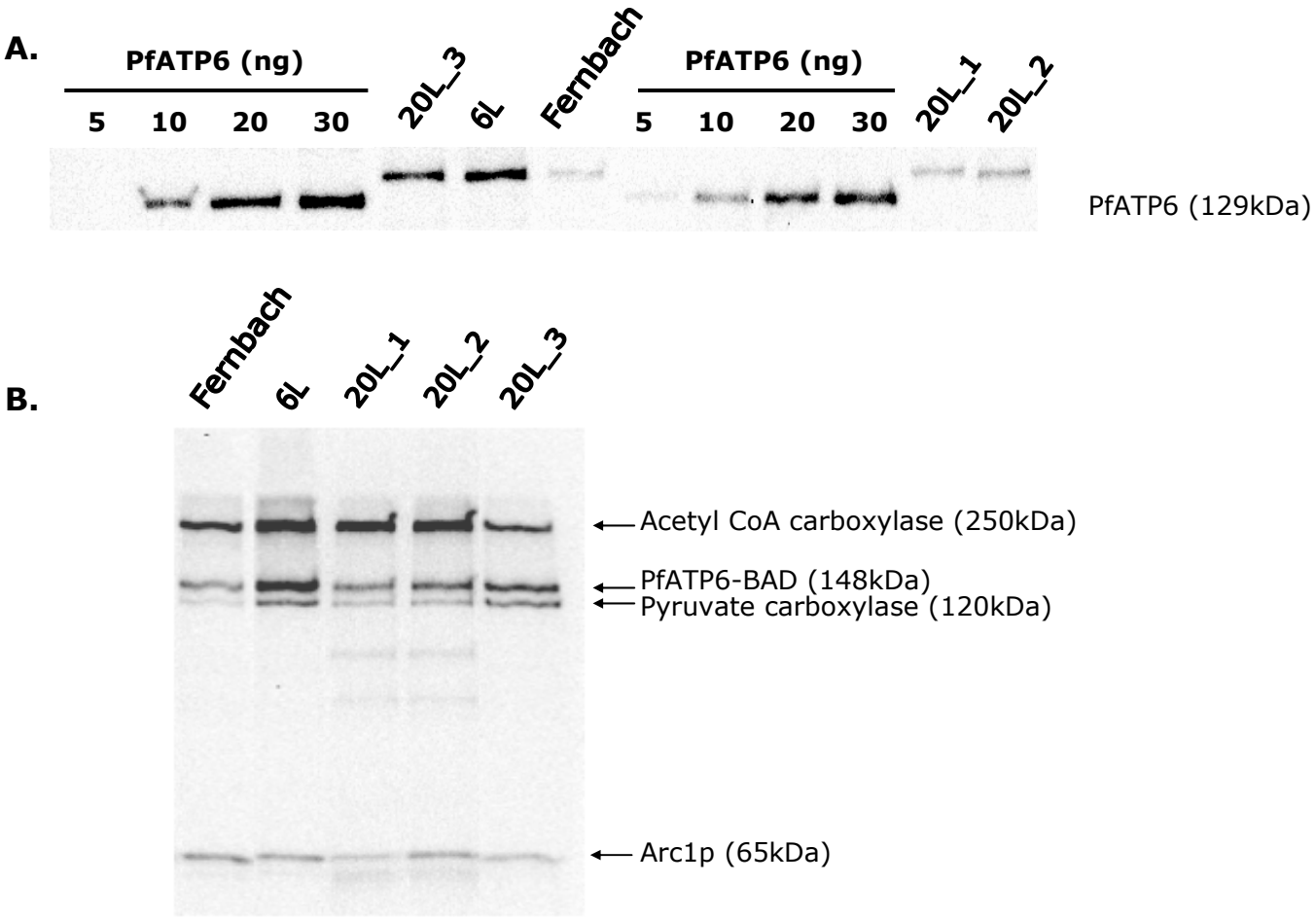

Figure III.2-12: Analysis of the amount of PfATP6-BAD in P3 fractions recovered after yeast culture in Fernbach and in fermentor and comparison of the biotinylation level.

*In panel **A** are presented Western-blot analyses with anti-PfATP6 antibodies and in panel **B** with avidin peroxidase.*
1µg of total proteins were loaded for each P3 fractions.

In panel A, quantified amounts of purified PfATP6 were loaded as standards. They were mixed with 1µg (total protein concentration) of P3 of yeasts transformed with an empty vector (see Article I).
By this way, the conditions are the same for each loaded samples and improve the quality of the quantification.

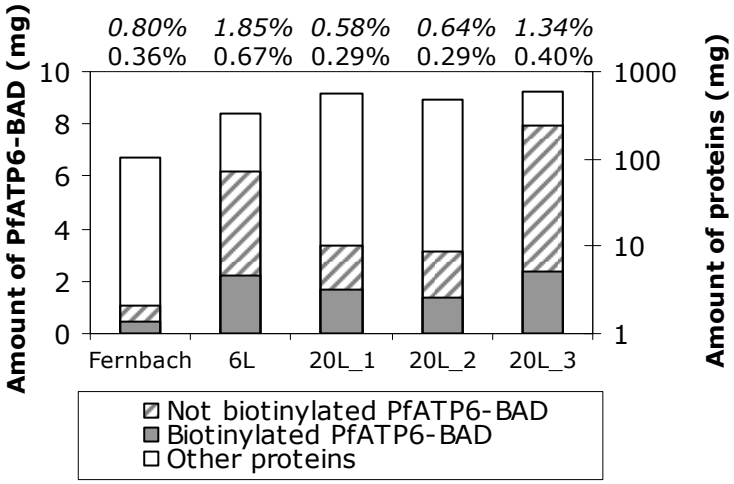

Figure III.2-13: Comparison of the expression level of PfATP6-BAD in light membranes after yeast culture in Fernbach flasks and in fermentor.

The values of total protein amounts were obtained from bicinchonic acid method and are related to the logarithmic scale on the right. Amounts of PfATP6-BAD were determined from quantification of the western blot presented in Fig. III.2-12 panel A. and amounts of biotinylated PfATP6-BAD were determined according to the analysis presented in Fig. III.2-11. Values correspond to 1L of culture.
Values on top of the histogram correspond respectively to the % (w/w) of total PfATP6-BAD (in italic) and biotinylated PfATP6-BAD (underneath) compared to the amount of total proteins.

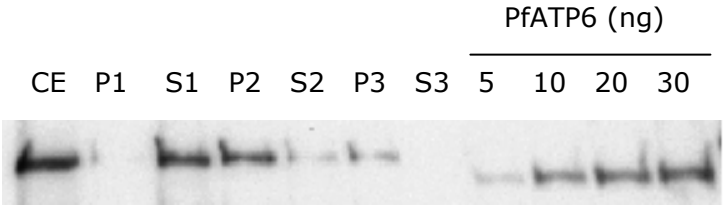

Figure III.2-14: Analysis of the amount of PfATP6-BAD in the different fractions recovered after yeast breaking and differential centrifugation of the crude extract (CE).
2.3µL of CE (i.e. 2.6µg of total protein) was loaded and the same volume was loaded for each derived fraction.
Quantified amounts of purified PfATP6 were loaded as standards with 1µg (total protein concentration) of P3 of yeasts transformed with an empty vector (see Article I).

As the objective was the functional study of PfATP6, as soon as a sufficient amount of expressed PfATP6-BAD was obtained to do functional experiments, the improvement of the expression was stopped. However, it would be interesting to carry on expression trials in order to find a protocol that would lead to a higher recovery of biotinylated PfATP6-BAD in the light membrane fractions.

For this purpose, it would be interesting to follow the distribution of biotinylated PfATP6-BAD between the heavy and the light membranes during the expression process to see if they are first stored into P3 or P2. Nevertheless, according to Cédric Montigny, results previously acquired by former members of our group with SERCA1a fused to a histidine tag (Pierre Falson and Guillaume Lenoir), showed that the Ca^{2+}-ATPases are first stored into light membranes and only when light membranes begin to be saturated, they are stored into heavy membranes. Based on this observation, one strategy could consist in growing yeast at higher density by keeping them in a fermentative state longer than they are. Then, as they left this state because of a lack of glucose, more glucose could be added to the medium. Yeast would be left to grow until they shift for a respiration mechanism (i.e. no glucose, which repressed galactose inducible promoters, remains in solution. The substrate becomes ethanol produced during glucose fermentation). Finally, once the induction would be triggered, a few hours would be sufficient to produce enough PfATP6-BAD in the P3 fraction which will be fully biotinylated (or closely).

I.12.2 Development of the purification of PfATP6

The purification of PfATP6 was based on the protocol previously developed in the lab for SERCA1a (Jidenko et al., 2005). The general procedure was kept but some improvements were necessary to increase the yield of purified PfATP6. The final method is described in article II. This section will aim at describing the stages of the process that were optimized.

I.12.2.1 Washing of light membranes

After the production of PfATP6 in yeast grown in fermentor, the amount of undesired soluble biotinylated proteins such as acetyl Co A carboxylase, pyruvate arboxylase and Arc1p was dramatically increased in light membranes. Two hypotheses could explain this increase. The yeast metabolism was forced to produce membranes and this might increase the production of proteins involved in the fatty acid synthesis like pyruvate carboxylase (a mitochondrial protein) and acetyl Co A carboxylase (a protein associated with the cytoplasmic surface of the endoplasmic reticulum). Their cellular localization justified that they are trapped in the light membranes fraction. Their presence could also

be due to a less efficient membrane fractionation. Indeed, volumes treated after an expression in fermentor are higher than in Fernbach flask and needed the scale up of centrifugation steps. Even if the centrifugation rates and times were calculated to be equivalent, dealing with higher volumes can introduce a bias in the preparation.

As the purification of PfATP6 is based on the binding of biotinylated proteins to streptavidin resin, removing these contaminants could increase the number of streptavidin sites available for the binding of PfATP6-BAD. This might result in a substantial economy of resin. These proteins are soluble whereas PfATP6 is a membrane protein. They might therefore be removed by a deep wash of the membranes.

In the lab, membrane stripping with high KCl buffer (0.72M) was previously attempted and showed an efficient removal of soluble proteins. This method was successfully used to improve the purity of SERCA1a when it was purified with Ni-NTA chromatography (Lenoir et al., 2002). With SERCA1a-BAD, this step did not significantly improve the purity of the protein and was therefore not added to the protocol of purification (Jidenko, 2005). In the case of light membranes of PfATP6, I tested if a KCl treatment of the membranes would remove the biotinylated contaminants. I noticed that washing membranes with 0.5M KCl was very efficient and eliminated almost all the soluble biotinylated proteins. Only some acetyl CoA carboxylase remained. The effect of this washing can be seen in article II, supplemental information.

In addition, I noted that the removal of these proteins increased, as expected, the amount of PfATP6-BAD bound onto streptavidin resin. These results will be detailed in section III.2.2.3.

I.12.2.2 Solubilization of PfATP6-BAD

PfATP6 and SERCA1a are orthologous proteins. PfATP6 is bigger than SERCA1a but the additional amino acids are mainly located in the cytosolic region and the number of transmembrane helices is conserved. This similarity was encouraging to apply to PfATP6-BAD the same solubilization conditions as SERCA1a-BAD.

The solubilization of SERCA1a-BAD consisted in diluting light membranes at 2mg/mL of total proteins in solubilization buffer containing 0.1M NaCl, adding DDM in a ratio 3:1 (detergent:protein, w/w), incubating 2h at room temperature and recovering the solubilized fraction after ultracentrifugation of the solution at 120000g_{av}, 4°C for 30min (type 45 Ti rotor).

Before my arrival, in the lab, it was decided to increase the time of centrifugation to 45min because 30 min were not sufficient to remove aggregated proteins and solubilized proteins. Thereby, the solubilization yield was decreased but the quality of the solublized proteins was higher.

While I just started the first trials of purification of PfATP6, we met Steven Karlish who advised us to try different conditions to improve our solubilization yields: using KCl instead of NaCl because KCl is necessary for the Ca^{2+}-ATPase and could prevent the calcium ATPase from deactivation and therefore aggregation. Moreover, salts may change the cmc of detergents and their solubilizing power.
He also advised us to replace incubation time by the use of a Potter type homogenizer to gain time. Waiting a shorter time might also decrease the formation of aggregates which might appear. Moreover, as we are dealing with higher amount of membranes, this would allow us to work at higher membrane concentrations with the same solubilization efficiency.

In order to test these suggestions, we worked with a material that we know the best: yeast membranes containing SERCA1a.

I.12.2.2.1 Solubilization tests with SERCA1a-BAD

With Bertrand Arnou who has a Post doc position in our lab, we designed a set of solubilization trials from the same membranes to see if this could improve the solubilization efficiency and if we could also spare some time and some detergent. We tested the effect of KCl in comparison with NaCl, the influence of a higher protein concentration, the benefit of the use of a Potter-type homogenizer and we also tried to use a lower amount of detergent. The conditions are summed up in table III.2-1.

The data presented in fig. III.2-15 and summarized in table III.2-1 showed that the use of a Potter-type homogenizer to solubilize higher concentrated membranes gives the same solubilization efficiency as the previous solubilization procedure while it is faster. Since then, this homogenizer has always been used in the lab to carry out the solubilization stages.
The use of potassium chloride instead of sodium chloride increased a little bit the solubilization yield. This latter was especially improved (~10%) with the use of a higher concentration of potassium chloride.
Although the highest yield was obtained with high concentration of potassium chloride and a DDM:proteins ratio of 3:1 (w/w), it is interesting to note that the previous yield of solubilization can be reached with less detergent if 0.5M KCl are used instead of 0.1M NaCl.

DDM:protein (w/w)	2:1		3:1				
Salt	KCl		NaCl	KCl			
Salt concentration (M)	0.25	0.5	0.1	0.1	0.25	0.5	
Protein concentration (mg/mL)	5		2	5			
DDM concentration (g/L)	10		6	15			
Homogeneization	With Potter-type homogenizer (20 slow up and down)		Stirring slowly with a magnet 2h	With Potter-type homogenizer (20 slow up and down)			
Condition number	1	2	3	4	5	6	7
% Solubilization	42%	60%	61%	60%	66%	68%	71%

Table III.2-1: Solubilization conditions tested
Protein referred to the total protein content
The amount of proteins used was 220mg

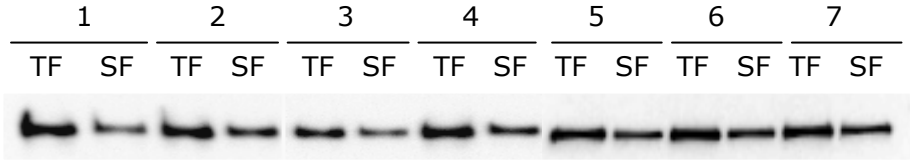

Figure III.2-15 : Solubilization efficiency in different conditions of detergent, homogeneization, protein concentration and salts

Western-blot analysis with anti SERCA1a antibodies

1 to 7 correspond to the conditions described in Table III-2.1
1, …, 7 except 3 : 2µg of total proteins
3 : 0.8 µg of total proteins

TF : Total Fraction, diluted membranes (P3) with detergent before removing unsolubilized content
SF : solubilized fraction, solubilized membranes

As suggested by Steven Karlish, the use of KCl influenced the solubilization process and improved its efficiency. In these experiments, we considered all the SERCA1a-BAD protein but in focusing on biotinylated ones, the solubilization ratios were better (data not shown). This suggests that the pool of proteins which can be purified is of better quality (not aggregated). Does the biotinylation help to select the properly folded proteins?

I.12.2.2.2 Solubilization of PfATP6-BAD

The best conditions of solubilization used with SERCA1a-BAD were applied to PfATP6-BAD: DDM:proteins, 3:1 (w/v); KCl 0.5M and most solubilizations were performed in these conditions. As larger preparations of solubilized PfATP6 were required, the use of more concentrated membranes was more convenient. Therefore, I increased the concentration of membranes to 10mg/mL of total proteins and I verified that this change did not alter the solubilization yield (data not shown).
Before knowing the best conditions of solubilization for SERCA1a-BAD, I attempted some solubilization trials of PfATP6-BAD in the conditions initially applied to SERCA1a-BAD and also replacing NaCl by KCl. The results (fig. III-2.16, panel C) showed a better efficiency of solubilization when using KCl instead of NaCl but as these tests were conducted on different membranes and only once, I will not conclude about a better efficiency of KCl compared to NaCl.
As noted with SERCA1a-BAD, biotinylated PfATP6-BAD were solubilized in a higher proportion than total PfATP6-BAD (fig. III-2.16, panel C).
At the beginning of this section, I mentioned that light membranes were contaminated by soluble biotinylated proteins. A way to remove these contaminants is to treat them with a buffer containing 0.5M KCl prior to their solubilization. To be sure this supplemental step did not affect the solubilization yield, this effect was checked but I did not notice a significant difference between both conditions (compare no treated membranes and washed membranes in fig. III-2.16, panel C).

Although the same conditions of solubilization as those for SERCA1a-BAD were applied to PfATP6-BAD, a lower solubilization yield was achieved. PfATP6-BAD is bigger than SERCA1a-BAD but most of the additional amino acids are likely to be located in the cytosolic region of the protein and the membrane region is rather conserved between these proteins. We could expect a better solubilization efficiency since the soluble part of the protein was extended but a different result was obtained. This could be explained by a proportion of misfolded proteins which can not be solubilized but other reasons could be considered. Indeed, the longer a protein is, the more difficult it is to fold it. Moreover, we do not know if PfATP6 needs some cofactors or post-translational modifications to be properly folded.

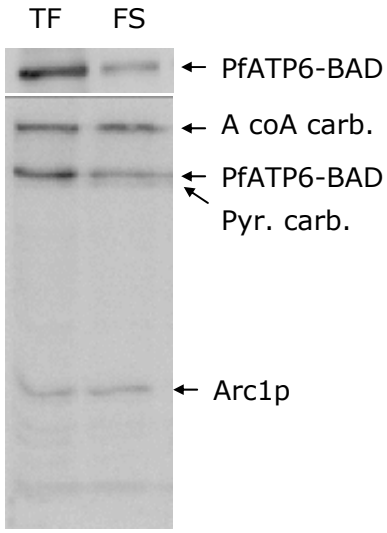

C.

		NaCl 0.1M	KCl 0.1M	KCl 0.5M
Not treated membranes	Total PfATP6-BAD	26%	36%	N.d.
	Biotinylated PfATP6-BAD	34%	50%	N.d.
Washed membranes	Total PfATP6-BAD	Not determined		
	Biotinylated PfATP6-BAD		38%	43±9%

Figure III-2.16: Solubilization ratio of PfATP6-BAD in function of the salt used and its concentration

The proteins were detected either with anti-PfATP6 antibodies (A.) or avidin peroxidase (B.). The % of solubilization (C.) were determined by western blot analysis of the light membranes before (TF, 1µg of total proteins, 0.4µL) and after (FS, 0.4µL) their solubilization (i.e. before and after ultracentrifugation of the membranes in presence of detergent). The values obtained for NaCl 0.1M and KCl 0.1M referred to one experiment only. For KCl 0.5M, 7 values were taken into account.
N.d.: Not determined

I.12.2.3 Optimization of the binding of PfATP6-BAD onto streptavidin-Sepharose resin

Affinity chromatography is considered to be optimal when the maximum of binding sites of the resin are occupied by proteins. In the case of streptavidin-biotin based interactions, the binding sites will catch all the biotinylated proteins until it remains no empty place. However, according to the manufacturer, the streptavidin sites are very close to each other on the resin which is not an optimal configuration for proteins that are much bigger than biotin. Indeed, when a protein binds to a streptavidin, it can mask the other streptavidin surrounding this site. Therefore, the binding capacity of this resin depends on the sample to purify and must be evaluated. To determine the optimal

amount of PfATP6 which will bind to the resin, different amount of proteins were incubated with the same amount of resin and resins were analyzed by Coomassie blue stained gels. This test was performed with two different samples. One sample corresponded to light membranes prepared from yeast grown in the condition "6L" (see III.2.1.3.2) and solubilized. This sample was rich in biotinylated PfATP6-BAD. The other corresponded to light membranes prepared from yeast grown in the condition "20L_1" (see III.2.1.3.2), washed with high KCl buffer and solubilized. These membranes contained a lower proportion of biotinylated PfATP6-BAD.

Although somewhat incomplete, the results presented in fig. III-2.17 showed that PfATP6-BAD binds in larger quantity on the resin when the light membranes were washed prior to be solubilized. As expected, removing the soluble biotinylated proteins freed some streptavidin sites for PfATP6-BAD and the same amount of resin will bind more PfATP6-BAD.

Besides, it appears that if higher amounts of proteins are incubated with the resin, the latter tends to bind more proteins. However, more proteins are also found afterwards in the flow through (data not shown). Under the conditions tried here, one milliliter of resin was able to bind up to 100µg of PfATP6-BAD. To avoid an important loss of PfATP6-BAD during protein binding, it is nevertheless better to use a lower amount of proteins.

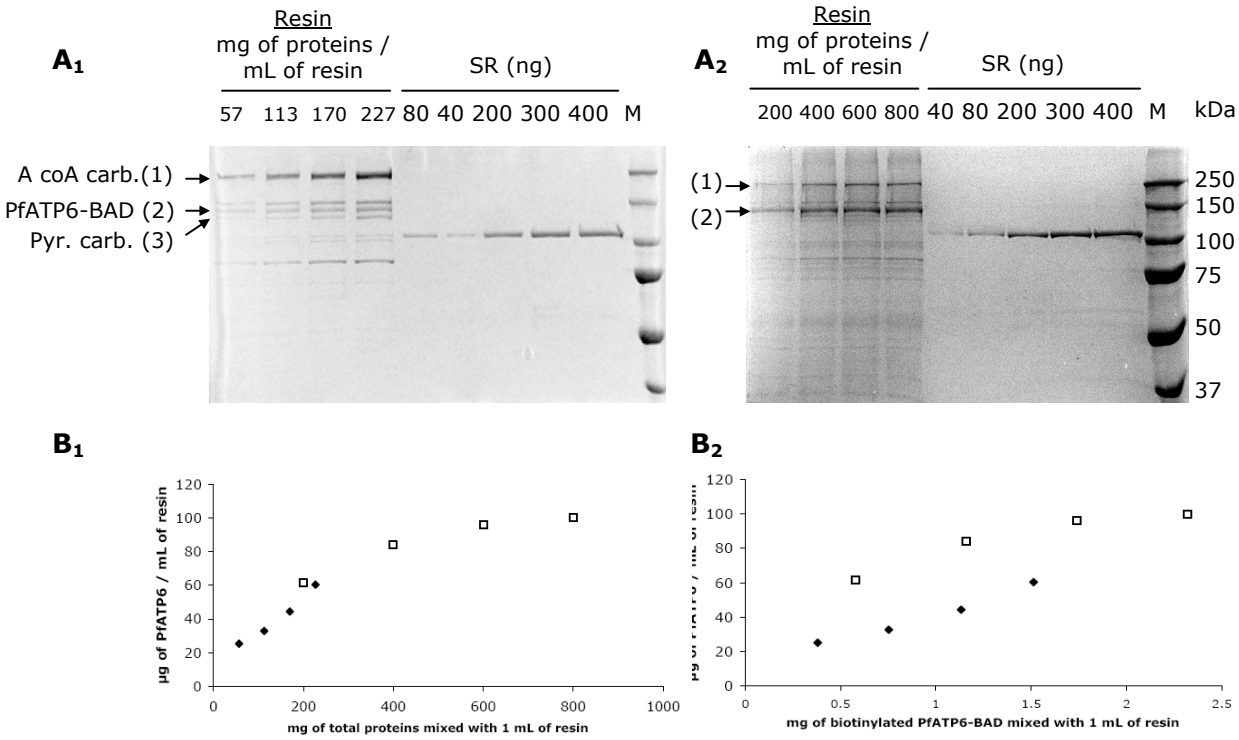

Figure III-2.17: Optimization of the amount of resin in function of the amount of proteins

Different amounts of proteins (mg) were loaded onto 1mL of streptavidin-Sepharose resin. Each amount corresponds to the total protein content of the light membranes before their treatment (washing, solubilization).

Panels A: analysis of these resins with Coomassie blue stained gels.
Each lane (Resin) contains 2.5µl of resin. Resins were incubated with different volumes of solubilized membranes and washed with high salt and low salt buffers.
In A1, light membranes of yeast expressed in the conditions "fermentor 6L" were used (6.7µg of biotinylated PfATP6/mg of total proteins in P3).
In A2, washed light membranes of yeast expressed in the conditions "fermentor 20L_1" were used (2.9µg of biotinylated PfATP6/mg of total proteins in P3).

Panels B: graphical analysis of the results
♦ corresponds to the condition A1 and □ to the condition A2
B1 allows the determination of the amount of bound PfATP6-BAD in function of the amount of total proteins used for the purification
B2 gives a view of the amount of bound PfATP6-BAD in function of the amount of biotinylated PfATP6-BAD used for the purification.

The loss occurring during the solubilization and the resin binding seems to be due to the protein quality. Aggregated proteins seem to be lost during the solubilization process and misfolded proteins during the binding to streptavidin. Although this would require further investigations, we could make the hypothesis that this purification step acts in selecting biotinylated proteins but also in selecting proteins of good quality and therefore potentially active proteins.

I.12.2.4 Effect of β-mercaptoethanol and lipids on the purification of PfATP6 and comparison of its purification with the streptavidin-Sepharose and avidin-agarose resins.

A.

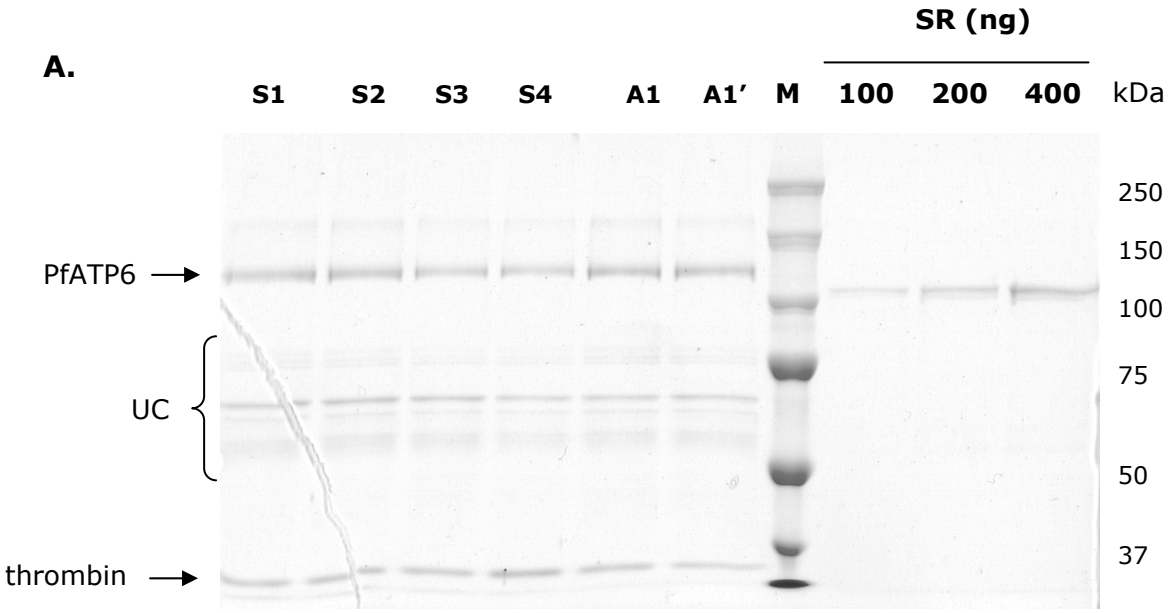

B.

	S1	S2	S3	S4	A1	A1'
Concentration of purified PfATP6 (ng/mL)	103	92	59	57	82	84
ATPase activity (µmol of ATP/mg of PfATP6/min) $C_{12}E_8$ 1mg/mL *	2.3	1.9	2.1	2	2.4	not measured

Figure III.2-18: Evaluation of the effect of β-mercaptoethanol and DOPC on the purification and comparison of streptavidin-Sepharose (S1 to S4) and avidin-agarose (A1, A1') resins

*The conditions **S1** correspond to the usual conditions, the purification was performed with buffers containing 1mM β-mercaptoethanol. This reducing agent was removed from the low salt buffer in **S2.***
***S3** and **S4** are the equivalent of S1 and S2 but the purification was performed with a buffer containing 0.2mg/mL of DDM and 0.05mg/mL of DOPC.*
***A1** and **A1'** are equivalent to S1 but avidin agarose resin was used. For A1', more proteins were incubated with the resin.*
***SR_{100}, SR_{200}, SR_{400}**: 5, 10 and 20µL of SR proteins at 20ng/µL*
The elution fractions recovered in each condition were analyzed on Coomassie blue stained gels (Panel A) to determine the amount of purified PfATP6. Then, their ATPase activities were measured (Panel B). UC=unspecific cleavages caused by thrombin.
** In article II and later in this thesis, we will see that, in fact, the protein is unstable without lipids. Here, the activity was measured on a short time period (2min).*

In the initial protocol of purification of SERCA1a developed in the lab (Jidenko et al., 2006), 1mM of β-mercaptoethanol was added in the solubilization buffer and also to the high salt and low salt buffers used to wash the resin. β-mercaptoethanol is a reducing agent which is used to protect proteins and maybe lipids against oxidation. As the aim of my PhD was to characterize the effect of artemisinin known to form active radicals, it was necessary to remove from the buffer all molecules that will react with these radicals and therefore β-mercaptoethanol.

β-mercaptoethanol has been already removed from the protocol of purification of SERCA1a when Alexandre Marchand, in our lab, studied oxidative cleavages of different mutated SERCA1a to investigate structural modifications of these mutants. He did not mention any modification of the purification process and any change in the ATPase activity of SERCA1a. To determine if the purification of PfATP6 and its activity was affected by the removal of β-mercaptoethanol, I prepared purified PfATP6 with and without this reducing agent. To do that, I only removed β-mercaptoethanol, in one case, from the low salt buffer.

The lack of reducing agent did not extensively affect the yield of purification since the amount of eluted PfATP6 was equivalent in both cases (compare lanes S1-S2, and S3-S4 on fig. III.2-18). Regarding the activity of PfATP6, it was a little lower in absence of β-mercaptoethanol but this difference was very small (~10%). I therefore felt confident to remove β-mercaptoethanol from the low salt buffer.

Steven Karlish and his group are adding lipids during the purification of the Na^+,K^+ ATPase. They showed that it increased the stability of the protein during the purification (Haviv et al., 2007). Indeed, during the purification process, proteins are washed with high volumes of buffers containing detergents and lipids essential for the protein are likely to be released. To verify if the addition of lipids could allow the recovery of more active proteins, the washing buffers of the resin (high salt and low salt buffers) were supplemented with 0.05mg/mL of DOPC and the concentration of detergent (DDM) was lowered to 0.2mg/mL (instead of 0.5). However, with this new buffer, 40% of the protein was not eluted from the resin (fig. III.2-18, compare lanes S1,S2 to lanes S3,S4) despite the fact that it was fully cleaved by thrombin (data not shown). Thus, cleaved PfATP6 seems to remain associated to the resin by unspecific binding and this is likely to be mediated by the presence of lipids. Besides this lower recovery, the ATPase activity of this purified sample was measured and it was not significantly different than in absence of DOPC (fig. III.2-18, panel B). As no better activities were obtained, this did not encourage me to add lipids during the purification of PfATP6 since it decreased too much the amount of purified PfATP6 recovered.

The last thing I wanted to compare was the global efficiency of purification of streptavidin-Sepharose resin compared to avidin-agarose resin, the former resin used with SERCA1a. Therefore, I followed the same protocol of purification for both resins and I compared the amount of eluted proteins. A lower amount of proteins was eluted from avidin-agarose compared to streptavidin-Sepharose (~80%). In parallel, a sample of avidin resin was also incubated with 1.5 times more proteins to see if more proteins could bind to avidin-agarose compared to streptavidin-Sepharose but in both conditions, more PfATP6-BAD were found in the flow through of avidin resins (data not shown). These results proved that the use of streptavidin-Sepharose resin instead of avidin-agarose resin was a benefit in terms of purification effectiveness but also in terms of financial view since streptavidin-Sepharose resin is twice cheaper than avidin-agarose resin!

I.12.2.5 Optimization of the thrombin cleavage

The aim was to determine the appropriate amount of thrombin necessary to cleave efficiently PfATP6-BAD without unspecific cleavages of PfATP6 or other bound proteins. For this purpose, I firstly used the same cleavage conditions as SERCA1a-BAD (25U of thrombin/mL of resin and incubation at room temperature for 30 min, twice) but they were inappropriate to PfATP6-BAD since some unspecific cleavages appeared (see eluted fractions on fig. III.2-18).

Consequently, it was necessary to test different cleavage conditions to find the best ones. Thus, streptavidin-Sepharose resin was incubated with washed and solubilized light membranes of yeast containing PfATP6-BAD. It was then divided in 5 equivalent samples and incubated with different amounts of thrombin at room temperature. An aliquot of each sample was taken at different time and was analyzed by electrophoresis. Coomassie blue stained gels are presented in fig. III.2-19. Taking into account that unspecific cleavages should be avoided, the best cleavage conditions found consisted in incubating the resin with 10U of thrombin per milliliter of resin for 30 min. From this experiment, I also noticed that incubating the resin with 20U of resin for 10 min did not lead to extensive unspecific cleavages. Consequently, in another experiment, I tried to incubate the resin with 10U/mL of resin for 10 min and then with 10 more units per milliliter of resin 10min and, again, for 10min. These conditions lead to almost complete cleavage of PfATP6-BAD with only few unspecific cleavages (see article II) and were then applied to all the purifications of PfATP6.

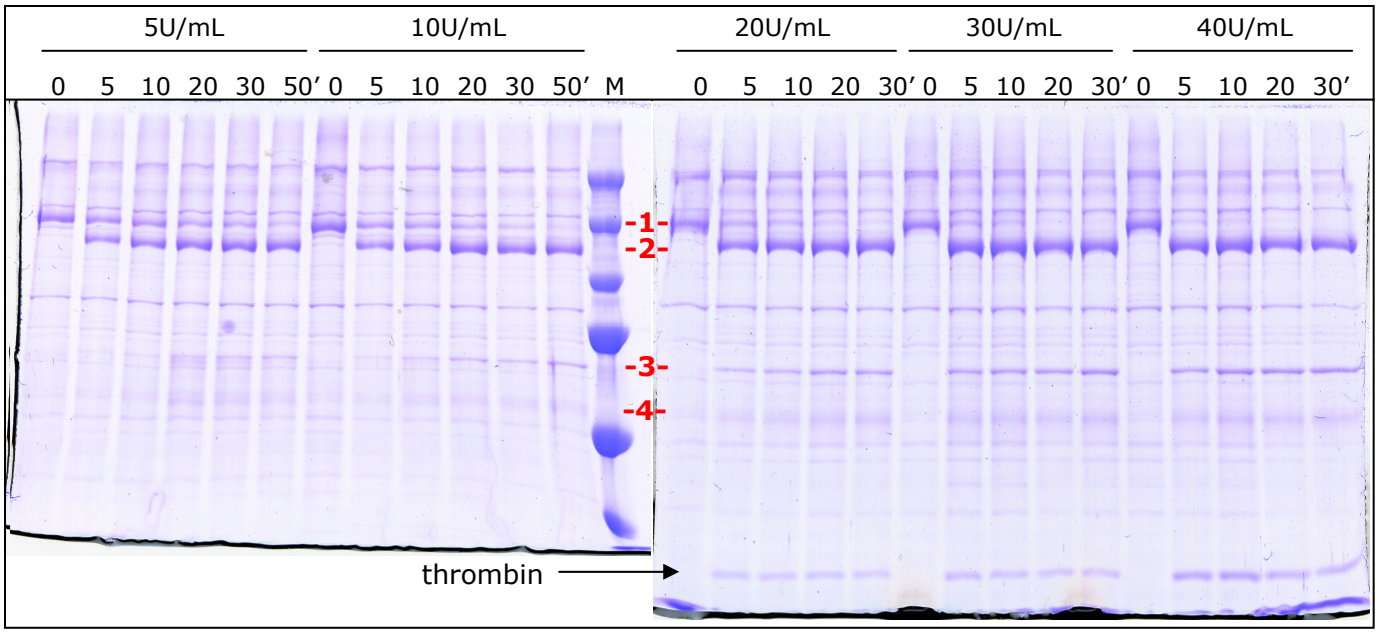

Figure III.2-19: Kinetic of the cleavage of PfATP6-BAD using different amounts of thrombin

Coomassie blue stained gels loaded with 2µL of streptavidin-Sepharose resin.

Resins loaded with PfATP6-BAD (-1-) were treated with different amounts of thrombin. These amounts are indicated in units of activity by mL of resin. During the incubation of thrombin (the time is indicated in minutes above the gels), PfATP6 (-2-) is released from the resin and other proteolytic cleavages occurred (-3-, -4-)

Under these conditions and even in the usual cleavage conditions of SERCA1a mentioned above, PfATP6-BAD was more efficiently cleaved than SERCA1a-BAD since almost 100% of PfATP6 was released whereas this yield reached only 60% with SERCA1a-BAD (Jidenko et al., 2006). This can be due to the longer C-terminus chain of PfATP6 which leaves more space for the thrombin to bind to its recognition site (between PfATP6 and BAD).

I.12.3 Reconstitution of PfATP6 in a lipid environment

When Ca^{2+}-ATPases are solubilized in detergent, their ATPase activity can be altered (Lund et al., 1989) and of course no calcium uptake can be measured because of a lack of closed compartment. One way to get rid of these problems is to reconstitute the proteins in tight and unilamellar proteoliposomes.

Since it is a difficult step, I tried different methods to reconstitute PfATP6 in a lipid environment.

One method used by Jesper V. Møller's lab (University of Aarhus, Denmark) to successfully prepare SERCA1a proteoliposomes, consists in forming unilamellar liposomes of DOPC by dialysis, combining detergent destabilized liposomes with membrane proteins in a ratio of 60:1 (w/w) in presence of glycerol and slowly removing detergent to form tight and unilamellar vesicles (see Materials and Methods). Glycerol protects membrane proteins during the reconstitution process (Geertsma et al., 2008). I therefore joined his group to learn from their experience in SERCA1a reconstitution and to perform some reconstitution assays of PfATP6.

As this reconstitution aimed at measuring calcium uptake, it is important to avoid a high intravesicular free calcium concentration. Indeed, a high intravesicular free calcium concentration inhibits the Ca^{2+}-ATPase for bioenergetic reasons (Moller et al., 2005). To sustain the activity of the Ca^{2+}-ATPase for the experimental time (~1h), vesicles are prepared in phosphate buffer. Phosphate will precipitate with intravesicular calcium which will maintain a low free calcium concentration inside the vesicles.
During the reconstitution process, Ca^{2+}-ATPases will be transferred from mixed micelles to detergent-saturated liposomes. This is achieved by using destabilized liposomes with a detergent concentration between Rsat and Rsol (see fig. III.2-20, β-octylglucoside). For the first reconstitution trial, a high cmc detergent was used: β-octylglucoside (cmc~6.5mg/mL). This detergent was shown to alter the ATPase activity of the rabbit Ca^{2+}-ATPase but was successfully used to reconstitute it (Jidenko et al., 2006). To avoid extensive alteration of the enzyme, the solution of lipid-protein-detergent was therefore not preincubated before starting the detergent removal and detergent was removed with a fast process, the use of polystyrene beads (Bio-beads SM2). However, to avoid the formation of undesired multilamellar vesicles by a too fast reconstitution process, detergent was progressively removed by several additions of small amounts of Bio-beads instead of a large amount in once.
The conditions of reconstitution are detailed in Table III.2-2.
In these conditions (1), the reconstituted sample showed a very low ATPase activity that represents only 7% of the activity of the protein before reconstitution. In parallel, a reconstitution of affinity-purified SERCA1a was performed under the same conditions, and in this case, the sample kept more than 30% of its activity before reconstitution. The reconstituted sample of PfATP6 showed a calcium accumulation inside the vesicles. According to his experience, JV Møller considered that the level of accumulation was consistent with an active transport. However, it can be noticed that PfATP6 and SERCA1a did not share a common behavior during this reconstitution process since SERCA1a remained more active (more than the 3 times expected from their activities measured in detergent).

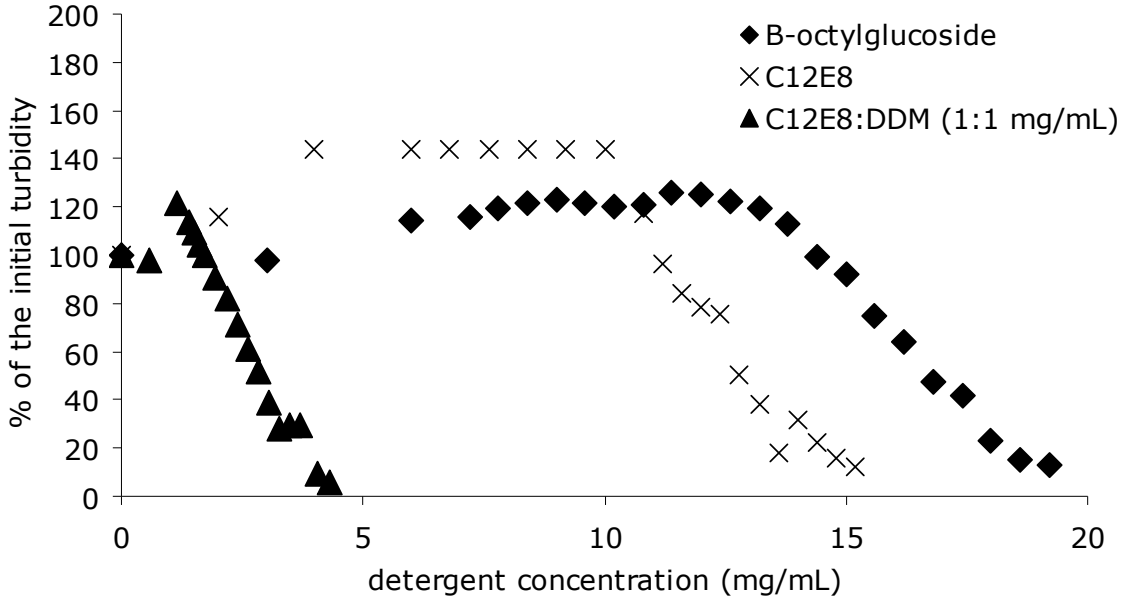

Figure III.2-20: Solubilization of DOPC vesicles with different detergent solutions

The turbidity corresponds to the optical density measured at 540nm after each addition of detergent.
β-octylglucoside and $C_{12}E_8$ were used to solubilize 3mg/mL of DOPC vesicles prepared by dialysis. $C_{12}E_8$:DDM was used to solubilize 4mg/mL of DOPC vesicles prepared by extrusion (200nm cut-off).

We made the hypothesis that PfATP6 could be more altered by β-octylglucoside than SERCA1a and we chose to use $C_{12}E_8$ (despite its lower cmc, 0.06mg/mL) still in a concentration between Rsat and Rsol (see table III.2-2 (2) and fig III.2-20, $C_{12}E_8$).
In spite of these new conditions no improvement was observed. We have therefore started to think about a problem of stability of PfATP6 during the reconstitution process.

Then, I came back to France and I set up new experiments.
However, as we did not have the material to prepare liposomes by dialysis, I tried to prepare them by extrusion (see Materials and Methods). This method has the advantage to be fast and to make calibrated vesicles. For this preparation, I followed the advices of Maïté Paternostre who has a strong experience in proteoliposomes preparation. She advised me to use filters of 100 or 200nm to be sure to obtain homogenous sizes of liposomes and unilamellar vesicles. Nevertheless, she also advised me to use first a filter of 400nm to make the extrusion easier. To check the homogeneity and the size of the extruded vesicle samples, they were analyzed by dynamic light scattering (DLS). The results of this analysis are presented in fig. III.2-21.

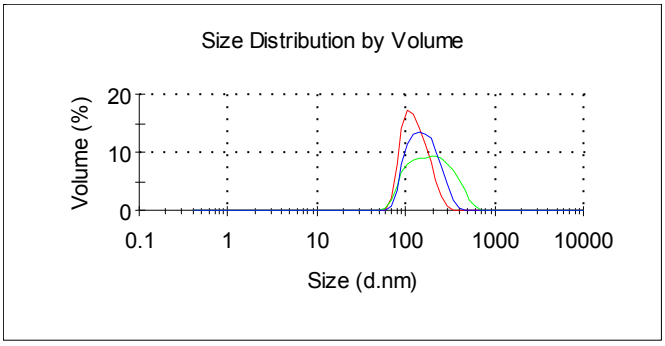

Figure III.2-21: DLS analysis of extruded vesicles

The green curve corresponds to DOPC sample filtered 10 times through a 400nm filter. The blue curve corresponds to the filtration of the former sample through a 200nm filter (2 times). The red curve corresponds to the filtration of the same sample (i.e. the one filtered through the 400nm filter) through a 100nm filter (2 times). The instrument for DLS measurement was not able to acquire a spectrum of the sample before extrusion because of a too large dispersity.

It can be seen that after treatment with the 400nm filter, the size distribution of the vesicles remains large. As expected, the second filtration (through 100nm or 200nm filters) allowed the formation of more calibrated vesicles.

From a solution of "200nm" vesicles, I decided to use DDM as solubilizing detergent since PfATP6 appeared stable in this mild detergent (see III.2.4). However, this detergent is known to solubilize DOPC vesicles with difficulties (de Foresta et al., 1989; Kragh-Hansen et al., 1993). This problem was solved with the use of mixed micelles of DDM and $C_{12}E_8$ (in a 1:1 ratio) which appeared to be a very efficient cocktail to solubilize these vesicles (fig. III.2-20, $C_{12}E_8$/DDM).

In this new reconstitution trial (table III.2-2 (3)), liposomes were again pre-treated with a detergent concentration between Rsat and Rsol but the reconstitution was performed at 4°C instead of room temperature to enhance the stability of PfATP6. The incubation of Bio-beads was therefore longer since it is known that the detergent adsorption by Bio-beads is divided by 2 each 12°C (Rigaud et al., 2003). To take into account this lower efficiency, I followed the procedure described for DDM removal at 4°C in the reconstitution process of another plasmodial membrane protein, the chloroquine resistant transporter (Tan et al., 2006). Despite these adjustments, the ATPase activity of PfATP6 was still low while SERCA1a solubilized from SR vesicles were successfully reconstituted under these conditions. In addition, reconstituted PfATP6 showed an identical calcium accumulation either in presence or in absence of ATP to trigger the activation of calcium the enzyme while reconstituted SR showed a relevant calcium uptake. Thus, we

concluded that the observed calcium accumulation was due to passive diffusion and not to active pumping. This reconstitution process was again efficient for SERCA1a but not for PfATP6.

As the main objective of this reconstitution was to measure an ATPase activity in a lipid environment rather than a detergent environment (to be closer to a native environment), I decided to try a "basic" reconstitution which was successful with native and mutated SERCA1a (Marchand et al., 2008). It only consists in adding DOPC (without preparation of calibrated and unilamellar vesicles) to the affinity purified Ca^{2+}-ATPase and removing detergent (DDM) with Bio-beads (table III.2-2 (4)). In this case the lipid/protein ratio was 3/1 (w/w) and the reconstitution was performed at a higher calcium concentration. In this case, the sample kept more than 25% of its initial activity.
This result suggests that DDM, as expected, is compatible with a successful reconstitution of PfATP6. However, this positive result could also be explained by the presence of a higher calcium concentration during the reconstitution process that may confer to PfATP6 a better stability.

With this promising result, I decided to use another solution of phosphatidylcholine lipids which can be easily solubilized by DDM: EYPC. I prepared "200nm" EYPC vesicles by extrusion and I followed their solubilization by DDM. Although the kinetic of interaction of this detergent with EYPC was faster than with DOPC, it was necessary to wait at least 2 minutes between the addition of detergent and the spectrum acquisition to ensure a total interaction of these components and therefore a reliable measurement. Once this curve was obtained, destabilized liposomes were prepared by adding DDM in the range of concentrations between Rsat and Rsol. After protein addition, detergent removal by Bio-beads was followed with radiolabeled DDM (^{14}C) until no detergent was remaining (fig. III.2-22). This reconstitution (table III.2-2 (5)) was again performed with a high calcium concentration but this time at 18°C. The resultant solution showed an ATPase activity of PfATP6 which represents 25% of the activity of the protein before reconstitution. Because of a too high calcium concentration, no calcium uptake could be performed but this result was promising. Because of a lack of time, I did not try the same experiments with a lower calcium concentration. This test would have given us evidence of the role of the calcium in the maintenance of the stability of PfATP6 and maybe good conditions for calcium uptake measurements.
Finally, I tried with this detergent-lipid couple to relipidate the protein in the same conditions as suggested by (Lenoir et al., 2002) (but without EYPS). In these last conditions, more than 50% of the initial activity was kept. Microscopy analysis after freeze-fracture of this sample was performed (Pictures are in article II). The micrographs

show several types of lipid organization but they confirm the presence of PfATP6 in the liposomes.

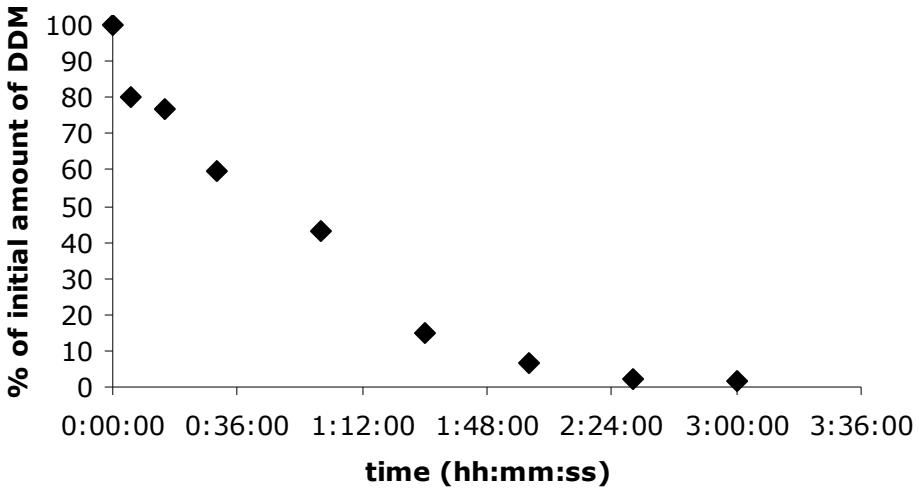

Figure III.2-22: Follow-up of DDM removal by Bio-Beads by radioactive counting during the reconstitution of sample 5 (see table III.2-2 (5)).

As these conditions gave the best results in term of ATPase activity, I have therefore chosen to apply these conditions for inhibition assays of PfATP6 by artemisinin.
In parallel, I have tried to form calibrated and tight sealed proteoliposomes from this relipidated sample by extrusion on 100nm filters. However, proteins seemed to remain bound to the filter used in this process since no protein could be detected on a Coomassie blue stained gel after extrusion whereas they were detectable before extrusion.

These assays lead to a successful protocol to relipidate PfATP6 and to keep it functional. Although it was not possible to measure a calcium-uptake of reconstituted PfATP6 from a solution of homogenous proteoliposomes, the results obtained show that it was probably due to a lack of stability of PfATP6 during the reconstitution process. DDM, EYPC and calcium seemed to be key elements to maintain this protein stable. Note that PfCRT was also successfully reconstituted with DDM destabilized vesicles of EYPC and *E. coli* total lipid extract. It could be interesting, now, to see if lower calcium concentrations would also lead to successful reconstitution of PfATP6. If it does, calcium-uptake measurement and thereby new characterizations of PfATP6 could be finally performed.

	Protein concentration (µg/mL)	Lipid				Detergent to destabilize vesicles		$[Ca^{2+}]_{free}$ (mM)	Reconstitution buffer	Detergent removal with Biobeads	ATPase activity	Calcium uptake	
		type	Calibrated vesicules	Mode of preparation	Concentration (mg/mL)	type	Concentration (mg/mL)					+ATP	~~ATP~~
1	50	DOPC	x	dialysis	3	β-octylglucoside	15	0.03	100mM NaH_2PO_4 pH 7.1, 1mM $MgCl_2$, 1mM NaN_3, 20% glycerol	200mg, 2h, RT 200mg, 1h, RT (300mg, 2h, RT)x2	0.2 S1a: 1.7 (30°C)	0.075 S1a : 0.165 (30°C)	ND
2						$C_{12}E_8$	12.8				0.2 SR: 1.2 (30°C)	0.045 SR: 0.366 (30°C)	ND
3	70			Extrusion	4	$C_{12}E_8$/DDM	1.7/1.7		50mM KH_2PO_4 pH 7, 20% glycerol	100mg, overnight, 4°C (100mg, 3h, 4°C)x2 200mg, 3h, 4°C	0.1 SR: 1.4 (30°C)	0.040 SR: 0.850 (30°C)	0.040 (30°C)
4	50		/	/	0.15	DDM brought with the protein	2	2.5	50mM MOPS-Tris pH7, 50mM KCl, 20% glycerol	200mg, 3h, 4°C	1.2 (37°C)	ND	ND
5	10	EYPC	X	Extrusion	0.5	DDM	1.2	1.9	50mM KH_2PO_4 pH 7, 1mM $MgCl_2$, 20% glycerol	(80mg, 1h, 18°C) x2 100mg, 1h, 18°C	0.5 SR : 3 (25°C)	ND	ND
6	330		/	/	1	DDM brought with the protein	0.25	2.5	50mM MOPS-Tris pH7, 50mM KCl, 20% glycerol	20mg, 3h, 18°C	2.9 (37°C)	ND	ND

Table III.2-2: Conditions of reconstitution of PfATP6 and functional characterization of the reconstituted samples
ATPase activities and calcium uptakes were measured in 50mM Tes-Tris pH 7.5, 100mM KCl, 6mM $MgCl_2$, 5mM ATP and 100µM of free calcium.
ATPase activities are in µmol of ATP/mg of Ca^{2+}-ATPases/min and calcium uptakes, in µmol of Ca^{2+}/ mg of Ca^{2+}-ATPases/min.
S1a corresponds to purified SERCA1a (by affinity chromatography) and SR, to solubilized rabbit sarcoplasmic reticulum provided by P. Champeil.
Solubilized SR (15mg/mL) was prepared by adding DDM in a 3:1 (w/w) ratio, to SR vesicles suspended in 100mM MOPS-Tris pH 7, 80mM KCl, 20% glycerol, 1mM $MgCl_2$, 2mM $CaCl_2$. Solubilized SR was recovered after centrifugation at 6°C and 120000g (rotor TLA 100, Beckman) for 35min. Prior to reconstitution, it was diluted in the same buffer as purified PfATP6.
RT: room temperature; ND: not determined.

I.12.4 Functional characterization of solubilized and relipidated PfATP6 and effect of artemisinin drugs

Functional characterization of purified PfATP6 was performed by the measurement of the ATPase activity of the protein in different conditions. Most of the functional characterization experiments and results are presented in article II. As the major aim of this study was to test the effect of artemisinin drugs on PfATP6, the characterization of this protein was mainly focused on finding stable conditions to do proper inhibition assays. I will sum up here most of these results and I will bring some additional information.

I.12.4.1 Effect of parameters such as fusion tag, detergents/lipids, pH, pCa, temperature, and stabilization on the ATPase activity of PfATP6

-Protein with fusion tag, before purification

For the first ATPase assays of PfATP6, the same conditions formerly used with native and mutated SERCA1a (50mM Tes-Tris pH 7.5, 0.1M KCl, 6mM $MgCl_2$, 5mM ATP, 1mM $C_{12}E_8$, 30°C) were applied (unless otherwise specified).

During the optimization of the purification procedure, I tried to measure an ATPase activity of PfATP6 when it was still bound onto the resin (before thrombin cleavage) and linked with its tag, BAD. Interestingly, an ATP hydrolysis was measured and stopped by the addition of EGTA, a chelating agent of calcium (fig. III.2-23). This fusion protein was therefore active and its activity was depending on calcium concentration, like a Ca^{2+}-ATPase. Linked to streptavidin, we can conclude that BAD did not prevent PfATP6 to be an active enzyme and neither SERCA1a (data not shown). However, in the case of PfATP6, the hydrolysis rate was not constant: it was decreasing over the time.
From this promising result, I wanted to try if it was possible to detect a thapsigargin dependent ATPase activity (i.e. a SERCA dependent activity) from solubilized yeast light membranes expressing PfATP6-BAD. For this purpose, I first tried to measure an ATPase activity of SERCA1a-BAD in solubilized yeast light membranes before purification. To inhibit the other ATPases present in these membranes, usual ATPase inhibitors were required (e.g. NaN_3 and bafilomycine to inhibit H^+-ATPases, ouabaïn to inhibit Na^+/K^+ ATPase). The SERCA-dependent activity corresponded to the ATPase activity measured after addition of all these inhibitors and before addition of thapsigargin. In these conditions it was not possible to measure a relevant thapsigargin dependent signal. This seems to suggest either that BAD prevents SERCA to be active or that only a low

proportion of expressed SERCA are functional. These results were also confirmed by phosphorylation experiments (personal communication of Philippe Champeil). BAD seems to influence a little the activity of the Ca^{2+}-ATPase since when it was not fused to a tag, the protein was fully functional in membranes (Menguy et al., 1998). As these measurements did not give clear answers about a thapsigargin dependent activity with SERCA1a-BAD from solubilized yeast light membranes, I did not try to perform them with PfATP6-BAD.

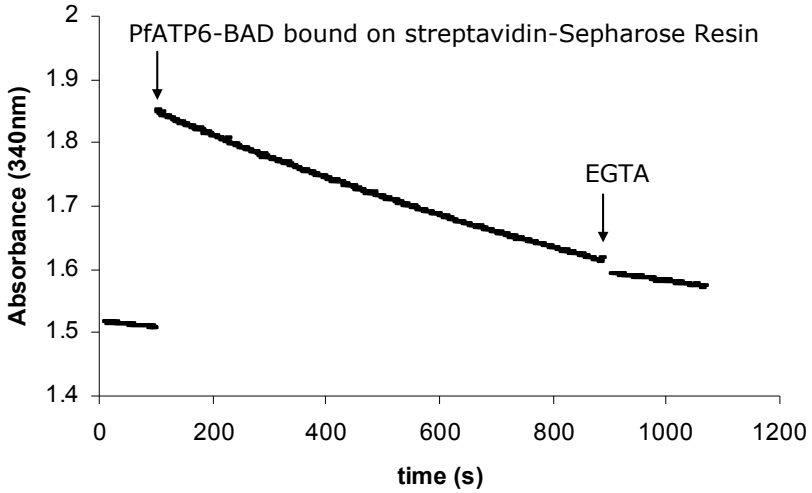

Figure III.2-23: ATPase activity of PfATP6-BAD bound on streptavidin-Sepharose resin

The ATPase activity at 37°C of ~2µg of PfATP6-BAD bound on streptavidin-Sepharose was measured at pH7.5 in 2mL of 50mM Tes-Tris pH 7.5, 0.1M KCl, 5mM ATP, 6mM $MgCl_2$ and 125µM $CaCl_2$ by coupled enzyme assay.
The increase in absorbance after sample addition is due to the resin.

-After purification: stabilization of PfATP6 with lipids and determination of its activity as a function of the pH, the pCa and the temperature.

After measuring a calcium dependent ATPase activity with PfATP6-BAD bound on resin, I confirmed, by measuring the activity in the same conditions, that after the release of BAD by thrombin cleavage, eluted PfATP6 kept this property. During this experiment, I also noticed the same decrease in the ATP hydrolysis rate that had been already observed before thrombin cleavage (see article II). PfATP6 seems to inactivate over the time in these conditions of detergent.

To improve the stability of PfATP6, I followed conditions described by the group of Steven Karlish to stabilize Na^+, K^+ ATPase (Haviv et al., 2007) and direct advices from Steven Karlish. I thereby added a mix of lipids and $C_{12}E_8$ (lipids:$C_{12}E_8$ 0.05:0.2 mg/mL) instead of $C_{12}E_8$ alone to the assay medium. It resulted on a better stability of the ATPase (see

article II). In article II, only DOPC is mentioned but I also tried DOPS and EYPC. Whatever the lipid used, the same stabilizing effect was observed and the resultant activity was the same (fig. III.2-24, compare A to B, C and D). The same stabilizing effect was observed with the addition of DDM in a 1:1 ratio but contrary to phospholipids, the activity of PfATP6 was dramatically decreased (fig III.2-24, compare A, B and E).
As I managed to find conditions in which PfATP6 had a stable activity, I did not explore different $C_{12}E_8$:lipid or $C_{12}E_8$:DDM ratios but it would have been interesting to test them to determine from what ratios the ATPase was stabilized.

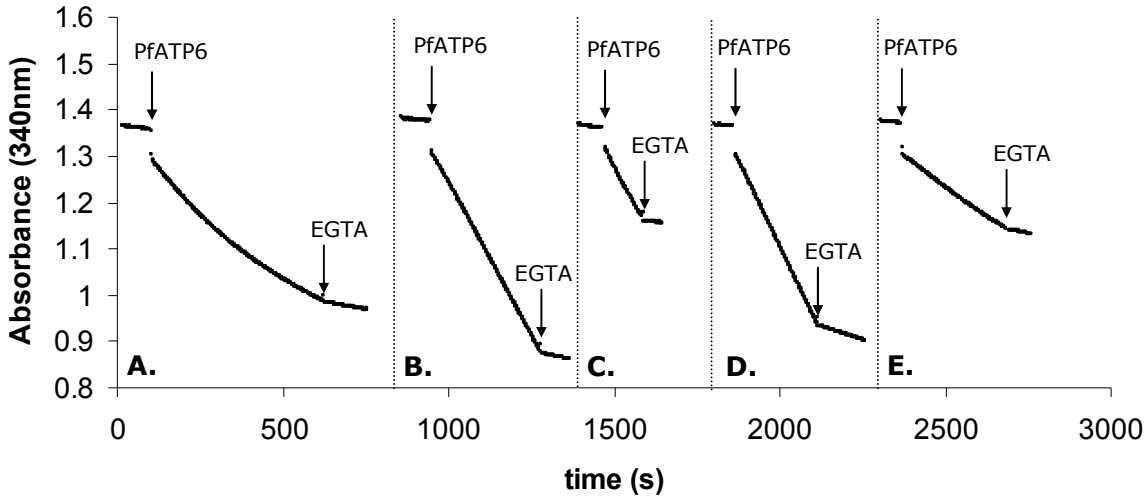

Figure III.2-24: Stabilization of the ATPase activity of PfATP6 measured in detergent by addition of phospholipids

ATPase activities of 5µg of PfATP6 were measured at 37°C and pH7.5 in 2mL of 50mM Tes-Tris pH 7.5, 0.1M KCl, 5mM ATP, 6mM $MgCl_2$ and 125µM $CaCl_2$ by coupled enzyme assay.
The reactions were triggered by addition of purified PfATP6 into the medium and stopped by addition of a final concentration of 750µM EGTA. They were carried out in presence of ***A.*** *$C_{12}E_8$ (0.2mg/mL),* ***B.*** *$C_{12}E_8$/DOPC (0.2/0.05 mg/mL),* ***C.*** *$C_{12}E_8$/EYPC (0.2/0.05 mg/mL),* ***D.*** *$C_{12}E_8$/DOPS (0.2/0.05 mg/mL),* ***E.*** *$C_{12}E_8$/DDM (0.5/0.5 mg/mL)*

Then, seeking for optimal pH and calcium concentration, I determined that PfATP6 reached its optimal activity at pH 7.5 and for a free calcium concentration between 1µM and 100µM (article II, supplemental data).

During the different measurements performed, I tried various temperatures from 20 to 37°C. Hence, it led to establish a temperature dependency of PfATP6 which is depicted in fig. III.2-25. Again, I did not carry out specific assays to determine the lower temperature that activates the enzyme and the temperature from which it was denatured

because it was not useful for this purpose. However, for a complete characterization of this protein, it would be interesting to determine it.

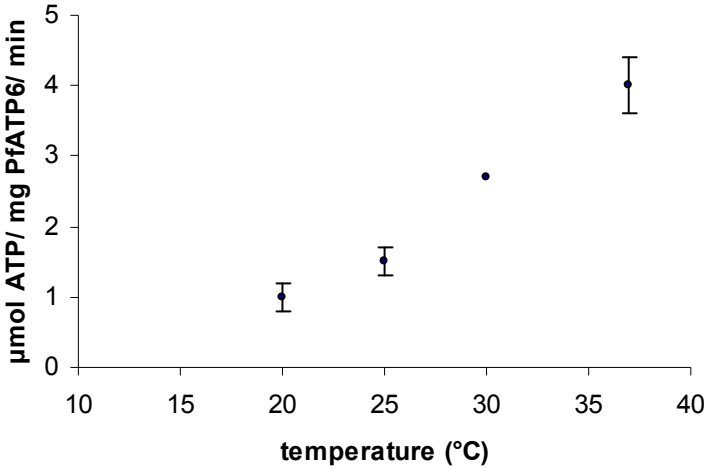

Figure III.2-25: Effect of the temperature on the ATPase activity of PfATP6

ATPase activities of PfATP6 were measured at pH7.5 in 50mM Tes-Tris pH 7.5, 0.1M KCl, 5mM ATP, 6mM $MgCl_2$ and 125µM $CaCl_2$ by couple enzyme assay and at different temperatures.
Except for 30°C, each value is an average of at least three measurements.

- Stability of PfATP6

In the same way, I tested the activity of streptavidin-purified PfATP6 at t=0 and after four days at 4°C. I measured a loss of 50% of the ATPase activity. To maintain a longer stability of the protein, it could be worth adding some lipids to PfATP6 after the step of affinity chromatography. Indeed, we have already seen (see III.2.2) that adding them during this purification step does not seem necessary because no difference of activity was observed between these eluted fractions and those only in detergent. Nevertheless, when conserved at -80°C in the elution buffer of affinity chromatography in presence of 40% glycerol, the protein kept its full activity at least for 6 months since the same activity was measured during this time period (data not shown).

- Activity of PfATP6 after reconstitution in lipids

Enzyme activity in detergent and in a membrane environment is different because the detergent micelles are more dynamic than membranes and it could alter or extensively facilitate the movement of a protein during its turnover (le Maire et al., 2000). For this reason, it seemed important to reconstitute PfATP6 in an environment closer to its native one: in lipids. As mentioned in III.2.3, suitable conditions were found to reconstitute purified PfATP6 in lipids but I could not demonstrate unambiguously a calcium transport.

However, relipidatation of this protein with EYPC allowed the measurement of an ATPase activity of the enzyme in lipids. Under these conditions, the ATPase activity of PfATP6 was a little lower than in detergent: more than 4 µmol ATP/mg PfATP6/min in $C_{12}E_8$/DOPC 0.2/0.05 mg/mL while it reached 3 µmol ATP/mg PfATP6/min without detergent. The reasons are still unclear but it seems to be due to a loss of activity of the protein during the reconstitution process. More extensive stability tests could be performed to understand this possible time-dependent inactivation in solution.

I.12.4.2 Inhibition assays of PfATP6

Taking into account the results previously described, inhibition assays of PfATP6 were performed either in a detergent/lipid environment or with relipidated proteins and in absence of detergent. This protein was shown to be sensitive to SERCA-type inhibitors like thapsigargin, BHQ and CPA. For thapsigargin, either solubilized in detergent or reconstituted in lipids, the range of inhibiting concentrations was higher than for SERCA1a. As mentioned in article II, *in vivo* results corroborate this observation. In the primary structure of this protein, amino acids that interact with thapsigargin are well conserved (SERCA1a F256, I765, Y843 i.e. PfATP6 F264; I977; Y1055) whereas the amino acids located in the binding pocket of thapsigargin are more or less conserved (see annexe 2 and compare with fig I.2-13). The explanation might therefore come from an alteration of the affinity of thapsigargin for its binding site by the surrounding amino acids (repulsive forces…). In addition, the folding of PfATP6 is likely to be somewhat different from SERCA1a and it could be more difficult to thapsigargin to reach its binding site. Structural data would be of major importance to answer this question.
CPA and BHQ bind SERCA1a in the same region than thapsigargin: 3µM and 100µM respectively are sufficient to fully inhibit that protein (see I.4). In the case of PfATP6, 100µM of BHQ inhibited more than 90% of its activity whereas 3µM of CPA inhibited only 65% of it (fig. III.2-26)**.** This also suggests a different conformation of the binding pocket. A Ki determination would be interesting to measure in order to know the behavior of PfATP6 related to the concentration of Tg, BHQ and CPA. However, although partial, these results are in favor of a SERCA-like behavior.

In addition, the activity of PfATP6 was also half-inhibited by 100µM vanadate. As vanadate bound into the nucleotide binding site, it is in competition with ATP and its binding depends also a lot of the protein turnover and therefore on the calcium concentration. This makes difficult the interaction of vanadate with the protein under the conditions of measurement tested and can explain this partial inhibition.

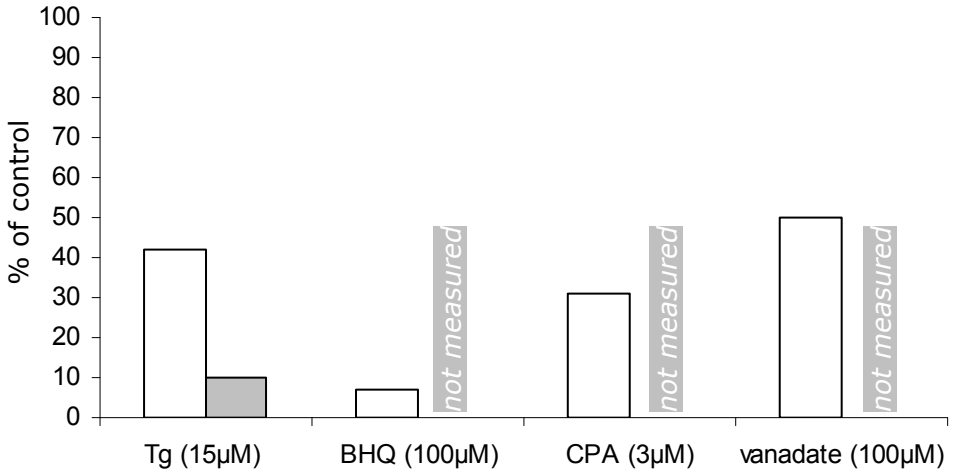

Figure III.2-26: Effect of SERCA-type inhibitors on the ATPase activity of PfATP6

ATPase activities of PfATP6 were measured at pH7.5 in 50mM Tes-Tris pH 7.5, 0.1M KCl, 5mM ATP, 6mM $MgCl_2$, 125µM $CaCl_2$ by couple enzyme assay at 25°C (except vanadate: Pi determination at 37°C).
White bars correspond to activities measured in $C_{12}E_8$/DOPC (0.2/0.05mg/mL). The inhibitors were added during the ATPase turnover.
The grey bar corresponds to the ATPase activity measured on relipidated PfATP6. The inhibitors were preincubated with the ATPase in 0.2µM of free calcium before measuring its enzyme activity at higher calcium concentration.
ATPase activities are expressed in % of control. Control was the ATPase activity of PfATP6 measured in presence of DMSO.

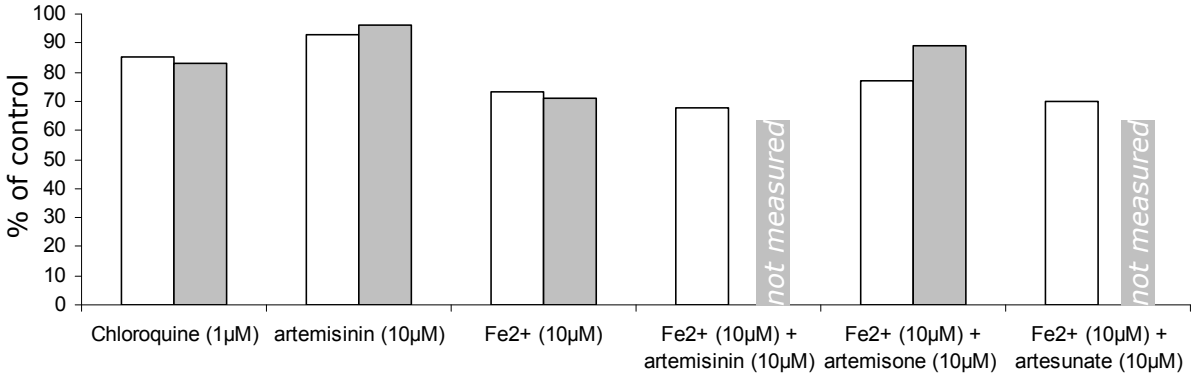

Figure III.2-27 : Effect of artemisinin drugs on PfATP6 in absence and in presence of iron and comparison with the effect of chloroquine

ATPase activities of PfATP6 were measured at pH7.5 in 50mM Tes-Tris pH 7.5, 0.1M KCl, 5mM ATP, 6mM $MgCl_2$, 125µM $CaCl_2$ by couple enzyme assay at 25°C.
White bars correspond to ATPase activities measured in $C_{12}E_8$/DOPC (0.2/0.05mg/mL). The inhibitors were added during the ATPase turnover.
Grey bars correspond to the ATPase activities measured on relipidated PfATP6. The inhibitors were preincubating with PfATP6 in 0.2µM of free calcium before measuring its ATPase activity at higher calcium concentration.

The main objective of my work was to characterize the interaction of artemisinin drugs with PfATP6. I therefore monitored the ATPase activity of PfATP6 in presence of these drugs. Several methods were applied but all aim to see if the ATPase activity of PfATP6 was stopped in presence of these drugs. These methods consist in adding drugs to the protein during its turnover or pre-incubating drugs with the protein (in presence or in absence of free calcium) before triggering the enzyme reaction by adding ATP and by varying the medium temperature. Whatever the method applied and the concentration of artemisinin drugs used (between 1 and 100µM), less than 10% of the ATPase activity of PfATP6 was inhibited (fig. III.2-27). This percentage of inhibition was not linked to a dose effect, it was almost the same whatever the drug concentration, while at such high concentrations, PfATP6 should have been completely inhibited (Eckstein-Ludwig et al., 2003).

As seen in introduction, many papers show that artemisinin reacts with iron and suggest that this ion is necessary to transform the drug as a killer agent of *Plasmodium* parasites. This may be due to a Fenton reaction between the peroxide bond of artemisinin and iron that could lead to free radicals formation and therefore protein cleavage or alkylation (see introduction). Indeed, this type of reaction has already been observed with SERCA1a in presence of iron II, H_2O_2 and ascorbate (Montigny et al., 2004). The reaction medium should already contain some iron ions brought up with water but as no reliable inhibition of the enzyme was observed under these conditions, 10µM of iron II (from freshly prepared $FeSO_4$ solution) were added to the medium. In this new reaction medium, the same assays as previously described were performed but in presence of artemisinin drugs and iron in a 1:1 molar ratio because they should react mole to mole. In presence of iron, the activity of PfATP6 was altered but no inhibition was observed with artemisinin drugs either in detergent or lipid environment. In addition, I tried to incubate a longer time PfATP6 with artemisone and iron (7min vs 1.5min usually) and I controlled the effect by repeating the same experiment but this time with DMSO and iron. With the control, some activity (30%) was lost while in presence of artemisone the activity was conserved (fig. III.2-28). These results suggest that artemisone reacts with iron preventing PfATP6 to get damaged by the presence of free iron in the medium.

For future experiments, it might be interesting to test the effect of heme-bound iron but this is unlikely to change the conclusion of this part (Zhang et al., 2008). Another way to proceed would be to add some reductive agent to the medium such as ascorbate or gluthation to reactivate the reaction. To do this, another way to measure ATPase activities will have to be used because ascorbate was not compatible with this coupled enzyme assay.

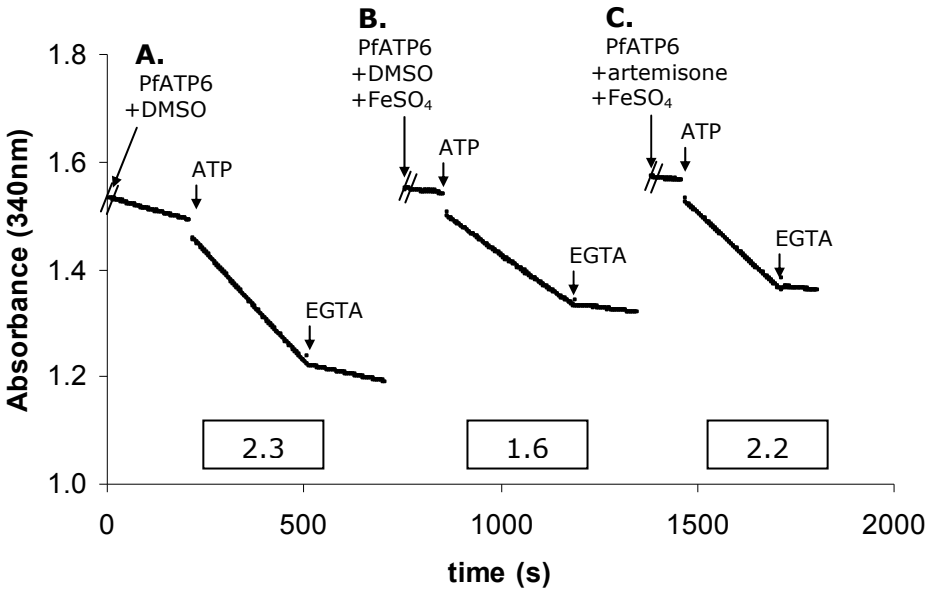

Figure III.2-28: Effect of long time pre-incubation of artemisone with PfATP6 in presence of iron

*ATPase activities of 2.5µg PfATP6 preincubated with 1% (v/v) DMSO (**A**), 1%(v/v) DMSO + 10µM $FeSO_4$ (**B**) and 10µM artemisone +10µM $FeSO_4$ (**C**) were measured at pH7.5 and 37°C in 2mL of 50mM Tes-Tris pH 7.5, 0.1M KCl, 6mM $MgCl_2$ by coupled enzyme assay in presence of 125µM $CaCl_2$. Solutions were incubated at 37°C for 7 min before adding 5mM ATP to trigger the reaction.*
The values indicated under each curve correspond to the specific activity (in µmol of ATP/mg of PATP6/min) measured for A, B and C.

I.12.5 Molecular weight control of PfATP6 by mass spectrometry

Before transforming *S. cerevisiae* with pYeDP60-Pfatp6-BAD vector, the cDNA of PfATP6-BAD and the nucleotides surrounding the region was checked by sequencing and no mistake was found. After expression, PfATP6 was fully translated since PfATP6-BAD was detected with anti-PfATP6 antibodies, targeting the N-domain of the protein, and also with avidin peroxidase which binds the biotinylated acceptor domain in the C-terminal region of the protein.

During the elution step of the affinity purification, thrombin releases PfATP6 from the biotin acceptor domain. After this cleavage, the protein can only be detected with anti-PfATP6 antibodies or by Coomassie blue staining and the size is approximated from the marker ladder. That will not attest that the protein did not loose amino acids during thrombin cleavage.

As PfATP6 was not inhibited by artemisinin, it was important to check that all the expected amino acids were present. The best way would have been to perform an Edmann sequencing of the protein because it would have confirmed the amino acid

sequence of the protein but as a first step, a molecular weight determination by mass spectrometry was carried out.

To estimate the precision that can be reached with this technique, the masses of known proteins must be measured. We used extracted SERCA1a from SR vesicles and yeast expressed affinity-purified SERCA1a as standards. Indeed, after thrombin cleavage, yeast expressed and purified SERCA1a has six more amino acids than native SERCA1a (2 glycines and 4 amino acids of the thrombin cleavage site) -and this is also true for PfATP6. This enabled us to check if this difference of 6 amino acids could be determined by mass spectrometry.

Previous experiments performed by the laboratory with Pierre Le Maréchal (IBBMC, University Paris XI, Orsay) determined suitable conditions to submit SERCA1a extracted from SR to MALDI-TOF mass spectrometry. Delipidated proteins stored in 50mM MOPS-Tris pH 6.8, NaCl 50mM, DDM 0.4mg/mL were shown to give a significant signal to noise ratio (supplemental data (Lenoir et al., 2004)). I thereby followed the same protocol to prepare SERCA1a and PfATP6.

Solubilized SR, affinity purified SERCA1a and PfATP6 were prepared by gel-filtration HPLC in 50mM MOPS-Tris pH 6.8, NaCl 50mM, DDM 0.4mg/mL as described in Materials and Methods section. The resulting spectra are presented in fig. III.2-29. It can be noticed that this step allowed the elimination of thrombin from affinity purified proteins. In addition, although PfATP6 has a higher molecular weight than SERCA1a, PfATP6 was eluted a few seconds later. PfATP6-detergent complex has therefore a slightly smaller hydrodynamic radius than SERCA1a-detergent complex in these buffer conditions.

Once the proteins were eluted, they were concentrated until they reached the concentration written in table III.2-3. Then, they were mixed with matrix solution (exact dilutions are described in table III.2-3), spotted onto the MALDI target and analyzed by MALDI-TOF mass spectrometry.

Sample	Sample concentration after HPLC and concentration	Mix for MS	Amount of loaded proteins	Expected molecular weight (Da)	Determined molecular weight (Da)
Solubilized SR	7 mg/mL (1)	1µL (1) + 19µL of matrix solution	3.2 pmol	109489	109497
SERCA1a	0.25mg/mL (2)	1µL (2) + 1µL of matrix solution	1.1 pmol	110069	110090
PfATP6	2mg/mL (3)	1µL (3) + 2µL of matrix solution	1.4 pmol	139994	140053

Table III.2-3: Sample preparation and molecular weight determination by mass spectrometry of native SERCA1a (solubilized SR), affinity purified SERCA1a and PfATP6

Matrix solution consists in saturated solution of sinapinic acid in 30% acetonitrile, 0.3% trifluoroacetic acid.
Expected molecular weight was calculated with the online software Protein calculator (www.scrips.edu/~cdputnam/protcalc.html) taking into account the isotopic mass of the constituent.
Determined molecular weight was obtained after MALDI-TOF analyses (the spectra are depicted in fig. III.2-30)

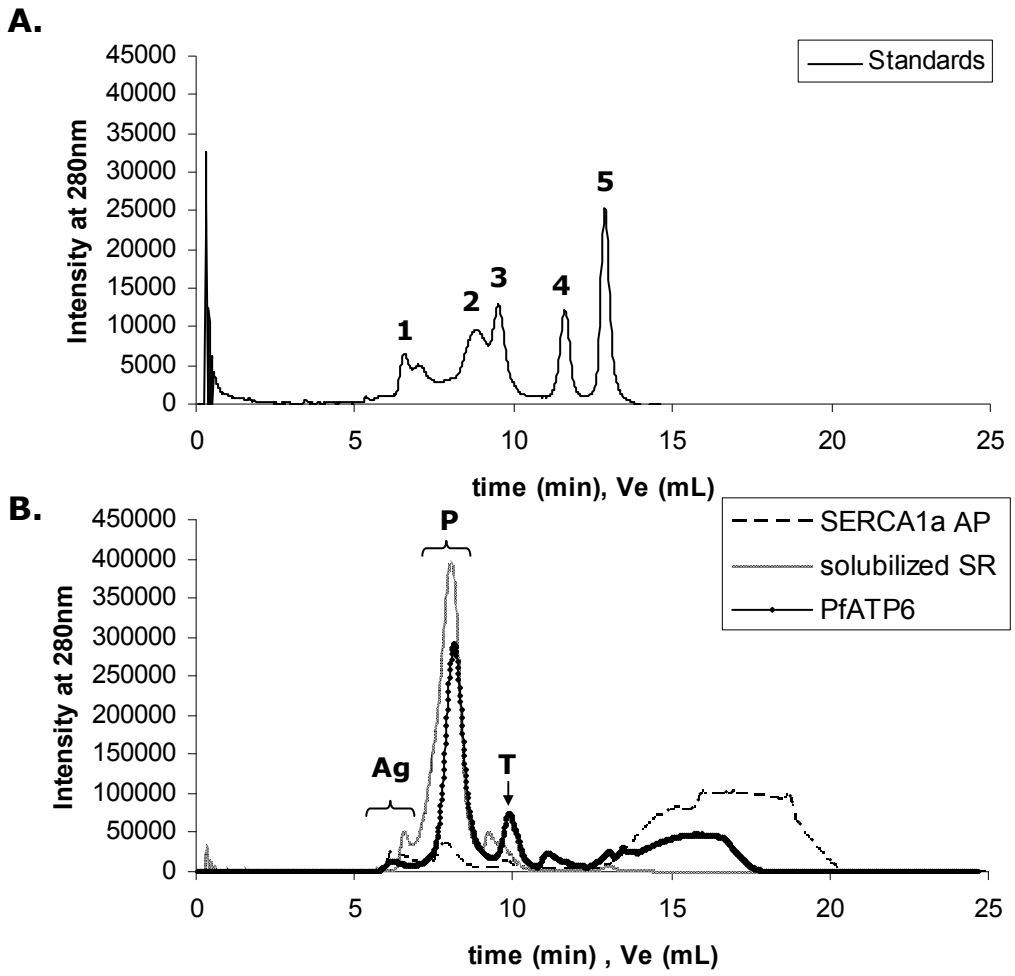

Figure III.2-29: Gel-filtration of Ca^{2+}-ATPases prior to MALDI-TOF analyses

Gel-filtration was performed in 50mM MOPS-Tris pH6.8; 50mM NaCl; DDM 0.4mg/mL, at 1mL/min.

*Chromatogram of the gel-filtration of molecular weight standards is depicted in panel **A**.*
*The molecular weight standards are: thyroglobulin (**1**, 670kDa, Stokes radius (Rh) 8.6nm); bovine γ-globulin (**2**, 158kDa, Rh 5.2nm); chicken ovalbumin (**3**, 44kDa, Rh 2.8nm) equine myoglobin (**4**, 17kDa, Rh 1.7nm) and vitamin B12 (**5**, 1.35kDa, Rh 0.85nm).*

*Chromatograms of the gel-filtration of SERCA1a (from solubilized SR and affinity purified SERCA1a) and PfATP6 are depicted in panel **B.***

Solubilized SR (500µg of SR in 50mM MOPS-Tris pH 6.8; 50mM NaCl; 10mg/mL DDM) was centrifuged 5min at 120000g (rotor TLA 100, Beckman) before injection. Affinity purified SERCA1a (SERCA1a AP, 30µg) and PfATP6 (300µg) were in 50 mM MOPS-Tris pH 7; 50mM KCl; 20% glycerol; 2.5mM $CaCl_2$; 0.5mg/mL DDM.

*During gel-filtration, proteins of interest (**P**) were separated from aggregates (**Ag**) and thrombin (**T**, 37kDa).*

Acquired spectra (fig. III.2-30) show that conditions for native SERCA1a fit also for affinity purified SERCA1a and PfATP6 since a signal was obtained in each case. The difference noted between the signal intensity of the samples can be assigned to the amount of proteins loaded on the target (compare table III.2-3 and fig. III.2-30).

The measured masses show that mass spectrometry is really accurate even with high molecular weight membrane proteins since a difference of less than one amino acid (average mass = 100Da) was found between the expected and the measured values. Purified SERCA1a was confirmed to be bigger than native SERCA1a and PfATP6 had its expected molecular weight. This confirms a good conservation of the protein during the purification and suggests that major post translational modifications are unlikely.

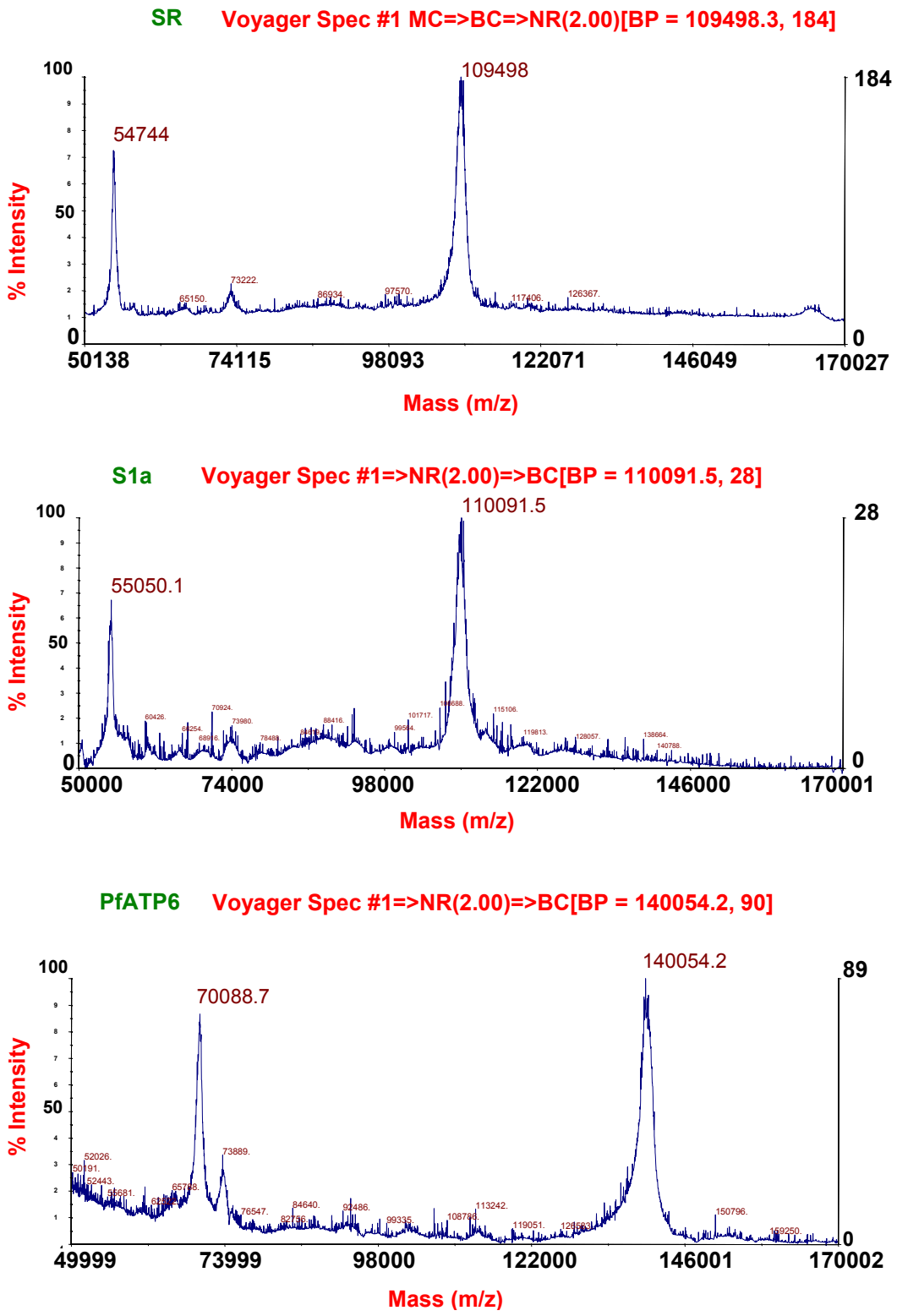

Figure III.2-30: MALDI-TOF MS spectra of native SERCA1a (SR), affinity purified SERCA1a (S1a) and PfATP6.

In red, on top of each spectrum, is indicated the m/z ratio of the major peak, corresponding to the molecular weight of the protein +1Da.

I.12.6 Toward structural study of PfATP6

I.12.6.1 Modeling of PfATP6 from the 3D structure of SERCA1a

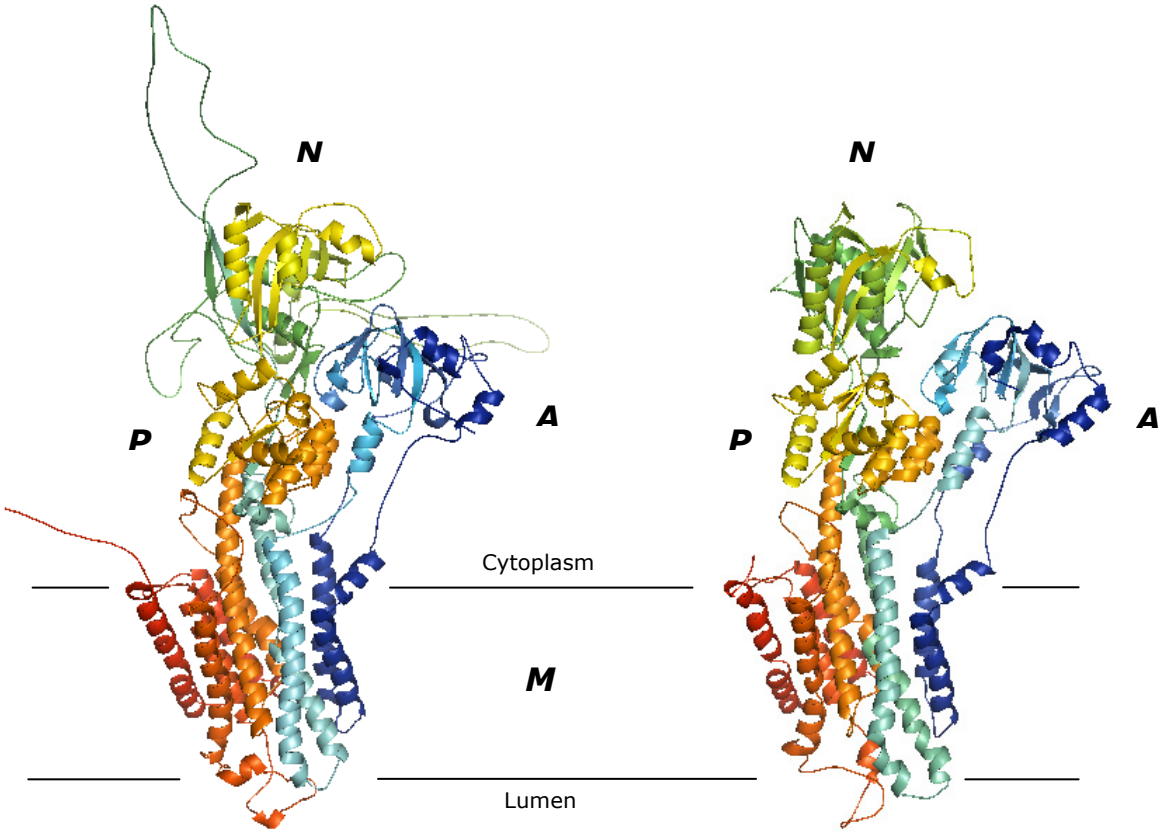

Model of PfATP6 *SERCA1a E2MgF$_4$ + CPA*

Figure III.2-31 : Model of PfATP6 compared to the structure of SERCA1a in E2 MgF$_4$ + CPA.

The structure of SERCA1a presented here corresponds to the one obtained by Takahashi et al. (2007)(PDB accession number: 2eas)
A : actuator domain ; N : nucleotide binding domain ; P : phosphorylation domain ; M : transmembrane domain
Colours change gradually from the amino acid terminus (blue) to the carboxy terminus (red).

A potential structure of PfATP6 was generated by Jens Preben Morth (Pumpkin, University of Aarhus) from the structure of SERCA1a in E2MgF4 with CPA bound (PDB accession number : 3fgo, unpublished). The general organization of PfATP6 compared to SERCA1a looks conserved. All main domains are present (A, N, P and as in SERCA1a, the membrane domain is composed of 10 α-helices). According to the alignment of PfATP6 with SERCA1a, the major inserts are found in the N-domain. At one point, these inserts made the structure impossible that is why there is a chain break between the residues

I677 and C678. In addition, it can be seen on the model that the structure of three extra loops in the N-domain remains to model. Among the extra inserts found in PfATP6 compared to SERCA1a, one starting at residue 851, corresponds exactly to the place where the Na^+,K^+ ATPase also have an insert (residues 630 to 660). J. Preben therefore made a hybrid structure to model this loop, assuming that this loop takes the same secondary structure as in the Na^+,K^+ ATPase structure. In the luminal part of PfATP6, one loop is longer than in SERCA1a and seems to organize as two short α-helices.

Although the primary structure of PfATP6 and this model gives information about the conservation of the main domains of SERCA (domains A, N and P), calcium binding sites, inhibitors binding sites…), this structural characterization remains partial. Thus, it would be of major interest to have its crystallographic structure. A complete structure of PfATP6 would allow a best docking of artemisinin with this protein (to see if one place would be favored) and would be useful for drug design. Indeed, PfATP6 would be a good drug target since, as shown in introduction, a deregulation of calcium homeostasis leads to the parasite death.

I.12.6.2 Crystallization attempts of PfATP6

As orthologous proteins, PfATP6 and SERCA1a share many functional and structural similarities. Both of them were even expressed and purified with the same procedure. For these reasons, it seemed worth trying to use, for PfATP6, crystallization conditions close to those successful for SERCA1a.

For this purpose, I was welcomed by the teams of Jesper V. Møller and Poul Nissen in Aarhus University (Denmark), who have a strong experience of the crystallization of P-type ATPases and also expressed and affinity-purified SERCA1a (Jidenko et al., 2005; Marchand et al., 2008), to set up the first crystallization assays of PfATP6. During the three weeks spent in Aarhus, I learned a lot from Dr. Claus Olesen, Dr. Anne-Marie Lund-Winter and Dr. Bertrand Arnou, who taught me how to develop and follow crystallization experiments. When I came back to France, with the support of Dr B. Arnou, I tried to apply what I learned in these labs to try again some crystallization assays of PfATP6. Dr Marie-Hélène Ledu (SB^2SM, iBiTec-S, CEA Saclay), Dr Thomas Sorensen (Diamond, UK) also helped me to some extent.

I.12.6.2.1 Sample preparation prior to crystallization assays of PfATP6

After streptavidin purification, PfATP6 is in solution with thrombin, used for the elution, and DDM as detergent. Regarding SERCA1a, no suitable crystal was obtained in DDM. Every structure resolutions was achieved from crystals grown in presence of $C_{12}E_8$ (e.g (Sorensen et al., 2004; Moncoq et al., 2007; Toyoshima, 2008)). A detergent exchange was therefore required to place the protein in the best crystallization environment. This exchange was successfully performed by gel filtration HPLC which allowed, in addition, the removal of thrombin (Jidenko et al., 2005). Then, the protein was concentrated to reach 5-15mg/mL and some lipids (DOPC) were added to stabilize it.

In a first attempt, I applied this strategy to PfATP6. The chromatogram of the gel filtration of PfATP6 compared to SERCA1a is presented in fig. III.2-32.

PfATP6 is eluted almost in the same time frame as SERCA1a. Thrombin was eluted, as expected, later than PfATP6. DDM micelles, according to the published results (Jidenko et al., 2005), are eluted between 9 and 11mL of elution buffer after sample injection. The collected fraction of PfATP6 (Ve=7,5-9mL) is therefore likely to be in solution only with $C_{12}E_8$ and not with DDM as demonstrated for SERCA1a (Jidenko et al., 2005). This fraction was then concentrated and DOPC was added according to the amount of $C_{12}E_8$ in solution ($C_{12}E_8$:DOPC, 3:1, (w/w), see Materials and Methods for calculation of the amount of $C_{12}E_8$ in solution). Adding DOPC to PfATP6 will also favor its stability during crystallization trials.

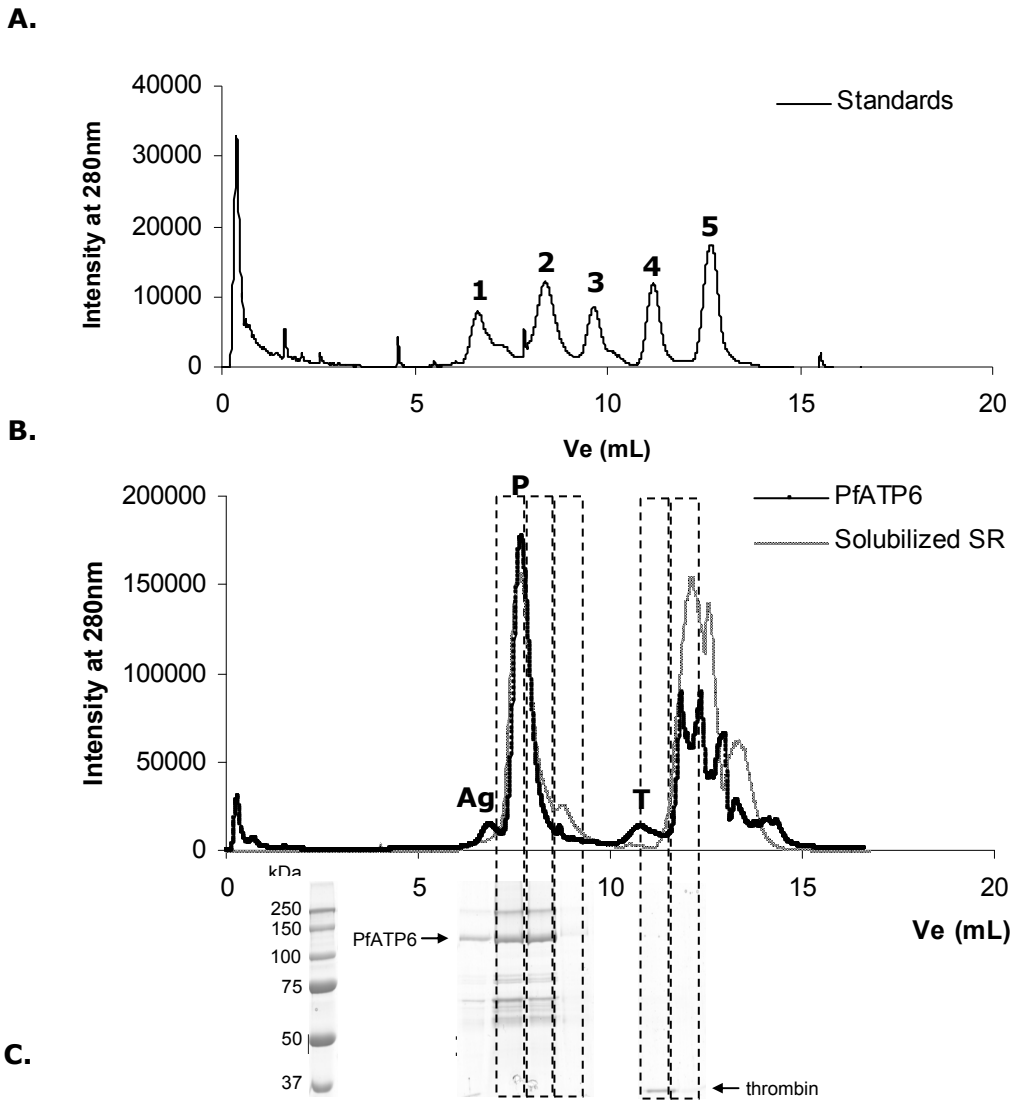

Figure III.2-32: Gel-filtration of Ca^{2+}-ATPases in $C_{12}E_8$ prior to crystallization assays

Gel-filtration was performed in 50mM MOPS-Tris pH6.8; 80mM KCl; 1mM $CaCl_2$, 1mM $MgCl_2$, 15% sucrose, 0.5mg/mL $C_{12}E_8$ at 1mL/min.

*Chromatogram of the gel-filtration of molecular weight standards is depicted in panel **A**.*
*The molecular weight standards are: thyroglobulin (**1**, 670kDa, Stokes radius (Rh) 8.6nm); bovine γ-globulin (**2**, 158kDa, Rh 5.2nm); chicken ovalbumin (**3**, 44kDa, Rh 2.8nm) equine myoglobin (**4**, 17kDa, Rh 1.7nm) and vitamin B12 (**5**, 1.35kDa, Rh 0.85nm).*
*Chromatograms of the gel-filtration of SERCA1a (from solubilized SR) and PfATP6 are depicted in panel **B.***
Solubilized SR (80µg of SR in 50mM MOPS-Tris pH 6.8; 50mM NaCl; 10mg/mL DDM) was solubilized in 50mM MOPS-Tris pH 6.8; 50mM NaCl; 10mg/mL DDM, centrifuged 5min at 120000g (rotor TLA 100, Beckman) before injection and diluted in 50mM MOPS-Tris pH 6.8; 50mM NaCl; 10mg/mL DDM.
Affinity purified PfATP6 (80µg) were in 50mM MOPS-Tris pH 7; 50mM KCl; 20% glycerol; 2.5mM $CaCl_2$; 0.5mg/mL DDM.
*During gel-filtration, proteins of interest (**P**) were separated from aggregates (**Ag**) and thrombin (**T**, 37kDa).*
*SDS-PAGE analysis of the injected PfATP6 sample (**IS**) and the collected fractions (rectangles in dotted lines) is depicted in panel **C**. (10µL of 5X concentrated fraction were loaded).*

In a second time, the elution buffer content was modified taking into account differences between PfATP6 and SERCA1a: the pI of PfATP6 is higher than SERCA1a since it reaches 7.2 while it is of 5.5 for SERCA1a; PfATP6 seems to be unstable when exclusively solubilized by $C_{12}E_8$ (see article II and section III.2.4).

As PfATP6 has a higher pI than SERCA1a, global charges of these proteins are different in the elution buffer. In the usual elution conditions, SERCA1a is negatively charged whereas PfATP6 is positively charged. Moreover, crystallization is known to be favored when the global charge of a protein is neutral. I therefore increased the pH of the elution buffer to 7.2.

In spite of the lack of stability of the ATPase activity of PfATP6 in $C_{12}E_8$ micelles, it seems to remain stable in mixed micelles of $C_{12}E_8$/DOPC (see article II and section III.2.4). I thereby added some DOPC to the elution buffer in the same detergent/lipids ratio used for ATPase activities measurement: 4/1 (w/w).

In these new elution conditions, proteins (PfATP6, SERCA1a and even thrombin) were eluted earlier than in the previous conditions but a similar elution profile was observed (see fig III.2-33). The collected fractions were then pooled and concentrated but no additional lipids were added.

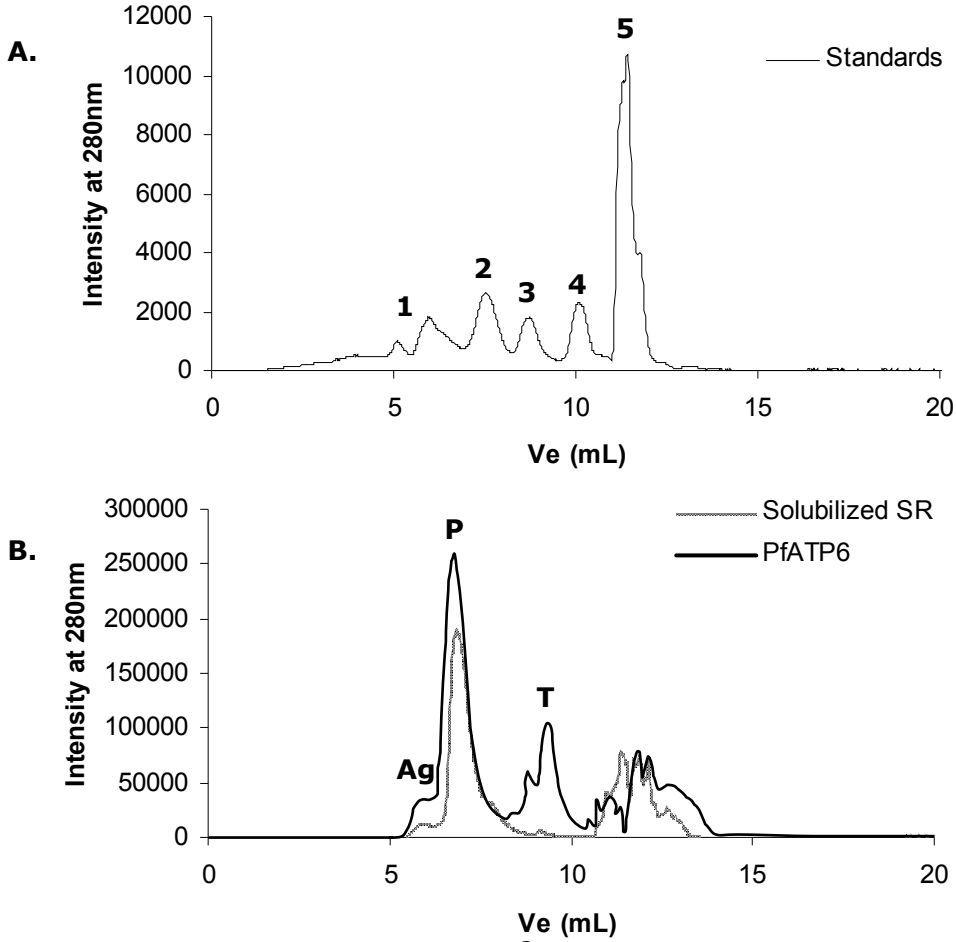

Figure III.2-33: Gel-filtration of Ca^{2+}-ATPases in $C_{12}E_8$/DOPC prior to crystallization assays

Gel-filtration was performed in 50mM MOPS-Tris pH7.2; 80mM KCl; 1mM $CaCl_2$, 1mM $MgCl_2$, 15% sucrose, 0.5mg/mL $C_{12}E_8$, 0.125 mg/mL DOPC, at 1mL/min

*Chromatogram of the gel-filtration of molecular weight standards is depicted in panel **A**.*
*The molecular weight standards are: thyroglobulin (**1**, 670kDa, Stokes radius (Rh) 8.6nm); bovine γ-globulin (**2**, 158kDa, Rh 5.2nm); chicken ovalbumin (**3**, 44kDa, Rh 2.8nm) equine myoglobin (**4**, 17kDa, Rh 1.7nm) and vitamin B12 (**5**, 1.35kDa, Rh 0.85nm).*

Chromatograms of the gel-filtration of SERCA1a (from solubilized SR).

*During gel-filtration, proteins of interest (**P**) were separated from aggregates (**Ag**) and thrombin (**T**, 37kDa).*

Solubilized SR (160µg of SR in 50mM MOPS-Tris pH 6.8; 50mM NaCl; 10mg/mL DDM) was solubilized in 50mM MOPS-Tris pH 6.8; 50mM NaCl; 10mg/mL DDM, centrifuged 5min at 120000g (rotor TLA 100, Beckman) before injection and diluted in 50mM MOPS-Tris pH 6.8; 50mM NaCl; 10mg/mL DDM.
Affinity purified PfATP6 (300µg) were in 50mM MOPS-Tris pH 7; 50mM KCl; 20% glycerol; 2.5mM $CaCl_2$; 0.5mg/mL DDM.

Before submitting PfATP6 to crystallization experiments, it is important to place the protein in a stable conformational state because only identically folded proteins will be able to get organize as a crystal. For this purpose, some inhibitors were added (specific inhibitors of SERCA-type proteins, BHQ and non hydrolysable ATP analog, AMPPCP) and calcium concentration was adjusted in function of the inhibitor used. For instance, BHQ is an inhibitor of the E2 conformation of SERCA-type proteins, low calcium concentrations are therefore necessary. The protein in presence of AMMPCP will be blocked in E1 conformation and in the case of SERCA1a, high calcium concentration (10mM) was required to crystallize under these conditions. Besides these additives, β-mercaptoethanol was also added in some cases because it was shown that sometimes, reductive conditions help to get crystals (Morth et al., 2007; Pedersen et al., 2007).
Final sample conditions for crystallization assays are described in table III.2-4.

Elution buffer	Sample volume (µL)	Protein (mg/mL)	$C_{12}E_8$ (mg/mL)	DOPC (mg/mL)	AMPPCP (mM)	Ca^{2+} (mM)	BHQ (mM)	EGTA (mM)	β-mercaptoethanol (mM)	Sample number
1	86	20 ***1:***	19 ***0.95*** **3:**	6.3 **1**	1	10	/	/	/	1
1	98	26 ***1:***	17.3 ***0.6*** **3:**	5.8 **1**	/	1	1	0.99	/	2[a]
									1	3[a]
					1	10	/	/	/	4
									1	5
2	70	6 ***1:***	15 ***2.5*** **4:**	3.8 **1**	1	10				6

Table III.2-4 : Sample conditions for crystallization attempts of PfATP6

Samples 1-5 were prepared in the Danish lab and sample 6 in the French lab.
*Buffer : **1**=50mM MOPS-Tris pH6.8; 80mM KCl; 1mM $CaCl_2$, 1mM $MgCl_2$, 15% sucrose, 0.5mg/mL $C_{12}E_8$; **2**=50mM MOPS-Tris pH7.2; 80mM KCl; 1mM $CaCl_2$, 1mM $MgCl_2$, 15%sucrose, 0.5mg/mL $C_{12}E_8$, 0.125 mg/mL DOPC*
Bold values correspond to mass ratios either between protein amount and $C_{12}E_8$ (in italic) or $C_{12}E_8$ and DOPC.
[a] : Snowy precipitates were observed in samples 2 and 3 that might be due to the DMSO brought with BHQ. DMSO represented 5% (v/v) of the protein sample.

I.12.6.2.2 Crystallization assays of PfATP6

Samples 1-5 were prepared and submitted to crystallization trials when I was in Denmark and sample 6 when I came back to France.

As described in Material and Methods, the crystallization method used was vapor diffusion either with sitting drop or hanging drop. Regarding the crystallizing solutions, four different screens were used (table III.2-5). Three were developed in Poul Nissen's lab based on the crystallizing conditions of purified SERCA1a and its mutants (see Materials and Methods). The last one was a commercial kit dedicated to membrane proteins, the MbClass I, supplied by Qiagen.

	SERCA1a screen 1		SERCA1a screen 2 (glycerol)		SERCA1a screen 3 (saccharose)		MbClass I	
PfATP6 samples	Sitting drop [a]	Hanging drop	Sitting drop [a]	Hanging drop	Sitting drop [a]	Hanging drop	Sitting drop [b]	Hanging drop
1	X	X	X		X			
2	X				X			
3	X				X			
4	X				X			
5	X				X			
6						X	X	

Table III.2-5 : Crystallization conditions attempted with PfATP6

Each x correspond to tested conditions.
Sitting drop plates were prepared either with Mosquito ([a]) or Cartesian ([b]) liquid handlers

Most conditions led to clear or dense precipitates with samples 1-5. Clear precipitates are often good starting points of crystallization but in these cases, no crystal was observed. In the case of sample 6, with Mbclass I, no crystal was observed either, but the list of precipitating conditions obtained is detailed table III.2-6. It can be noticed that most of precipitating conditions were obtained in presence of salts used to design screens of SERCA1a. Nevertheless, with SERCA1a screen 3, interesting precipitates were observed. Indeed, in presence of KCl, one condition (fig. III.2-34, panel 3) led to a precipitate in which some regions seemed to aggregate. I observed an evolution of the number and the density of these kinds of aggregates that increased during the incubation time. It could mean that PfATP6 molecules tend to organize. Besides, in presence of LiCl, one condition (fig. III.2-34, panel 4) led to a clear precipitate and four small organized structures. Other conditions, all in presence of $MgSO_4$, even led to crystalline precipitates and crystalline objects appeared (fig. III.2-34, panels 1-3). Surprisingly, only single crystalline objects were observed in the drops and they appeared lately (more than one month). Although strange, to try to know if it is a protein, a salt or a detergent crystal, it might be worth analyzing them by X-ray diffraction.

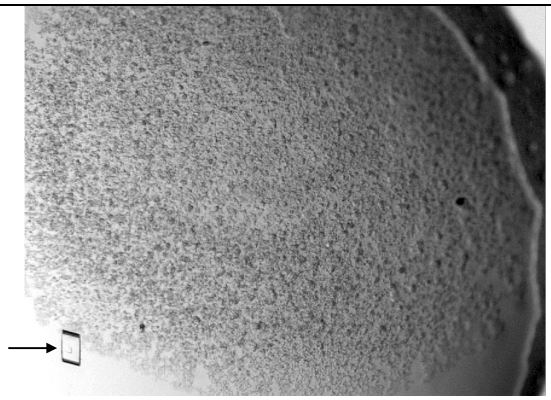

10% sucrose, 16% PEG6000, 0.2M Mg SO_4, 3% t-BuOH

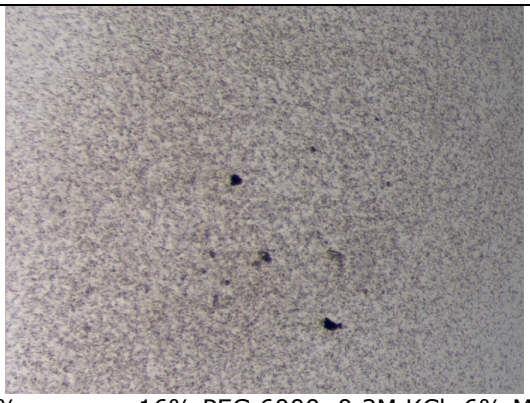

10% sucrose, 16% PEG 6000, 0.2M KCl, 6% MPD

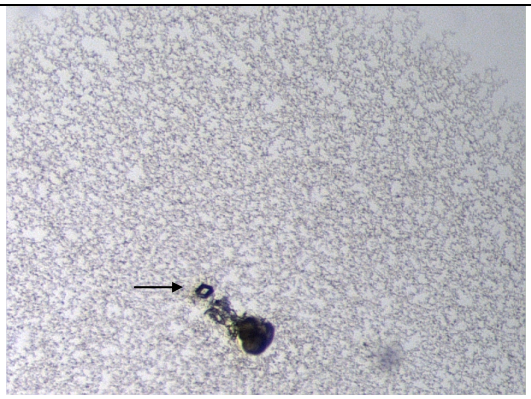

10% sucrose, 12% PEG 2000, 0.2M $MgSO_4$, 3% t-BuOH

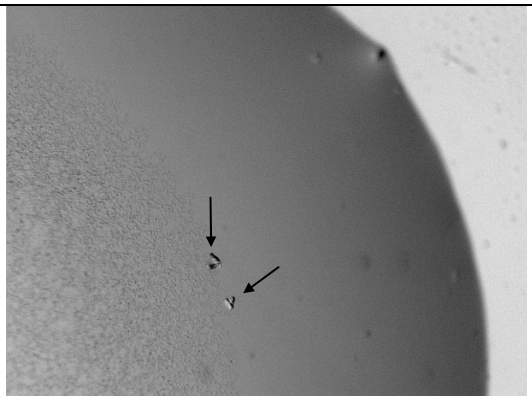

10% sucrose, 8% PEG6000, 0.2M LiCl, 6% MPD

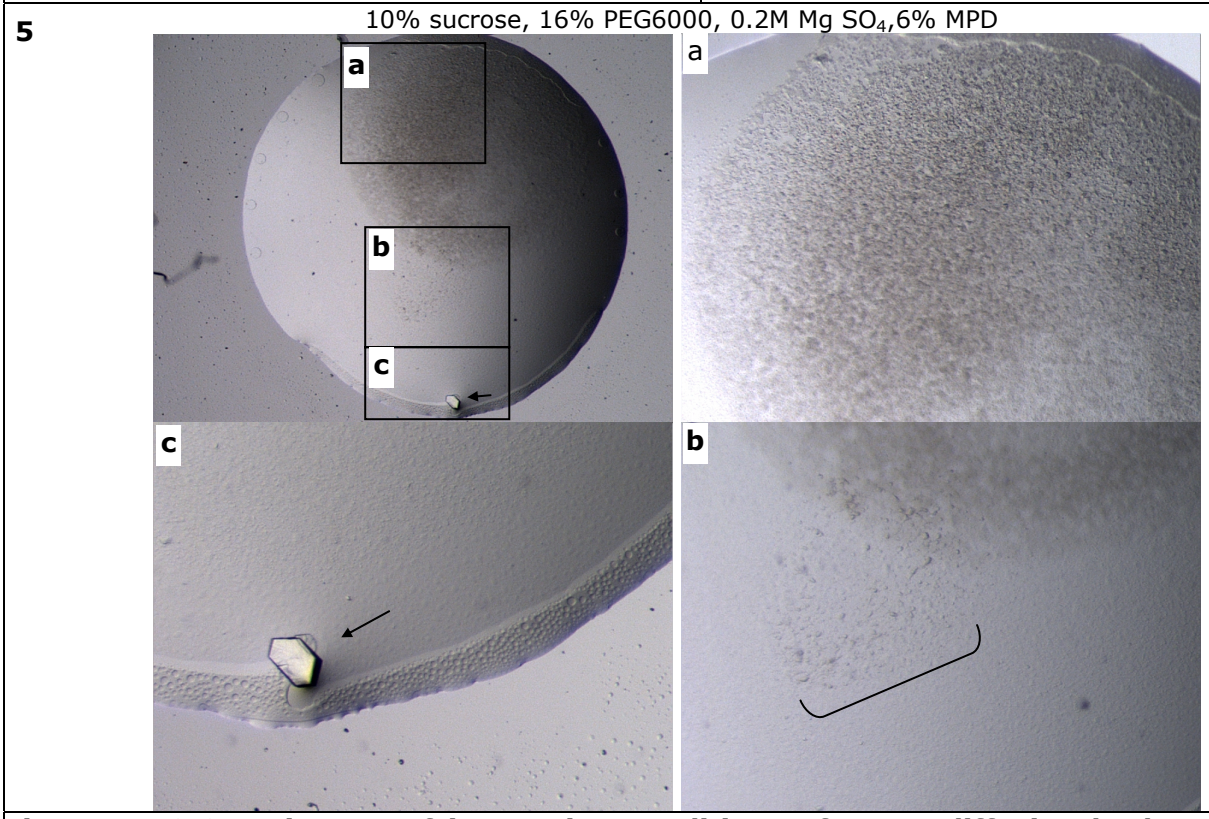

Figure III.2-34: Pictures of interesting conditions of vapor diffusion by hanging drop obtained with PfATP6 (sample 6) mixed with crystallizing solutions of SERCA1a screen 3

***a**, **b** and **c** are magnifications of the drop **5** : **a** focus on the crystalline precipitate ; **b** focus on a second type of crystalline precipitate and **c** focus on a crystalline object.*
Arrows points crystalline objects.

	Salt	Buffer	Precipitant
1	0.1 M Sodium citrate tribasic dihydrate	0.1 M Sodium citrate tribasic dihydrate pH 5.6	10 % v/v 2-Propanol
2	0.1 M Sodium chloride	0.1 M Sodium acetate anhydrous pH 4.6	12 % v/v 2-Propanol
3	0.2 M Calcium chloride	0.1 M Sodium acetate anhydrous pH 4.6	30 % w/v 2-Propanol, 20 % w/v Glycerol anhydrous
4		0.1 M Tris-HCl pH 8.5	0.5 M Ammonium sulfate
5		1 M Sodium/Potassium phosphate pH 7.5	0.7 M Ammonium sulfate
6		0.1 M ADA pH 6.5	1 M Ammonium sulfate
7		0.1 M Tris-HCl pH 8.5	1.2 M Ammonium sulfate
8	0.1 M Ammonium acetate		1.4 M Ammonium sulfate, 4 % w/v 2-Propanol
9		0.1 M Sodium citrate tribasic dihydrate pH 5.6	2 M Ammonium sulfate
10	0.25 M Sodium chloride	0.05 M Sodium/Potassium phosphate pH 7.5	3.5 M Ammonium sulfate
11		0.1 M ADA pH 6.5	1 M di-Ammonium hydrogen phosphate
12	0.1 M Ammonium sulfate	0.1 M HEPES Sodium salt pH 7.5	0.5 M di-Sodium hydrogen phosphate, 0.5 M di-Potassium hydrogen phosphate
13	0.1 M di-Ammonium hydrogen phosphate	0.1 M Tris-HCl pH 8.5	0.5 M di-Sodium hydrogen phosphate, 0.5 M di-Potassium hydrogen phosphate
14	0.5 M Lithium chloride		1 M Sodium citrate tribasic dihydrate pH 5.6
15		0.1 M Tris-HCl pH 8.5	0.2 M Lithium sulfate monohydrate
16	0.1 M Potassium sodium tartrate tetrahydrate	0.1 M Tris-HCl pH 8.5	0.4 M Magnesium sulfate hydrate
17	0.1 M Magnesium chloride hexahydrate	0.1 M Sodium citrate tribasic dihydrate pH 5.6	4 % v/v MPD
18	0.6 M Magnesium sulfate hydrate	0.1 M HEPES Sodium salt pH 7.5	4 % v/v MPD
19	0.1 M Sodium chloride	0.1 M Sodium acetate anhydrous pH 4.6	12 % v/v MPD
20	0.1 M Sodium chloride	0.1 M Sodium citrate tribasic dihydrate pH 5.6	12 % v/v MPD
21		0.1 M ADA pH 6.5	12 % v/v MPD
22	0.1 M Sodium citrate tribasic dihydrate	0.1 M HEPES Sodium salt pH 7.5	12 % v/v MPD
23	0.1 M Lithium sulfate monohydrate	0.1 M Tris-HCl pH 8.5	12 % v/v MPD
24	0.1 M Sodium chloride	0.1 M Tris-HCl pH 8.5	12 % v/v MPD
25		0.1 M Bis-Tris Propane pH 7	25 % w/v MPD
26		0.3 M Sodium citrate tribasic dihydrate pH 5.6	30 % w/v MPD
27	0.1 M Lithium sulfate monohydrate	0.1 M Sodium citrate tribasic dihydrate pH 5.6	4 % v/v PEG 400
28	0.3 M Lithium sulfate monohydrate	0.1 M ADA pH 6.5	4 % v/v PEG 400
29	0.6 M Magnesium sulfate hydrate	0.1 M HEPES Sodium salt pH 7.5	4 % v/v PEG 400
30	0.1 M Sodium citrate tribasic dihydrate	0.1 M Tris-HCl pH 8.5	5 % v/v PEG 400
31	0.2 M Calcium chloride	0.1 M HEPES Sodium salt pH 7.5	15 % w/v PEG 400, 15 % w/v Glycerol anhydrous
32	0.1 M Magnesium chloride hexahydrate	0.1 M Sodium acetate anhydrous pH 4.6	18 % v/v PEG 400
33	0.1 M Sodium chloride	0.1 M Sodium citrate tribasic dihydrate pH 5.6	18 % v/v PEG 400
34	0.1 M Magnesium chloride hexahydrate	0.1 M HEPES Sodium salt pH 7.5	18 % v/v PEG 400
35	0.1 M Ammonium sulfate	0.1 M HEPES Sodium salt pH 7.5	18 % v/v PEG 400
36	0.05 M Magnesium acetate	0.05 M Sodium acetate anhydrous pH 4.6	25 % w/v PEG 400
37	0.05 M Sodium sulfate, 0.05 M Lithium sulfate monohydrate	0.05 M Tris-HCl pH 8.5	30 % w/v PEG 400
38	0.2 M Calcium chloride	0.1 M HEPES Sodium salt pH 7.5	48 % w/v PEG 400
39		0.01 M Tris-HCl pH 7.5	20 % w/v PEG 550 MME
40	0.1 M Magnesium chloride	0.05 M Tris-HCl pH 8.5	30 % w/v PEG 550 MME
41			35 % w/v PEG 600
42	0.35 M Sodium chloride	0.1 M Tricine pH 8	28 % w/v PEG 1000, 10 % w/v Glycerol anhydrous
43	0.1 M Magnesium chloride, 0.1 M Sodium chloride		10 % w/v PEG 1500, 5 % w/v Ethanol
44			5 % w/v PEG 2000
45	0.5 M Magnesium chloride	0.05 M Tris-HCl pH 8.5	10 % w/v PEG 2000
46	0.02 M Sodium citrate	0.1 M Sodium dihydrogen phosphate pH 6.2	15 % w/v PEG 2000
47	0.5 M Sodium chloride	0.1 M Sodium dihydrogen phosphate pH 6.8	15 % w/v PEG 2000
48		0.02 M Bis-Tris propane pH 7	15 % w/v PEG 2000
49	0.1 M Magnesium chloride	0.05 M HEPES Sodium salt pH 7.5	15 % w/v PEG 2000
50			15 % w/v PEG 2000
51	0.1 M Lithium chloride		15 % w/v PEG 2000
52	0.3 M Magnesium nitrate	0.1 M Tris-HCl pH 8	20 % w/v PEG 2000, 2 % w/v MPD
53	0.3 M Magnesium chloride	0.1 M Bicine pH 9	25 % w/v PEG 2000, 15 % w/v Glycerol anhydrous
54		0.1 M Sodium acetate anhydrous pH 4.6	8 % w/v PEG 2000 MME
55		0.1 M Sodium citrate tribasic dihydrate pH 5.6	10 % w/v PEG 2000 MME, 3 % w/v PEG 200, 20 % w/v Glycerol anhydrous
56	0.5 M Sodium chloride	0.05 M Tris-HCl pH 7.5	12 % w/v PEG 2000 MME
57	0.15 M Sodium chloride	0.05 M Sodium citrate tribasic dihydrate pH 5.6	10 % w/v PEG 3350
58		0.05 M Tris-HCl pH 7.5	2 % w/v PEG 4000
59	0.1 M Sodium chloride	0.05 M Sodium-MES pH 6.5	5 % w/v PEG 4000, 10 % w/v Glycerol anhydrous
60		0.05 M Sodium dihydrogen phosphate pH 6.7	5 % w/v PEG 4000
61			5 % w/v PEG 4000
62	0.1 M Potassium chloride		5 % w/v PEG 4000
63	0.2 M Ammonium sulfate	0.1 M Sodium acetate anhydrous pH 4.6	10 % w/v PEG 4000
64	0.1 M Sodium chloride	0.1 M HEPES Sodium salt pH 7.5	10 % w/v PEG 4000
65	0.1 M Ammonium sulfate	0.1 M HEPES Sodium salt pH 7.5	10 % w/v PEG 4000
66	0.5 M Sodium chloride	0.05 M Tris-HCl pH 8.5	10 % w/v PEG 4000
67	0.1 M Lithium sulfate monohydrate	0.1 M ADA pH 6.5	12 % w/v PEG 4000
68	0.1 M Lithium sulfate monohydrate	0.1 M ADA pH 6.5	12 % w/v PEG 4000, 2 % v/v 2-propanol
69		0.05 M Sodium dihydrogen phosphate pH 6.8	12 % w/v PEG 4000
70	0.5 M Potassium chloride	0.05 M MOPS pH 7	12 % w/v PEG 4000, 20 % w/v Glycerol anhydrous
71	0.1 M Lithium chloride	0.01 M Tris-HCl pH 7.5	15 % w/v PEG 4000
72	0.5 M Sodium chloride	0.1 M Bis-Tris propane pH 7	20 % w/v PEG 4000
73	0.5 M Sodium chloride	0.1 M Sodium dihydrogen phosphate pH 7	20 % w/v PEG 4000
74	0.15 M Zinc acetate, 0.05 M Zinc chloride	0.05 M Tris-HCl pH 7.5	20 % w/v PEG 4000
75		0.05 M Tricine pH 8	22 % w/v PEG 4000
76	0.5 M Sodium chloride	0.05 M Tris-HCl pH 8.5	22 % w/v PEG 4000
77			30 % w/v PEG 4000
78	0.1 M Magnesium acetate	0.1 M Sodium citrate tribasic dihydrate pH 5.6	10 % w/v PEG 5000 MME
79	0.1 M Magnesium sulfate		5 % w/v PEG 6000
80	0.15 M Zinc acetate, 0.05 M Zinc chloride	0.05 M Tris-HCl pH 7.5	10 % w/v PEG 6000
81	0.1 M Lithium sulfate monohydrate	0.1 M Sodium citrate tribasic dihydrate pH 5.6	12 % w/v PEG 6000
82	0.15 M Sodium chloride	0.1 M Tris-HCl pH 8.5	12 % w/v PEG 6000
83		0.05 M Sodium succinate pH 6.5	15 % w/v PEG 6000
84	0.025 M Potassium dihydrogen phosphate		12 % w/v PEG 8000, 10 % w/v MPD
85	0.1 M Magnesium acetate	0.1 M Sodium citrate tribasic dihydrate pH 5.6	8 % w/v PEG 10000
86			0.05 M Potassium dihydrogen phosphate pH 8
87			1.5 M Potassium dihydrogen phosphate pH 7
88	0.1 M Lithium sulfate monohydrate	0.1 M HEPES Sodium salt pH 7.5	0.1 M Potassium sodium tartrate tetrahydrate
89		0.1 M Tris-HCl pH 8.5	0.1 M Sodium acetate trihydrate
90		0.1 M Sodium citrate tribasic dihydrate pH 5.6	0.1 M Sodium chloride
91		0.1 M Tris-HCl pH 8.5	0.1 M Sodium chloride
92		0.1 M Sodium acetate anhydrous pH 4.6	1.5 M Sodium chloride
93	0.1 M Sodium formate		2 M Sodium chloride
94			0.1 M Sodium citrate tribasic dihydrate pH 4.8
95		0.1 M HEPES Sodium salt pH 7.5	1 M Sodium citrate tribasic dihydrate
96			1 M Sodium citrate tribasic dihydrate

Table III.2-6: Results of the follow up of vapor diffusion experiments of PfATP6 (in E1~Ca^{2+}-AMPPCP) with Mbclass I kit performed by sitting drop

Grey lines correspond to conditions that led to precipitation.

CONCLUDING COMMENTS

AND PROSPECTS

Xenopus laevis oocytes were initially chosen as expression system for the mutant E255L of SERCA1a and for PfATP6, without subsequent purification steps of these proteins (Eckstein-Ludwig et al., 2003; Uhlemann et al., 2005). The oocyte system did not allow a high expression level of proteins due to the limited number of eggs that can be injected. The presence of the protein in these oocytes was only validated by a statistical increase of the ATPase activity of mRNA-injected oocytes compared to water-injected oocytes and unpublished immunofluorescence data performed only recently to highlight PfATP6 (S. Krishna, personal communication). No information about the presence of the full-length protein (e.g. with a western-blot) is available. The functional study of PfATP6 and SERCA1a E255L was only performed from oocyte membranes and, as mentioned above, never with purified proteins. It was therefore interesting to be able to express at a high level this protein and also to purify it.

For this purpose, we used the method of heterologous expression in yeast and purification by affinity chromatography of SERCA1a developed by our lab (Jidenko et al., 2005; Jidenko et al., 2006) to first study SERCA1a E255L. Without any modification of the protocol of expression and only a small modification of the purification protocol (change of the resin motivated by a lower cost), similar yields were obtained. These results validate, one more time, the reliability of this method (see also (Marchand et al., 2008). The resulting purified mutant was, as expected, active and still inhibited by thapsigargin in presence of detergent. However, it was not inhibited by artemisinin, even in presence of iron, a potential activator. Facing this unexpected result, we tried to think about reasons that could explain this non-inhibition. The explanation that seems the most obvious for us was the main difference that exists between a pure protein and a membrane fraction containing the protein of interest but also many other proteins, lipids, cofactors… This environment can be more (or less) suitable to reveal the activity of artemisinin or lead to bias observations. In any case, after expression in oocytes, this mutant was shown to be less sensitive to artemisinin than PfATP6. Therefore we found important to see if purified PfATP6, the described target of this drug, could be inhibited by artemisinin.

However, contrary to SERCA1a, PfATP6 had never been expressed in yeast. As a first trial, we therefore decided to strictly apply the same protocols developed for SERCA1a. For this purpose, we sub-cloned the native gene coding for PfATP6 in the vector of expression designed for SERCA1a and following advices of S. Krishna based on observations that plasmodial proteins do not express properly in heterologous hosts such as yeasts, we also sub-cloned a codon-optimized version of the gene for its expression in yeast. We encountered a large number of problems to fulfill these steps, mainly due to the known difficulty to amplify plasmodial DNA which are very AT-rich. Both versions of the gene led to the expression of PfATP6 but the wild-type cDNA gave a very low amount

of proteins whereas with the codon-optimized cDNA, almost the same amount of what was obtained with SERCA1a was reached. Thus, this optimized gene was chosen for larger expressions. At this point, it can be interesting to keep in mind that an optimized gene can lead to a (partially) misfolded protein because of the difference of codon usage between the native and the heterologous host. This remark is also true for non-optimized genes expressed heterologously.

Although PfATP6 was expressed at an expression level close to the one of SERCA1a with its optimized gene, it was at least three times less expressed than SERCA1a. However, thanks to the use of a more controlled follow-up of the yeast culture by using a fermentor, we were able to reach the level of SERCA1a produced in Fernbach flasks. This expression level was actually multiplied about four times like it was for SERCA1a. Lenoir et al. had increased the level of expression of SERCA1a by genetically modifying the yeast strain and increasing the induction time (Lenoir et al., 2002). Here we optimized it by changing the parameters of culture and therefore the yeast metabolism. Regarding the protocol of expression, it could still be optimized (maybe by producing more yeasts but stopping the step of protein expression before yeasts accumulate too many heterologous proteins in their membranes, see Results and Discussion) because we suspect that besides the high-quality proteins that we are able to purify, proteins of lower quality are produced and cannot be solubilized and/or purified.

The solubilization of PfATP6 with DDM was a little less efficient than for SERCA1a but the use of KCl instead of NaCl in the solubilization buffer as suggested by Steven Karlish, allowed a higher recovery. That was also true for SERCA1a. The subsequent purification, performed in batch instead of column, as previously described (Jidenko et al., 2006), was successful for SERCA1a and could be easily transposed to PfATP6 once the proper protein:resin ratio was determined. Then, we had the good surprise that the thrombin cleavage was facilitated with PfATP6, probably due to its longer C-terminus part than SERCA1a. Finally, almost the same amounts of protein could be recovered from 1mL resin with PfATP6 compared with SERCA1a. All purification protocols have to be checked when dealing with new proteins but in this case, no deep modifications (like different buffer composition, different detergent) were necessary. This validates, once again, the method developed by Jidenko et al. to efficiently purify Ca^{2+}-ATPases by affinity chromatography.

Contrary to the proteins expressed with *X. laevis* oocytes, here, we confirmed by Western-blot analysis, Coomassie blue stained gels and MALDI-TOF analyses, that we produced and purified a protein of a correct size. In the future, mass spectrometry analyses could also be performed to look for post-translational modifications of the protein and see if some of these modifications are essential or not. In addition, we were able to measure a specific ATPase activity of PfATP6 with the same qualitative

characteristics as rabbit SR. The gene optimization does not seem thereby to have generated a misfolded protein. PfATP6 was nevertheless less active and was inhibited with a higher amount of thapsigargin than the one necessary to inhibit SERCA1a revealing functional differences between both proteins.

PfATP6 was stable in DDM. We have nevertheless noticed that PfATP6 was less stable in $C_{12}E_8$ than SERCA1a. This problem was solved by the addition of some phospholipids during ATPase assays but to reconstitute the protein in DOPC proteoliposomes, this was not sufficient. In this case, a first step was reached by using a more stabilizing detergent, DDM, and EYPC as lipids because they can be solubilized by DDM faster than DOPC. Because of a lack of time, I could not test, in suitable conditions, this detergent/lipid couple with preformed liposomes but it should lead to a successful reconstitution of PfATP6. Thus, Ca^{2+}-uptake measurements and therefore a deeper characterization of PfATP6 will be able to be performed with these tight sealed proteoliposomes. Plasmodial membrane protein reconstitutions were carried out with DDM and a mix of EYPC and *E. coli* total lipid extract (Tan et al., 2006). Thereby, the addition of *E. coli* total lipid extract could also be attempted.

The use of DDM and DOPC could also be a solution to stabilize PfATP6 in crystallization experiments. Regarding crystallization assays, they were performed at a pH close to the pI of the protein whereas in the case of SERCA1a, crystallization buffer was at pH 6.8 (Jidenko, 2005), a pH higher than the pI of the protein. A higher pH could be tested to have a global charge of the protein which is negative rather than being positive. I therefore suggest trying pH 8 because PfATP6 is still active at this pH.

Once the conditions of stable ATPase activity of PfATP6 were defined, we tested the inhibition capacity of artemisinin toward PfATP6. However, in these conditions (in detergent/lipid or only in lipids), artemisinin drugs did not inhibit PfATP6, even in presence of iron. We therefore concluded that artemisinin can not inhibit directly PfATP6 as previously claimed. We were not nevertheless able to exclude an indirect interaction of these entities. Thus, it could be interesting to add oocyte membranes together with purified PfATP6 to see if in these new conditions, PfATP6 could be inhibited by artemisinin. Another way to measure ATPase activity such as phosphorylation experiments with radioactive labeled phosphate or ATP followed by electrophoresis with Sarkadi gel could also be attempted in parallel with oocyte membranes, yeast light membranes expressing PfATP6 and purified PfATP6 in presence/absence of artemisinin in order to have a comparative picture.

Many other effects of artemisinin were noted on *Plasmodium* which are sometimes consistent with an effect on calcium homeostasis which might be linked to PfATP6 but some also pinpoints a different target between artemisinin and thapsigargin. Indeed these two drugs did not trigger the same rise of cytosolic calcium (de Pilla Varotti et al.,

2008). Artemisinin can still induce the release of calcium after thapsigargin addition while the contrary is not possible. This suggests another target than exclusively the endoplasmic reticulum. It is as if artemisinin could open the endoplasmic reticulum, acidocalcisomes and/or, mitochondria known as calcium storage places. Does artemisinin act on all these calcium storage compartments? Does artemisinin target another protein? Does artemisinin alkylate heme or iron-containing proteins such as suggested by other groups (see introduction). The main questions remain why artemisinin is concentrated in parasite infected erythrocyte and what is the first effect caused by this drug. The first question might find its answer in the fact that infected erythrocyte membranes are more permeable than healthy red blood cells (Kirk, 2001). The answer to the second question might be a reaction between hemoglobin and artemisinin leading to the dicrease of bioavailable hemoglobin for the parasite, or contained in the five artemisinin-alkylated parasite proteins highlighted with radiolabeled artemisinin (Asawamahasakda et al., 1994). It could therefore be of major importance to highlight these proteins by mass-spectrometry.

In parallel of this research about the mechanism of action of artemisinin, purified PfATP6, an essential protein for *P. falciparum* (since thapsigargin, its specific inhibitor kills *P. falciparum* parasites with an IC_{50} of 2.6µM with chloroquine sensitive parasites, (Eckstein-Ludwig et al., 2003)) can be considered as a new therapeutic target. For this purpose, chemical banks could be screened to find inhibiting drugs of PfATP6 that do not inhibit SERCA1a. In addition, efforts have to be carried out on the crystallization of PfATP6 to access rapidly to its three dimensional structure. With the structure of PfATP6, the research of the "perfect" inhibitor might be facilitated because PfATP6 has a cytosolic organization different from SERCA1a. We saw that the cytosolic domains of the proteins move a lot during the enzyme cycle of SERCA1a. Thus, a linker of the cytosolic domains might therefore deeply disturb the function of PfATP6 and lead to its inhibition.

In conclusion, this work has allowed the production and the purification of a parasite membrane protein, PfATP6, a potential therapeutic target against malaria and has demonstrated that the mechanism of action of artemisinin is more complicated than simply related to the binding of artemisinin on the single SERCA of the malaria parasite. It is therefore urgent to reconsider the mechanism of action of artemisinin.

REFERENCES

Abdin, M. Z., M. Israr, R. U. Rehman and S. K. Jain (2003). "Artemisinin, a novel antimalarial drug: biochemical and molecular approaches for enhanced production." Planta Med **69**(4): 289-99.

Accardo, A., S. A. Laurent, H. Mazarguil, M. Meyer, A. Robert and B. Meunier (2007). "Interaction of iron(II)-heme and artemisinin with a peptide mimic of Plasmodium falciparum HRP-II." J Inorg Biochem **101**(11-12): 1739-47.

Adovelande, J., B. Bastide, J. Deleze and J. Schrevel (1993). "Cytosolic free calcium in Plasmodium falciparum-infected erythrocytes and the effect of verapamil: a cytofluorimetric study." Exp Parasitol **76**(3): 247-58.

Amoah, L. E., J. K. Lekostaj and P. D. Roepe (2007). "Heterologous expression and ATPase activity of mutant versus wild type PfMDR1 protein." Biochemistry **46**(20): 6060-73.

Andersen, J. P., T. L. Sorensen, K. Povlsen and B. Vilsen (2001). "Importance of transmembrane segment M3 of the sarcoplasmic reticulum Ca2+-ATPase for control of the gateway to the Ca2+ sites." J Biol Chem **276**(26): 23312-21.

Angov, E., C. J. Hillier, R. L. Kincaid and J. A. Lyon (2008). "Heterologous protein expression is enhanced by harmonizing the codon usage frequencies of the target gene with those of the expression host." PLoS ONE **3**(5): e2189.

Arsenault, P. R., K. K. Wobbe and P. J. Weathers (2008). "Recent advances in artemisinin production through heterologous expression." Curr Med Chem **15**(27): 2886-96.

Asawamahasakda, W., I. Ittarat, Y. M. Pu, H. Ziffer and S. R. Meshnick (1994). "Reaction of antimalarial endoperoxides with specific parasite proteins." Antimicrob Agents Chemother **38**(8): 1854-8.

Avery, M. A., F. Gao, W. K. Chong, S. Mehrotra and W. K. Milhous (1993). "Structure-activity relationships of the antimalarial agent artemisinin. 1. Synthesis and comparative molecular field analysis of C-9 analogs of artemisinin and 10-deoxoartemisinin." J Med Chem **36**(26): 4264-75.

Avery, M. A., S. Mehrotra, J. D. Bonk, J. A. Vroman, D. K. Goins and R. Miller (1996). "Structure-activity relationships of the antimalarial agent artemisinin. 4. Effect of substitution at C-3." J Med Chem **39**(15): 2900-6.

Balint, G. A. (2001). "Artemisinin and its derivatives: an important new class of antimalarial agents." Pharmacol Ther **90**(2-3): 261-5.

Bardi, L., C. Crivelli and M. Marzona (1998). "Esterase activity and release of ethyl esters of medium-chain fatty acids by Saccharomyces cerevisiae during anaerobic growth." Can J Microbiol **44**(12): 1171-6.

Basco, L. K., O. Dechy-Cabaret, M. Ndounga, F. S. Meche, A. Robert and B. Meunier (2001). "In vitro activities of DU-1102, a new trioxaquine derivative, against Plasmodium falciparum isolates." Antimicrob Agents Chemother **45**(6): 1886-8.

Bhisutthibhan, J., X. Q. Pan, P. A. Hossler, D. J. Walker, C. A. Yowell, J. Carlton, J. B. Dame and S. R. Meshnick (1998). "The Plasmodium falciparum translationally controlled tumor protein homolog and its reaction with the antimalarial drug artemisinin." J Biol Chem **273**(26): 16192-8.

Bhisutthibhan, J., M. A. Philbert, H. Fujioka, M. Aikawa and S. R. Meshnick (1999). "The Plasmodium falciparum translationally controlled tumor protein: subcellular localization and calcium binding." Eur J Cell Biol **78**(9): 665-70.

Bhisutthibhan, J. and S. R. Meshnick (2001). "Immunoprecipitation of [(3)H]dihydroartemisinin translationally controlled tumor protein (TCTP) adducts from Plasmodium falciparum-infected erythrocytes by using anti-TCTP antibodies." Antimicrob Agents Chemother **45**(8): 2397-9.

Burk, O., K. A. Arnold, A. K. Nussler, E. Schaeffeler, E. Efimova, B. A. Avery, M. A. Avery, M. F. Fromm and M. Eichelbaum (2005). "Antimalarial artemisinin drugs induce cytochrome P450 and MDR1 expression by activation of xenosensors pregnane X receptor and constitutive androstane receptor." Mol Pharmacol **67**(6): 1954-65.

Centeno, F., S. Deschamps, A. M. Lompre, M. Anger, M. J. Moutin, Y. Dupont, M. G. Palmgren, J. M. Villalba, J. V. Moller, P. Falson and et al. (1994). "Expression of the sarcoplasmic reticulum Ca(2+)-ATPase in yeast." FEBS Lett **354**(1): 117-22.

Champeil, P., F. Guillain, C. Venien and M. P. Gingold (1985). "Interaction of magnesium and inorganic phosphate with calcium-deprived sarcoplasmic reticulum adenosinetriphosphatase as reflected by organic solvent induced perturbation." Biochemistry **24**(1): 69-81.

Chayen, N. E. (2004). "Turning protein crystallisation from an art into a science." Curr. Opin. Struct. Biol. **14**(5): 577-83.

Chen, D. C., B. C. Yang and T. T. Kuo (1992). "One-step transformation of yeast in stationary phase." Curr Genet **21**(1): 83-4.

Chen, P. Q., G. Q. Li, X. B. Guo, K. R. He, Y. X. Fu, L. C. Fu and Y. Z. Song (1994). "The infectivity of gametocytes of Plasmodium falciparum from patients treated with artemisinin." Chin Med J (Engl) **107**(9): 709-11.

Cheng, F., J. Shen, X. Luo, W. Zhu, J. Gu, R. Ji, H. Jiang and K. Chen (2002). "Molecular docking and 3-D-QSAR studies on the possible antimalarial mechanism of artemisinin analogues." Bioorg Med Chem **10**(9): 2883-91.

Clarke, D. M., K. Maruyama, T. W. Loo, E. Leberer, G. Inesi and D. H. MacLennan (1989). "Functional consequences of glutamate, aspartate, glutamine, and asparagine mutations in the stalk sector of the Ca2+-ATPase of sarcoplasmic reticulum." J Biol Chem **264**(19): 11246-51.

Clausen, J. D., B. Vilsen, D. B. McIntosh, A. P. Einholm and J. P. Andersen (2004). "Glutamate-183 in the conserved TGES motif of domain A of sarcoplasmic reticulum Ca2+-ATPase assists in catalysis of E2/E2P partial reactions." Proc Natl Acad Sci U S A **101**(9): 2776-81.

Cojean, S., V. Hubert, J. Le Bras and R. Durand (2006). "Resistance to dihydroartemisinin." Emerg Infect Dis **12**(11): 1798-9.

Collins, W. E. and J. W. Barnwell (2008). "A hopeful beginning for malaria vaccines." N Engl J Med **359**(24): 2599-601.

Cornelius, F. and J. V. Moller (1991). "Electrogenic pump current of sarcoplasmic reticulum Ca(2+)-ATPase reconstituted at high lipid/protein ratio." FEBS Lett **284**(1): 46-50.

Cosledan, F., L. Fraisse, A. Pellet, F. Guillou, B. Mordmuller, P. G. Kremsner, A. Moreno, D. Mazier, J. P. Maffrand and B. Meunier (2008). "Selection of a trioxaquine as an antimalarial drug candidate." Proc Natl Acad Sci U S A **105**(45): 17579-84.

Dahlstrom, S., M. I. Veiga, P. Ferreira, A. Martensson, A. Kaneko, B. Andersson, A. Bjorkman and J. P. Gil (2008). "Diversity of the sarco/endoplasmic reticulum Ca(2+)-ATPase orthologue of Plasmodium falciparum (PfATP6)." Infect Genet Evol **8**(3): 340-5.

Damsky, C. H. (1976). "Environmentally induced changes in mitochondria and endoplasmic reticulum of Saccharomyces carlsbergensis yeast." J Cell Biol **71**(1): 123-35.

de Foresta, B., M. le Maire, S. Orlowski, P. Champeil, S. Lund, J. V. Moller, F. Michelangeli and A. G. Lee (1989). "Membrane solubilization by detergent: use of brominated phospholipids to evaluate the detergent-induced changes in Ca2+-ATPase/lipid interaction." Biochemistry **28**(6): 2558-67.

de Pilla Varotti, F., A. C. Botelho, A. A. Andrade, R. C. de Paula, E. M. Fagundes, A. Valverde, L. M. Mayer, J. S. Mendonca, M. V. de Souza, N. Boechat and A. U. Krettli (2008). "Synthesis, antimalarial activity, and intracellular targets of MEFAS, a new hybrid compound derived from mefloquine and artesunate." Antimicrob Agents Chemother **52**(11): 3868-74.

Dechy-Cabaret, O., F. Benoit-Vical, C. Loup, A. Robert, H. Gornitzka, A. Bonhoure, H. Vial, J. F. Magnaval, J. P. Seguela and B. Meunier (2004). "Synthesis and antimalarial activity of trioxaquine derivatives." Chemistry **10**(7): 1625-36.

Docampo, R. and S. N. Moreno (2001). "The acidocalcisome." Mol Biochem Parasitol **114**(2): 151-9.

Docampo, R., W. de Souza, K. Miranda, P. Rohloff and S. N. Moreno (2005). "Acidocalcisomes - conserved from bacteria to man." Nat Rev Microbiol **3**(3): 251-61.

Drueckes, P., R. Schinzel and D. Palm (1995). "Photometric microtiter assay of inorganic phosphate in the presence of acid-labile organic phosphates." Anal Biochem **230**(1): 173-7.

Dupont, Y. (1980). "Occlusion of divalent cations in the phosphorylated calcium pump of sarcoplasmic reticulum." Eur J Biochem **109**(1): 231-8.

Duraisingh, M. T. and A. F. Cowman (2005). "Contribution of the pfmdr1 gene to antimalarial drug-resistance." Acta Trop **94**(3): 181-90.

Dyer, M., M. Jackson, C. McWhinney, G. Zhao and R. Mikkelsen (1996). "Analysis of a cation-transporting ATPase of Plasmodium falciparum." Mol Biochem Parasitol **78**(1-2): 1-12.

Eckstein-Ludwig, U., R. J. Webb, I. D. Van Goethem, J. M. East, A. G. Lee, M. Kimura, P. M. O'Neill, P. G. Bray, S. A. Ward and S. Krishna (2003). "Artemisinins target the SERCA of Plasmodium falciparum." Nature **424**(6951): 957-61.

Falson, P., T. Menguy, F. Corre, L. Bouneau, A. G. de Gracia, S. Soulie, F. Centeno, J. V. Moller, P. Champeil and M. le Maire (1997). "The cytoplasmic loop between putative transmembrane segments 6 and 7 in sarcoplasmic reticulum Ca2+-ATPase binds Ca2+ and is functionally important." J Biol Chem **272**(28): 17258-62.

Ferreira, I. D., A. Martinelli, L. A. Rodrigues, E. L. do Carmo, V. E. do Rosario, M. M. Povoa and P. Cravo (2008). "Plasmodium falciparum from Para state (Brazil) shows satisfactory in vitro response to artemisinin derivatives and absence of the S769N mutation in the SERCA-type PfATPase6." Trop Med Int Health **13**(2): 199-207.

Fidock, D. A., R. T. Eastman, S. A. Ward and S. R. Meshnick (2008). "Recent highlights in antimalarial drug resistance and chemotherapy research." Trends Parasitol **24**(12): 537-44.

Fishwick, J., G. Edwards, S. A. Ward and W. G. McLean (1998). "Morphological and immunocytochemical effects of dihydroartemisinin on differentiating NB2a neuroblastoma cells." Neurotoxicology **19**(3): 393-403.

Fujioka, H. and M. Aikawa (2002). "Structure and life cycle." Chem Immunol **80**: 1-26.

Garcia, C. R., A. R. Dluzewski, L. H. Catalani, R. Burting, J. Hoyland and W. T. Mason (1996). "Calcium homeostasis in intraerythrocytic malaria parasites." Eur J Cell Biol **71**(4): 409-13.

Garcia, C. R. (1999). "Calcium homeostasis and signaling in the blood-stage malaria parasite." Parasitol Today **15**(12): 488-91.

Gardner, M. J., et, al. and - (2002). "Genome sequence of the human malaria parasite Plasmodium falciparum." Nature **419**(6906): 498-511.

Gazarini, M. L. and C. R. Garcia (2004). "The malaria parasite mitochondrion senses cytosolic Ca2+ fluctuations." Biochem Biophys Res Commun **321**(1): 138-44.

Gazarini, M. L., C. A. Sigolo, R. P. Markus, A. P. Thomas and C. R. Garcia (2007). "Antimalarial drugs disrupt ion homeostasis in malarial parasites." Mem Inst Oswaldo Cruz **102**(3): 329-34.

Geering, K., I. Theulaz, F. Verrey, M. T. Hauptle and B. C. Rossier (1989). "A role for the beta-subunit in the expression of functional Na+-K+-ATPase in Xenopus oocytes." Am J Physiol **257**(5 Pt 1): C851-8.

Geering, K. (2001). "The functional role of beta subunits in oligomeric P-type ATPases." J Bioenerg Biomembr **33**(5): 425-38.

Geertsma, E. R., N. A. Nik Mahmood, G. K. Schuurman-Wolters and B. Poolman (2008). "Membrane reconstitution of ABC transporters and assays of translocator function." Nat Protoc **3**(2): 256-66.

Gietz, R. D., R. H. Schiestl, A. R. Willems and R. A. Woods (1995). "Studies on the transformation of intact yeast cells by the LiAc/SS-DNA/PEG procedure." Yeast **11**(4): 355-60.

Golenser, J., A. Domb, B. Leshem, P. Kremsner and A. Luty (2003). "Iron chelators as drugs against malaria pose a potential risk." Redox Rep **8**(5): 268-71.

Golenser, J., J. H. Waknine, M. Krugliak, N. H. Hunt and G. E. Grau (2006). "Current perspectives on the mechanism of action of artemisinins." Int J Parasitol **36**(14): 1427-41.

Gordi, T. and E. I. Lepist (2004). "Artemisinin derivatives: toxic for laboratory animals, safe for humans?" Toxicol Lett **147**(2): 99-107.

group, Q. A. C. r. (1979). "Antimalaria studies on Qinghaosu." Chin Med J (Engl) **92**(12): 811-6.

Gu, H. M., D. C. Warhurst and W. Peters (1984). "Uptake of [3H] dihydroartemisinine by erythrocytes infected with Plasmodium falciparum in vitro." Trans R Soc Trop Med Hyg **78**(2): 265-70.

Hasselbach, W. and M. Makinose (1963). "[on the Mechanism of Calcium Transport across the Membrane of the Sarcoplasmic Reticulum.]." Biochem Z **339**: 94-111.

Haviv, H., E. Cohen, Y. Lifshitz, D. M. Tal, R. Goldshleger and S. J. Karlish (2007). "Stabilization of Na(+),K(+)-ATPase purified from Pichia pastoris membranes by specific interactions with lipids." Biochemistry **46**(44): 12855-67.

Haynes, R. K. and S. Krishna (2004). "Artemisinins: activities and actions." Microbes Infect **6**(14): 1339-46.

Haynes, R. K., B. Fugmann, J. Stetter, K. Rieckmann, H. D. Heilmann, H. W. Chan, M. K. Cheung, W. L. Lam, H. N. Wong, S. L. Croft, L. Vivas, L. Rattray, L. Stewart, W. Peters, B. L. Robinson, M. D. Edstein, B. Kotecka, D. E. Kyle, B. Beckermann, M. Gerisch, M. Radtke, G. Schmuck, W. Steinke, U. Wollborn, K. Schmeer and A. Romer (2006). "Artemisone--a highly active antimalarial drug of the artemisinin class." Angew Chem Int Ed Engl **45**(13): 2082-8.

Haynes, R. K., W. C. Chan, C. M. Lung, A. C. Uhlemann, U. Eckstein, D. Taramelli, S. Parapini, D. Monti and S. Krishna (2007). "The Fe2+-mediated decomposition, PfATP6 binding, and antimalarial activities of artemisone and other artemisinins: the unlikelihood of C-centered radicals as bioactive intermediates." ChemMedChem **2**(10): 1480-97.

Hedfalk, K., N. Pettersson, F. Oberg, S. Hohmann and E. Gordon (2008). "Production, characterization and crystallization of the Plasmodium falciparum aquaporin." Protein Expr Purif **59**(1): 69-78.

Hoppe, H. C., D. A. van Schalkwyk, U. I. Wiehart, S. A. Meredith, J. Egan and B. W. Weber (2004). "Antimalarial quinolines and artemisinin inhibit endocytosis in Plasmodium falciparum." Antimicrob Agents Chemother **48**(7): 2370-8.

Hotta, C. T., M. L. Gazarini, F. H. Beraldo, F. P. Varotti, C. Lopes, R. P. Markus, T. Pozzan and C. R. Garcia (2000). "Calcium-dependent modulation by melatonin of the circadian rhythm in malarial parasites." Nat Cell Biol **2**(7): 466-8.

Inesi, G., M. Kurzmack, C. Coan and D. E. Lewis (1980). "Cooperative calcium binding and ATPase activation in sarcoplasmic reticulum vesicles." J Biol Chem **255**(7): 3025-31.

Inesi, G., D. Lewis, C. Toyoshima, A. Hirata and L. de Meis (2008). "Conformational fluctuations of the Ca2+-ATPase in the native membrane environment. Effects of pH, temperature, catalytic substrates, and thapsigargin." J Biol Chem **283**(2): 1189-96.

Ionita, M., S. Krishna, P. M. Leo, C. Morin and A. P. Patel (2007). "Interaction of O-(undec-10-en)-yl-D-glucose derivatives with the Plasmodium falciparum hexose transporter (PfHT)." Bioorg Med Chem Lett **17**(17): 4934-7.

Ittarat, W., A. Sreepian, A. Srisarin and K. Pathepchotivong (2003). "Effect of dihydroartemisinin on the antioxidant capacity of P. falciparum-infected erythrocytes." Southeast Asian J Trop Med Public Health **34**(4): 744-50.

Jambou, R., E. Legrand, M. Niang, N. Khim, P. Lim, B. Volney, M. T. Ekala, C. Bouchier, P. Esterre, T. Fandeur and O. Mercereau-Puijalon (2005). "Resistance of Plasmodium falciparum field isolates to in-vitro artemether and point mutations of the SERCA-type PfATPase6." Lancet **366**(9501): 1960-3.

Jensen, A. M., T. L. Sorensen, C. Olesen, J. V. Moller and P. Nissen (2006). "Modulatory and catalytic modes of ATP binding by the calcium pump." EMBO J. **25**(11): 2305-14.

Jiang, J. B., G. Jacobs, D. S. Liang and M. Aikawa (1985). "Qinghaosu-induced changes in the morphology of Plasmodium inui." Am J Trop Med Hyg **34**(3): 424-8.

Jidenko, M. (2005). "Etude de l'ATPase Ca2+ du réticulum sarco/endoplasmique : Mise au point d'une nouvelle méthode de purification de SERCA1a de lapin exprimée chez S. cerevisiae permettant sa cristallisation et applications au mutant E309Q-Etude d'une autre isoforme, SERCA3a." PhD Thesis.

Jidenko, M., R. C. Nielsen, T. L. Sorensen, J. V. Moller, M. le Maire, P. Nissen and C. Jaxel (2005). "Crystallization of a mammalian membrane protein overexpressed in Saccharomyces cerevisiae." Proc Natl Acad Sci U S A **102**(33): 11687-91.

Jidenko, M., G. Lenoir, J. M. Fuentes, M. le Maire and C. Jaxel (2006). "Expression in yeast and purification of a membrane protein, SERCA1a, using a biotinylated acceptor domain." Protein Expr Purif **48**(1): 32-42.

Jung, M., H. Kim, K. Y. Nam and K. T. No (2005). "Three-dimensional structure of Plasmodium falciparum Ca2+ -ATPase(PfATP6) and docking of artemisinin derivatives to PfATP6." Bioorg Med Chem Lett **15**(12): 2994-7.

Juul, B., H. Turc, M. L. Durand, A. Gomez de Gracia, L. Denoroy, J. V. Moller, P. Champeil and M. le Maire (1995). "Do transmembrane segments in proteolyzed sarcoplasmic reticulum Ca(2+)-ATPase retain their functional Ca2+ binding properties after removal of cytoplasmic fragments by proteinase K?" J Biol Chem **270**(34): 20123-34.

Kannan, R., D. Sahal and V. S. Chauhan (2002). "Heme-artemisinin adducts are crucial mediators of the ability of artemisinin to inhibit heme polymerization." Chem Biol **9**(3): 321-32.

Kannan, R., K. Kumar, D. Sahal, S. Kukreti and V. S. Chauhan (2005). "Reaction of artemisinin with haemoglobin: implications for antimalarial activity." Biochem J **385**(Pt 2): 409-18.

Kaplan, J. H. (2002). "Biochemistry of Na,K-ATPase." Annu Rev Biochem **71**: 511-35.

Kimchi-Sarfaty, C., J. M. Oh, I. W. Kim, Z. E. Sauna, A. M. Calcagno, S. V. Ambudkar and M. M. Gottesman (2007). "A "silent" polymorphism in the MDR1 gene changes substrate specificity." Science **315**(5811): 525-8.

Kimura, M., Y. Yamaguchi, S. Takada and K. Tanabe (1993). "Cloning of a Ca(2+)-ATPase gene of Plasmodium falciparum and comparison with vertebrate Ca(2+)-ATPases." J Cell Sci **104 (Pt 4)**: 1129-36.

Kirk, K. (2001). "Membrane transport in the malaria-infected erythrocyte." Physiol Rev **81**(2): 495-537.

Klayman, D. L. (1985). "Quinghasu (Artemisinin): an antimalarial drug from China." Science **228**: 1049-1055.

Komar, A. A., T. Lesnik and C. Reiss (1999). "Synonymous codon substitutions affect ribosome traffic and protein folding during in vitro translation." FEBS Lett **462**(3): 387-91.

Kombila, M., T. H. Duong, D. Dufillot, J. Koko, V. Guiyedi, C. Guiguen, A. Ferrer and D. Richard-Lenoble (1997). "Light microscopic changes in Plasmodium falciparum from Gabonese children treated with artemether." Am J Trop Med Hyg **57**(6): 643-5.

Kragh-Hansen, U., M. le Maire, J. P. Noel, T. Gulik-Krzywicki and J. V. Moller (1993). "Transitional steps in the solubilization of protein-containing membranes and liposomes by nonionic detergent." Biochemistry **32**(6): 1648-56.

Kramer, R. and H. Ginsburg (1991). "Calcium transport and compartment analysis of free and exchangeable calcium in Plasmodium falciparum-infected red blood cells." J Protozool **38**(6): 594-601.

Krishna, S., C. Woodrow, R. Webb, J. Penny, K. Takeyasu, M. Kimura and J. M. East (2001). "Expression and functional characterization of a Plasmodium falciparum Ca2+-ATPase (PfATP4) belonging to a subclass unique to apicomplexan organisms." J Biol Chem **276**(14): 10782-7.

Krishna, S., A. C. Uhlemann and R. K. Haynes (2004). "Artemisinins: mechanisms of action and potential for resistance." Drug Resist Updat **7**(4-5): 233-44.

Krishna, S., L. Bustamante, R. K. Haynes and H. M. Staines (2008). "Artemisinins: their growing importance in medicine." Trends Pharmacol Sci **29**(10): 520-7.

Krungkrai, J., D. Burat, S. Kudan, S. Krungkrai and P. Prapunwattana (1999). "Mitochondrial oxygen consumption in asexual and sexual blood stages of the human malarial parasite, Plasmodium falciparum." Southeast Asian J Trop Med Public Health **30**(4): 636-42.

Kuhlbrandt, W. (2004). "Biology, structure and mechanism of P-type ATPases." Nat Rev Mol Cell Biol **5**(4): 282-95.

Kumar, N. and H. Zheng (1990). "Stage-specific gametocytocidal effect in vitro of the antimalaria drug qinghaosu on Plasmodium falciparum." Parasitol Res **76**(3): 214-8.

Kumar, S., A. K. Gupta, Y. Pal and S. K. Dwivedi (2003). "In-vivo therapeutic efficacy trial with artemisinin derivative, buparvaquone and imidocarb dipropionate against Babesia equi infection in donkeys." J Vet Med Sci **65**(11): 1171-7.

Kurland, C. and J. Gallant (1996). "Errors of heterologous protein expression." Curr Opin Biotechnol **7**(5): 489-93.

Lacount, D. J., L. W. Schoenfeld and S. Fields (2009). "Selection of yeast strains with enhanced expression of Plasmodium falciparum proteins." Mol Biochem Parasitol **163**(2): 119-22.

le Maire, M., J. V. Moller and C. Tanford (1976). "Retention of enzyme activity by detergent-solubilized sarcoplasmic Ca2+ -ATPase." Biochemistry **15**(11): 2336-42.

le Maire, M., P. Champeil and J. V. Moller (2000). "Interaction of membrane proteins and lipids with solubilizing detergents." Biochim Biophys Acta **1508**(1-2): 86-111.

Leida, M. N., J. R. Mahoney and J. W. Eaton (1981). "Intraerythrocytic plasmodial calcium metabolism." Biochem Biophys Res Commun **103**(2): 402-6.

Lenoir, G., T. Menguy, F. Corre, C. Montigny, P. A. Pedersen, D. Thines, M. le Maire and P. Falson (2002). "Overproduction in yeast and rapid and efficient purification of the rabbit SERCA1a Ca(2+)-ATPase." Biochim Biophys Acta **1560**(1-2): 67-83.

Lenoir, G., M. Picard, J. V. Moller, M. le Maire, P. Champeil and P. Falson (2004). "Involvement of the L6-7 loop in SERCA1a Ca2+-ATPase activation by Ca2+ (or Sr2+) and ATP." J Biol Chem **279**(31): 32125-33.

Li, W., W. Mo, D. Shen, L. Sun, J. Wang, S. Lu, J. M. Gitschier and B. Zhou (2005). "Yeast model uncovers dual roles of mitochondria in action of artemisinin." PLoS Genet **1**(3): e36.

Lund, S., S. Orlowski, B. de Foresta, P. Champeil, M. le Maire and J. V. Moller (1989). "Detergent structure and associated lipid as determinants in the stabilization of solubilized Ca2+-ATPase from sarcoplasmic reticulum." J Biol Chem **264**(9): 4907-15.

Lutsenko, S. and J. H. Kaplan (1993). "An essential role for the extracellular domain of the Na,K-ATPase beta-subunit in cation occlusion." Biochemistry **32**(26): 6737-43.

Lytton, J., M. Westlin, S. E. Burk, G. E. Shull and D. H. MacLennan (1992). "Functional comparisons between isoforms of the sarcoplasmic or endoplasmic reticulum family of calcium pumps." J Biol Chem **267**(20): 14483-9.

MacLennan, D. H. (1970). "Purification and properties of an adenosine triphosphatase from sarcoplasmic reticulum." J Biol Chem **245**(17): 4508-18.

MacLennan, D. H., C. J. Brandl, B. Korczak and N. M. Green (1985). "Amino-acid sequence of a Ca2+ + Mg2+-dependent ATPase from rabbit muscle sarcoplasmic reticulum, deduced from its complementary DNA sequence." Nature **316**(6030): 696-700.

Maeno, Y., T. Toyoshima, H. Fujioka, Y. Ito, S. R. Meshnick, A. Benakis, W. K. Milhous and M. Aikawa (1993). "Morphologic effects of artemisinin in Plasmodium falciparum." Am J Trop Med Hyg **49**(4): 485-91.

Marchand, A., A. M. Winther, P. J. Holm, C. Olesen, C. Montigny, B. Arnou, P. Champeil, J. D. Clausen, B. Vilsen, J. P. Andersen, P. Nissen, C. Jaxel, J. V. Moller and M. le Maire (2008). "Crystal structure of D351A and P312A mutant forms of the mammalian sarcoplasmic reticulum Ca(2+) -ATPase reveals key events in phosphorylation and Ca(2+) release." J Biol Chem **283**(21): 14867-82.

Marchesini, N., S. Luo, C. O. Rodrigues, S. N. Moreno and R. Docampo (2000). "Acidocalcisomes and a vacuolar H+-pyrophosphatase in malaria parasites." Biochem J **347 Pt 1**: 243-53.

Maruyama, K. and D. H. MacLennan (1988). "Mutation of aspartic acid-351, lysine-352, and lysine-515 alters the Ca2+ transport activity of the Ca2+-ATPase expressed in COS-1 cells." Proc Natl Acad Sci U S A **85**(10): 3314-8.

Matsumoto, Y., G. Perry, L. W. Scheibel and M. Aikawa (1987). "Role of calmodulin in Plasmodium falciparum: implications for erythrocyte invasion by the merozoite." Eur J Cell Biol **45**(1): 36-43.

Mehlin, C., E. Boni, F. S. Buckner, L. Engel, T. Feist, M. H. Gelb, L. Haji, D. Kim, C. Liu, N. Mueller, P. J. Myler, J. T. Reddy, J. N. Sampson, E. Subramanian, W. C. Van Voorhis, E. Worthey, F. Zucker and W. G. Hol (2006). "Heterologous expression of proteins from Plasmodium falciparum: results from 1000 genes." Mol Biochem Parasitol **148**(2): 144-60.

Menguy, T., F. Corre, L. Bouneau, S. Deschamps, J. V. Moller, P. Champeil, M. le Maire and P. Falson (1998). "The cytoplasmic loop located between transmembrane segments 6 and 7 controls activation by Ca2+ of sarcoplasmic reticulum Ca2+-ATPase." J Biol Chem **273**(32): 20134-43.

Meshnick, S. R., A. Thomas, A. Ranz, C. M. Xu and H. Z. Pan (1991). "Artemisinin (qinghaosu): the role of intracellular hemin in its mechanism of antimalarial action." Mol Biochem Parasitol **49**(2): 181-9.

Meshnick, S. R., Y. Z. Yang, V. Lima, F. Kuypers, S. Kamchonwongpaisan and Y. Yuthavong (1993). "Iron-dependent free radical generation from the antimalarial agent artemisinin (qinghaosu)." Antimicrob Agents Chemother **37**(5): 1108-14.

Meshnick, S. R., T. E. Taylor and S. Kamchonwongpaisan (1996). "Artemisinin and the antimalarial endoperoxides: from herbal remedy to targeted chemotherapy." Microbiol Rev **60**(2): 301-15.

Miras, R., M. Cuillel, P. Catty, F. Guillain and E. Mintz (2001). "Purification of heterologous sarcoplasmic reticulum Ca2+-ATPase Serca1a allowing phosphoenzyme and Ca2+-affinity measurements." Protein Expr Purif **22**(2): 299-306.

Moller, J. V., K. E. Lind and J. P. Andersen (1980). "Enzyme kinetics and substrate stabilization of detergent-solubilized and membraneous (Ca2+ + Mg2+)-activated ATPase from sarcoplasmic reticulum. Effect of protein-protein interactions." J Biol Chem **255**(5): 1912-20.

Moller, J. V., B. Juul and M. le Maire (1996). "Structural organization, ion transport, and energy transduction of P-type ATPases." Biochim Biophys Acta **1286**(1): 1-51.

Moller, J. V., P. Nissen, T. L. Sorensen and M. le Maire (2005). "Transport mechanism of the sarcoplasmic reticulum Ca2+ -ATPase pump." Curr Opin Struct Biol **15**(4): 387-93.

Moller, J. V., C. Olesen, A. M. Jensen and P. Nissen (2005). "The structural basis for coupling of Ca2+ transport to ATP hydrolysis by the sarcoplasmic reticulum Ca2+-ATPase." J Bioenerg Biomembr **37**(6): 359-64.

Moncoq, K., C. A. Trieber and H. S. Young (2007). "The molecular basis for cyclopiazonic acid inhibition of the sarcoplasmic reticulum calcium pump." J Biol Chem **282**(13): 9748-57.

Montigny, C., C. Jaxel, A. Shainskaya, J. Vinh, V. Labas, J. V. Moller, S. J. Karlish and M. le Maire (2004). "Fe2+ -catalyzed oxidative cleavages of Ca2+ -ATPase reveal novel features of its pumping mechanism." J Biol Chem **279**(42): 43971-81.

Morth, J. P., B. P. Pedersen, M. S. Toustrup-Jensen, T. L. Sorensen, J. Petersen, J. P. Andersen, B. Vilsen and P. Nissen (2007). "Crystal structure of the sodium-potassium pump." Nature **450**(7172): 1043-9.

Nagamune, K. and L. D. Sibley (2006). "Comparative genomic and phylogenetic analyses of calcium ATPases and calcium-regulated proteins in the apicomplexa." Mol Biol Evol **23**(8): 1613-27.

Nagamune, K., W. L. Beatty and L. D. Sibley (2007). "Artemisinin induces calcium-dependent protein secretion in the protozoan parasite Toxoplasma gondii." Eukaryot Cell **6**(11): 2147-56.

Nagamune, K., S. N. Moreno and L. D. Sibley (2007). "Artemisinin-resistant mutants of Toxoplasma gondii have altered calcium homeostasis." Antimicrob Agents Chemother **51**(11): 3816-23.

Nagamune, K., S. N. Moreno, E. N. Chini and L. D. Sibley (2008). "Calcium regulation and signaling in apicomplexan parasites." Subcell Biochem **47**: 70-81.

Nagelschmitz, J., B. Voith, G. Wensing, A. Roemer, B. Fugmann, R. K. Haynes, B. M. Kotecka, K. H. Rieckmann and M. D. Edstein (2008). "First assessment in humans of the safety, tolerability, pharmacokinetics, and ex vivo pharmacodynamic antimalarial activity of the new artemisinin derivative artemisone." Antimicrob Agents Chemother **52**(9): 3085-91.

Nessler, S., O. Friedrich, N. Bakouh, R. H. Fink, C. P. Sanchez, G. Planelles and M. Lanzer (2004). "Evidence for activation of endogenous transporters in Xenopus laevis oocytes expressing the Plasmodium falciparum chloroquine resistance transporter, PfCRT." J Biol Chem **279**(38): 39438-46.

Newby, Z. E., J. O'Connell, 3rd, Y. Robles-Colmenares, S. Khademi, L. J. Miercke and R. M. Stroud (2008). "Crystal structure of the aquaglyceroporin PfAQP from the malarial parasite Plasmodium falciparum." Nat Struct Mol Biol **15**(6): 619-25.

Noedl, H., Y. Se, K. Schaecher, B. L. Smith, D. Socheat and M. M. Fukuda (2008). "Evidence of artemisinin-resistant malaria in western Cambodia." N Engl J Med **359**(24): 2619-20.

O'Neill, P. M. (2005). "The therapeutic potential of semi-synthetic artemisinin and synthetic endoperoxide antimalarial agents." Expert Opin Investig Drugs **14**(9): 1117-28.

Obara, K., N. Miyashita, C. Xu, I. Toyoshima, Y. Sugita, G. Inesi and C. Toyoshima (2005). "Structural role of countertransport revealed in Ca(2+) pump crystal structure in the absence of Ca(2+)." Proc Natl Acad Sci U S A **102**(41): 14489-96.

Olesen, C., T. L. Sorensen, R. C. Nielsen, J. V. Moller and P. Nissen (2004). "Dephosphorylation of the calcium pump coupled to counterion occlusion." Science **306**(5705): 2251-5.

Olesen, C., M. Picard, A. M. Winther, C. Gyrup, J. P. Morth, C. Oxvig, J. V. Moller and P. Nissen (2007). "The structural basis of calcium transport by the calcium pump." Nature **450**(7172): 1036-42.

Olliaro, P. L., R. K. Haynes, B. Meunier and Y. Yuthavong (2001). "Possible modes of action of the artemisinin-type compounds." Trends Parasitol **17**(3): 122-6.

Palmgren, M. G. and K. B. Axelsen (1998). "Evolution of P-type ATPases." Biochim Biophys Acta **1365**(1-2): 37-45.

Pandey, A. V., B. L. Tekwani, R. L. Singh and V. S. Chauhan (1999). "Artemisinin, an endoperoxide antimalarial, disrupts the hemoglobin catabolism and heme detoxification systems in malarial parasite." J Biol Chem **274**(27): 19383-8.

Parapini, S., N. Basilico, M. Mondani, P. Olliaro, D. Taramelli and D. Monti (2004). "Evidence that haem iron in the malaria parasite is not needed for the antimalarial effects of artemisinin." FEBS Lett **575**(1-3): 91-4.

Pashynska, V. A., H. Van den Heuvel, M. Claeys and M. V. Kosevich (2004). "Characterization of noncovalent complexes of antimalarial agents of the artemisinin-type and FE(III)-heme by electrospray mass spectrometry and collisional activation tandem mass spectrometry." J Am Soc Mass Spectrom **15**(8): 1181-90.

Passos, A. P. and C. R. Garcia (1997). "Characterization of Ca2+ transport activity associated with a non-mitochondrial calcium pool in the rodent malaria parasite P. chabaudi." Biochem Mol Biol Int **42**(5): 919-25.

Passos, A. P. and C. R. Garcia (1998). "Inositol 1,4,5-trisphosphate induced Ca2+ release from chloroquine-sensitive and -insensitive intracellular stores in the intraerythrocytic stage of the malaria parasite P. chabaudi." Biochem Biophys Res Commun **245**(1): 155-60.

Paulusma, C. C. and R. P. Oude Elferink (2005). "The type 4 subfamily of P-type ATPases, putative aminophospholipid translocases with a role in human disease." Biochim Biophys Acta **1741**(1-2): 11-24.

Pedersen, B. P., M. J. Buch-Pedersen, J. P. Morth, M. G. Palmgren and P. Nissen (2007). "Crystal structure of the plasma membrane proton pump." Nature **450**(7172): 1111-4.

Pompon, D., B. Louerat, A. Bronine and P. Urban (1996). "Yeast expression of animal and plant P450s in optimized redox environments." Methods Enzymol **272**: 51-64.

Prieto, J. H., S. Koncarevic, S. K. Park, J. Yates, 3rd and K. Becker (2008). "Large-scale differential proteome analysis in Plasmodium falciparum under drug treatment." PLoS ONE **3**(12): e4098.

Rasmussen, U., S. Broogger Christensen and F. Sandberg (1978). "Thapsigargine and thapsigargicine, two new histamine liberators from Thapsia garganica L." Acta Pharm Suec **15**(2): 133-40.

Rawlings, D. J. and D. C. Kaslow (1992). "A novel 40-kDa membrane-associated EF-hand calcium-binding protein in Plasmodium falciparum." J Biol Chem **267**(6): 3976-82.

Reeves, D. C., D. A. Liebelt, V. Lakshmanan, P. D. Roepe, D. A. Fidock and M. H. Akabas (2006). "Chloroquine-resistant isoforms of the Plasmodium falciparum chloroquine resistance transporter acidify lysosomal pH in HEK293 cells more than chloroquine-sensitive isoforms." Mol Biochem Parasitol **150**(2): 288-99.

Reis, E. M., E. Kurtenbach, A. R. Ferreira, P. J. Biselli, C. W. Slayman and V.-A. S. (1999). "N-terminal chimeric constructs improve the expression of sarcoplasmic reticulum Ca(2+)-ATPase in yeast." Biochim Biophys Acta **1461**(1): 83-95.

Reungpatthanaphong, P. and S. Mankhetkorn (2002). "Modulation of multidrug resistance by artemisinin, artesunate and dihydroartemisinin in K562/adr and GLC4/adr resistant cell lines." Biol Pharm Bull **25**(12): 1555-61.

Rigaud, J. L., G. Mosser, J. J. Lacapere, A. Olofsson, D. Levy and J. L. Ranck (1997). "Bio-Beads: an efficient strategy for two-dimensional crystallization of membrane proteins." J Struct Biol **118**(3): 226-35.

Rigaud, J. L. and D. Levy (2003). "Reconstitution of membrane proteins into liposomes." Methods Enzymol **372**: 65-86.

Robert, A., J. Cazelles and B. Meunier (2001). "Characterization of the Alkylation Product of Heme by the Antimalarial Drug Artemisinin We are grateful to the CNRS for financial support, and to the French Ministery of Education for a PhD grant to J.C. Dr. Yannick Coppel (LCC-CNRS) is gratefully acknowledged for discussions on NMR data." Angew Chem Int Ed Engl **40**(10): 1954-1957.

Robert, A., F. Benoit-Vical, C. Claparols and B. Meunier (2005). "The antimalarial drug artemisinin alkylates heme in infected mice." Proc Natl Acad Sci U S A **102**(38): 13676-80.

Robert, A., C. Bonduelle, S. A.-L. Laurent and M. B. (2006). "Heme alkylation by artemisinin and trioxaquines." Journal of physical organic chemistry **19**: 562-569.

Robson, K. J. and M. W. Jennings (1991). "The structure of the calmodulin gene of Plasmodium falciparum." Mol Biochem Parasitol **46**(1): 19-34.

Rohrbach, P., O. Friedrich, J. Hentschel, H. Plattner, R. H. Fink and M. Lanzer (2005). "Quantitative calcium measurements in subcellular compartments of Plasmodium falciparum-infected erythrocytes." J Biol Chem **280**(30): 27960-9.

Sacarlal, J., J. J. Aponte, P. Aide, I. Mandomando, Q. Bassat, C. Guinovart, A. Leach, J. Milman, E. Macete, M. Espasa, O. Ofori-Anyinam, J. Thonnard, S. Corachan, M. C. Dubois, M. Lievens, F. Dubovsky, W. R. Ballou, J. Cohen and P. L. Alonso (2008). "Safety of the RTS,S/AS02A malaria vaccine in Mozambican children during a Phase IIb trial." Vaccine **26**(2): 174-84.

Sagara, Y. and G. Inesi (1991). "Inhibition of the sarcoplasmic reticulum Ca2+ transport ATPase by thapsigargin at subnanomolar concentrations." J Biol Chem **266**(21): 13503-6.

Saheki, S., A. Takeda and T. Shimazu (1985). "Assay of inorganic phosphate in the mild pH range, suitable for measurement of glycogen phosphorylase activity." Anal Biochem **148**(2): 277-81.

Sanger, F., S. Nicklen and A. R. Coulson (1977). "DNA sequencing with chain-terminating inhibitors." Proc Natl Acad Sci U S A **74**(12): 5463-7.

Schmid, G. and W. Hofheinz (1983). "Total Synthesis of Qinghaosu." Journal of the American Chemical Society **105**(3): 624-625.

Scholl, P. F., A. K. Tripathi and D. J. Sullivan (2005). "Bioavailable iron and heme metabolism in Plasmodium falciparum." Curr Top Microbiol Immunol **295**: 293-324.

Schultz, L. D., K. J. Hofmann, L. M. Mylin, D. L. Montgomery, R. W. Ellis and J. E. Hopper (1987). "Regulated overproduction of the GAL4 gene product greatly increases expression from galactose-inducible promoters on multi-copy expression vectors in yeast." Gene **61**(2): 123-33.

Schwarzer, E., F. Turrini and P. Arese (1994). "A luminescence method for the quantitative determination of phagocytosis of erythrocytes, of malaria-parasitized erythrocytes and of malarial pigment." Br J Haematol **88**(4): 740-5.

Seidler, N. W., I. Jona, M. Vegh and A. Martonosi (1989). "Cyclopiazonic acid is a specific inhibitor of the Ca2+-ATPase of sarcoplasmic reticulum." J Biol Chem **264**(30): 17816-23.

Sharp, P. M. and W. H. Li (1987). "The codon Adaptation Index--a measure of directional synonymous codon usage bias, and its potential applications." Nucleic Acids Res **15**(3): 1281-95.

Sibley, C. H., V. H. Brophy, S. Cheesman, K. L. Hamilton, E. G. Hankins, J. M. Wooden and B. Kilbey (1997). "Yeast as a model system to study drugs effective against apicomplexan proteins." Methods **13**(2): 190-207.

Sinou, V. (1998). "Nouvelles approches dans la morphogenèse du Plasmodium et du Trypanosome : Incidences en chimiothérapie. ." PhD Thesis.

Skerjanc, I. S., T. Toyofuku, C. Richardson and D. H. MacLennan (1993). "Mutation of glutamate 309 to glutamine alters one Ca(2+)-binding site in the Ca(2+)-ATPase of sarcoplasmic reticulum expressed in Sf9 cells." J Biol Chem **268**(21): 15944-50.

Smith, P. K., R. I. Krohn, G. T. Hermanson, A. K. Mallia, F. H. Gartner, M. D. Provenzano, E. K. Fujimoto, N. M. Goeke, B. J. Olson and D. C. Klenk (1985). "Measurement of protein using bicinchoninic acid." Anal Biochem **150**(1): 76-85.

Sorensen, T. L., J. V. Moller and P. Nissen (2004). "Phosphoryl transfer and calcium ion occlusion in the calcium pump." Science **304**(5677): 1672-5.

Soulie, S., L. Denoroy, J. P. Le Caer, N. Hamasaki, J. D. Groves and M. le Maire (1998). "Treatment with crystalline ultra-pure urea reduces the aggregation of integral membrane proteins without inhibiting N-terminal sequencing." J Biochem **124**(2): 417-20.

Stoute, J. A., M. Slaoui, D. G. Heppner, P. Momin, K. E. Kester, P. Desmons, B. T. Wellde, N. Garcon, U. Krzych and M. Marchand (1997). "A preliminary evaluation of a recombinant circumsporozoite protein vaccine against Plasmodium falciparum malaria. RTS,S Malaria Vaccine Evaluation Group." N Engl J Med **336**(2): 86-91.

Sullivan, D. J., Jr., I. Y. Gluzman and D. E. Goldberg (1996). "Plasmodium hemozoin formation mediated by histidine-rich proteins." Science **271**(5246): 219-22.

Tadini-Buoninsegni, F., G. Bartolommei, M. R. Moncelli, R. Guidelli and G. Inesi (2006). "Pre-steady state electrogenic events of Ca2+/H+ exchange and transport by the Ca2+-ATPase." J Biol Chem **281**(49): 37720-7.

Takahashi, M., Y. Kondou and C. Toyoshima (2007). "Interdomain communication in calcium pump as revealed in the crystal structures with transmembrane inhibitors." Proc Natl Acad Sci U S A **104**(14): 5800-5.

Tan, W., D. M. Gou, E. Tai, Y. Z. Zhao and L. M. Chow (2006). "Functional reconstitution of purified chloroquine resistance membrane transporter expressed in yeast." Arch Biochem Biophys **452**(2): 119-28.

Tanabe, K., R. B. Mikkelsen and D. F. Wallach (1982). "Calcium transport of Plasmodium chabaudi-infected erythrocytes." J Cell Biol **93**(3): 680-4.

Tanabe, K., A. Izumo, M. Kato, A. Miki and S. Doi (1989). "Stage-dependent inhibition of Plasmodium falciparum by potent Ca2+ and calmodulin modulators." J Protozool **36**(2): 139-43.

Tanford, C., J. A. Reynolds and E. A. Johnson (1985). "Thermodynamic and kinetic cooperativity in ligand binding to multiple sites on a protein: Ca2+ activation of an ATP-driven Ca pump." Proc Natl Acad Sci U S A **82**(14): 4688-92.

Targett, G., C. Drakeley, M. Jawara, L. von Seidlein, R. Coleman, J. Deen, M. Pinder, T. Doherty, C. Sutherland, G. Walraven and P. Milligan (2001). "Artesunate reduces but does not prevent posttreatment transmission of Plasmodium falciparum to Anopheles gambiae." J Infect Dis **183**(8): 1254-9.

ter Kuile, F., N. J. White, P. Holloway, G. Pasvol and S. Krishna (1993). "Plasmodium falciparum: in vitro studies of the pharmacodynamic properties of drugs used for the treatment of severe malaria." Exp Parasitol **76**(1): 85-95.

Toovey, S., L. Y. Bustamante, A. C. Uhlemann, J. M. East and S. Krishna (2008). "Effect of artemisinins and amino alcohol partner antimalarials on mammalian sarcoendoplasmic reticulum calcium adenosine triphosphatase activity." Basic Clin Pharmacol Toxicol **103**(3): 209-13.

Toyoshima, C., M. Nakasako, H. Nomura and H. Ogawa (2000). "Crystal structure of the calcium pump of sarcoplasmic reticulum at 2.6 A resolution." Nature **405**(6787): 647-55.

Toyoshima, C. and H. Nomura (2002). "Structural changes in the calcium pump accompanying the dissociation of calcium." Nature **418**(6898): 605-11.

Toyoshima, C. and G. Inesi (2004). "Structural basis of ion pumping by Ca2+-ATPase of the sarcoplasmic reticulum." Annu Rev Biochem **73**: 269-92.

Toyoshima, C. and T. Mizutani (2004). "Crystal structure of the calcium pump with a bound ATP analogue." Nature **430**(6999): 529-35.

Toyoshima, C., Y. Norimatsu, S. Iwasawa, T. Tsuda and H. Ogawa (2007). "How processing of aspartylphosphate is coupled to lumenal gating of the ion pathway in the calcium pump." Proc Natl Acad Sci U S A **104**(50): 19831-6.

Toyoshima, C. (2008). "How Ca(2+)-ATPase pumps ions across the sarcoplasmic reticulum membrane." Biochim Biophys Acta.

Troullier, A., J. L. Girardet and Y. Dupont (1992). "Fluoroaluminate complexes are bifunctional analogues of phosphate in sarcoplasmic reticulum Ca(2+)-ATPase." J Biol Chem **267**(32): 22821-9.

Uhlemann, A. C., A. Cameron, U. Eckstein-Ludwig, J. Fischbarg, P. Iserovich, F. A. Zuniga, M. East, A. Lee, L. Brady, R. K. Haynes and S. Krishna (2005). "A single amino acid residue can determine the sensitivity of SERCAs to artemisinins." Nat Struct Mol Biol **12**(7): 628-9.

Uyemura, S. A., S. Luo, S. N. Moreno and R. Docampo (2000). "Oxidative phosphorylation, Ca(2+) transport, and fatty acid-induced uncoupling in malaria parasites mitochondria." J Biol Chem **275**(13): 9709-15.

van Agtmael, M. A., T. A. Eggelte and C. J. van Boxtel (1999). "Artemisinin drugs in the treatment of malaria: from medicinal herb to registered medication." Trends Pharmacol Sci **20**(5): 199-205.

van Es, H. H., S. Karcz, F. Chu, A. F. Cowman, S. Vidal, P. Gros and E. Schurr (1994). "Expression of the plasmodial pfmdr1 gene in mammalian cells is associated with increased susceptibility to chloroquine." Mol Cell Biol **14**(4): 2419-28.

Varotti, F. P., F. H. Beraldo, M. L. Gazarini and C. R. Garcia (2003). "Plasmodium falciparum malaria parasites display a THG-sensitive Ca2+ pool." Cell Calcium **33**(2): 137-44.

Vedadi, M., J. Lew, J. Artz, M. Amani, Y. Zhao, A. Dong, G. A. Wasney, M. Gao, T. Hills, S. Brokx, W. Qiu, S. Sharma, A. Diassiti, Z. Alam, M. Melone, A. Mulichak, A. Wernimont, J. Bray, P. Loppnau, O. Plotnikova, K. Newberry, E. Sundararajan, S. Houston, J. Walker, W. Tempel, A. Bochkarev, I. Kozieradzki, A. Edwards, C. Arrowsmith, D. Roos, K. Kain and R. Hui (2007). "Genome-scale protein expression and structural biology of Plasmodium falciparum and related Apicomplexan organisms." Mol Biochem Parasitol **151**(1): 100-10.

Vivas, L., L. Rattray, L. B. Stewart, B. L. Robinson, B. Fugmann, R. K. Haynes, W. Peters and S. L. Croft (2007). "Antimalarial efficacy and drug interactions of the novel semi-synthetic endoperoxide artemisone in vitro and in vivo." J Antimicrob Chemother **59**(4): 658-65.

Vyas, N., B. A. Avery, M. A. Avery and C. M. Wyandt (2002). "Carrier-mediated partitioning of artemisinin into Plasmodium falciparum-infected erythrocytes." Antimicrob Agents Chemother **46**(1): 105-9.

Walker, D. J., J. L. Pitsch, M. M. Peng, B. L. Robinson, W. Peters, J. Bhisutthibhan and S. R. Meshnick (2000). "Mechanisms of artemisinin resistance in the rodent malaria pathogen Plasmodium yoelii." Antimicrob Agents Chemother **44**(2): 344-7.

Waller, R. F. and G. I. McFadden (2005). "The apicoplast: a review of the derived plastid of apicomplexan parasites." Curr Issues Mol Biol **7**(1): 57-79.

Wang, H., H. C. Ye, B. Y. Liu, Z. Q. Li and G. F. Li (2003). "[Advances in molecular regulation of artemisinin biosynthesis]." Sheng Wu Gong Cheng Xue Bao **19**(6): 646-50.

Wasserman, M., C. Alarcon and P. M. Mendoza (1982). "Effects of Ca++ depletion on the asexual cell cycle of Plasmodium falciparum." Am J Trop Med Hyg **31**(4): 711-7.

White, N. J. (2008). "Qinghaosu (artemisinin): the price of success." Science **320**(5874): 330-4.

Wictome, M., F. Michelangeli, A. G. Lee and J. M. East (1992). "The inhibitors thapsigargin and 2,5-di(tert-butyl)-1,4-benzohydroquinone favour the E2 form of the Ca2+,Mg(2+)-ATPase." FEBS Lett **304**(2-3): 109-13.

Woodrow, C. J., R. K. Haynes and S. Krishna (2005). "Artemisinins." Postgrad Med J **81**(952): 71-8.

Wu, Y. (2002). "How might qinghaosu (artemisinin) and related compounds kill the intraerythrocytic malaria parasite? A chemist's view." Acc Chem Res **35**(5): 255-9.

Wuytack, F., L. Raeymaekers and L. Missiaen (2002). "Molecular physiology of the SERCA and SPCA pumps." Cell Calcium **32**(5-6): 279-305.

Zhang, G., Y. Guan, B. Zheng, S. Wu and L. Tang (2008). "No PfATPase6 S769N mutation found in Plasmodium falciparum isolates from China." Malar J **7**: 122.

Zhang, H., E. M. Howard and P. D. Roepe (2002). "Analysis of the antimalarial drug resistance protein Pfcrt expressed in yeast." J Biol Chem **277**(51): 49767-75.

Zhang, S. and G. S. Gerhard (2008). "Heme activates artemisinin more efficiently than hemin, inorganic iron, or hemoglobin." Bioorg Med Chem **16**(16): 7853-61.

Zhang, Z., D. Lewis, C. Strock, G. Inesi, M. Nakasako, H. Nomura and C. Toyoshima (2000). "Detailed characterization of the cooperative mechanism of Ca(2+) binding and catalytic activation in the Ca(2+) transport (SERCA) ATPase." Biochemistry **39**(30): 8758-67.

APPENDICES

Appendix 1: alignment of SERCA1a with PfATP6

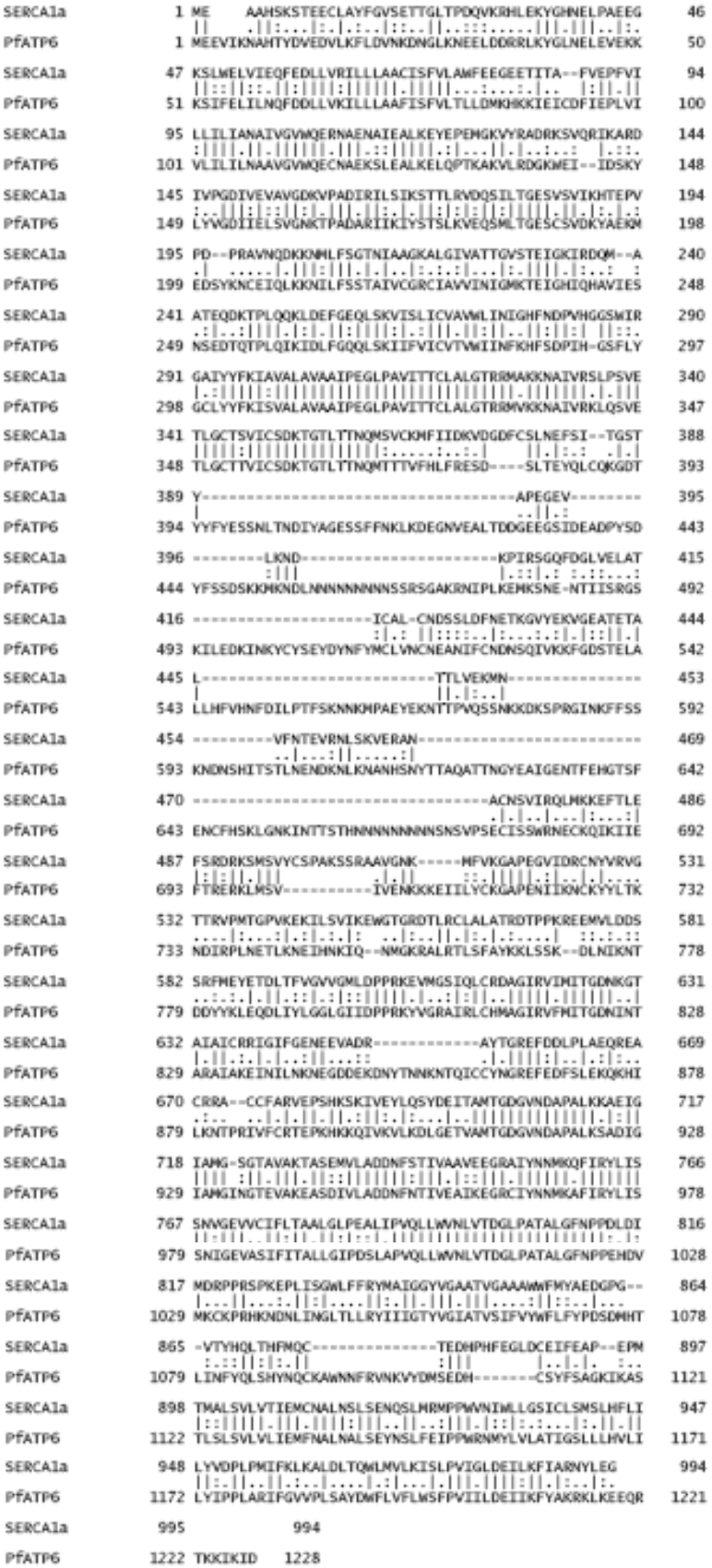

Appendix 2 : alignment of Pfatp6 co and wt

```
PfATP6wt atg gaa gag gtt att aag aat gct cat aca tac gat gtt gag gat gta cta aaa ttt ttg
PfATP6co atg gaa gaa gtt att aaa aac gct cat act tat gat gtt gaa gat gtt ttg aaa ttt ttg
         ||| ||| ||. ||| ||| ||. ||. ||| ||| ||. ||. ||| ||| ||. ||| ||. .|. ||| ||| |||
PfATP6wt gat gta aac aaa gat aat ggt tta aag aat gag gaa ttg gat gat aga aga tta aaa tat
PfATP6co gat gtt aac aaa gat aat ggt tta aaa aac gaa gaa ttg gat gat aga aga ttg aaa tat
         ||| ||. ||| ||| ||| ||| ||| ||| ||. ||. ||. ||| ||| ||| ||| ||| ||| ||. ||| |||
PfATP6wt ggt ttg aat gaa tta gaa gta gaa aag aag aaa agt att ttt gaa ttg ata tta aat caa
PfATP6co ggt tta aac gaa ttg gaa gtt gaa aaa aaa aaa tct att ttc gaa ttg att ttg aat cag
         ||| ||. ||. ||| ||. ||| ||. ||| ||. ||. ||| ..| ||| ||. ||| ||| ||. ||. ||| ||.
PfATP6wt ttt gat gat tta tta gta aag ata tta tta cta gct gca ttc att agt ttc gtg tta act
PfATP6co ttt gat gat ttg ttg gtt aag att ttg ttg ttg gct gct ttt att tct ttt gtt ttg act
         ||| ||| ||| ||. ||. ||. ||| ||. ||. ||. .|. ||| ||. ||. ||| ..| ||. ||. ||. |||
PfATP6wt tta tta gat atg aaa cat aaa aaa ata gaa ata tgt gat ttt att gaa cca tta gtt ata
PfATP6co ttg ttg gat atg aaa cat aaa aag att gaa att tgt gat ttt att gaa cca ttg gtt att
         ||. ||. ||| ||| ||| ||| ||| ||. ||. ||| ||. ||| ||| ||| ||| ||| ||| ||. ||| ||.
PfATP6wt gta tta ata tta ata tta aat gct gcc gta ggt gta tgg caa gaa tgt aat gct gaa aaa
PfATP6co gtt ttg att ttg att tta aac gct gct gtt ggt gtt tgg caa gaa tgt aat gct gaa aaa
         ||. ||. ||. ||. ||. ||| ||. ||| ||. ||. ||| ||. ||| ||| ||| ||| ||| ||| ||| |||
PfATP6wt tct tta gaa gct tta aaa gaa tta caa cct acc aaa gct aaa gta tta cga gat ggg aag
PfATP6co tct ttg gaa gct tta aag gaa ttg caa cca act aaa gct aaa gtt ttg aga gat ggt aaa
         ||| ||. ||| ||| ||| ||. ||| ||. ||| ||. ||. ||| ||| ||| ||. ||. .|| ||| ||. ||.
PfATP6wt tgg gaa att att gat agt aaa tat tta tat gtt ggt gat att att gaa ttg agt gtt ggt
PfATP6co tgg gaa att att gat agt aaa tac tta tat gtt ggt gat att att gaa ttg tct gtt ggt
         ||| ||| ||| ||| ||| ||| ||| ||. ||| ||| ||| ||| ||| ||| ||| ||| ||| ..| ||| |||
PfATP6wt aat aaa act ccc gct gat gca aga ata att aaa ata tat tca aca agt tta aaa gtt gaa
PfATP6co aac aaa act cca gct gat gct aga att att aaa att tat tct act tct ttg aaa gtt gaa
         ||. ||| ||| ||. ||| ||| ||. ||| ||. ||| ||| ||. ||| ||. ||. ..| ||. ||| ||| |||
PfATP6wt cag agt atg tta aca gga gaa tcc tgt tca gtt gac aaa tat gct gaa aaa atg gaa gat
PfATP6co caa tca atg ttg act ggt gaa tct tgt tct gtt gat aag tat gca gaa aag atg gaa gat
         ||. ... ||| ||. ||. ||. ||| ||. ||| ||. ||| ||. ||. ||| ||. ||| ||. ||| ||| |||
PfATP6wt agt tat aaa aat tgt gaa ata cag ttg aaa aaa aat att tta ttt tca tct acc gct att
PfATP6co tct tac aaa aat tgt gaa att caa ttg aaa aaa aac att ttg ttt tct tct act gct att
         ..| ||. ||| ||| ||| ||| ||. ||. ||| ||| ||| ||. ||| ||. ||| ||. ||| ||. ||| |||
PfATP6wt gta tgt ggt aga tgt ata gct gtt gta atc aac ata ggt atg aag act gaa ata ggt cat
PfATP6co gtt tgt ggt aga tgt att gct gtt gtt att aac att gga atg aaa act gaa att ggt cat
         ||. ||| ||| ||| ||| ||. ||| ||| ||. ||. ||| ||. ||. ||| ||. ||| ||| ||. ||| |||
PfATP6wt att cag cat gct gtt ata gaa tca aat agt gaa gat act caa aca cct tta caa ata aaa
PfATP6co att caa cat gct gtt att gaa tct aat tca gaa gat act caa act cca ttg caa att aag
         ||| ||. ||| ||| ||| ||. ||| ||. ||| ... ||| ||| ||| ||| ||. ||. ||. ||| ||. ||.
PfATP6wt atc gat tta ttt ggt caa caa tta tca aaa atc att ttt gta ata tgt gta act gta tgg
PfATP6co att gat ttg ttt ggt caa caa ttg tct aag att att ttc gtt att tgt gtt act gtt tgg
         ||. ||| ||. ||| ||| ||| ||| ||. ||. ||. ||. ||| ||. ||. ||. ||| ||. ||| ||. |||
PfATP6wt att att aat ttt aaa cat ttc tca gat cca att cat ggt tca ttt tta tat ggt tgt tta
PfATP6co att att aac ttc aaa cat ttt tct gat cca att cat ggt tct ttc tta tac ggt tgt ttg
         ||| ||| ||. ||. ||| ||| ||. ||. ||| ||| ||| ||| ||| ||. ||. ||| ||. ||| ||| ||.
PfATP6wt tat tat ttt aaa att agt gtt gct tta gct gtt gct gct ata cca gaa gga ttg cca gca
PfATP6co tat tat ttc aaa att tct gtt gct ttg gca gtt gct gct att cca gaa ggt tta cca gct
         ||| ||| ||. ||| ||| ..| ||| ||| ||. ||. ||| ||| ||| ||. ||| ||| ||. ||. ||| ||.
PfATP6wt gtc ata aca act tgt tta gct tta gga aca aga aga atg gta aaa aaa aat gct ata gta
PfATP6co gtt att act act tgt ttg gct ttg ggt act aga aga atg gtt aaa aaa aat gct att gtt
         ||. ||. ||. ||| ||| ||. ||| ||. ||. ||. ||| ||| ||| ||. ||| ||| ||| ||| ||. ||.
PfATP6wt aga aaa tta caa agt gtt gag acg tta gga tgt aca acg gtt ata tgt tct gat aaa aca
PfATP6co aga aaa ttg caa tct gtt gaa act ttg ggt tgt act act gtt att tgt tct gat aaa act
         ||| ||| ||. ||| ..| ||| ||. ||. ||. ||. ||| ||. ||. ||| ||. ||| ||| ||| ||| ||.
PfATP6wt ggt acc ctt aca aca aat caa atg aca aca acc gtg ttt cat ttg ttt aga gaa tct gat
PfATP6co ggt act ttg act act aat caa atg act act aca gtt ttt cat ttg ttc aga gaa tct gat
         ||| ||. .|. ||. ||. ||| ||| ||| ||. ||. ||. ||. ||| ||| ||| ||. ||| ||| ||| |||
```

PfATP6wt tct tta aca gaa tac caa cta tgt caa aaa ggg gat acc tat tac ttt tat gaa agt tca
PfATP6co tct ttg aca gaa tat caa ttg tgt caa aaa ggt gat act tat tac ttt tat gaa tct tct

PfATP6wt aac tta aca aat gat ata tat gca ggt gaa tca tct ttt ttt aat aaa tta aaa gat gaa
PfATP6co aat ttg act aac gat att tat gct ggt gaa tca tct ttt ttc aac aaa ttg aaa gat gaa

PfATP6wt gga aat gtt gaa gct tta acg gat gat gga gaa gaa gga tca att gat gaa gct gat cca
PfATP6co ggt aat gtt gaa gct ttg act gat gat ggt gaa gaa ggt tct att gac gaa gct gat cca

PfATP6wt tat agt gat tat ttt tct agt gat agt aag aaa atg aaa aat gat tta aac aac aac aat
PfATP6co tat tct gat tac ttt tct tct gat tca aaa aag atg aaa aac gat tta aac aac aat aat

PfATP6wt aat aat aat aat aat agt agt agg agt ggt gct aag agg aat att cct tta aaa gaa atg
PfATP6co aac aac aac aac aat tct tca aga tca ggt gct aag aga aat att cca ttg aag gaa atg

PfATP6wt aaa tca aat gaa aat aca ata ata agt aga ggt agt aaa ata tta gaa gat aaa att aat
PfATP6co aaa tct aac gaa aat act att att tca aga ggt tct aag att ttg gaa gat aag att aac

PfATP6wt aaa tat tgt tat tca gaa tat gat tat aat ttt tat atg tgt tta gta aat tgt aat gaa
PfATP6co aaa tat tgt tat tct gaa tac gat tac aat ttt tac atg tgt ttg gtt aat tgt aat gaa

PfATP6wt gca aat att ttc tgt aac gat aat agt caa ata gta aaa aaa ttt gga gac agt acc gaa
PfATP6co gca aac att ttt tgt aat gat aat tct caa att gtt aaa aag ttt ggt gat tct act gaa

PfATP6wt tta gct tta tta cat ttt gta cat aat ttt gat ata tta cca aca ttc tct aaa aat aat
PfATP6co ttg gct tta ttg cat ttt gtt cat aat ttc gat att ttg cca act ttt tct aaa aac aac

PfATP6wt aaa atg cca gca gaa tat gaa aaa aat aca aca cct gta caa tca tca aat aag aag gat
PfATP6co aaa atg cca gct gaa tac gaa aaa aac act act cca gtt caa tct tct aac aaa aaa gat

PfATP6wt aaa tca cca agg ggt atc aac aaa ttc ttt agt tca aaa aat gat aac agt cat att acc
PfATP6co aaa tct cca aga ggt att aac aaa ttt ttc tct tct aaa aac gat aat tct cat att act

PfATP6wt agt aca ttg aat gaa aat gat aag aat tta aag aat gct aac cat tct aat tat act aca
PfATP6co tct act ttg aac gaa aac gat aaa aac tta aaa aac gct aat cat tct aat tat act act

PfATP6wt gct cag gca aca aca aat gga tat gaa gct ata gga gaa aat aca ttt gag cat ggc aca
PfATP6co gct caa gct act act aat ggt tac gaa gct att ggt gaa aat act ttt gaa cat ggt aca

PfATP6wt agt ttt gaa aat tgt ttc cac tca aaa ttg ggt aat aaa ata aat acc aca tca aca cat
PfATP6co tct ttc gaa aat tgt ttt cat tct aaa ttg ggt aac aaa att aac act act tct act cat

PfATP6wt aat aat aat aac aac aat aat aat aat agt aat agt gtt cca agt gaa tgt atc tcg agt
PfATP6co aac aac aac aac aac aat aat aac aat tct aat tca gtt cca tca gaa tgt att tct tca

PfATP6wt tgg aga aat gaa tgt aaa caa ata aaa att att gaa ttc act aga gaa agg aaa ctt atg
PfATP6co tgg aga aat gaa tgt aaa caa att aag att att gaa ttt act aga gaa aga aaa ttg atg

PfATP6wt agt gtt att gtt gaa aat aaa aaa aaa gaa ata ata ttg tat tgt aaa ggt gca cct gag
PfATP6co tct gtt att gtt gaa aac aaa aaa aag gaa att att ttg tat tgt aaa ggt gct cca gaa

PfATP6wt aat ata ata aaa aat tgt aaa tat tat tta acg aaa aat gat ata cgt cca tta aat gaa
PfATP6co aat att att aaa aat tgt aaa tac tat ttg aca aaa aac gat att aga cca tta aac gaa

PfATP6wt act tta aaa aat gaa att cat aat aag att caa aat atg gga aaa aga gca tta aga aca
PfATP6co acc tta aaa aac gaa att cat aac aaa att caa aat atg ggt aaa aga gct ttg aga act

```
PfATP6wt ctt agc ttt gct tat aaa aaa tta agt agt aaa gat tta aat att aag aat aca gat gat
PfATP6co ttg tct ttt gct tac aaa aaa ttg tca tca aaa gat ttg aac att aaa aac act gat gat
         .|. ... ||| ||| ||. ||| ||| ||. ... ... ||| ||| ||. ||. ||| ||. ||. ||. ||| |||
PfATP6wt tat tat aaa tta gaa caa gat tta att tat tta ggt gga tta ggt att att gat cca cca
PfATP6co tat tac aaa ttg gaa caa gat ttg att tat ttg gga ggt tta ggt att att gat cca cct
         ||| ||. ||| ||. ||| ||| ||| ||. ||| ||| ||. ||. ||. ||| ||| ||| ||| ||| ||| ||.
PfATP6wt cgt aaa tat gta gga aga gca att aga tta tgc cat atg gct ggt ata cgt gta ttt atg
PfATP6co aga aaa tat gtt ggt aga gct att aga ttg tgt cat atg gct ggt att aga gtt ttt atg
         .|. ||| ||| ||. ||. ||| ||. ||| ||| ||. ||. ||| ||| ||| ||| ||. .|. ||. ||| |||
PfATP6wt att aca ggt gat aat att aat acg gcc aga gct ata gct aaa gaa att aat ata tta aat
PfATP6co att aca ggt gat aac att aat act gct aga gct att gct aag gaa att aac att tta aac
         ||| ||| ||| ||| ||. ||| ||| ||. ||. ||| ||| ||. ||| ||. ||| ||| ||. ||. ||| ||.
PfATP6wt aaa aat gaa ggg gat gat gaa aag gat aat tat aca aat aat aaa aat aca caa ata tgt
PfATP6co aaa aac gaa ggt gat gat gaa aaa gat aat tac act aac aac aaa aat act caa att tgt
         ||| ||. ||| ||. ||| ||| ||| ||. ||| ||| ||. ||. ||. ||. ||| ||| ||. ||| ||. |||
PfATP6wt tgt tat aat gga aga gaa ttt gaa gat ttt tca tta gaa aag caa aaa cat att tta aaa
PfATP6co tgt tat aat ggt aga gaa ttt gaa gat ttt tct ttg gaa aaa caa aaa cat att ttg aaa
         ||| ||| ||| ||. ||| ||| ||| ||| ||| ||| ||. ||. ||| ||. ||| ||| ||| ||| ||. |||
PfATP6wt aat aca cca aga att gtt ttc tgt aga act gaa cct aaa cat aaa aaa caa ata gta aaa
PfATP6co aat act cca aga att gtt ttt tgt aga aca gaa cca aaa cat aaa aaa caa att gtt aag
         ||| ||. ||| ||| ||| ||| ||. ||| ||| ||. ||| ||. ||| ||| ||| ||| ||| ||. ||. ||.
PfATP6wt gta cta aaa gac tta gga gaa aca gtt gct atg aca ggt gat ggt gta aat gat gca cca
PfATP6co gtt tta aaa gat ttg ggt gaa act gtt gct atg act ggt gat ggt gtt aat gat gct cca
         ||. .|| ||| ||. ||. ||. ||| ||. ||| ||| ||| ||. ||| ||| ||| ||. ||| ||| ||. |||
PfATP6wt gca ttg aaa tca gct gac ata gga ata gct atg ggt att aat gga acg gag gta gct aaa
PfATP6co gct ttg aaa tct gca gat att ggt att gct atg ggt att aat ggt aca gaa gtt gct aag
         ||. ||| ||| ||. ||. ||. ||. ||. ||. ||| ||| ||| ||| ||| ||. ||. ||. ||. ||| ||.
PfATP6wt gaa gca tca gat att gtt tta gct gat gat aat ttt aat act ata gtt gaa gca att aaa
PfATP6co gaa gct tca gat att gtt ttg gct gat gat aat ttc aat act att gtt gaa gct att aag
         ||| ||. ||| ||| ||| ||| ||. ||| ||| ||| ||| ||. ||| ||| ||. ||| ||| ||. ||| ||.
PfATP6wt gaa gga aga tgt ata tat aat aat atg aaa gca ttt atc cgt tat cta att agt agt aat
PfATP6co gaa gga aga tgt att tac aac aat atg aaa gct ttt att aga tac tta att tct tct aat
         ||| ||| ||| ||| ||. ||. ||. ||| ||| ||| ||. ||| ||. .|. ||. .|| ||| ..| ..| |||
PfATP6wt ata gga gaa gtt gca tcc att ttt ata aca gcc tta ttg ggt ata cct gac agt tta gct
PfATP6co att ggt gaa gtt gct tct att ttc att act gct ttg ttg ggt att cca gat tct ttg gca
         ||. ||. ||| ||| ||. ||. ||| ||. ||. ||. ||. ||. ||| ||| ||. ||. ||. ..| ||. ||.
PfATP6wt ccc gtt cag tta ttg tgg gta aat ttg gtt act gac gga tta cca gca aca gca cta ggg
PfATP6co cca gtt caa ttg ttg tgg gtt aac ttg gtt aca gat ggt tta cct gct act gct ttg ggt
         ||. ||| ||. ||. ||| ||| ||. ||. ||| ||| ||. ||. ||. ||| ||. ||. ||. ||. .|. ||.
PfATP6wt ttc aat cca cca gaa cat gac gta atg aag tgc aag ccg aga cac aaa aac gac aat tta
PfATP6co ttt aat cca cca gaa cat gat gtt atg aaa tgt aag cca aga cat aaa aac gat aac tta
         ||. ||| ||| ||| ||| ||| ||. ||. ||| ||. ||. ||| ||. ||| ||. ||| ||| ||. ||. |||
PfATP6wt ata aac ggt cta act tta tta aga tat ata att att gga aca tat gta gga ata gct aca
PfATP6co att aac ggt tta act tta ttg aga tat att att att ggt act tat gtt ggt att gca aca
         ||. ||| ||| .|| ||| ||| ||. ||| ||| ||. ||| ||| ||. ||. ||| ||. ||. ||. ||. |||
PfATP6wt gtc tca ata ttt gtg tac tgg ttt tta ttt tat cca gat tca gat atg cac acg ttg ata
PfATP6co gtt tct att ttt gtt tat tgg ttt tta ttc tat cca gat tct gat atg cat act ttg att
         ||. ||. ||. ||| ||. ||. ||| ||| ||| ||. ||| ||| ||| ||. ||| ||| ||. ||. ||| ||.
PfATP6wt aac ttt tat caa tta tca cat tat aac caa tgt aaa gca tgg aat aac ttc cgt gta aat
PfATP6co aat ttc tat caa ttg tct cat tac aat caa tgt aaa gct tgg aac aat ttt aga gtt aac
         ||. ||. ||| ||| ||. ||. ||| ||. ||. ||| ||| ||| ||. ||| ||. ||. ||. .|. ||. ||.
PfATP6wt aag gtt tat gat atg tct gag gat cac tgt tca tat ttt tca gca gga aaa att aag gca
PfATP6co aaa gtt tac gat atg tca gaa gat cat tgt tct tat ttt tct gct ggt aaa att aaa gct
         ||. ||| ||. ||| ||| ||. ||. ||| ||. ||| ||. ||| ||| ||. ||. ||. ||| ||| ||. ||.
PfATP6wt agc acc tta tct tta tcc gtt tta gtt tta ata gaa atg ttt aat gct ttg aat gcc ttg
PfATP6co tct act ttg tct ttg tct gtt ttg gtt tta att gaa atg ttt aat gct tta aat gct ttg
         ... ||. ||. ||| ||. ||. ||| ||. ||| ||| ||. ||| ||| ||| ||| ||| ||. ||| ||. |||
```

```
PfATP6wt  agt gag tat aat tcc tta ttt gaa ata cca cca tgg aga aat atg tac cta gta tta gct
PfATP6co  tca gaa tac aat tct ttg ttt gaa att cca cca tgg aga aac atg tat ttg gtt ttg gct
          ... ||. ||. ||| ||. ||. ||| ||| ||. ||| ||| ||| ||| ||. ||| ||. .|. ||. ||. |||
PfATP6wt  act ata ggt tcc tta ctt tta cat gtc tta ata ctt tac att cca ccc tta gct cgt att
PfATP6co  act att ggt tct ttg ttg ttg cat gtt ttg att tta tac att cca cca ttg gct aga att
          ||| ||. ||| ||. ||. .|. ||. ||| ||. ||. ||. .|. ||| ||| ||| ||. ||. ||| .|. |||
PfATP6wt  ttt ggt gtt gtt cca tta agt gca tat gac tgg ttc tta gta ttc ttg tgg tcc ttc cca
PfATP6co  ttt ggt gtt gtt cca ttg tct gct tat gat tgg ttt ttg gtt ttt ttg tgg tct ttt cca
          ||| ||| ||| ||| ||| ||. ..| ||. ||| ||. ||| ||. ||. ||. ||. ||| ||| ||. ||. |||
PfATP6wt  gtt att ata ctt gac gaa att att aaa ttc tat gca aag agg aaa tta aag gaa gag caa
PfATP6co  gtt att att ttg gat gaa att att aaa ttt tac gca aag aga aaa ttg aaa gaa gaa caa
          ||| ||| ||. .|. ||. ||| ||| ||| ||| ||. ||. ||| ||| ||. ||| ||. ||. ||| ||. |||
PfATP6wt  aga acc aag aaa att aaa att gat taa
PfATP6co  aga act aaa aag att aag att gat taa
          ||| ||. ||. ||. ||| ||. ||| ||| |||
```

Appendix 3 : comparison of codon usage tables between two genomes...

Codontable 1 (red):

Saccharomyces_cerevisiae

Codontable 2 (black):

Plasmodium_falciparum

Mean difference: 22.13 %

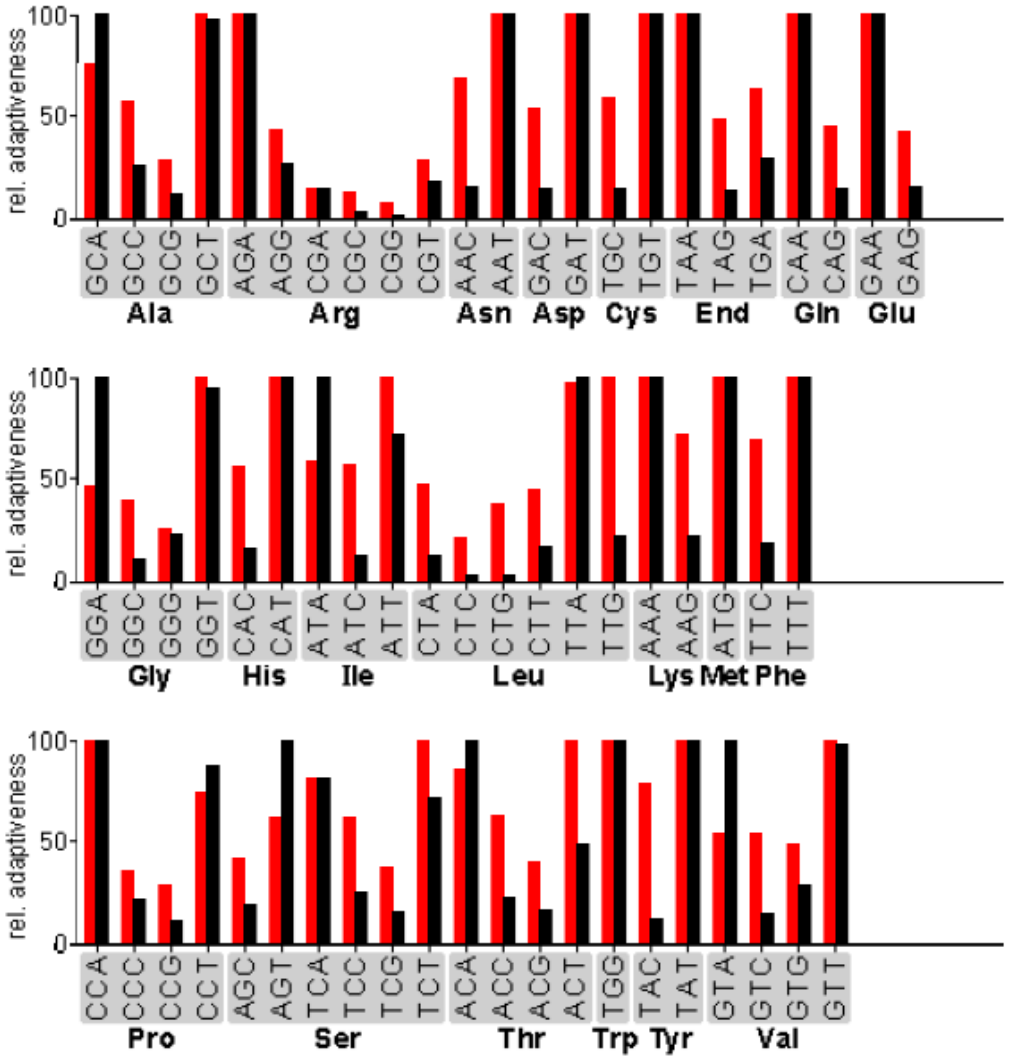

…and between a gene (Pfatp6 wt, in red) and a genome (*S. cerevisiae*, black)

Codontable (black):
Saccharomyces_cerevisiae

Mean difference: 19.95 %

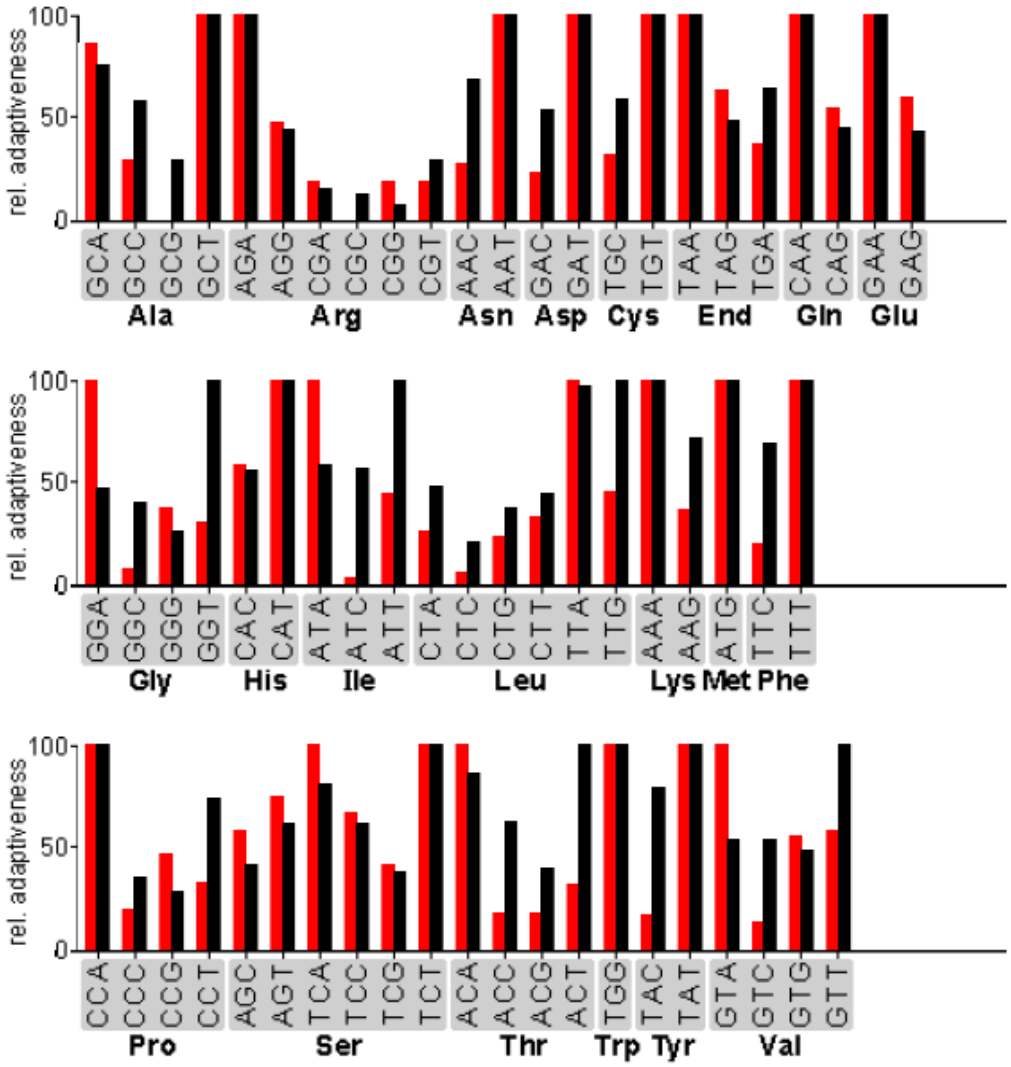

These graphics were generated from http://gcua.schoedl.de/

ARTICLES

ARTICLE I

Heterologous Expression and Affinity Purification of Eukaryotic Membrane Proteins in view of Functional and Structural Studies: the example of the sarcoplasmic reticulum Ca^{2+}-ATPase

to be published in Methods in Molecular Biology

Delphine Cardi[§ 1], Cédric Montigny[§ 1], Bertrand Arnou[§ 1], Marie Jidenko[§], Estelle Marchal[§], Marc le Maire[§] and Christine Jaxel[§]*

§ CEA, iBiTecS (Institut de Biologie et Technologies de Saclay), SB^2SM, CNRS, URA 2096, LRA17V University of Paris-Sud, F 91191 Gif-sur-Yvette, France

* To whom correspondence should be addressed. Phone: 33-1-6908-3379. Fax: 33-1-6908-8139. E-mail: christine.jaxel@cea.fr. Mail : Dr C. Jaxel, iBiTec-S & URA 2096 CNRS, CEA Saclay, 91191 Gif-sur-Yvette cedex, France.

[1] These three authors contributed equally to this work.

Running title: Affinity purification of P-type ATPases for structural studies.

Abstract

Heterologous SERCA1a Ca^{2+}-ATPase (sarco-endoplasmic reticulum Ca^{2+}-ATPase isoform 1a) from rabbit was expressed in yeast *S. cerevisiae* as a fusion protein, with a Biotin Acceptor Domain (BAD) linked to the Serca C-terminus by a thrombin cleavage site. Thanks to the pYeDP60 vector, the recombinant protein was expressed under the control of a galactose-inducible promoter. Biotinylation of the protein occurred directly in yeast. Optimizing the number of galactose induction steps and increasing the amount of Gal4p transcription factor both improved expression. Lowering the temperature from 28°C to 18°C during expression enhanced the recovery of detergent-extractible active protein. In the "light membrane fraction", thought to mainly contain internal membranes, we are able to recover about 14-18 mg Ca^{2+}-ATPase per liter of yeast culture in a bioreactor. Solubilization of this membrane fraction by n-Dodecyl β–D-maltopyranoside (DDM) allowed us to recover the largest amount of active protein. The *in vivo* biotinylated recombinant protein was then bound to a streptavidin-Sepharose resin. Selective elution of the biotinylated Serca1a was carried out after thrombin action on the resin-bound protein. Thereby we are able to obtain 200-500 µg/L of yeast culture of a 50 % pure SERCA1a which displays an ATPase activity similar to that of the native rabbit Ca^{2+}-ATPase. To succeed in crystallization, an additional size exclusion chromatography step was necessary. This step increases purity to 70 %, removes aggregated protein and exchanges DDM for $C_{12}E_8$.

Key words: membrane protein, heterologous expression, yeast, bioreactor, Ca^{2+}-ATPase, biotin-streptavidin affinity.

1. Introduction

We have worked out a procedure for affinity purification of rabbit SERCA1a heterologously expressed in yeast cells, producing sufficient amounts for crystallization and biophysical studies. The wild type form gives a crystal that is isomorphous to the native SERCA1a protein from rabbit ***(1)***. Later on the crystal structures of two mutant forms, D351A and P312A as well as some of their functional characterization ***(2)*** have been described. Our procedure for heterologous expression and affinity purification ***(3)*** has also been recently applied to *Plasmodium falciparum* PfATP6, a SERCA-type protein ***(4)***.

In fact, recently, a few other eukaryotic membrane proteins have yielded high-resolution X-ray or electron diffraction data after recombinant expression (1 in 2005, 2 in 2006, 5 in 2007, see review ***(5)*** and refs. ***(6-9)*** for more recent data). The expression systems which were used in these other successful cases are diverse: *E. coli* (one successful case), yeast, *Pichia pastoris* or *Saccharomyces cerevisiae* (4 cases), insect cells (3 cases) or even mammalian cells (1 case). The type of detergents and or lipids used for solubilization or crystallization does not give obvious clues for best choices, except maybe that a mixture of lipid with the detergent is often present in the final crystallization steps. An emerging concept in the field is that it is very important to aim at purifying a *native* protein together with improving the expression yield and the purity assessed on SDS-PAGE. In line with this idea of looking for an active protein, we believe that there was a key factor for the success in our case: *in vivo* yeast biotinylation of the biotin acceptor domain (BAD) added as a tag to SERCA1a was essential to purification of a small subfraction of fully active proteins. This procedure implies a positive selection of properly folded enzymes, a procedure similar to the one developed by Drew and coworkers ***(10)***, also recently successful. Although many parameters must always be optimized (choice of detergent, expression temperature…) this type of approach could open the way for easier crystallization of this important class of protein.

In our case the optimization has been a long process starting in 1994 with the expression of the protein ***(11)***, followed by its purification, first using a poly-His tag ***(12)***, then more recently using the BAD domain mentioned above ***(1, 3)***. Here, we present our recent advances in the scale-up of the expression protocol using a 20-liters bioreactor to follow and to control precisely the yeast culture parameters. This new protocol made possible to increase both the yeast density and the proportion of expressed protein compared to results obtained in glass vessels. In fact, the yields in glass vessels are more variable than in the bioreactor and depend on various parameters such as the volume of yeast cultures. In general, the new protocol results in an increase of the total expression per liter of culture by a factor of 4.

2. Materials

2.1 Yeast culture

All culture media are from Becton Dickinson Biosciences (Gibco BRL, Fisher Scientific Bioblock). All chemical products were purchased from Sigma-Aldrich except if noted otherwise.

1- YPD (A) medium: 1% (w/v) bactopeptone, 1% (w/v) yeast extract, 1% (w/v) glucose, 20 µg/mL adenine: a 10% over-concentrated medium containing only bactopeptone and yeast extract is prepared. It is sterilized for 20 min at 120°C. Glucose and adenine are added after cooling from respectively 20 % (w/v) and 10 mg/mL stock solutions (see below).

2- S1 buffer: 100 mM Li acetate, 40 % PEG 4000, 100 mM DTT.

3- S6 (A) minimum medium: 0.1 % (w/v) bactocasamino acids, 0.7 % (w/v) yeast nitrogen base, 2 % (w/v) glucose, 20 µg/mL adenine: a 10 % over-concentrated medium containing only bactocasamino acids and yeast nitrogen base is prepared. It is sterilized for 20 min at 120°C. Glucose and adenine are added after cooling from respectively 20 % (w/v) and
10 mg/mL stock solutions (see below).

4- S6 (A) agar minimum medium: 0.1 % (w/v) bactocasamino acids, 0.7 % (w/v) yeast nitrogen base, 2 % (w/v) glucose, 20 µg/mL adenine, 1.5 % agar. Medium is prepared as described for S6 (A) minimum medium with agar being present since the beginning of the preparation.

5- S5 (A) minimum medium: 0.1 % (w/v), bactocasamino acids, 0.7 % (w/v) yeast nitrogen base, 2 % (w/v) galactose, 20 µg/mL adenine. The sterilization 20 min at 120°C is done before the addition of galactose and adenine. Medium is prepared as described for S6 (A) minimum medium. 20 % (w/v) galactose is prepared as described below.

6- 20 % (w/v) glucose stock solution is sterilized by filtration onto a 0.22 µm Steritop filter (Millipore S.A.) and is added in the various media after sterilization and cooling at 40°C.

7- 20 % (w/v) galactose stock solution is sterilized by filtration onto a 0.22 µm Steritop filter (Millipore S.A.) and is added in the various media after sterilization and cooling at 40°C.

8- A solution of 10 mg/mL adenine is prepared in 0.1 N HCl and filtrated onto a 0.22 µm Steritop filter (Millipore S.A.) and is added in the various media after sterilization and cooling at 40°C.

9- A 50 % (w/v) trichloroacetic acid (TCA) stock solution is prepared from powder in Milli-Q water. It can be stored for some months at 4°C. A working solution of 2 % (w/v) TCA is prepared just before use by dilution of the 50 % stock solution in water.

10- Glass beads (0.5 mm diameter, Biospec Products) are stored at 4°C. They are reusable after decontamination with fungicidal solution, intensive rinsing with water and sterilization with ethanol. Beads are dried by incubation in a Pasteur oven before storage at 4°C.

11- The incubator is a Multitron incubator shaker system (INFORS HT) and the bioreactor is a Techfors-S apparatus (INFORS HT) coupled to a recirculating cryostat (FE1100, Julabo).

12- YPGE2x rich medium: 2 % (w/v) Bacto™ Peptone, 2 % (w/v) yeast extract, 1 % (w/v) glucose and 2.7 % (v/v) ethanol. The medium without glucose and ethanol is sterilized directly in the bioreactor. Final volume takes into account the 10 % water evaporation occurring during the sterilization process.

13- Highly concentrated solution of galactose at 50 % (w/v) is prepared by heating the solution in a microwave.

14- Antifoam A concentrate is used.

2.2 Membrane preparation

1- Yeast are centrifuged in bottles (polycarbonate bottles with screw caps assemblies, Beckman Coulter), each one inwardly covered with a liner (harvestLineTM system liners, Beckman Coulter). *JLA8.1000*, *JLA10.500*, *45Ti* and *Type 19* rotors used are from Beckman Coulter.

2- MilliQ water: 4 liters are stored at 4°C.

3- TEKS buffer: 50 mM Tris-HCl pH 7.5, 1 mM EDTA, 0.6 M sorbitol, 0.1 M KCl; 1 liter is prepared beforehand and stored at 4°C.

4- TES buffer: 50 mM Tris-HCl pH 7.5, 1 mM EDTA, 0.6 M sorbitol; 2 liters are prepared beforehand and stored at 4°C.

5- Phenylmethanesulfonyl fluoride (PMSF) is dissolved to 0.2 M in ethanol; 10 mL are prepared beforehand and could be stored at 4°C for some weeks.

6- Hepes-sucrose buffer: 20 mM Hepes-Tris pH 7.5, 0.3 M sucrose (LABOSI, Elancourt, France), 0.1 mM $CaCl_2$.

7- Reagents for protein assay: bicinchoninic acid (BCA) and $CuSO_4$ 4 %.

2.3 Solubilization of SERCA

1- Pre-solubilization buffer: 50 mM MOPS-Tris pH 7.0, 100 mM KCl, 20 % glycerol (w/w), 1 mM $CaCl_2$, 1 mM PMSF and complete EDTA-free antiprotease cocktail (in our hands, it was sufficient to use half of the recommended amount *i.e.* 1 tablet for 100 mL (Roche Diagnostics) plus possibly 1 mM β-mercaptoethanol or 1 mM DTT.

2.4 Purification of SERCA by affinity chromatography

1- Streptavidin-Sepharose™ High Performance resin is from G.E. Healthcare, Courtaboeuf, France.

2- Solubilization buffer: 50 mM MOPS-Tris pH 7.0, 100 mM KCl, 20 % glycerol (w/w), 1 mM $CaCl_2$ and 15 mg/mL DDM (Anatrace) (the DDM amount depends on protein concentration, see **3.4**).

3- High salt (HS) washing buffer: 50 mM MOPS-Tris pH 7.0, 1 M KCl, 20 % glycerol (w/w), 1 mM $CaCl_2$ and 0.5 mg/mL DDM.

4- Low salt (LS) washing buffer: 50 mM MOPS-Tris pH 7.0, 100 mM KCl, 20 % glycerol (w/w), 2.5 mM $CaCl_2$ and 0.5 mg/mL DDM.

5- Bovine thrombin is from VWR International.

6- Filter tube after thrombin reaction is a Handee™ Centrifuge Column, PIERCE.

2.5 Purification of SERCA by Size Exclusion Chromatography (SEC)

1- Centricon Ultracel-YM 3000 DA are from Amicon, Millipore.

2- Resin is a 0.78 cm x 30 cm TosoHaas TSK-gel G3000SWXL column mounted on a Gold HPLC System (Beckman Coulter).

3- SEC buffer: 100 mM MOPS-Tris pH 6.8, 80 mM KCl, 1 mM $CaCl_2$,1 mM $MgCl_2$, 15 % sucrose, and 0.5 $mg.mL^{-1}$ $C_{12}E_8$ (Nikko Chemicals).

4- DOPC (1,2-dioleoyl-*sn*-Glycero-3-Phosphocholine, Avanti Polar lipids, Inc.) is dissolved at 40 mg/mL in chloroform and then, chloroform is evaporated and a thin layer of N_2-dried DOPC is formed in a tube.

2.6 SDS-PolyAcrylamide Gel Electrophoresis (SDS-PAGE)

1- Mini-protean 3 cell system is used (Bio-Rad S.A.).

2- Separating gel solution : 375 mM Tris-HCl pH 8.8; 8 % acrylamide (w/v); 0.1 % SDS; 0.1 % ammonium persulfate; 0.06 % TEMED (v/v).

3- Stacking gel solution : 125 mM Tris-HCl pH 6.8; 5% acrylamide (w/v); 0.1 % SDS; 0.1 % ammonium persulfate; 0.1 % TEMED (v/v).

4- Denaturing buffer 2x-concentrated: 100 mM Tris-HCl pH 8, 1.4 M β-mercaptoethanol, 4 % SDS (w/v), 1 mM EDTA, 8 M urea, 0.05 % bromophenol blue (w/v).

5- Running buffer: 25 mM Tris, 250 mM glycine, 0.1 % SDS.

6- Coomassie blue staining solution: 0.05 % Coomassie blue R, 40 % methanol, 10 % acetic acid.

2.7 Western Blotting for SERCA

1- Mini Trans-Blot Mini-protean 3 cell system cell is used (Bio-Rad S.A.).

2- CAPS buffer: 10 mM CAPS, 10 % methanol, pH 11.1 adjusted with NaOH. One liter is prepared per electrophoresis tank (for 1 or 2 blots, Miniprotean 2 or 3 systems). It is stored at 4°C with stirring for 2-3 h for cooling.

3- The polyvinylidene-difluoride (PVDF) membranes are from Millipore S.A. and chromatography paper from ATGC Biotechnologie.

4- Precision Plus Protein all blue Standards (PPPS) is a markers solution from Bio-Rad.

5- PBS-T buffer: phosphate buffer pH 7.4 (10 mM KH_2PO_4, 90 mM K_2HPO_4), 100 mM NaCl, 0.2 % Tween 20.
6- The anti-SERCA1a primary antibody is either (79B), a guinea pig antibody, a gift from Dr. A.-M. Lompré (INSERM U 621, Paris, France), or a mouse monoclonal anti-Serca1a (IIH11 clone).
6- The secondary antibody is either an anti-guinea pig goat antibody conjugated to horse radish peroxidase purchased from TEBU Bio, coupled to the 79B antibody, or a goat anti-mouse IgG1 (γ) (Caltag Laboratories), coupled to the monoclonal anti-SERCA1a antibody.
7- Avidin peroxidase conjugate is a commercial solution (Sigma-Aldrich) frozen for single use (5 µL) aliquots at -70°C.
8- Enhanced chemiluminescent (ECL) reagents are from G.E. Healthcare and detection is made by using a G:BOX camera, Syngene distributed by Ozyme.

3. Methods

In order to express SERCA1a in yeast, we use plasmid pYeDP60 initially given by Denis Pompon ***(13)*** and described after modification in ***(1, 3 and 12)***(see **Fig. 1**). It contains a bacterial part to amplify the DNA in bacteria and a yeast part for vector replication and for expression of the recombinant protein. For the selection of transformed yeast, the plasmid contains two auxotrophy markers to allow the synthesis of uracile and adenine. The gene of interest is under the transcriptional control of a hybrid promoter containing the inducible part of GAL10 and the strong promoter of CYC1. The *Saccharomyces cerevisiae* strain used for the expression is W303.1b Gal4-2 (*a*, *leu2*, *his3*, *trp1::TRP1-GAL10-GAL4*, *ura3*, *ade2-1*, *can*^{r}, *cir*$^+$) and is auxotrophous to uracile and adenine. This strain has a low constitutive expression level of GAL4p transactivation factor (1 to 3 copies of molecules per cell). It has been genetically modified to induce expression of that transactivator, under the control of a *GAL10* promoter. In presence of glucose, the system is repressed by constitutive binding of an inhibitor to GAL4p. When glucose is entirely consumed and galactose is added to the medium, GAL4p constitutives copies are released and it can activate the GAL10 promoter. This event allows firstly, high synthesis of transactivator from the yeast genome and secondly, induction of the expression of the protein of interest from the plasmid. This expression is induced when a sufficient concentration of yeast has been obtained and for a duration defined to avoid toxicity (see below).
Finally, the gene coding SERCA1a is cloned in the same open reading frame of a sequence coding a C-terminal biotin acceptor domain (BAD) separated by a sequence coding a thrombin cleavage site. By this way, the fusion protein, which is expressed, can be biotinylated directly in yeast in order to allow its purification by affinity chromatography onto a streptavidin Sepharose resin ***(14, 15)***. The direct cleavage by

thrombin on the resin allows simultaneous elution of SERCA1a and removal of the tag. For an improvement of the purity of the protein preparation, a second step of purification by SEC is added.

For all these expression and purification steps, the protein is detected on polyacrylamide gel revealed by Coomassie blue staining (purity) or by western-blot stained either by a specific antibody (that recognizes SERCA1a) or by an avidin probe coupled to HRP which binds to the biotin already linked to BAD. In our case, the enzymatic activity of SERCA1a cannot be easily detected directly on yeast membrane but is nicely estimated using the purified protein.

In order to broaden this procedure, several DNA vectors have been prepared. The aim is to allow the purification of other membrane proteins. For some of them, the position of the tag on the N-terminal side may be desirable.

3.1 Yeast culture

3.1.1 Yeast transformate

First of all, intact yeast cells are transformed with pYeDP60 modified plasmids for the expression of SERCA1a by the protocol developed by Chen *et al.* ***(16)*** using the LiAc/single stranded DNA/ PEG method ***(17)***. After an overnight culture of yeast at 28°C and at 200 rpm in YPD (A) medium, 5.10^7 cells, in stationary phase, are pelleted 5 min at 4°C and 3000g_{av}. The pellet is gently resuspended on ice in cold mix containing 90 µL of S1 buffer, 5 µL of denatured single stranded carrier DNA (10 mg/mL) and about 1µg of plasmid DNA. Yeasts were then heat-shocked at 45°C for 45 min in a water-bath to help DNA to enter into the competent cells and transferred onto S6 (A) agar plates and incubated at 28°C for 48 h. This minimum medium is deprived of uracile. As *S. cerevisiae* W303.1b Gal4-2 is auxotrophous for uracile, only those transformed with vectors derived from pYeDP60 will have the ability to grow on this minimum medium since this plasmid will complement the *ura3* genotype of this yeast.

3.1.2 Selection of individual clones in minimum medium

1- A colony streaked onto a S6 (A) agar minimum medium storage plate (*see* **Note 1**) is toothpicked into 5 mL of S6 (A) minimum medium and grown at 28°C during 24 h in a shaking incubator at 200 rpm (*see* **Note 2**).

2- For each assay, 500 µL of the previous S6 (A) precultures are centrifuged 5 min at 4°C and 1000xg_{av} and resuspended in 5 mL of S5 (A) minimum medium to induce expression. These cultures are incubated at 28°C during a 15-18 h in a shaking incubator at 200 rpm.

3- For each culture, 5 OD_{600nm} were centrifuged 5 min, at 4°C and 8000xg_{av} in 2 mL tubes. The pellets are washed with water, resuspended and centrifuged 5 min, at 4°C and 1000xg_{av}.

4- The supernatants are removed and the pellets are resuspended in 400 µL of cooled 2 % TCA. Glass beads are added to reach the meniscus. The suspensions are mixed with a vortex at maximal speed for 8 min at room temperature to break the cells.

5- The tubes are then placed on ice and glass beads are sedimented. The supernatant is removed by pipetting and that crude extract is kept on ice.

6- Glass beads are washed 3 times with 400 µL of 2 % TCA and these 3 collected supernatants are gathered with the crude extract.

7- The resulting solution is kept 15 min on ice for protein precipitation. Then, the samples are centrifuged 15 min, at 4°C and 30000xg_{av}.

8- The pellets are resuspended in 100 µL of 100 mM Tris-HCl pH 7.5 (*see* **Note 3**). These samples are analyzed by Western blotting in order to choose the best clones. These ones may be stored, starting from the S6 (A) minimum medium precultures either on storage plates or in 20 % glycerol samples stored at -70°C.

3.1.3 Large scale expression of Serca1a

The procedure here is described for 6 liters of yeast culture in a bioreactor but that protocol may be easily adapted for 20 liters.

1- For large scale expression, a colony streaked onto a S6 (A) agar minimum medium storage plate is toothpicked into 5 mL of S6 (A) minimum medium and is grown at 28°C during 24 h in a shaking incubator at 200 rpm (the cell density reaches saturation : $OD600_{nm}$ = 3, corresponding to 9-15.10^7 cells per mL).

2- This culture is used to inoculate 40 mL of S6 (A) minimum medium and is grown at 28°C during 24 h in a shaking incubator at 200 rpm (density also reaches saturation, *see* **Note 4**).

3- This second culture is used to inoculate 400 mL of S6 (A) minimum medium and grown at 28°C during about 10 h in a shaking incubator at 200 rpm. In the mean time, 6 liters of YPGE2x medium without ethanol are pre-equilibrated at 28°C and saturated with air under high aeration (1 volume of air per volume of medium per min *i.e.*, 1 vvm) and agitation at 300 rpm during 12 h.

4- The bioreactor is inoculated with the culture of 400 mL at exponential phase (OD_{600nm} = 0.6 or 2.10^7 cells per mL) (*see* **Note 5**): the final density inside the fermentor must be OD_{600nm} = 0.03 (corresponding to 10^6 cells per mL). 0.0001 % of foam suppresser Antifoam A is added and the culture is performed at 28°C, 300 rpm and 1 vvm.

5- 15-18 h after inoculation, ethanol is added (*see* **Note 6**). A regulation sequence between the rate of agitation and the aeration is activated to maintain the dissolved dioxygen up to 20 %. This fixed parameter allows maintaining of yeast in aerobiosis. In that condition, continuous measurement of the dissolved dioxygen, using a probe, induces automatic regulation of stirring, from 300 to 1000 rpm and air flow between 6 to 18 L.min^{-1} (*i.e.* 1 to 3 vvm in the case of a 6 L-culture).

6- 34 h after inoculation ($OD600_{nm}$ = 30 corresponding to 9-15.10^8 cells per mL), the aeration is reduced to 2 L.min^{-1} and the agitation is lowered to 300 rpm (*see* **Note 7**) to maintain cells in anaerobiosis. At the same time, the temperature of the medium is lowered to 18°C to slow down the yeast metabolism and consequently favours the folding of expressed membrane proteins. We wait for 1 generation time (~2 h) so that the culture can adapt to the new conditions.

7- 36 h after inoculation, 2 % galactose are added from a fresh 50 % stock solution to induce the expression of recombinant proteins.

8- 49 h after inoculation, a second induction is triggered by addition of 2 % galactose and the culture is pursued during 5 h under the same conditions.

9- After 54 h, the culture is stopped by decreasing the temperature to 6°C. The stirring is maintained to 300 rpm to avoid yeast sedimentation in the bioreactor before harvesting (see **Fig. 2**).

3.2 Membrane preparation

The procedure is described for 6 liters of yeast culture (about 350-400 g of yeast).

1- At the end of the fermentation, yeast are recovered directly in three 1 liter centrifugation bottles, using the sampling/harvesting valve of the bioreactor. They are centrifuged for 9 min, at 4°C and 4500xg_{av} and the supernatants are removed. The bottles are filled and centrifuged again with the remaining yeast until the bioreactor is empty. The same liners are used all along the steps 1 to 4: rubber tubing is used to poor out each centrifugation supernatant without the need to cut it and the resuspensions of the pellets are easily carried out directly in the liners by hand kneading.

2- The yeast pellets are washed with resuspension in 2.1 L (700 mL per liner, the volume equivalent to five times the mass of yeast) of cooled milliQ water and centrifuged 9 min, at 4°C and 4500xg_{av} in a JLA8.1000 rotor. After removing the supernatants, the pellets are weighed. Usually, about 50 g of yeast per liter are obtained.

3- The pellets are resuspended in 700 mL (in fact 240 mL per liner, corresponding to about 2 mL per gram of yeast) of TEKS buffer. The solution is incubated 15 min at 4°C and then centrifuged 9 min, at 4°C and 4500xg_{av} in a JLA8.1000 rotor.

4- The pellets are resuspended in the same volume of TES buffer (700 mL, corresponding to about 2 mL per gram of yeast) and supplemented with 1 mM PMSF and 1 tablet of complete EDTA-free antiprotease cocktail per 100 mL (for an alternate protocol stop here membrane preparation, *see* **Note 8**).

The pH is controlled: it must be at 7.0-7.5 (*see* **Note 9**).

5- The yeast suspension is distributed in several 500 mL centrifugation plastic bottles (about 80 mL per bottle). Cold glass beads are added until they reach the meniscus (about 450 g of beads per bottle, bottles have to be not more than half full to improve breaking). The bottles are tightly closed with screw caps and Para-Film to avoid leaks.

Beads are released from the bottom side of the bottles by manual agitation and the bottles are placed horizontally on the tray of an INFORS Multitron incubator and fixed with adhesive tape. Agitation is then performed during 20 min at 350 rpm (orbital agitation) and the room temperature set at 17°C to break yeast membranes. The culture will warm up from 4°C and the temperature has to be less than 12°C at the end of shaking to prevent protein degradation. Otherwise, breaking step can be done in successive phases of shaking-cooling.

All subsequent steps are performed at 4°C in a cold room.

6- For recovering the crude extract from the bottles, a vacuum pump is connected to a filtering flask as a trap (3 liters erlenmeyer), that is itself connected to a 25 mL pipette (without cotton plug). This home made pump system allows the efficient sucking of the crude extract from the beads into the trap.

7- The glass beads are washed in three successive steps with 1.1 L (3 times 40 mL per bottle (and 10 bottles), corresponding to about three times the mass of yeast) of the TES buffer supplemented with 1 mM PMSF and complete EDTA-free antiproteases cocktail. The last supernatant should be clear indicating that the beads are properly washed. The pH of the total crude extract (the first extract plus 3 washes will make up about 1.5 liter) is controlled: it must be at 7.0-7.5. Otherwise, pH is adjusted to 7.5 by adding NaOH 10 N.

8- The total crude extract is centrifuged in 500 mL bottles for 15 min, at 4°C and $1000xg_{av}$ in a JLA10.500 rotor. The pellet (P1), containing non- and partially-broken cells is discarded.

9- The first supernatant (S1) is centrifuged in 500 mL bottles for 15 min, at 4°C and $18000xg_{av}$ in a JLA10.500 rotor. The second supernatant (S2) is removed with great care and the pellet (P2), containing heavy membranes, is resuspended in about 15 mL of the TES buffer (with 1 mM PMSF and complete EDTA-free) per bottle and saved for further analyses.

10- This S2 supernatant is then centrifuged in 250 mL bottles for 5 h, at 10°C and $29000xg_{av}$ in a Type 19 rotor. The third supernatant (S3) is removed.

11- The pellet (P3), containing light membranes, is resuspended in 70 mL of the Hepes-sucrose buffer, *i.e.* 0.2 mL per gram of yeast. The membrane suspension is homogenized using a Potter-type mixing system and is conserved at -70°C after fast cooling in liquid nitrogen (see **Fig. 3**).

3.3 Estimation of total membrane protein concentration

Estimation of the membrane protein concentration is performed by bicinchoninic acid (BCA) assay ***(18)*** which has been adapted in a microplate format. The active reagent is prepared just before use to avoid premature oxidation by mixing bicinchoninic acid and $CuSO_4$ 4 % with a 50/1 (v/v) ratio. Each sample (20 µL of the sample to be

quantified, 12 µL of water and 8 µL of 10 % SDS) is compared to a reference curve obtained by using a concentration range of BSA samples (from 1 to 8 µg/mL) in a total volume of 40 µL. To be valuable, the BSA has to be diluted in the same buffer as the sample to be quantified, *i.e.* TES or Hepes-sucrose buffer, and has to contain a final concentration of 2 % (w/v) SDS. After adding 200 µL of BCA active reagent, each sample is incubated for 30 min at 37°C and absorbance at 540_{nm} is measured. This method is preferentially used for the estimation of membrane proteins because it is more robust in the presence of detergent; in fact, presence of SDS is strictly necessary to allow complete removal and denaturation of the membranous parts of proteins. At the end, the protein concentration of the light membranes (P3) is about 40 mg/mL with a content of about 3 % recombinant Ca^{2+}-ATPase. This ratio is estimated from western-blots.

3.4 Washing of light membranes and solubilization of membrane proteins (see **Fig. 4**)

1- Light membranes P3 are thawed using a water-bath at 20°C and diluted at 5 $mg.mL^{-1}$ of total proteins in the pre-solubilization buffer (**Fig. 4**, lane T_w). 1 mM β-mercaptoethanol or DTT can be added to prevent lipids and proteins from oxidation (*see* **Note 10**). This washing step is optional. However, we observe that the level of expression of yeast endogenous biotinylated proteins (Acetyl-CoA carboxylase, pyruvate carboxylase and Arc1p) was remarkably increased during expression phase as it can be expected from yeast metabolic pathways adaptation in anaerobiosis. Those soluble or extrinsic proteins were dragged with the P3 pellet and represent the major contaminants for affinity chromatography. This washing step by simple dilution enables to remove most of those proteins (*see* **Note 11**).

2- Diluted membranes are centrifuged for 1 h, at 10°C and $100000xg_{av}$ in a 45Ti rotor. The supernatant is discarded (**Fig. 4**, lane S_w).

3- Solubilization is performed at the final ratio DDM / total proteins of 3/1 (w/w). The membrane pellet is resuspended using a Potter-type homogenizer in the pre-solubilization buffer at a final concentration of 10 $mg.mL^{-1}$. At the same time, detergent is dissolved in the pre-solubilization buffer at a final concentration of 30 $mg.mL^{-1}$ and equilibrated for 1 h at 20°C before use. Then, both solutions (proteins and detergent) are mixed and kept at 20°C under gentle agitation for 5 min. Resulting concentrations are about 5 and 15 $mg.mL^{-1}$ respectively for total proteins and DDM. This solution is homogenized using a Potter-type homogenizer (~10 up and down). The solution becomes clearer (**Fig. 4**, lane T_{DM}).

4- Finally, the solution is centrifuged for 1 h at 10°C and $100000xg_{av}$ in a 45Ti rotor. The obtained supernatant contains the solubilized proteins (**Fig. 4**, lane S_{DM}).

3.5 Batch purification of SERCA by affinity chromatography (see **Fig. 4**)

The purification is carried out with 1 mL of resin for 4 mg of total Ca^{2+}-ATPase contained in the P3 fraction. Note that it might be useful to adjust this ratio according to the relative amount of the other biotinylated proteins compared to the level of expression of the protein of interest. Indeed, those proteins will compete for binding onto the streptavidin resin (*see* **Note 12**). In our hands, this ratio seems to be optimal for WT SERCA1a but it was not the case for some mutants and other isoforms.

We use a batch procedure throughout: each step consists in gently mixing the resin with the appropriate solution (5 min), centrifuging for 15 min, at 4°C and 1000xg_{av} in a « swinging bucket » rotor 11133 from Sigma.

1- The resin, stored in ethanol by the provider, has to be washed with 10 resin volumes of milli-Q water and equilibrated twice with 10 resin volumes of solubilization buffer.

2- This equilibrated resin is then added to the solution of solubilized proteins and the whole is gently stirred at 4°C overnight. However, thanks to the high affinity of streptavidin for biotin, this step may also be carried out for 2 h at 20°C.

All subsequent steps are done in 50 mL centrifuge tubes

3- The resin is collected in 50 mL centrifuge tubes by successive centrifugations: each tube is (i) filled with the suspension from 2-, (ii) centrifuged 5 min at 4°C and 1000xg_{av}, (iii) the supernatant is removed and these 3 steps are repeated until each tube contains about a maximum volume of 5 mL resin. All supernatants are pooled and this fraction is named flow through (**Fig. 4**, lane FT).

4- The resin is washed twice with 10 resin volumes of high salt (HS) washing buffer to remove unspecific bound proteins (**Fig. 4**, lane HS).

5- The resin is washed twice with 10 resin volumes of low salt (LS) washing buffer to reduce the KCl concentration before elution of SERCA1a and to increase the calcium concentration required for the thrombin cleavage (**Fig. 4**, lane LS)

6- 1 Volume of LS buffer (kept at 20°C) is added to the resin and this suspension is stirred 5 min on a wheel in order to equilibrate the temperature at 20°C (**Fig. 4**, lane R_0).

7- 25 units of thrombin per mL of resin are added to the solution. They are stirred slowly to prevent foaming on the wheel during 30 min at 20°C (**Fig. 4**, lane $R_{30'}$).

8- 25 more units of thrombin per mL of resin are added and the incubation is performed in the same conditions (**Fig. 4**, lane $R_{60'}$).

9- The thrombin cleavage is stopped by adding 1 mM PMSF and a complete EDTA-free antiproteases cocktail. The solution is then stirred 5 min at 20°C on the wheel and, at the end, is transferred into a filter tube.

10- SERCA1a is finally removed from the resin by centrifugation 2 min at 10°C and 1000xg_{av} (**Fig. 4**, lanes E1 and E2).

This protocol allows us to produce routinely milligrams of pure Ca^{2+}-ATPase depending on the level of expression for mutants and obviously on the amount of membranes used at the start of the purification. Note that this eluted fraction can be directly used for functional assays like ATPase activity measurements. For storage, it is frozen in liquid nitrogen and conserved at -70°C after adjusting the glycerol concentration to 40 %.

3.6 Detergent exchange by Size Exclusion Chromatography

DDM is exchanged with $C_{12}E_8$ by size-exclusion chromatography (SEC), an additional step that also improves the purity of the Ca^{2+}-ATPase preparation and the delipidation of the sample. This step is optional for functional analysis but is essential for structural studies as crystallogenesis trials.

1- SERCA1a eluted from affinity chromatography resin (typically 30 mL) is first concentrated on Centricon Ultracel-YM 30 until the volume is smaller than 500 µL.

2- This concentrate is applied at 0.5 mL/min into a silica gel-filtration column (0.78 cm x 30 cm TosoHaas TSK-gel G3000SWXL column), mounted on a Gold HPLC System, and equilibrated with 100 mM MOPS-Tris pH 6.8, 80 mM KCl, 1 mM $CaCl_2$,1 mM $MgCl_2$, 15 % sucrose, and 0.5 $mg.mL^{-1}$ $C_{12}E_8$.

3- The eluted fractions containing the Ca^{2+}-ATPase peak are pooled (about 1.5 mL total volume) and concentrated on Centricon-30 to a final volume of about 50 µL. The final protein concentration is about 10 $mg.mL^{-1}$ and $C_{12}E_8$ is estimated to be about 17-20 $mg.mL^{-1}$ on the basis of previous $C_{12}E_8$ binding data ***(19)***.

4- The concentrated, delipidated, and $C_{12}E_8$-solubilized Ca^{2+}ATPase is supplemented with phospholipid DOPC, to reach a $C_{12}E_8$: DOPC ratio of 3:1 (w/w). This is done by adding the protein sample in a centrifuge tube that had been already deposited with a thin layer of N_2-dried DOPC, gently vortexing the tube, and storing it overnight at 4°C for equilibration.

5- Finally, the sample was subjected to centrifugation at 120,000xg_{av} in a TLA-100 rotor for 20 min to remove aggregated (inactive) proteins just before the crystallization assays (see **Fig. 5**).

3.7 SDS-PolyAcrylamide Gel Electrophoresis (SDS-PAGE)

1- Gels are prepared according to the Laemmli procedure ***(20)***. 0.75 mm gels at 8 % acrylamide are prepared by mixing 1 mL of 1.5 M Tris-HCl pH 8.8 with 1.07 mL of 30 % acrylamide/bis solution (29/1), 1.85 mL of water, 40 µL of 10 % SDS, 40 µL of 10 % ammonium persulfate and 2.4 µL of TEMED (ammonium persulfate and TEMED are added just before pooring) for a total of 4 mL corresponding to one gel.

The gel (3.2 mL) is poored, leaving space for a stacking gel and over lay with water. The gel should polymerize in about 30 min.

2- The stacking gel is prepared by mixing 250 µL of 1 M Tris-HCl pH 6.8 with 330 µL of 30 % acrylamide/bis solution, 1.38 mL of water, 20 µL of 10 % SDS, 20 µL of 10 %

ammonium persulfate and 2 µL of TEMED (ammonium persulfate and TEMED are added just before pooring) for a total of 2 mL corresponding to one gel. The water is removed and the amount of stacking gel allowing at least one centimeter below the wells is poored and the comb is inserted. The gel should polymerize in about 30 min at 20°C.

3- The running buffer is added to the upper and lower chambers of the gel unit.

4- For SDS-PAGE, samples from membrane preparation and purification are diluted in the corresponding low salt washing buffer, mixed with an equal volume of denaturing buffer 2x-concentrated and immediately heated at 100°C for 1 min to denature proteases which could be very harmful for our proteins in presence of SDS. Note that the presence of urea is crucial in order to avoid the aggregation of membrane proteins ***(21)***. The samples are then cooled and loaded onto the gels. The gel is run at 120 V -25 mA during 1 hour.

5- Proteins are stained with Coomassie brilliant blue: the gel is incubated 10 min in the Coomassie blue staining solution and then rinsed several times (3-4 times for some seconds) with water. After removing the excess of the staining solution, the gel in water is destained by using microwave oven (about 1 min at 900 W, stop it just before boiling). Destaining is improved by adding a piece of absorbent paper in the hot water and by shaking gently the gel until complete disappearance of the background.

3.8 Western Blotting for SERCA

1- Samples that have been separated by SDS-PAGE can be transferred to PVDF membrane. Prestained standard (PPPS) can be used to check transfer efficiency. The transfer is done in CAPS buffer. This buffer allows a better electrophoretic mobility of the proteins. In those conditions we are able to transfer all the proteins (MW about 20 to 200 kDa) from an 8% Laemmli type gel in less than 1 h at 250 mA and about 80-90V instead of many hours in classical Tris-glycine buffer. Nevertheless, one has to be careful to proceed in presence of an ice cooling unit in the tank to prevent warming which can modify the mobility of proteins.

2- In the case of an immunodetection, the membranes are blocked for 10 min at 20°C in presence of PBS-T supplemented with 5% dry milk. 79B anti-Serca1a guinea-pig antibody (that recognizes the N-terminal part of SERCA1a) is added in the blocking media at 1/20000 dilution for 1 h. The membrane is rinsed once using PBS-T. Anti-guinea-pig antibody coupled to horse raddish peroxidase is then added at 1/10000 in PBS-T and incubated for 1 h. In the case of the other couple of antibodies, the mouse monoclonal anti-SERCA1a (IIH11 clone) is diluted 1/2500 and the goat anti-mouse IgG1 (γ) is diluted 1/2000. In case of very low protein expression, a better signal/noise ratio can be obtained by heating the PVDF membrane in SDS/β-mercaptoethanol ***(22)***.

3- In the case of detection of biotinylated proteins by avidin-peroxidase probe, the procedure is slightly different: it is indispensable to avoid incubation of the probe with dry milk because of the presence of biotinylated proteins in it. So after the first step

consisting in blocking membrane with PBS-T supplemented with 5 % dry milk, we wash it three times for 10 min with PBS-T in order to remove milk. The probe is added at a 1/50000 dilution in PBS-T and incubated for 1 h at 20°C.

4- For the two systems of detection, membranes are washed 3 times for 10 min with PBS-T buffer. The bound antibodies are revealed with ECL reagents and emitted light is detected using a CCD cooled camera.

In order to quantify the amount of SERCA proteins, the intensities of the bands are compared to a range of native Ca^{2+}-ATPase isolated from the rabbit sarcoplasmic reticulum (SR membranes provided by Dr. Philippe Champeil). In the case of membranous solutions, the comparison may suffer from the presence of many other membrane proteins. To be more relevant, a similar amount of P3 membrane prepared from yeast transformed with the empty expression vector is added to the SR range. This addition is particularly important when the detection system is not very sensitive and when the relative amount of expressed proteins is very low.

4. Notes

1- The plates have to be prepared less than one week before. Otherwise, an additional preculture must be done.

2- For each clone, several colonies are checked in order to choose the best one.

3- These samples may be stored as aliquots (15 µL) at -70°C.

4- Both cultures are performed in erlenmeyer-type flasks containing a volume of at least 10 times the medium volume in order to allow an optimal aeration of the yeast cultures.

5- This procedure allows to obtain cells in a synchronous state and at exponential phase for the following inoculation in the bioreactor.

6- A chiller is connected in order to cool the effluents and thus limit the ethanol evaporation.

7- The anaerobiosis stimulates the production of networks of internal membranes which is convenient for storing overexpressed membrane proteins.

8- At this step, the pellets may be resuspended in only one volume V of TES buffer with 1 mM PMSF and complete EDTA-free antiprotease cocktail corresponding to 1 time the weight of yeast (350 mL for 6 initial liters of yeast culture) and stored at -70°C after fast freezing in liquid nitrogen. In this case, the solution is rapidly thawed in water in a bath-water at 20°C and one additional volume V of TES buffer with 1 mM PMSF and complete EDTA-free antiprotease cocktail is added before the breaking of the yeast.

9- The pH may be lower if yeast cells are altered by an efflux of lysosomal contents.

10- The membrane protein solution can be diluted in the range of 2-10 mg/mL. Nevertheless, note that you will need to be careful to adjust the subsequent centrifugation time in function of the final concentration.

11- Note that KCl concentration may be increased to 600 mM to improve the removal of extrinsic proteins from the membranes. However, this treatment may somewhat induce protein proteolysis ***(12)***.

12- Note that it might be of interest to verify the biotinylation level of the protein beforehand.

Acknowledgments

The authors would like to thank Dr. Philippe Champeil for the gift of SR membranes and for discussions. This work was supported by grants from the Commissariat à l'Energie Atomique (CEA) program Signalisation et transport membranaires and by the Agence Nationale de la Recherche (Grant ANR-06-BLAN-0239-01).

References

1. Jidenko, M., Nielsen, R. C., Sørensen, T. L-M., Møller, J.V., le Maire, M., Nissen, P., and Jaxel, C. (2005) Crystallization of a mammalian membrane protein overexpressed in *Saccharomyces cerevisiae*. *Proc. Natl. Acad. Sci. USA* **102**, 11687-11691.

2. Marchand, A., Winther, A. M. L., Holm, P. J., Olesen, C., Montigny, C., Arnou, B. Champeil, P. Clausen, J. D., Vilsen, B., Andersen, J. P., Nissen, P., Jaxel, C., Møller, J. V., and le Maire, M. (2008) Crystal Structure of D351A and P312A Mutant Forms of the Mammalian Sarcoplasmic Reticulum Ca^{2+}-ATPase Reveals Key Events in Phosphorylation and Ca^{2+} Release. *J. Biol. Chem.* **283**, 14867-14882.

3. Jidenko, M., Lenoir, G., Fuentes, J. M., le Maire, M., and Jaxel, C. (2006) Expression in yeast and purification of a membrane protein, SERCA1a, using a biotinylated acceptor domain. *Protein Expr. Purif.* **48**, 32-42.

4. Cardi, D. et al., in preparation.

5. Midgett, C. R., and Madden, D. R. (2007) Breaking the bottleneck: eukaryotic membrane protein expression for high-resolution structural studies. *J. Struct. Biol.* **160**, 265-274.

6. Ferguson, A. D., McKeever, B. M., Xu, S., Wisniewski, D., Miller, D. K., Yamin, T-T., Spencer, R. H., Chu, L., Ujjainwalla, F., Cunningham, B. R., Evans, J. F., and. Becker, J. W. (2007) Crystal structure of inhibitor-bound human 5-lipoxygenase-activating protein. *Science* **317**, 510-512.

7. Jasti, J., Furukawa, H., Gonzales, E. B., and Gouaux, E. (2007) Structure of acid-sensing ion channel 1 at 1.9 Å resolution and low pH. *Nature* **449**, 316-323.

8. Kobilka, B. K. & co-workers, see News and Views by Sprang, S. R. (2007) A receptor unlocked. *Nature* **450**, 355-356.

9. Pedersen, B. P., Buch-Pedersen, M. J., Morth, J. B., Palmgren, M. G., and Nissen, P. (2007) Crystal structure of the plasma membrane proton pump. *Nature* **450**, 1111-1114.
10. Drew, D., Newstead, S., Sonoda1, Y., Kim, H., von Heijne, G., and Iwata, S. (2008) GFP-based optimization scheme for the overexpression and purification of eukaryotic membrane proteins in *Saccharomyces cerevisiae*. *Nature Protocols* **3**, 784 - 798.
11. Centeno, P., Deschamps, S., Lompré, A.-M., Anger, M., Moutin, M. J., Dupont, Y., Palmgren, M. G., Møller, J. V., Falson, P., and le Maire, M. (1994) Expression of the sarcoplasmic reticulum Ca^{2+}-ATPase in yeast. *FEBS Lett.* **354**, 117-122.
12. Lenoir, G., Menguy, T., Corre, F., Montigny, C., Pedersen, P. A., Thinès, D., le Maire, M., and Falson, P. (2002) Over-production in yeast and rapid and efficient purification of the rabbit SERCA1a Ca^{2+}-ATPase. *Biochim. Biophys. Acta , Biomembranes* **1560**, 67-83.
13. Pompon, D., Louerat, B., Bronine, A., and Urban, P. (1996) Yeast expression of animal and plants P450s in optimized redox environmants. *Methods Enzymol.* **272**, 51-64.
14. Cronan J. E., Jr (1990) Biotination of proteins *in vivo*. A post-translational modification to label, purify, and study proteins. *J. Biol. Chem.* **265**, 10327-10333.
15. Pouny, Y., Weitzman, C., and Kaback, H. R. *In vitro* biotinylation provides quantitative recovery of highly purified active lactose permease in a single step. *Biochemistry* **37**, 15713-15719.
16. Chen, D.C., Yang, B.C., and Kuo, T.T. (1992) One-step transformation of yeast in stationary phase. *Curr. Genet.* **21**, 83-84.
17. Gietz, D., St Jean, A., Woods, R. A., and Schiestl, R.H. (1992) Improved method for high efficiency transformation of intact yeast cells. *Nucleic Acids Res.* **20**, 1425.
18. Smith, P. K., Krohn, R. I., Hermanson, G. T., Mallia, A. K., Gartner, M. D., Provenzano, M. D., Fugimoto, E. K., Goeke, N. M., Olson, B. J., and Klenk, D. C. (1985) Measurement of protein using bicinchoninic acid. *Anal. Biochem.* **150,** 76–85.
19. Møller, J. V., and le Maire, M. (1993) Detergent binding as a measure of hydrophobic surface of integral membrane proteins. *J. Biol. Chem.* **268**, 18659-18672.
20. Laemmli, U. K. (1970) Cleavage of structural proteins during the assembly of the head of bacteriophage T4. *Nature* **227**, 680-685.
21. Soulié, S., Møller, J. V., Falson, P., and le Maire, M. (1996) Urea reduces the aggregation of membrane proteins on sodium dodecyl sulfate-polyacrylamide gel electrophoresis. *Anal. Biochem.* **236**, 363-364.
22. Fuentes, J. M., Lompré, A.-M., Møller, J. V., Falson, P., le Maire, M. (2000) Clean Western blots of membrane proteins after yeast heterologous expression following a shortened version of the method of Perini et al. . *Anal. Biochem.* **285**, 276-278.

Figures legends

Figure 1. Plasmid used for the heterologous expression of Serca1a-BAD

Cloning and amplification in E. coli (light grey): Ori bact., bacterial replication origin; Amp^R, gene coding for β-lactamase to allow resistance to ampicillin (selection marker). *Amplification in yeast (dark grey)*: ADE2, auxotrophy selection marker for adenine; URA3, auxotrophy selection marker for uracile; 2μ, yeast replication origin.

Expression (white): GAL10-CYC1, fusion promoter of the inducible part of GAL10 and RNA polymerase binding part of CYC1; PGK, Phosphoglycerate Kinase terminator sequence; SERCA1a, coding sequence for Ca^{2+}-ATPase; Thr, sequence coding for thrombin cleavage site; BAD, Biotin Acceptor Domain. Serca1a, Thr and BAD sequences were cloned in the same coding frame to allow expression of the fusion protein SERCA1a-BAD.

Figure 2. Follow-up of culture parameters during expression process

6 L of YPGE2x medium were inoculated with yeast strain containing vector for SERCA1a-BAD overexpression as described in Methods. Cells density is estimated by optical density measurements at 600 nm using a Novaspec spectrophotometer (closed circles and continuous line). Dissolved dioxygen concentration (dO_2, dark and short dashed line), pH (long dashed line) and temperature are measured continuously thanks to a probe connected to the recording system. dO_2 and pH are used as real-time reporter of yeast metabolism. *First phase going from inoculation to 34 h:* yeast growth is optimized by maintaining dissolved dioxygen up to 20% by automatic control of air flow rate and stirring. *Second phase corresponding to expression phase:* temperature is lowered at 18°C to slowdown cell division. Expression is induced by two successive galactose additions (grey arrows at 36 and 49 h). *Last phase after 54 h:* growth and expression are suddenly stopped by decreasing temperature to 6°C and stirring at 300 rpm.

Figure 3. Membrane preparation

A. Principle of the fractionation. TCE, total crude extract; S1 and P1, supernatant and pellet from first centrifugation respectively; S2 and P2, supernatant and pellet from second centrifugation respectively; S3 and P3, supernatant and pellet from third centrifugation respectively. B. Western blot analysis of various aliquots from the membrane preparation: samples (1 μg of total proteins) were analysed by SDS-PAGE. For the SR samples, they were added to 1 μg of P3 membrane prepared from yeast transformed with the empty expression vector. Proteins were transferred onto a PVDF membrane and immunostained with a specific antibody directed against SERCA1a (79B) or revealed with avidin peroxidase probe (AP) which can bound to all the biotinylated proteins. SR, SERCA1a extracted from rabbit sarcoplasmic reticulum; AcoA. carb., Acetyl-CoA carboxylase; pyr. carb., pyruvate carboxylase.

Figure 4. Purification of Serca1a by streptavidin affinity chromatography

In all cases, 20 µL of the sample to be tested are mixed with 20 µL of denaturing buffer 2x-concentrated and 20 µL of this mix is loaded onto the gel.

A. Coomassie blue stained SDS-PAGE. MWM, Molecular Weight Marker; T_W, diluted membrane fraction in pre-solubilization buffer; S_W, supernatant of membrane washing containing eliminated proteins; T_{DM}, membrane pellet resuspended in pre-solubilization buffer supplemented with DDM; S_{DM}, solubilized fraction; FT, flow-through; HS, washing at 1 M KCl; LS, washing at 50 mM KCl; R_0 - $R_{30'}$ - $R_{60'}$, resin samples taken at time 0 – 30 min and 60 min during thrombin cleavage step; Res, resin after elution of SERCA1a; E1 and E2, first and second elutions; Co, elution pool concentrated on YM-30 membranes (diluted 20-fold); SR0.1 and SR0.5, 0.1 and 0.5 mg native rabbit sarcoplasmic reticulum Ca^{2+}-ATPase (SR) used as standards. B. Western-blot and immunodetection using anti-SERCA1a antibody. Samples from T_W to L_S fractions were 10-fold, resin and eluted fractions samples 50-fold and "Co" fraction 1000-fold diluted in LS buffer, respectively. After electrophoresis, proteins were transferred to PVDF membranes and SERCA1a was detected thanks to the use of mouse monoclonal anti-SERCA1a (IIH11 clone) as a primary antibody and goat anti-mouse IgG1 (γ) as a secondary antibody. Intensities of bands are compared to standard amount of 10 and 50 ng of SR for quantitative estimation. C. Western-blot and detection using avidin-HRP probe. Previous membranes are stripped by incubation in a 2 % SDS, 1 mM EDTA, 0.1 M β-mercaptoethanol and 50 mM Tris-Cl pH 6.8 buffer during 30 min. After extensive washing with PBS-T buffer, avidin-peroxidase probe is added. In this case, only biotinylated proteins are detected, the purified SERCA1a protein is not visible. SR, extracted from rabbit sarcoplasmic reticulum; S1a-BAD, SERCA1a fused to BAD; S1a, SERCA1a; ACoA Carb, Acetyl-CoA carboxylase; Pyr.Carb, pyruvate carboxylase.

Figure 5. SEC-HPLC purification step for crystallization attempts

The figure depicts the elution profile at 280 nm (in arbitrary units, Arb. U.) from size-exclusion chromatography of SERCA1a after affinity chromatography. The absorption peaks corresponding to aggregates, monomeric SERCA1a or thrombin are indicated by arrows. The inset shows (A) the SDS-PAGE profile of SERCA1a after SEC-HPLC purification (SERCA1a is indicated by an arrow) and (B) crystals obtained using the protein analyzed in A. Crystals were obtained by the vapour diffusion method in hanging drops using PEG2000 as the precipitant and *ter*-butanol as additive.

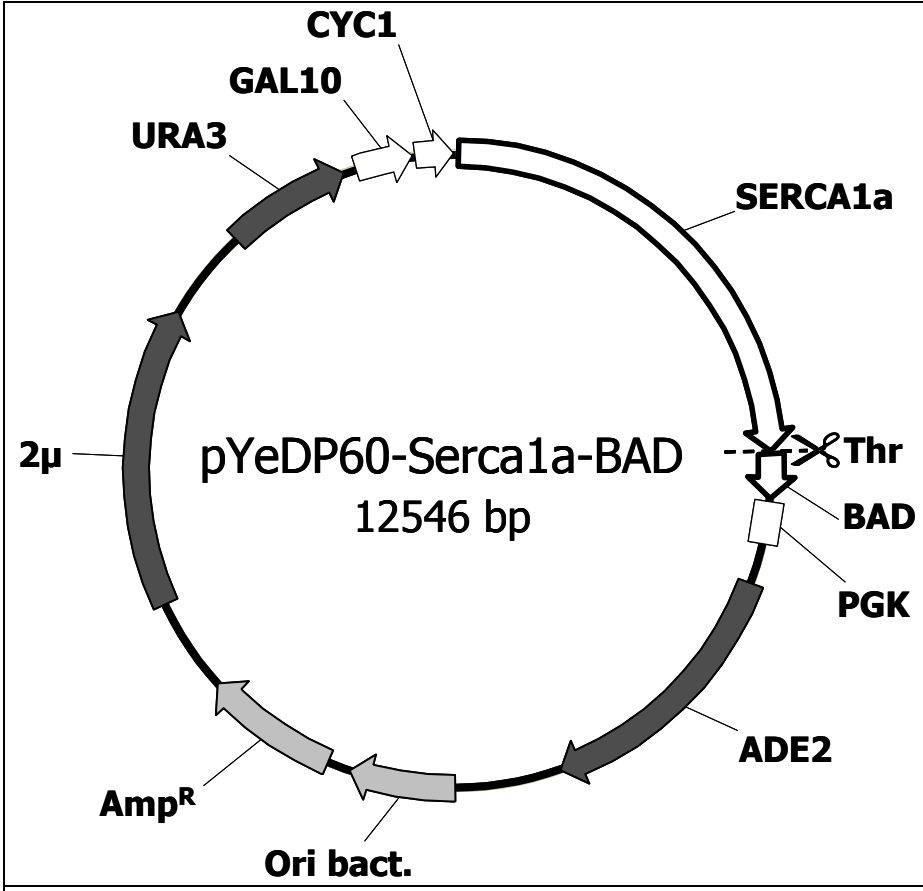

Fig. 1. Plasmid used for the heterologous expression of SERCA1a-BAD

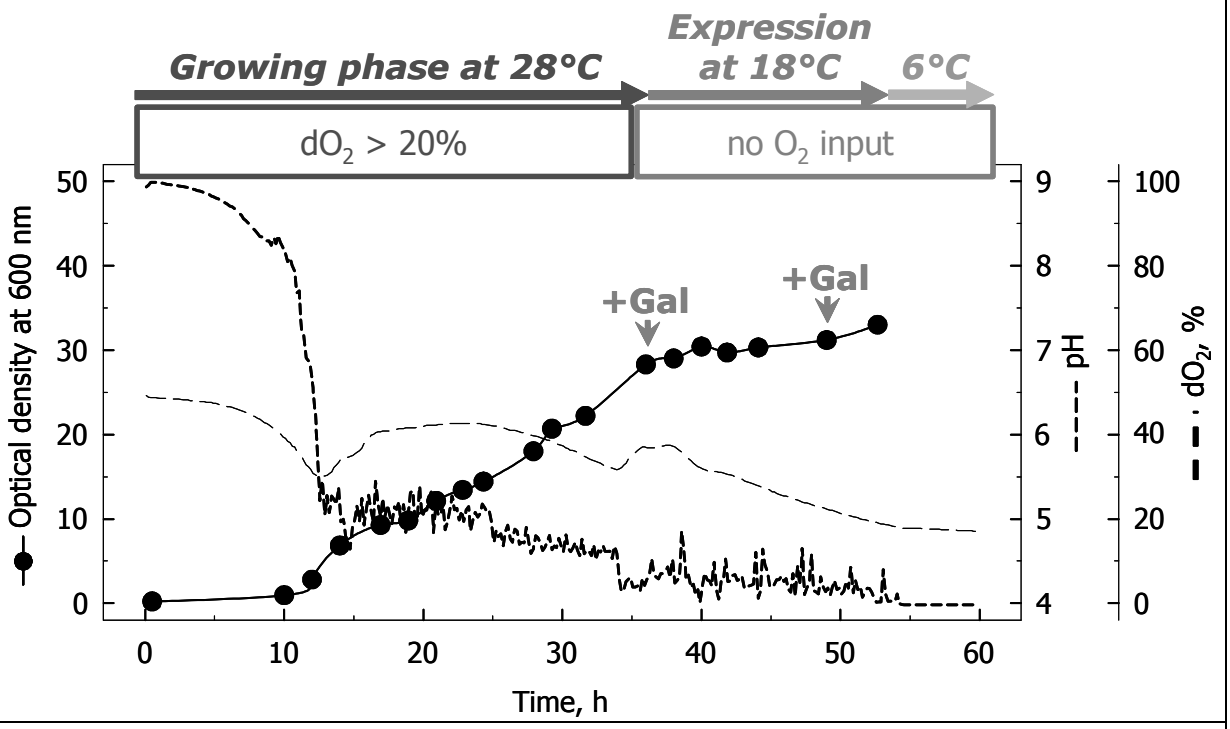

Figure 2. Follow-up of culture parameters during expression process

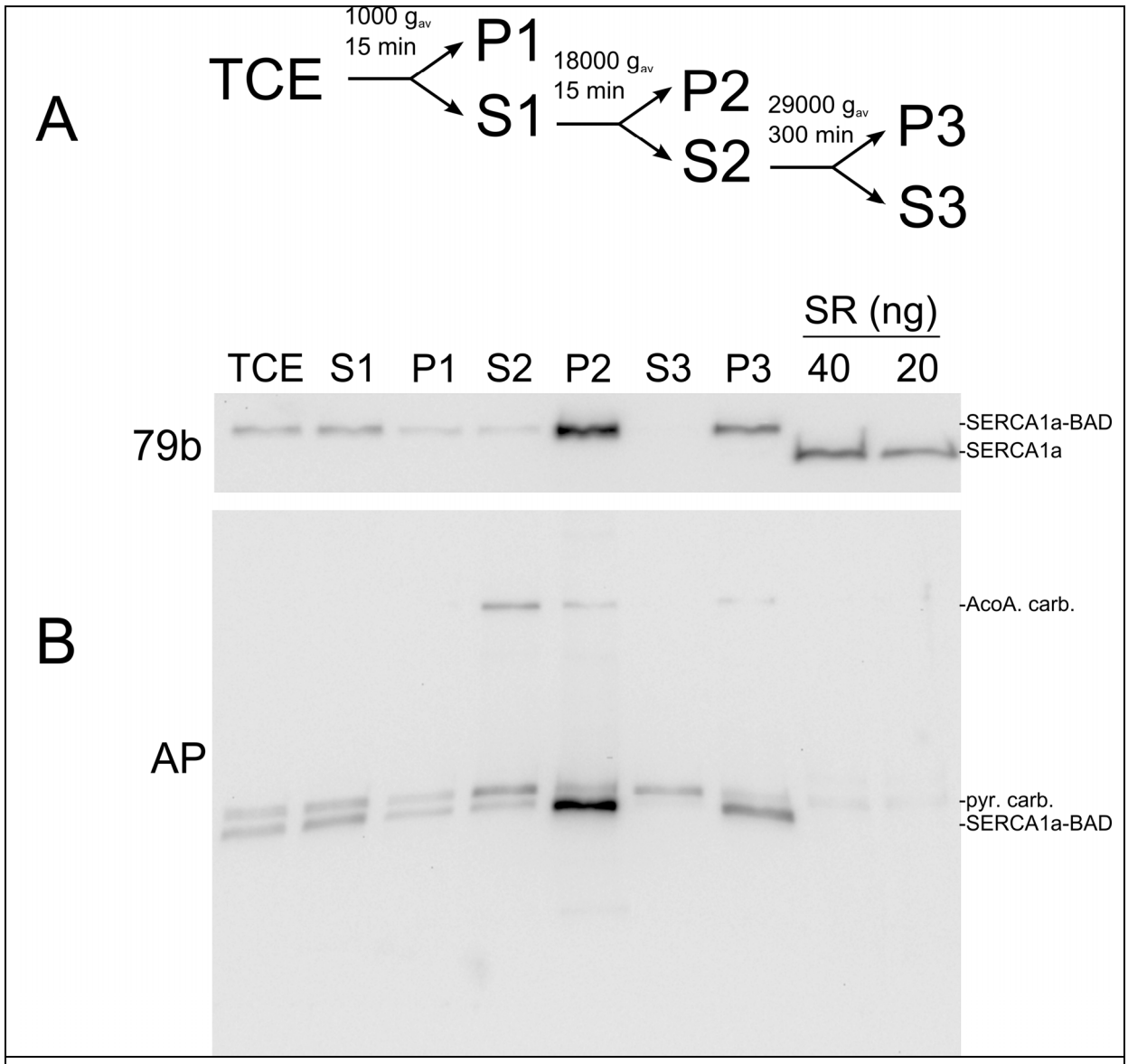

Fig. 3. Membrane preparation

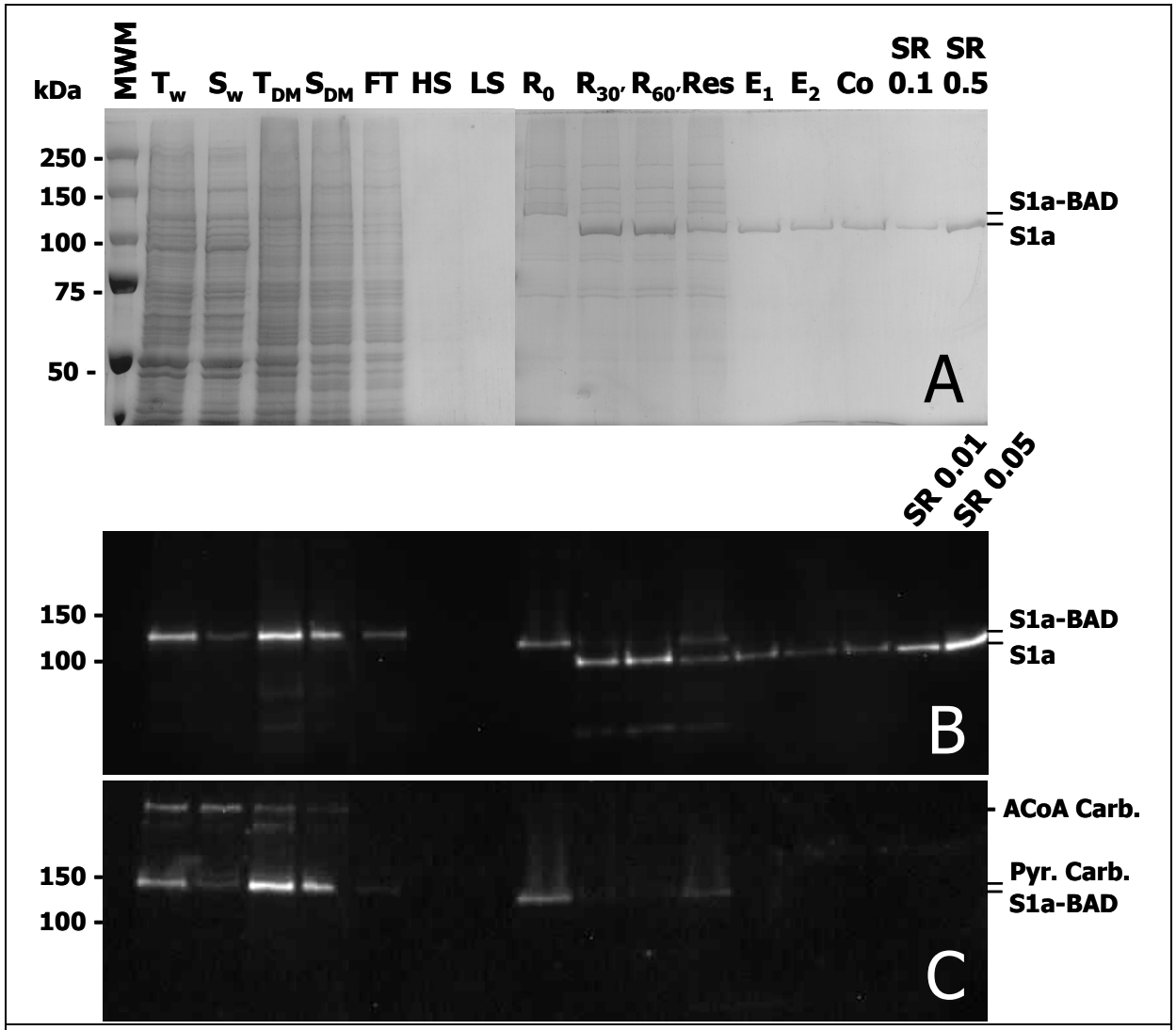

Fig. 4. Purification of Serca1a by streptavidin affinity chromatography

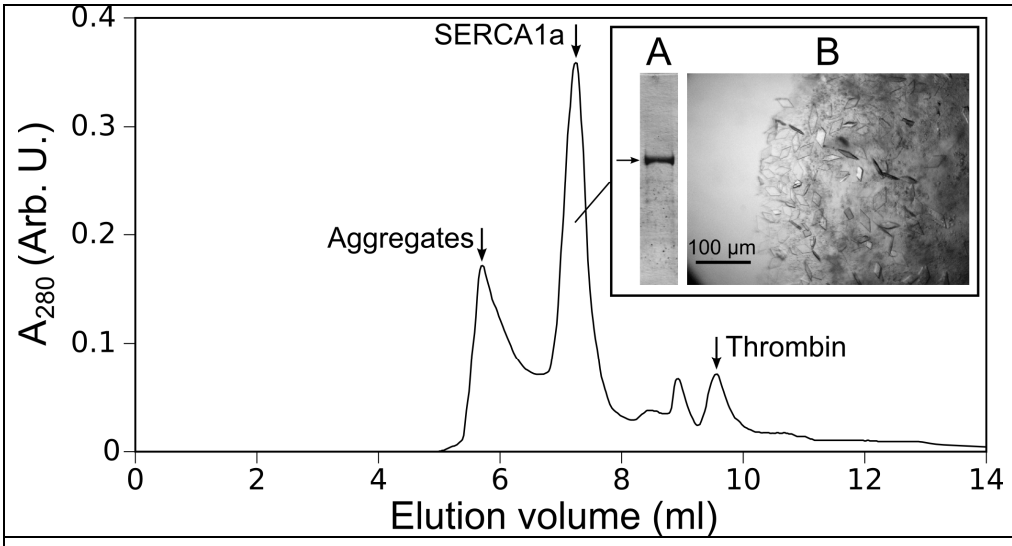

Fig. 5. SEC-HPLC purification step for crystallization attempts

ARTICLE II

Purified E255L mutant SERCA1a and purified PfATP6 are sensitive to SERCA-type inhibitors but insensitive to artemisinins.

Delphine Cardi*, Estelle Marchal*, Sanjeev Krishna†, Jesper V. Møller‡, Marc le Maire*, and Christine Jaxel*§

*Commissariat à l'Energie Atomique (CEA), Institut de Biologie et de Technologies de Saclay, SB2SM, URA CNRS 2096, Laboratoire de Recherche Associé 17V University of Paris-Sud, Gif sur Yvette, F-91191, France. †Centre for Infection, Division of Cellular and Molecular Medicine, St George's University of London, London, UK. ‡ Department of Physiology and Biophysics, Centre for Membrane Pumps in Cells and Disease-PUMPKIN, Danish National Research Foundation, Institute of Physiology and Biophysics, University of Aarhus, Ole Worms Alle´ 1185 and 1160, Aarhus C DK-8000, Denmark

Corresponding author: §Christine Jaxel, URA CNRS 2096, iBiTec-S/SB2SM/LPM, CEA Saclay, 91191 Gif-sur-Yvette, France, tel: 33169083379, fax: 33169088139, christine.jaxel@.cea.fr

Correspondence could also be addressed to Marc le Maire (marc.lemaire@cea.fr).

Manuscript information: 22 pages for text, 3 figures and 1 table.

Abbreviations: SR, sarcoplasmic reticulum; ER, endoplasmic reticulum; SERCA1a, 1a isoform of the SR Ca^{2+}-ATPase; BAD, biotin acceptor domain; PfATP6, P. falciparum Ca2+-ATPase; DDM, dodecylmaltoside; $C_{12}E_8$,dodecyl octaethylene glycol monoether; DOPC, dioleylphosphatidyl-choline**;** Tg, thapsigargin; BHQ, 2, 5-Di(tert-butyl)-1, 4-benzohydroquinone; and CPA, cyclopiazonic acid.

Abstract

Artemisinins are sesquiterpene trioxane lactones that contain an endoperoxide bridge essential for antimalarial activity. Artemisinins are effective against both asexual and early sexual stages of infection caused by *Plasmodium falciparum*. Artemisinins have been described as inhibitors of PfATP6 (*P. falciparum* ATP6), a SERCA (sarcoplasmic–endoplasmic reticulum

Ca^{2+}-ATPase)-type ATPase, after expression in *Xenopus* oocytes. Mutation of an amino acid residue in mammalian SERCA1 (E255) to the equivalent one predicted in PfATP6 (L) was reported to induce sensitivity to artemisinin after assay of Ca^{2+} dependent ATPase hydrolysis in the oocyte system. However, after purification of the mammalian SERCA1a E255L expressed in *Saccharomyces cerevisiae* we show that artemisinin and its derivatives do not inhibit Ca^{2+}-ATPase activity. Moreover, we find that artemisinin does not inhibit the Ca^{2+}-ATPase activity of PfATP6 when purified with streptavidin

chromatography after expression as a biotinylated protein in *S. cerevisiae*. Purified PfATP6 has enabled us to characterize several of its properties including optimal Ca^{2+} concentrations and pH, and to determine ATPase activity in the presence of detergent and lipids. Under these conditions, PfATP6, is somewhat less sensitive to thapsigargin than to rabbit SERCA1 and retains full sensitivity to CPA (cyclopiazonic acid) and BHQ (2, 5-Di(tert-butyl)-1, 4-benzohydroquinone) inhibitors. On the other hand, the insensitivity of purified PfATP6 to artemisinins suggests that the mechanism of action of this class of drugs is complex and cannot be ascribed to direct inhibition of PfATP6 as previously considered. Furthermore, the successful purification of PfATP6 affords the opportunity to develop new antimalarials by screening for inhibitors against PfATP6.

Introduction

Malaria is a major infectious disease with about 500 million cases and one million deaths every year. Human malaria is caused by five species of protozoan parasites of the genus *Plasmodium* transmitted to humans by female *Anopheles* mosquitoes. Infections with *Plasmodium falciparum* are responsible for most severe disease and deaths. Without a vaccine, drug treatment is a critical part of malaria control strategies. However, drug-resistant parasites are severely compromising effectiveness of many therapies (1, 2). The artemisinins have maintained their efficacy despite the emergence of drug resistance to other classes of antimalarial, although even this class now exhibits clinically relevant resistance in some areas (3). Artemisinins kill parasites faster (4) and with less toxicity (5) than other drugs but their mechanism of action is not yet clearly known. Artemisinin is extracted from *Artemisia annua,* a herb long used to treat fevers in traditional Chinese medicine, and derivatives have been developed to improve their potency, solubility, stability and pharmacokinetic properties (6-9). Artemisinins are sesquiterpene trioxane lactones that contain an endoperoxide bridge essential for antimalarial activity (10). They are effective against the blood stages of *Plasmodium* and especially the early ring-and sexual stages (gametocytes) of the parasite life cycle (4, 11, 12). Artemisinins accumulate preferentially in infected erythrocytes (13, 14) and are located in parasite membranes and in the red blood cell tubovesicular membrane network (15). The generation of free radicals by artemisinins may be critical for killing parasites, an observation that is consistent with the importance of the endoperoxide bridge for drug efficacy (16). The nature of these radicals, and how they are generated is debated, with hypotheses including roles for iron or heme catalysing Fenton-like reactions (17, 18).

Artemisinin inhibits the endocytosis of red blood cell cytoplasmic macromolecules by the parasite (19), possibly via an increase in the cytosolic level of Ca^{2+}. Efficacy, against *Toxoplasma gondii,* has also been related to changes in calcium homeostasis in this member of the apicomplexan family of parasites that includes *Plasmodium* spp (20,21). Several P-type ATPases (PfATP6, a SERCA type protein; PfATP4, a PMR-like protein, 3

putative ATPases which seem to belong to Golgi-ER-type family) and a single Ca^{2+}/H^{+} exchanger were identified to be involved in the maintenance of calcium homeostasis in *Plasmodium falciparum* (22).

Recently, Krishna and colleagues (23, 24) observed that the ATPase activity of the single sarco(endo)plasmic reticulum calcium ATPase (SERCA) of *P. falciparum*, PfATP6, expressed in *Xenopus laevis* oocyte was inhibited by artemisinin (Ki : ~150 nM). Isobologram analysis, and competition studies with fluorophore derivatives localizing to parasites were consistent with a common target for artemisinin and thapsigargin (Tg), a specific inhibitor of SERCA-type proteins, because an antagonism was observed in the action of these drugs. PfATP6 and SERCA1 share an overall 40 % homology with a well conserved transmembrane region, while the cytosolic sequence of the parasite Ca^{2+}-ATPase contains about 200 additional residues. Mutation studies on PfATP6 expressed in oocytes suggested that in particular Leu 263 modulates the sensitivity of this enzyme to artemisinin (25). This was in part based on the finding that rabbit SERCA1, whose Tg binding site is near F256 (26), is insensitive to artemisinin and its aminoacid sequence contains at the homologous position of Leu 263 a glutamate (Glu 255). When the Leu 263 of PfATP6 was mutated to glutamate, sensitivity to artemisinin was decreased (25), and conversely when the glutamate residue of SERCA1 was mutated to a leucine, SERCA1 became sensitive to artemisinin (25).

These results suggest that PfATP6 is a target for artemisinins, with further support derived from correlation between certain point mutations in PfATP6 in field isolates showing reduced *in vitro* sensitivity to artemether (27) and dihydroartemisinin (28) although all the cases of artemisinin resistance are not related to these mutations (18, 29, 30).

Up to now, only two of these transporters (PfATP6, PfATP4) and mutated SERCA1a E255L have been studied in the *Xenopus laevis* oocyte system (23, 31). To characterize this Ca^{2+} ATPase (functionally and structurally) and to understand the interaction of artemisinins with PfATP6 and SERCA1a E255L, it is important to purify these proteins. Our group recently developed a method to purify rabbit SERCA1a by affinity chromatography after its expression in yeast (32) and this method was successfully used for studying and crystallizing wild type (33) and mutated SERCA1a (34).

These methods were applied to purify and functionally characterize SERCA1a E255L and PfATP6, and to study the effects of artemisinin and other drugs when combined with detergent or lipids.

Results and Discussion

Study of the mutant SERCA1a E255L: purification and enzymatic properties.

The yeast light membranes for SERCA1a E255L mutant (endoplasmic reticulum and secretion vesicles) were prepared by membrane fractionation, as previously described

(32). From one liter of culture containing about 35 g of yeast, 325 mg of membrane proteins, containing the SERCA1a E255L mutant, was obtained in the light membrane fraction. The subsequent solubilization with DDM and purification by streptavidin chromatography was performed as described in (34) and led to the recovery of 150 µg of mutated protein at a concentration of about 30 µg/mL, as determined by Coomassie blue gel staining and western blotting (see Fig. 1A and 1B). The protein was well purified as shown on the Coomassie blue staining gel (about 70 %- most of the impurity is due to inhibited thrombin, Fig. 1A).

To determine the effect of artemisinin on the SERCA1a E255L mutant, the specific ATPase activity of the protein was measured spectrophotometrically by a coupled enzyme system. We found that the maximal rate of ATP hydrolysis of the SERCA1a E255L mutant was about 1.6 µmol of hydrolysed ATP min^{-1} (mg Ca^{2+}-ATPase)$^{-1}$ as measured in the presence of 1 mg/mL $C_{12}E_8$ and 25°C. By comparison, the specific activity of the wild type SERCA1a protein, overexpressed in yeast and measured under the same conditions was 4.4 µmol of hydrolysed ATP min^{-1} (mg Ca^{2+}-ATPase)$^{-1}$. Thus the mutation appears to slow down the ATP hydrolysis rate. Although this is in line with the effect of other mutations in this region (35), it is still somewhat surprising because the mutant E255A studied after over-expression in COS cells did not show any significant functional differences from that of the native protein (35). The Ca^{2+} dependent-ATPase activity of the mutant, like that of the wild type, could be stopped both by thapsigargin (specific inhibitor for SERCA type ATPases) and by EGTA (chelating agent of calcium ions) (Fig. 1C, panel A), supporting the suggestion that main calcium pumping function of this protein, is retained in the mutant. To perform the assay under optimal conditions, we have adopted the use of lipid/detergent mixtures. The presence of DOPC in the assay media, forming mixed micelles with $C_{12}E_8$, both increased the stability and enzymatic activity of solubilized Ca^{2+}-ATPase. We found that optimal conditions were obtained in the presence of 0.2 mg/mL of $C_{12}E_8$ and 0.05 mg/mL of DOPC (Fig. 1C, panel B) and this resulted in an increase of the specific activity from 4.4 - (Fig. 1C, panel A) to 7.1 µmol of hydrolysed ATP min^{-1} (mg Ca^{2+}-ATPase)$^{-1}$. The phospholipid-dependent increase in activity of purified P-type ATPases had already been observed (see (36), with the Na^+/K^+ ATPase for a recent example). The addition of artemisinin to the SERCA1a E255L mutant solubilized in this medium did not inhibit Ca^{2+}-ATPase activity (Fig. 1C, panel C). Some studies suggested that artemisinin needs the presence of iron to be an efficient inhibitor (23). The effect of artemisinin in the presence of iron (Fe^{2+}) was also tested (Fig. 1C, panel E) and compared with the effect of iron alone (Fig. 1C, panel D). There was no inhibitory effect of artemisinin and iron on the SERCA1a E255L mutant ATPase activity with the combination giving a slight but insignificant increase in activity. On the basis of these results, we were unable to confirm earlier findings of a specific artemisinin inhibition of Ca^{2+}-ATPase activity by the E255L mutant, obtained after expression in the oocyte

system (23). There is thus no evidence for an artemisinin binding site with a putative localization in the binding region for thapsigargin when tested with the purified and detergent-solubilized ATPase mutant.

Study of PfATP6: purification.

We then proceeded to investigate the plasmodial protein PfATP6. Although the codon adaptation index (which is a measure of the similarity of the codon usage of a gene to that of the proposed host organism (37)) is high (0.843) for the wild type PfATP6 gene and *S. cerevisiae*, only very low levels of the protein were obtained by heterologous expression in yeast (see supporting information, Fig. S1). As genes of *Plasmodium* are often very AT-rich, we designed a sequence that took into account optimal codon usage for yeast and removed most of the poly A or T tracts in the native sequence to avoid premature transcriptional termination as observed for other plasmodial proteins expressed in *S. cerevisiae* (38) and in *P. pastoris* (38-40). Gene optimization increased the codon adaptation index to a very high value (0.959) and enormously increased expression of PfATP6 (see supporting information, Fig. S1). This was the case despite leaving the GC content almost unchanged (27.9 % for the wild type sequence and 28.6 % after modification). This optimized sequence was therefore used for a subsequent large scale expression of PfATP6.

Like the mutant SERCA1a E255L, PfATP6 was expressed in yeast at high level; this expression has been optimized in particular by using a fermentor (see supporting information, SI Materials and Methods). After expression, we recovered light membranes (LM) containing 8 mg of PfATP6 per liter of culture of which about 30 % was biotinylated (2.4 mg, data not shown). The subsequent treatment of these membranes with DDM leads to the solubilization of 30 % of the biotinylated PfATP6 proteins (see supporting information, Fig. S2 and S3).

The fraction solubilized by DDM was loaded onto a streptavidin-Sepharose resin in a ratio of 4:1 w/v (8 mg of PfATP6 contained in LM in 2 mL of resin (i.e. ~600 µg of biotinylated and solubilized PfATP6)), in order to optimize the binding capacity of the resin. In these conditions, we estimated that ~240 µg of PfATP6-BAD was bound to 2 mL of resin. The thrombin cleavage between the sequence of PfATP6 and the biotinylated acceptor domain was followed by Coomassie Blue staining gel (Fig. 2A) and by immunodetection with anti-PfATP6 antibodies (Fig. 2B). Then, PfATP6 without its tag (BAD) was eluted from the resin and the corresponding fractions were well purified (lanes E1 and E2 in Fig. 2A). The purity of the protein reached about 70 % (the remaining 30 % being mainly due to thrombin) according to the evaluation performed by densitometry of Coomassie blue stained gel. This purification procedure gave a total amount of at least 160 µg of purified PfATP6 starting from 1 liter of yeast culture and therefore a yield of 7 % compared to the amount of biotinylated PfATP6-BAD contained in the light membranes.

Other plasmodial membrane proteins were produced in *Pichia pastoris* and Ni-NTA purified generally in better yield (38-40). In spite of our lower yield, we can expect to recover functional proteins since the yeast *in vivo* biotinylation that our protocol implies tends to select properly folded proteins (33).

Study of the enzymatic properties of the purified PfATP6

We first measured the specific ATPase activity of the purified PfATP6 with the aid of the coupled enzyme assay as described for SERCA1a E255L and in the presence of 1 mg/mL $C_{12}E_8$ (Fig. 2C, panel A) and 0.2 mg $C_{12}E_8$/mL (Fig. 2C, panel B). As can be seen the major part of ATP hydrolysis was stopped by the addition of EGTA, indicative of calcium-dependent ATPase activity. However, both at the high and low $C_{12}E_8$ concentrations, we observed a decrease of the hydrolytic rate with time suggesting that under these conditions the protein is inactivated during turnover. By addition of lipids (0.05 mg/mL of DOPC) together with 0.2 mg/mL $C_{12}E_8$, we were able to maintain a stable hydrolysis of ATP that was still inhibited by EGTA (Fig. 2C, panel C). Under these conditions, the specific activity at 37°C of the purified PfATP6 was 4.5 µmol of hydrolyzed ATP .min^{-1}. (mg of PfATP6)$^{-1}$, which is about 30 % of the activity of rabbit SERCA1.

The dependence of PfATP6 on Ca^{2+} concentration and pH shows the same characteristics as observed for rabbit SERCA1a (see SI results for Fig. S4 and S5). We then tested the effect of specific inhibitors of mammalian SERCA proteins (Fig. S6) including thapsigargin (Tg), 2, 5-Di(tert-butyl)-1, 4-benzohydroquinone (BHQ), and cyclopiazonic acid (CPA). These assays were performed with the $C_{12}E_8$/DOPC mixture at 25°C, a temperature at which the protein could be more stable. A small degree of inhibition was observed with 1.5 µM Tg, and Ca^{2+} dependent ATP hydrolysis became almost completely inhibited (by about 90 %) with 46.5 µM Tg (Table 1). This means that PfATP6 is significantly less sensitive than rabbit SERCA1a to Tg since the latter is inhibited by concentrations of Tg in the nM range (41)

These differences are well correlated with the observations of Varotti et al. (42) who, on parasites, found a similar difference in the maximum effect of Tg between *Plasmodium* parasites and mammalian cells. According to their results, for *Plasmodium*, 25 µM of Tg were necessary to inhibit Ca^{2+} release in the cytoplasm while 500 nM Tg were sufficient for producing the same effect in mammalian cells. Note also that higher concentrations of thapsigargin with an IC_{50}~2.6 µM are needed to kill chloroquine sensitive parasites (23). Two other SERCA pump inhibitors were then assayed. We observed that 100 µM of BHQ was able to inhibit more than 90 % of the activity of PfATP6 (Fig. S6C and Table 1) and that the addition of 3 µM of CPA resulted in a loss of about 70 % of this activity (Fig. S6D and Table 1), similar to what is observed with rabbit SERCA1a. Another P-type ATPase inhibitor, vanadate, acting as a phosphate analog, was also able to inhibit the activity of this Ca^{2+}-ATPase (Table 1). Therefore, PfATP6 is less sensitive to Tg, but like rabbit

SERCA1a, sensitive to BHQ and CPA that act at slightly different membrane sites on the transporter (43, 44). All these results show that the purified PfATP6 qualitatively behaves the same way as a mammalian SERCA protein.

We then proceeded to test the effect of artemisinin and some derivatives on PfATP6. By addition of 10 µM artemisinin, we were not able to detect inhibition (whatever the temperature in the range of 20-37°C), since more than 90 % of the activity was conserved after addition of this drug to PfATP6 (Fig. 2C, panel E and Table 1), while under these conditions PfATP6 was previously reported to be completely inhibited (23). We also tested lower and higher concentrations of artemisinin (1 to 100 µM for artemisinin and 1 to 500 µM for artemisone), but were never able to demonstrate any effect on PfATP6 dependent Ca^{2+}-ATPase activity (data not shown).

As was done with SERCA1a E255L, we also checked the effect of artemisinin in the presence of iron (10 µM Fe^{2+}) by comparing the effect with that obtained in the presence of iron alone (Fig. S7B). This was carried out by preincubating PfATP6 with iron together with artemisinin before triggering the reaction. This does not enhance the effect of this drug since no significant inhibition was observed (Fig. S7C and Table 1). In addition, other artemisinin derivatives were also tested: artemisone, which was also used in the oocyte tests (25), and artesunate (Fig. 7D and 7E). The use of these derivatives did not inhibit ATPase activity of PfATP6.

One of the differences between our ATPase assays and those done with oocytes is the presence of detergent. Consequently, as the detergent could interfere with artemisinin drugs, the protein was relipidated and detergent was completely removed using Bio-beads (Fig. 3A). Relipidated PfATP6 was then submitted to the same type of inhibition assays at 37°C but without any detergent in solution (Fig. 3B and Table 1). Again, artemisone, was not able to inhibit PfATP6 even in presence of iron. These results clearly show that under our conditions, the purified PfATP6 enzyme is not inhibited by artemisinin and its derivatives.

Concluding comments

The *Xenopus* oocyte was initially chosen as an expression system for the mutated E255L SERCA1 and for PfATP6. Oocyte membranes were then used to test the action of artemisinin (23, 25). The oocyte membrane is very complex, with hundreds of other proteins being present together with the expressed protein. These other putative proteins or proteolipid components could interact with PfATP6 or with the tested drug, which could thus be required for activity at its target. In our expression system the proteins are purified- and thus available for future structural studies, and clearly identified by specific antibodies but no direct effect of artemisinin was found on the detergent-solubilized enzymes or even on the lipid-reconstituted PfATP6.

Many puzzling facts come to mind when trying to pinpoint the target of artemisinin. For instance antimalarial activity of artemisinin is sensitive to steric effect and different derivatives do not have the same inhibition ability. Nevertheless, enantiomers of artemisinin are still effective in killing parasites. This is surprising because if a specific protein binding site is targeted, the stereospecificity should appear as an important point (9). Clearly artemisinin is affecting Ca^{2+} homeostasis as demonstrated e.g. with Ca^{2+}-sensitive dyes (see e.g. (45)). However this effect (rise of cytosolic Ca^{2+}) was also observed after thapsigargin addition suggesting an intracellular target distinct from the endoplasmic reticulum (45). On the other hand, after artemisinin addition, thapsigargin could no longer elicit Ca^{2+} release (45). In other experiments, artemisinin was shown to induce swelling of mitochondria and to interfere with mitochondrial electron transport in a yeast model (46 and references therein) and it was suggested that an activated species of artemisinin could depolarize the mitochondrial membrane. However, this was not observed in *Toxoplasma* exposed to artemisinin (20, 21). Since mitochondria are also a site of Ca^{2+} storage, this may still be related to the Ca^{2+} homeostasis effect but it is by no means the only possible mechanism of action.

In more direct investigations of the target it was shown that activated artemisinin formed covalent adducts with four major membrane-associated proteins but only one of them was identified turning out to be an homolog of the Translationnally Controlled Tumor Protein with a still unknown function (47, 48). In future experiments it will be important to reconcile findings on the mechanisms of action of artemisinins obtained in apicomplexan parasites and in genetics studies, with findings from heterologous expression studies and with the present results to reassess the target of artemisinin. The present data do not favor a direct action of artemisinins on PfATP6, but artemisinin may need some transformations before becoming active or it could act indirectly on PfATP6 after binding to another protein. Alternatively, the drug may act on other proteins involved in Ca^{2+} homeostasis. However, we note that we have described a system that has potential for high throughput screening with novel classes of inhibitor acting against a key parasite transport protein.

Materials and Methods

The Materials and Methods describing various protocols are presented in the Supporting Information. These protocols are related to: plasmid constructions, yeast transformation and selection of individual clones, expression of SERCA1a-E255L in Fernbach flasks, expression of PfATP6 in fermentor, procedure for solubilization and batch purification of PfATP6 by streptavidin-Sepharose chromatography, protein estimation and Ca^{2+}-ATPase quantification, the SDS-PAGE and western-blotting, lipids preparation and detergent removal and relipidation.

ATPase activity measurement

ATPase activity was assayed using a spectrophotometric method as described (49, 50). In general, from 1 to 10 µg of proteins was used in 2 mL of reaction buffer (50 mM Tes-Tris pH 7.5, 0.1 M KCl, 5 mM ATP, 6 mM $MgCl_2$, 0.3 mM NADH, 1 mM phosphoenolpyruvate, 0.1 mg/mL of lactate dehydrogenase, 0.1mg/mL of pyruvate kinase containing 0.1 mM Ca^{2+} and 0.2:0.05 mg/mL $C_{12}E_8$:DOPC). Changes in reaction conditions, detergents, amount of proteins, variations in reaction temperature are indicated in the figure legends. The reaction was started by addition of the protein to the medium and stopped by addition of a final concentration of 750 µM EGTA. The difference between the slopes obtained before and after addition of EGTA is considered to be due to the Ca^{2+}-ATPase activity. To obtain the specific activity, the concentration of Ca^{2+}-ATPase (SERCA1a E255L or PfATP6) was determined from Coomassie blue stained gels after SDS-PAGE.

The inhibition assays were performed in the general conditions described above except with vanadate. The drugs used (stock solutions at 1.5 mM and 15 mM Tg, 100 mM BHQ, 3 mM CPA, 10 mM artemisinin, 10 mM artemisone and 10 mM artesunate) were dissolved in DMSO. All the inhibition assays were performed by addition of 2 µL of each drug solution. The protein was preincubated with these drugs for a few minutes (but longer incubations were not more efficient) before ATP addition which triggers the start of the reaction (as explained in the figure legends).

Acknowledgements

We are grateful to Dr. Jean-Marc Verbavatz for freeze-fracture electron microscopy data, to Dr. Manuel Garrigos for inhibition assays with vanadate and to Birte Nielsen for expert technical assistance. We thank Cedric Montigny in particular for his help in the fermentor story. D. C. is grateful to Leyla Bustamante-Rodriguez and to Dr. Charles Woodrow for interesting discussion. We thank Drs Bertrand Arnou, Anthony Lee, Steven Karlish, Maïté Paternostre, Anne Robert and Philippe Champeil for many helpful suggestions. This work was supported by the Danish Medical Research Council, the Danish Natural Science Research Council (Center for Structural Biology, the Dansync program), the Aarhus University Research Foundation, the Novo-Nordic Foundation (Denmark), by the CEA and the CNRS (France). SK is funded by the Commission of the European Communities ANTIMAL Grant: 018834 and Wellcome Trust Grant 074395/Z/04/Z. We thank Professor Richard Haynes for artemisone.

References

1. White, N. J. (2008) *Qinghaosu (artemisinin): the price of success.* Science **320,** 330-4.

2. Fidock, D. A., Eastman, R. T., Ward, S. A. & Meshnick, S. R. (2008) *Recent highlights in antimalarial drug resistance and chemotherapy research.* Trends Parasitol **24,** 537-44.
3. Noedl, H.*, et al.* (2008) *Evidence of artemisinin-resistant malaria in western Cambodia.* N Engl J Med **359,** 2619-20.
4. ter Kuile, F., White, N. J., Holloway, P., Pasvol, G. & Krishna, S. (1993) *Plasmodium falciparum: in vitro studies of the pharmacodynamic properties of drugs used for the treatment of severe malaria.* Exp Parasitol **76,** 85-95.
5. Woodrow, C. J., Haynes, R. K. & Krishna, S. (2005) *Artemisinins.* Postgrad Med J **81,** 71-8.
6. Burk, O.*, et al.* (2005) *Antimalarial artemisinin drugs induce cytochrome P450 and MDR1 expression by activation of xenosensors pregnane X receptor and constitutive androstane receptor.* Mol Pharmacol **67,** 1954-65.
7. Haynes, R. K.*, et al.* (2006) *Artemisone--a highly active antimalarial drug of the artemisinin class.* Angew Chem Int Ed Engl **45,** 2082-8.
8. Meshnick, S. R., Taylor, T. E. & Kamchonwongpaisan, S. (1996) *Artemisinin and the antimalarial endoperoxides: from herbal remedy to targeted chemotherapy.* Microbiol Rev **60,** 301-15.
9. O'Neill, P. M. (2005) *The therapeutic potential of semi-synthetic artemisinin and synthetic endoperoxide antimalarial agents.* Expert Opin Investig Drugs **14,** 1117-28.
10. Avery, M. A., Gao, F., Chong, W. K., Mehrotra, S. & Milhous, W. K. (1993) *Structure-activity relationships of the antimalarial agent artemisinin. 1. Synthesis and comparative molecular field analysis of C-9 analogs of artemisinin and 10-deoxoartemisinin.* J Med Chem **36,** 4264-75.
11. Kumar, N. & Zheng, H. (1990) *Stage-specific gametocytocidal effect in vitro of the antimalaria drug qinghaosu on Plasmodium falciparum.* Parasitol Res **76,** 214-8.
12. Kombila, M.*, et al.* (1997) *Light microscopic changes in Plasmodium falciparum from Gabonese children treated with artemether.* Am J Trop Med Hyg **57,** 643-5.
13. Vyas, N., Avery, B. A., Avery, M. A. & Wyandt, C. M. (2002) *Carrier-mediated partitioning of artemisinin into Plasmodium falciparum-infected erythrocytes.* Antimicrob Agents Chemother **46,** 105-9.
14. Gu, H. M., Warhurst, D. C. & Peters, W. (1984) *Uptake of [3H] dihydroartemisinine by erythrocytes infected with Plasmodium falciparum in vitro.* Trans R Soc Trop Med Hyg **78,** 265-70.
15. Olliaro, P. L., Haynes, R. K., Meunier, B. & Yuthavong, Y. (2001) *Possible modes of action of the artemisinin-type compounds.* Trends Parasitol **17,** 122-6.

16. Ittarat, W., Sreepian, A., Srisarin, A. & Pathepchotivong, K. (2003) *Effect of dihydroartemisinin on the antioxidant capacity of P. falciparum-infected erythrocytes.* Southeast Asian J Trop Med Public Health **34,** 744-50.
17. Golenser, J., Waknine, J. H., Krugliak, M., Hunt, N. H. & Grau, G. E. (2006) *Current perspectives on the mechanism of action of artemisinins.* Int J Parasitol **36,** 1427-41.
18. Zhang, G., Guan, Y., Zheng, B., Wu, S. & Tang, L. (2008) *No PfATPase6 S769N mutation found in Plasmodium falciparum isolates from China.* Malar J **7,** 122.
19. Hoppe, H. C.*, et al.* (2004) *Antimalarial quinolines and artemisinin inhibit endocytosis in Plasmodium falciparum.* Antimicrob Agents Chemother **48,** 2370-8.
20. Nagamune, K., Moreno, S. N. & Sibley, L. D. (2007) *Artemisinin-resistant mutants of Toxoplasma gondii have altered calcium homeostasis.* Antimicrob Agents Chemother **51,** 3816-23.
21. Nagamune, K., Beatty, W. L. & Sibley, L. D. (2007) *Artemisinin induces calcium-dependent protein secretion in the protozoan parasite Toxoplasma gondii.* Eukaryot Cell **6,** 2147-56.
22. Nagamune, K. & Sibley, L. D. (2006) *Comparative genomic and phylogenetic analyses of calcium ATPases and calcium-regulated proteins in the apicomplexa.* Mol Biol Evol **23,** 1613-27.
23. Eckstein-Ludwig, U.*, et al.* (2003) *Artemisinins target the SERCA of Plasmodium falciparum.* Nature **424,** 957-61.
24. Toovey, S., Bustamante, L. Y., Uhlemann, A. C., East, J. M. & Krishna, S. (2008) *Effect of artemisinins and amino alcohol partner antimalarials on mammalian sarcoendoplasmic reticulum calcium adenosine triphosphatase activity.* Basic Clin Pharmacol Toxicol **103,** 209-13.
25. Uhlemann, A. C.*, et al.* (2005) *A single amino acid residue can determine the sensitivity of SERCAs to artemisinins.* Nat Struct Mol Biol **12,** 628-9.
26. Toyoshima, C. & Nomura, H. (2002) *Structural changes in the calcium pump accompanying the dissociation of calcium.* Nature **418,** 605-11.
27. Jambou, R.*, et al.* (2005) *Resistance of Plasmodium falciparum field isolates to in-vitro artemether and point mutations of the SERCA-type PfATPase6.* Lancet **366,** 1960-3.
28. Cojean, S., Hubert, V., Le Bras, J. & Durand, R. (2006) *Resistance to dihydroartemisinin.* Emerg Infect Dis **12,** 1798-9.
29. Ferreira, I. D.*, et al.* (2008) *Plasmodium falciparum from Para state (Brazil) shows satisfactory in vitro response to artemisinin derivatives and absence of the S769N mutation in the SERCA-type PfATPase6.* Trop Med Int Health **13,** 199-207.
30. Krishna, S., Bustamante, L., Haynes, R. K. & Staines, H. M. (2008) *Artemisinins: their growing importance in medicine.* Trends Pharmacol Sci **29,** 520-7.

31. Krishna, S.*, et al.* (2001) *Expression and functional characterization of a Plasmodium falciparum Ca2+-ATPase (PfATP4) belonging to a subclass unique to apicomplexan organisms.* J Biol Chem **276,** 10782-7.
32. Jidenko, M., Lenoir, G., Fuentes, J. M., le Maire, M. & Jaxel, C. (2006) *Expression in yeast and purification of a membrane protein, SERCA1a, using a biotinylated acceptor domain.* Protein Expr Purif **48,** 32-42.
33. Jidenko, M.*, et al.* (2005) *Crystallization of a mammalian membrane protein overexpressed in Saccharomyces cerevisiae.* Proc Natl Acad Sci U S A **102,** 11687-91.
34. Marchand, A.*, et al.* (2008) *Crystal structure of D351A and P312A mutant forms of the mammalian sarcoplasmic reticulum Ca(2+) -ATPase reveals key events in phosphorylation and Ca(2+) release.* J Biol Chem **283,** 14867-82.
35. Andersen, J. P., Sørensen, T. L., Povlsen, K. & Vilsen, B. (2001) *Importance of transmembrane segment M3 of the sarcoplasmic reticulum Ca2+-ATPase for control of the gateway to the Ca2+ sites.* J Biol Chem **276,** 23312-21.
36. Haviv, H.*, et al.* (2007) *Stabilization of Na(+),K(+)-ATPase purified from Pichia pastoris membranes by specific interactions with lipids.* Biochemistry **46,** 12855-67.
37. Sharp, P. M. & Li, W. H. (1987) *The codon Adaptation Index--a measure of directional synonymous codon usage bias, and its potential applications.* Nucleic Acids Res **15,** 1281-95.
38. Zhang, H., Howard, E. M. & Roepe, P. D. (2002) *Analysis of the antimalarial drug resistance protein Pfcrt expressed in yeast.* J Biol Chem **277,** 49767-75.
39. Hedfalk, K., Pettersson, N., Oberg, F., Hohmann, S. & Gordon, E. (2008) *Production, characterization and crystallization of the Plasmodium falciparum aquaporin.* Protein Expr Purif **59,** 69-78.
40. Tan, W., Gou, D. M., Tai, E., Zhao, Y. Z. & Chow, L. M. (2006) *Functional reconstitution of purified chloroquine resistance membrane transporter expressed in yeast.* Arch Biochem Biophys **452,** 119-28.
41. Sagara, Y. & Inesi, G. (1991) *Inhibition of the sarcoplasmic reticulum Ca2+ transport ATPase by thapsigargin at subnanomolar concentrations.* J Biol Chem **266,** 13503-6.
42. Varotti, F. P., Beraldo, F. H., Gazarini, M. L. & Garcia, C. R. (2003) *Plasmodium falciparum malaria parasites display a THG-sensitive Ca2+ pool.* Cell Calcium **33,** 137-44.
43. Obara, K.*, et al.* (2005) *Structural role of countertransport revealed in Ca(2+) pump crystal structure in the absence of Ca(2+).* Proc Natl Acad Sci U S A **102,** 14489-96.

44. Moncoq, K., Trieber, C. A. & Young, H. S. (2007) *The molecular basis for cyclopiazonic acid inhibition of the sarcoplasmic reticulum calcium pump.* J Biol Chem **282,** 9748-57.
45. de Pilla Varotti, F.*, et al.* (2008) *Synthesis, antimalarial activity, and intracellular targets of MEFAS, a new hybrid compound derived from mefloquine and artesunate.* Antimicrob Agents Chemother **52,** 3868-74.
46. Li, W.*, et al.* (2005) *Yeast model uncovers dual roles of mitochondria in action of artemisinin.* PLoS Genet **1,** e36.
47. Asawamahasakda, W., Ittarat, I., Pu, Y. M., Ziffer, H. & Meshnick, S. R. (1994) *Reaction of antimalarial endoperoxides with specific parasite proteins.* Antimicrob Agents Chemother **38,** 1854-8.
48. Bhisutthibhan, J.*, et al.* (1998) *The Plasmodium falciparum translationally controlled tumor protein homolog and its reaction with the antimalarial drug artemisinin.* J Biol Chem **273,** 16192-8.
49. Falson, P.*, et al.* (1997) *The cytoplasmic loop between putative transmembrane segments 6 and 7 in sarcoplasmic reticulum Ca2+-ATPase binds Ca2+ and is functionally important.* J Biol Chem **272,** 17258-62.
50. Møller, J. V., Lind, K. E. & Andersen, J. P. (1980) *Enzyme kinetics and substrate stabilization of detergent-solubilized and membraneous (Ca2+ + Mg2+)-activated ATPase from sarcoplasmic reticulum. Effect of protein-protein interactions.* J Biol Chem **255,** 1912-20.

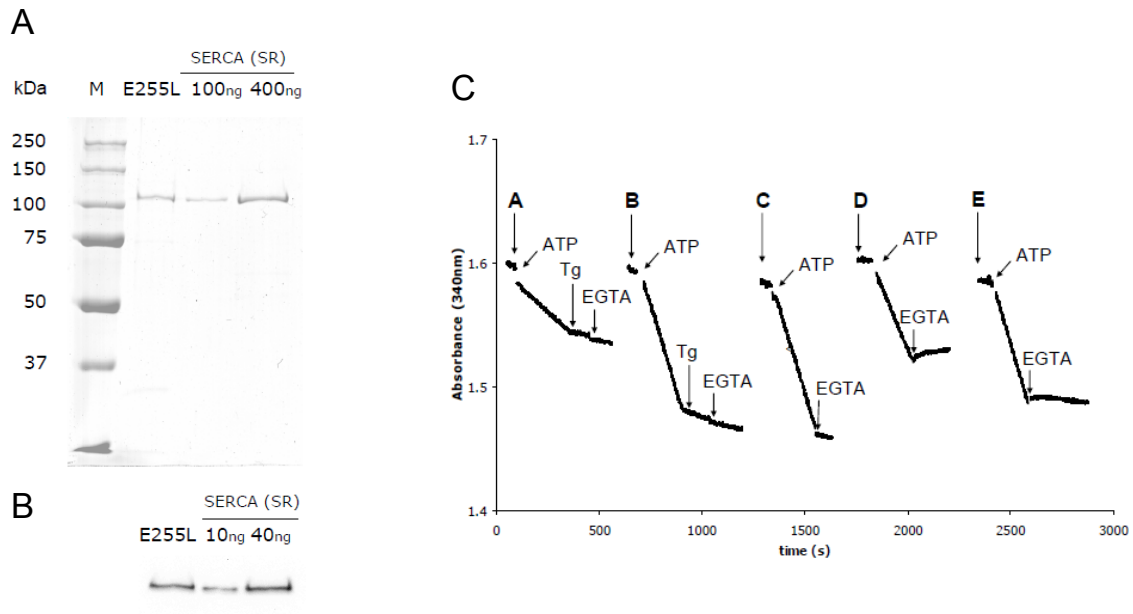

Fig. 1 Characteristics of purified SERCA1a-E255L mutant: purification and ATPase activity.

A. SDS-PAGE followed by Coomassie Blue staining. 7.5 µL of the eluted fraction was loaded (E255L) and to quantify the amount of SERCA-E255L in this sample, 100 and 400 ng of the wild type SERCA (SR) preparation were loaded. M is the molecular mass markers lane. *B Western-blot analysis with anti-SERCA1a antibodies*. 0.75 µL of the eluted fraction (E255L) and 10 and 40 ng of the SERCA (SR) preparation were loaded. *C. ATPase activities at 25°C of SERCA1a-E255L in $C_{12}E_8$ (1 mg/mL) and $C_{12}E_8$/DOPC (0.2/0.05 mg/mL) and inhibition assays with thapsigargin and artemisinin*. Purified SERCA1a-E255L was diluted to 1.5 µg/mL in the ATPase assay medium (50 mM Tes-Tris pH 7.5, 0.1 M KCl, 5 mM ATP, 6 mM $MgCl_2$, 0.3 mM NADH, 1 mM phosphoenolpyruvate, 0.1 mg/mL of lactate dehydrogenase, 0.1 mg/mL of pyruvate kinase). The medium contained also 125µM Ca^{2+} and either $C_{12}E_8$ 1 mg/mL (panel **A**) or $C_{12}E_8$/DOPC 0.2/0.05 mg/mL (panels **B**, **C**, **D** and **E**) and hydrolytic activity was monitored continuously with a coupled enzyme system by recording NADH oxidation at 340 nm. The reactions were triggered by addition of 5 mM ATP and stopped by the addition of 750 µM EGTA. The inhibition effect of 1.5 µM thapsigargin (Tg) was first checked (panels **A** and **B**) and then the effect of artemisinin was tested by preincubation of the protein with 10 µM artemisinin (**C**) and 10 µM Fe^{2+} + 10 µM artemisinin (panel **E**). The effect of Fe^{2+} + DMSO was controlled by addition of 10 µM Fe^{2+} + 2 µL DMSO (panel **D**).

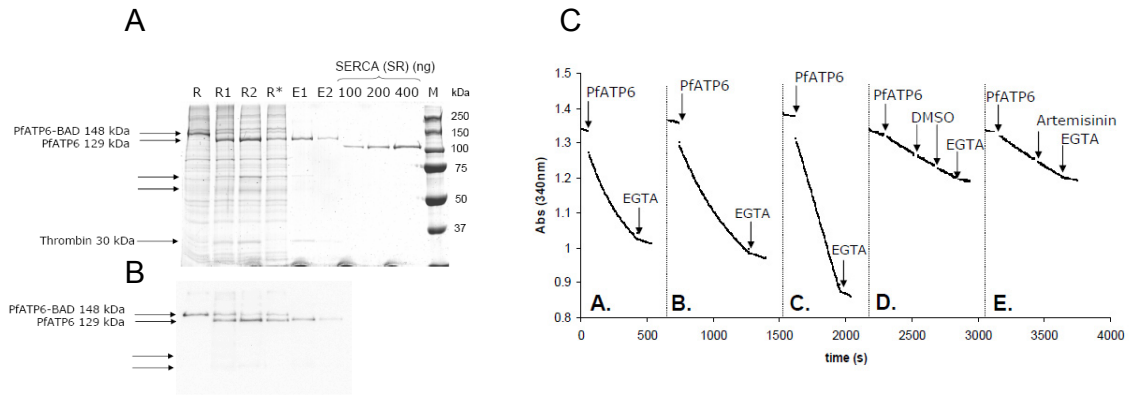

Fig. 2 Characteristics of purified PfATP6 protein: purification and ATPase activity.

A. SDS-PAGE followed by Coomassie blue staining. Except for the molecular mass marker (**M**) and the SERCA (SR) fractions, 7.5 µL of each fraction were loaded. To check the action of thrombin in the cleavage of PfATP6-BAD (% of cleavage) and the efficiency of elution, the resin before (**R**), after the first incubation with thrombin (about 60 % of cleavage, **R1**) and after the second one (about 90 % of cleavage, **R2**) and also the resin after elution (**R***) were analysed. To quantify the amount of PfATP6 recovered after the first (**E1**) and the second (**E2**) elution, 100, 200 and 400 ng of the wild type SERCA (SR) preparation were loaded. An approximate concentration of 30 µg/mL is determined for the first elution and of 10 µg/mL for the second elution. 20 % of PfATP6 were still retained on the resin (Lane R*). The arrows indicate potential unspecific cleavages of PfATP6. *B. Western blot analysis with anti-PfATP6 antibodies*. The same fractions as in A were analyzed but only 0.75 µL were loaded in each lane. Cleavage products of PfATP6 are hardly detectable (indicated by the arrows). *C. ATPase activities*. They were measured at 37°C and pH 7.5 with 5 µg of proteins in 2 mL of assay buffer (see legend to Fig. 1). The reaction was triggered by addition of purified PfATP6 into the medium and stopped by addition of a final concentration of 750 µM EGTA. The reactions were carried out in the presence of: panel **A**, $C_{12}E_8$ (1 mg/mL); panel **B**, $C_{12}E_8$ (0.2 mg/mL), and panel **C,** $C_{12}E_8$/DOPC (0.2/0.05 mg/mL). Panel **E**, the effect of 10 µM artemisinin was tested as followed: measurement at 25°C and pH 7.5, with 3 µg of protein in the same buffer as in **A**, **B** and **C**. The reaction was triggered by addition of ATP into the medium. The reaction was carried out in the presence of $C_{12}E_8$/DOPC (0.2/0.05 mg/mL). Panel **D**, control with DMSO. The rapid decrease in absorption just after the addition of PfATP6 was due to a dilution effect.

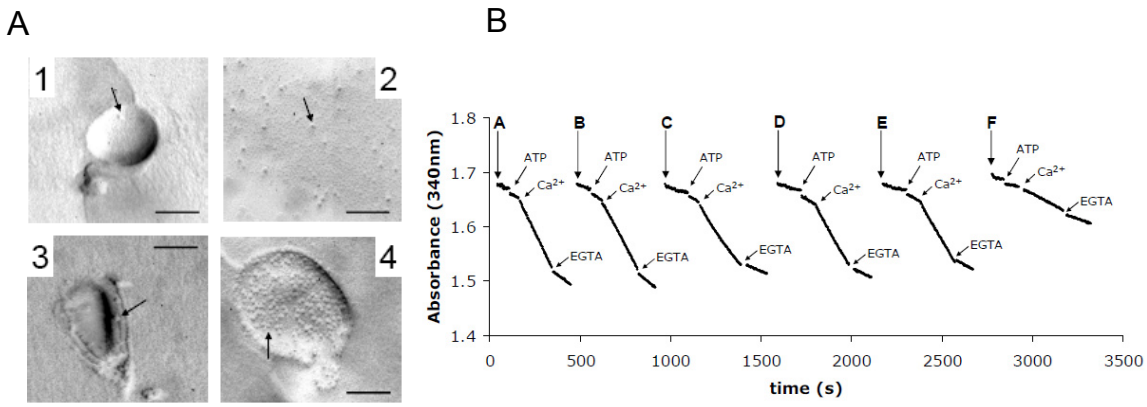

Fig. 3 Effect of artemisone and thapsigargin on the ATPase activity of relipidated PfATP6.

A. Relipidated PfATP6 with EYPC. Freeze-fracture electron microscopy analysis of relipidated PfATP6. Bar = 100nm. The sample is heterogenous and contains different lipid structures: vesicles with one membrane protein (**1**), large membranous structures with dispersed proteins (**2**), multilamellar vesicles (**3**) and vesicles with membrane proteins clusters (**4**). Each arrow shows one molecule of PfATP6. *B. ATPase activities*. They were performed

B. ATPase activities. They were performed with 1.75 µg/mL of reconstituted PfATP6 at 37°C. They were triggered by successive additions of 5 mM ATP and 100 µM of free Ca^{2+}, and stopped by the addition of 750 µM EGTA. Artemisone was added with 2 µL of solutions at 10 mM or 100 mM prepared in DMSO. The effects of artemisone were tested by preincubation of the protein in 150 µM EGTA with 10 µM artemisone (panel **B**), 10 µM Fe^{2+} + 2 µL of DMSO (panel **C**), 10 µM Fe^{2+} + 10 µM artemisone (panel **D**), 10 µM Fe^{2+} + 100 µM artemisone (panel **E**) before starting the reaction. The effect of 15 µM thapsigargin was tested in the same conditions (panel **F**). The effect of DMSO and Fe^{2+} + DMSO was controlled by addition of 2 µL of DMSO (panel **A**) and 10 µM Fe^{2+} + 2 µL DMSO (panel **C**) to the protein before starting the reaction.

	Control DMSO	Thapsigargin (46.5µM) or (*15µM*)	BHQ (100µM)	CPA (3.0µM)	Vanadate (100µM)	Artemisinin (10µM) or *artemisone (10µM)*	Fe^{2+} (10µM)	Fe^{2+} (10µM) +		
								artemisinin (10µM)	artemisone (10 or *100* µM)	artesunate (10µM)
1. Specific activity (µmol of ATP. min^{-1} /mg of PfATP6)	1.36	0.11	0.1	0.42		1.26	0.99	0.93	1.05	0.95
Percentage of activity (%)	100	8	7	31	50[a]	93	73	68	77	70
2. Specific activity (µmol of ATP. min^{-1} /mg of PfATP6)	2.8	*0.3*				2.7	~2[b]		2.5 / 2.2	
Percentage of activity (%)	100	*10*				96	~71[b]		89 / *79*	

Table 1 : Summary of the effect of specific inhibitors of SERCA and artemisinin drugs on the ATPase activities of PfATP6 measured as described in Fig. 3, S6 and S7.

Table 1: **Summary of the effect of specific inhibitors of SERCA and artemisinin drugs on the ATPase activities of PfATP6 measured as described in Fig. 3, S6 and S7.**

1. Activities measured with solubilized PfATP6 at 25°C. [a]This percentage was determined from ATPase activities measured at 37°C. The activity of the protein without vanadate was 3 µmol ATP.min-1. mg of PfATP6. 2. Activities measured with relipidated PfATP6 at 37°C. [b]The ATP hydrolysis rate was not constant in this condition. This value was calculated from the initial rate as if it was linear.

Supporting Information

SI Materials and Methods

Chemicals. All chemical products were purchased from Sigma-Aldrich (Saint-Quentin Fallavier, France) unless specified otherwise. PfuTurbo® DNA polymerase was from Stratagene and Electroelution G-capsules from G-Biosciences (AGRO-BIO, La Ferté Saint Aubin, France). Phusion® High fidelity polymerase was from Finnzymes (Ozyme, Saint Quentin en Yvelines, France). Restriction and modification enzymes were from New England Biolabs (Ozyme, Saint Quentin en Yvelines, France). High activity bovine thrombin was from Calbiochem (VWR International, Fontenay sous Bois, France), the Streptavidin Sepharose™ High Performance was purchased from GE Healthcare Biosciences AB (Orsay, France). All products for yeast and bacteria cultures were purchased from Difco (BD Biosciences, Le Pont de Claix, France). 1,2-Dioleoyl-sn-Glycero3-Phosphocholine (DOPC) was from Avanti Polar Lipids (Alabaster, AL, USA), n-dodecyl β-D-maltoside (DDM) was from Anatrace (Maumee, OH, USA) and octaethylene glycol mono-n-dodecyl ether ($C_{12}E_8$) was purchased from Nikkol Chemical (Tokyo, Japan). Precision protein standards were from Bio-Rad (Hercules, CA, USA). Immobilon-P membranes were from Millipore (Bedford, MA, USA). Avidin–peroxidase conjugate was from Sigma.

Plasmid constructions. The expression plasmid pYeDP60-SERCA1a-BAD was used for the constructions described in this work (Jidenko et al., 2006). The BAD cDNA fragment is a 300 bp fragment issued from the *Klebsiella pneumoniae* C-terminal oxaloacetate decarboxylase gene and it was kindly provided by R. Kaback, UCLA, USA.

E255L mutant : Overlap extension PCR with PfuTurbo DNA polymerase was utilized for the substitution of Glu^{255} with leucine in the rabbit SERCA1a cDNA. The 3' promoter primer sequence (5') CGC AAA CAC AAA TAC ACA CAC TAA ATT CC (3') was complementary to the 3' end of the promoter CYC1, located upstream the cDNA of SERCA1a. The Leu c primer sequence (5') AG CTG CTC CCC GAA **CAG** ATC CAG CTT CTG CT (3') was complementary to the region of SERCA1a encoding the 255^{th} amino acid of SERCA1a and mutated in order to code for a leucine (in bold). The Leu primer is complementary to Leu c. The BssHII 3' primer (5') GA TCT CAT CGT AGG ACT GCA GGT ATT CCA CGA TCT (3') was complementary to a region in 3' of a BssHII restriction site (internal site at + 2038 in SERCA1a). Two DNA fragments (818 bp and 1338 bp) were amplified, gel-purified, combined to act as template, and PCR amplified in a hybridization-extension reaction. The resultant mutated fragment (2130 bp) was digested with EcoRI (cut on the plasmid upstream the cDNA of SERCA1a) and BssHII, gel-purified, inserted into electroeluted digested pYeDP60-SERCA1a-BAD, and transformed into *Escherichia coli* JM109.

PfATP6wt and PfATP6co: The plasmid pYeDP60-SERCA1a-BAD was mutated to remove a BamHI restriction site (internal site at +3313 in 3' of the region encoding BAD) by

substitution of a C to a A. This new plasmid is called pYeDP60-SERCA1a-BAD_2.

PfATP6wt: The plasmid XA6A.40 contains the wild type sequence of PfATP6 (Pfatp6wt) EMBL: X71765, Tanabe, J. Cell Science, 1993). In order to subclone Pfatp6wt into pYeDP60-Serca1a-BAD_2, a previous overlap extension PCR was performed with Phusion® High fidelity polymerase on the plasmid XA6A.40 to add an EcoRI and a BamHI restriction sites in 5' and 3' of the sequence of PfATP6wt and to remove an unsuitable EcoRI restriction site located in the middle of the Pfatp6 sequence. The 5' Pfatp6wt primer sequence (5') CTA AAT TAC CGA ATT CTA GT**A TGG AAG AGG TTA TTA AGA ATG CTC** (3') was complementary to the 3' end of the promoter CYC1 in pYeDP60 containing an EcoRI restriction site (underlined) and the 5' end of Pfatp6 (bold). The XA6A.40 2079 c primer sequence (5') G TTT CCT TTC TCT AGT **A**AA TTC AAT AAT TTT TAT TTG (3') was complementary to a region containing a EcoRI restriction site (internal site at +2075 in Pfatp6, underlined) and mutated inside the restriction site, on the position 2079 from a G to a A (in bold) to remove it. The XA6A.40 2079 primer sequence was complementary to which of XA6A.40 2079 c. The 3' Pfatp6wt-tcs-bad primer (5') CGT ***GGA TCC TCT TGG AAC CAA*** **ACC ACC** ATC AAT TTT AAT TTT CTT GGT TCT TTG (3') was complementary to a region in 3' of the cDNA of Pfatp6, two codons coding for a glycine (in bold), a sequence coding for the thrombin cleavage site (in italic) including a BamHI restriction site (dotted line). Two DNA fragments (2133 bp and 1656 bp) were PCR amplified in a hybridization-extension reaction as described above. The resultant mutated gene of 3752 bp was digested with EcoRI and BamHI, gel-purified, inserted into electroeluted digested pYeDP60-SERCA1a-BAD_2, and treated as described for the E255L mutant.

PfATP6co: The plasmid YA6 contains the codon optimized sequence of PfATP6 (Pfatp6co) for the expression in *S. cerevisiae* (Geneart AG, Regensburg, Germany). In order to subclone Pfatp6co into pYeDP60-Serca1a-BAD_2, a previous PCR was performed on the plasmid YA6 for adding restriction sites (EcoRI and BamHI) in 5' and 3' of the sequence of PfATP6co. The 5' Pfatp6co primer sequence (5') CTA AAT TAC CGA ATT C TA GT**A TGG AAG AAG TTA TTA AAA ACG CTC** was complementary to the 3' end of the promoter CYC1 in pYeDP60 containing an EcoRI restriction site (underlined) and the 5' end of Pfatp6 (bold). The 3' Pfatp6co-tcs-bad primer (5') CGT ***GGA TCC TCT TGG AAC CAA*** **ACC ACC** ATC AAT CTT AAT CTT TTT AGT TCT TTG (3') was complementary to a region in 3' of the cDNA of Pfatp6co with the same additional sequences as for the wild sequence. The resultant fragment of 3752 bp was treated as described for the wild sequence.

The recombinant plasmids were colony-purified using Wizard® Plus SV Minipreps DNA Purification System (Promega, Charbonnières les Bains, France). All these contructs were checked by DNA sequencing.

Yeast transformation and selection of individual clones. The *S. cerevisiae* yeast strain W303.1b/Gal4 (*a*, *leu2*, *his3, trp1::TRP1-GAL10-GAL4, ura3, ade2-1, can*^{r}, *cir*$^{+}$) was the same as previously described (Lenoir et al., 2002). Transformation was performed according to the lithium acetate/single-stranded carrier DNA/PEG method (Gietz et al., 1995). Growth conditions and criteria for expression of the Ca^{2+}-ATPase were carried out as described for the test of individual clones and for the expression on minimal medium (Centeno et al., 1994; Lenoir et al., 2002). A colony streaked onto a minimum medium storage plate was toothpicked into minimum medium (0.1 % bactocasamino acids, 0.7 % yeast nitrogen base, 2 % glucose (w/v), 20 µg/mL adenine) and grown at 28°C during 24 h with shaking (200 rpm). For each assay, 500 µL of the minimum medium precultures were centrifuged 5 min at 4°C and 1000xg_{av} (rotor AM2.19, Jouan MR22i) and resuspended in 5 mL of minimum medium with 2 % galactose instead of glucose to induce expression. These cultures were incubated at 28°C during 18 h with shaking. For each culture, 4 OD_{600nm} were centrifuged 5 min, at 4°C and 8000xg_{av}. After washing with water, the pellets were resuspended in cooled 2 % TCA. Glass beads were added and the suspensions were mixed with a vortex at maximal speed for 8 min at room temperature to break the cells. The tubes were then placed on ice and glass beads were sedimented. The supernatant was kept on ice. After 3 washing with 2 % TCA, all the collected supernatants were gathered. The resulting solution was kept 15 min on ice for protein precipitation. Then, the samples were centrifuged 15 min, at 4°C and 30000xg_{av}. The pellets were resuspended in 100 µL of 50 mM Tris-Cl pH 7.5. These samples were analyzed by Western blotting in order to choose the best expressing clones.

Expression of SERCA1a-E255L in Fernbach flasks. Growth conditions of yeast and induction of the expression of the mutant were the same as previously published for native SERCA1a expressed in yeast (Jidenko et al., 2006).

Growth of yeast cells and large scale expression of PfATP6 using a fermentor (Techfors-S apparatus, INFORS HT, Massy, France)**.** This method is based on the one developed for SERCA1a in Fernbach flasks with the following modifications: twenty liters of YPGE2X were inoculated with 1.2 liters of a culture at exponential phase in minimum medium (~6.10^6 cells/mL). Culture was performed at 28°C under high aeration (1 vol air per vol per min; stirring rate 300 rpm) at the beginning of the culture and then regulated to maintain a dioxygen saturation of 20 % until the cell density reached 3.10^8 cells/mL. The culture was then cooled to 18°C, the regulation of dioxygen saturation was stopped, stirring rate was maintained at 300 rpm but aeration was lowered to 0.15 vol air per vol per min. Thirty minutes later, a solution of sterile galactose (500 g/L) was added to a final concentration of 20 g/L and the culture was continued for 13 h (Pompon et al., 1996).

Preparation of light membrane fractions. The light membrane fraction (LM) was obtained after breaking yeast cells with glass beads and differential centrifugation of the crude extract (CE). They were finally resuspended in Hepes-sucrose buffer (20 mM Hepes-Tris (pH 7.5), 0.3 M sucrose, 0.1 mM $CaCl_2$, 1 mM PMSF) at a final volume corresponding to 0.5 ml per g of the initial yeast pellet. The membranes can be stored at -80°C until use. The amount of the protein of interest is estimated by Western blot analysis using the appropriate antibody.

Solubilization and batch purification of PfATP6 by streptavidin-Sepharose chromatography. The light membrane fraction (LM), suspended in the Hepes-sucrose buffer, was washed twice to remove contaminant and soluble biotinylated proteins (Acetyl-CoA Carboxylase, Pyruvate Carboxylase and Arc1p) by diluting the membranes at 10 mg/ml in a buffer containing 50 mM MOPS-Tris (pH 7), 0.5 M KCl, 20 % glycerol, 1 mM $CaCl_2$, 1 mM β-mercaptoethanol, and 1 mM PMSF. Light membranes were then pelleted at 120,000 g for 90 min at 10°C and the supernatant containing soluble proteins was discarded.

After the second washing step, the pellet was resuspended in the same buffer and solubilized by DDM (30 mg/mL) at a protein concentration of 10 mg/mL. After mixing the solution with a Potter homogenizer and stirring for 5 min at room temperature, non-solubilized material was pelleted by centrifugation at 120,000 g for 45 min at 4°C. All subsequent steps (unless otherwise specified) were then performed at 4°C. The supernatant after the centrifugation step was mixed with streptavidin Sepharose™ High Performance resin at a ratio of 25:1 (v/v), using typically 25 mL of solubilized PfATP6 per mL of resin, and stirred gently overnight at 4°C. The suspension was then pelleted into 50 mL tubes (5 mL maximum of resin / tube) for 10 min at 1000xg_{av} (rotor 11133, SIGMA) and washed, twice with a "high-salt" buffer (50 mM MOPS-Tris (pH 7), 1 M KCl, 20 % glycerol, 1 mM $CaCl_2$, 0.05 % DDM, 1 mM β-mercaptoethanol) (buffer:resin, 10:1 (v:v)), and then twice with a "low salt" buffer (50 mM MOPS-Tris (pH 7), 50 mM KCl, 20 % glycerol, 2.5 mM $CaCl_2$, 0.05 % DDM) (buffer:resin, 10:1 (v:v)). The resin was resuspended in the "low salt" buffer (buffer:resin, 1:1 (v:v)) and thrombin was added (10 U thrombin/mL resin) and the mixture was placed on a wheel and gently stirred at room temperature for 15 min, followed by a second addition of thrombin and stirring for another 15 min. During this step, it was critical to adjust the thrombin concentration and the incubation time to avoid undesired digestions of PfATP6 while keeping a sufficient efficiency of cleavage. To inactivate thrombin, 2.5 mM PMSF was then added, and the solution of resin was transferred into Handee™ Centrifuge columns (Perbio Science France SAS, Brebieres, France). The proteolytically cleaved PfATP6 proteins were eluted from the column by centrifugation (1000 g, 5 min). A second elution was performed by a second centrifugation after the resin resuspension in one volume of low salt buffer (buffer:resin, 1:1 (v:v)). The eluted fractions containing the Ca^{2+}-ATPase were pooled

and glycerol concentration was increased to 40 % before freezing the samples in liquid nitrogen and storage at -80°C.

Protein estimation and Ca^{2+}-ATPase quantification. Protein concentrations were measured by the bicinchoninic acid procedure (Smith et al., 1985) in the presence of 2 % SDS (w/v) with bovine serum albumin as a standard. SERCA1a from rabbit muscle (SR), used as a standard for protein estimation, was prepared as previously described (Champeil et al., 1985). Ca^{2+}-ATPase quantification was performed either by Coomassie blue staining gel after SDS-PAGE or western blot using known amounts of SR as standards.

SDS-PAGE and western-blotting

For SDS-PAGE, samples were mixed with an equal volume of denaturing buffer, heated at 90°C for 2 min and loaded onto a Laemmli-type 8 % (w/v) polyacrylamide gels (Soulie et al., 1998). Amounts of proteins or volumes of initial samples loaded in each well are indicated in the figure legends. After separation by SDS-PAGE, gels were stained with Coomassie blue or proteins were electroblotted onto PVDF Immobilon P membrane (Juul et al., 1995). For each gel, molecular mass markers (Precision Protein standards, Biorad) were loaded.

The western blotting was followed by detection with avidin-peroxidase for the recognition of biotinylated proteins or by immunodetection with either the polyclonal antibody anti-SERCA1a 79B (a gift from A.-M. Lompré, INSERM, France) as previously described (Jidenko et al., 2006).

Immunodetection with anti-PfATP6. For immunodetection with anti-PfATP6 antibody, the polyclonal antibody anti PfATP6 generated in goat from the peptide CQSSNKKDKSPRGINK (the sequence Q to K corresponds to the 574-588 region of PfATP6) was used. Anti PfATP6 antibodies were purchased to BETHYL group. After electroblotting, membrane was blocked for 10 min in PBST (90 mM K_2HPO_4, 10 mM KH_2PO_4 (pH 7.7), 100 mM NaCl, 0.2 % (v/v) Tween 20) containing 5 % powdered skim milk. The primary antibody (1:10000) was then added to the solution and incubated for 1 h at room temperature. The membrane was washed once 10 min in PBST and then incubated with horseradish peroxidase-conjugated secondary rabbit anti-goat antibody (1:10000) in PBST containing 5 % powdered skim milk. After three washes with PBST, 10 min each, detection of proteins is performed with ECL (GE Healthcare, Vélizy, France). The chemiluminescence signal was acquired with a GBox HR 16 apparatus coupled with GeneSnap acquisition software and analyzed with GeneTools analysis software (Syngene, Ozyme, France).

Lipids preparation. Phospholipids (DOPC or EYPC) dissolved in chloroform were dried in a stream of nitrogen. Dried DOPC was then dissolved at 5 mg/mL in $C_{12}E_8$ 20 mg/mL.

Detergent removal and relipidation. After purification and before glycerol concentration adjustment, PfATP6 was concentrated onto 100 kDa cut-off concentrator

unit (Centricon YM100, Millipore). EYPC were then added to concentrated PfATP6 at a final concentration of 1 mg/mL and a lipid to protein ratio of 3:1 (w/w). To remove detergent, Bio-beads SM2, prepared as described (Rigaud et al., 1997), were added to the solution at a Bio-Beads:detergent ratio of 200:1 (w/w) and the whole solution was gently stirred at 18°C for 3 h. Biobeads were then removed and the solution was kept at 4°C.

ATPase activity measurement. The Ca^{2+}-dependence of the activity of purified PfATP6 was determined with the same enzymatic system, starting with a concentration of Ca^{2+} of 1.7 mM. Increasing amounts of EGTA were added to have the desired decreasing concentrations of free Ca^{2+}. These values were calculated with Maxchelator (http://www.stanford.edu/%7Ecpatton/webmaxc/webmaxc S.htm).

The pH-dependence of the activity of purified PfATP6 was also determined with the same enzymatic system, but using the following buffers according to the desired pH: 100 mM Mes-Tris pH 6.5; 100 mM MOPS-Tris pH 7; 100 mM Tes-Tris pH 7.5 and 100 mM Tris-Cl pH 8 and a concentration of $MgCl_2$ increased to 10 mM.

SI Results for Figs. S1, S2 and S3

Expression and purification of PfATP6 in yeast

Production of PfATP6 using an assay of expression on minimal medium as described previously was attempted in parallel from the wild type and the codon optimized genes. In both cases, proteins were expressed but the level of protein production with the codon optimized sequence was much higher than with the wild type one as detected by immunodetection with anti-PfATP6 antibodies (Fig. S1). In this figure, lane 1, an aggregated form of PfATP6-BAD is present. This is likely to be due to the TCA precipitation used for the recovery of the total protein content: this represents a drastic treatment of proteins that leads to their denaturation. After the expression of PfATP6-BAD from its wild type cDNA in particular, several proteins were identified as PfATP6 but smaller than the expected size. As the wild type sequence of Pfatp6 is richer in regions that may form hairpins, they might mimic a termination signal of transcription which might result in an anticipated transcription termination and therefore in the synthesis of truncated proteins. The expression of wild type Pfatp6 leading mainly to the synthesis of truncated form of PfATP6-BAD as well as a lower amount of proteins, we decided to use the optimized construct for a large scale expression of PfATP6 through the use of a fermentor for the yeast culture. In these conditions, 50 g of wet cells were recovered by liter of culture. After the yeast membrane preparation, Western blot analyses with avidin peroxidase and anti PfATP6 antibodies confirmed that PfATP6-BAD was expressed and *in vivo* biotinylated (Fig. S2A). PfATP6 is a SERCA type protein. In their original environment, these proteins are located in the light membranes (endoplasmic reticulum). Hence, we have focused on this membrane fraction for the next steps. The amount of

PfATP6-BAD contained in the light membranes (LM) represents about 2 % of the total protein content as determined by Western blot revealed with anti-PfATP6 antibodies (Fig. S2B) and 8 mg by liter of culture. We also evaluated that about 30 % of it was biotinylated (data not shown) and can therefore be purified. It can be noted that naturally biotinylated yeast proteins (ACC, Acetyl-CoA Carboxylase, 250 kDa; PC, Pyruvate Carboxylase, 120 kDa; Arc1p, Arc1p protein, 65 kDa) are mainly eliminated with the soluble fraction (Fig. S2A). Nevertheless, these soluble proteins that remain in the LM fraction can interfere with the binding of PfATP6-BAD onto the streptavidin resin. As these proteins are soluble, a washing of the membranes with a high-KCl buffer helped to remove the contaminant proteins before the solubilisation (Fig. S3). Sometimes, two washes were necessary to succeed in an efficient removal with a relatively low loss of the protein of interest. Once the membranes were washed, they were solubilized with DDM, a mild detergent used successfully with SERCA1a-BAD. The same detergent to protein ratio (3:1, w/w) was used but the protein and detergent were five times more concentrated than previously described with SERCA1a-BAD (Jidenko et al., 2006). Under these conditions, the solubilization ratio was about 30 % (Fig. S3, compare lanes WP and SF). Among the non-retained proteins, a small amount corresponded to PfATP6-BAD (Fig. S3, lane FT). This could be due to either an exceeding of the binding capacity of the resin, a partial biotinylation of PfATP6-BAD or an inappropriate folding of the protein.

SI Results for Figs. S4 and S5

Study of the enzymatic properties of the purified PfATP6

We measured the rate of hydrolysis of ATP, carried out by PfATP6, in function of different calcium concentrations (Fig. S4). In this medium, PfATP6 is activated by a small amount of free Ca^{2+} (pCa ~ 7) and the optimal activities are obtained in the pCa interval 6-4 with a maximal stimulation around pCa 4. During this experiment, free calcium concentration was adjusted by the addition of an increasing amount of EGTA. As EGTA is also, with a lower affinity, a chelating agent of Mg^{2+}, the concentration of free Mg^{2+} was increased to 5 mM in order to maintain a sufficient amount of free Mg^{2+} required for the ATP hydrolysis reaction. Moreover, EGTA is an acid which can modify the pH of the medium if this latter is not buffered enough. Therefore, the concentration in buffer agent (Tes-Tris) was increased to 100 mM to keep a constant pH during the experiment. In this medium, PfATP6 is activated by a small amount of free Ca^{2+} (pCa ~ 7) and the optimal activities are obtained in the pCa interval 6-4 with a maximal stimulation around pCa 4. Over this concentration, the activity is gradually inhibited by the increasing amount of free Ca^{2+}. This pCa dependence profile is also in agreement with the one described for rabbit SERCA1a solubilized in $C_{12}E_8$ (Moller et al., 1980).

Then, under the same conditions but at a lower temperature (20°C), the ATPase activity of PfATP6 was measured at different pH in order to determine the optimal one (Fig. S5).

A low ATPase activity was observed at pH 6.5 that was improved at pH 7, optimal at pH 7.5 (2.3 µmol of hydrolyzed ATP.min^{-1}.(mg of PfATP6)$^{-1}$) and a little lower at pH 8 (Fig. S5). This is in agreement with what was previously measured for SERCA1a (MacLennan, 1970).

SI Results for Fig. S6 and S7

Study of the enzymatic properties of the purified PfATP6; effect of inhibitors.

In some experiments, the effect of inhibitors was investigated by adding them during the ATPase turnover. As Fe^{2+} ions were sometimes used in the assays, a 10 mM $FeSO_4$ solution was freshly prepared and kept on ice (Montigny et al., 2004). Vanadate could not be used together with NADH since it oxidizes NADH (Lenoir et al., 2004). Therefore, to test its effect on PfATP6, the ATPase activity was estimated at 37°C by a colorimetric assay revealing the amount of Pi released during the reaction. 7.5 µg/mL of PfATP6 were added to 60 µL of assay medium, containing 50 mM Tes-Tris pH7.5, 0.1 M KCl, 6 mM $MgCl_2$, 5 mM ATP, 0.1 mM Ca^{2+}, 0.2:0.05 mg/mL $C_{12}E_8$:DOPC with or without 100 µM vanadate. The hydrolysis of ATP was triggered by the addition of ATP and stopped by addition of 60 µL of 3 mM EGTA. Inorganic phosphate was revealed with molybdate by adding 200 µL of a solution prepared by mixing one volume of 4 % ammonium molybdate in 15 mM zinc acetate pH 5 with 5 volumes of 0.1 g/mL freshly prepared ascorbic acid at pH 5. The blue color developed over 30 min at 37°C (Saheki et al., 1985; Drueckes et al., 1995) was read as duplicates in 96-well microtiter plates, at 690 nm on a Multiskan bichromatic spectrophotometer. The concentration of phosphate was calculated from standard curves (0-0.3 mM) prepared in the presence and absence of vanadate.

As inhibitors were prepared in DMSO, it could affect the enzyme activity of PfATP6 so we measured it (Fig. S6A). As expected, we noted that 2 µL of DMSO lowered the rate of hydrolysis of ATP by about 0.1 µmol ATP min^{-1} (mg protein)$^{-1}$. This remains low but we took into account this value to calculate the specific effect of the inhibitors.

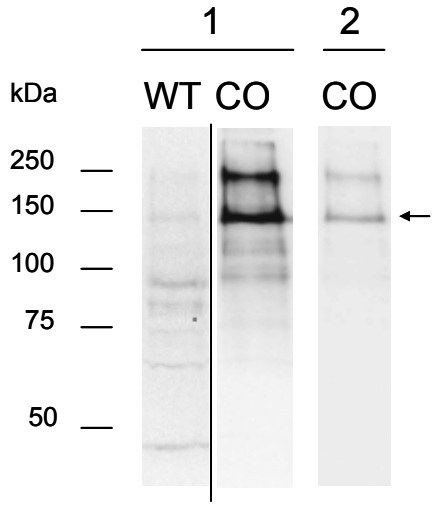

Fig. S1 Expression of PfATP6 on minimal medium.
*Western blot analysis with anti PfATP6 antibodies of the level of expression of PfATP6-BAD expressed from the wild type cDNA of Pfatp6 (**WT**) and the codon optimized one (**CO**).*
10µL of each protein solution after expression assay were loaded corresponding respectively to 8 and 10 µg of proteins for the WT and CO samples.
1 and **2** correspond to a signal acquisition of 14 and 2 min respectively.
The arrow indicates the band corresponding to monomeric PfATP6-BAD

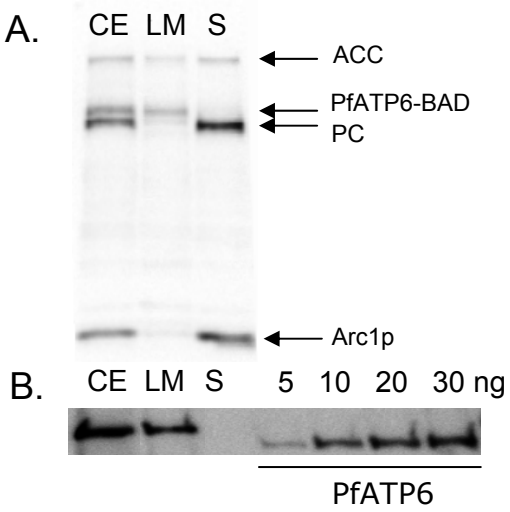

Fig. S2 Expression of PfATP6 and membrane fractionation.
Analyses of fractions recovered during the membrane preparation.

• *Western blot analysis with avidin peroxidase.* A fraction of 2µg of total proteins of crude extract (**CE**) and 1µg of total proteins of light membrane (**LM**) and soluble fraction (**S**) were loaded. Arrows indicate the biotinylated proteins endogenous to the yeast *S. cerevisiae* (ACC, Acetyl-CoA Carboxylase, 250kDa; PC, Pyruvate Carboxylase, 120kDa; Arc1p, Arc1p protein, 65kDa).

B. Western blot analysis with anti-PfATP6 antibodies. The same samples as in panel A were loaded. To quantify the amount of PfATP6-BAD in the LM fraction, 5, 10, 20 and 30 ng of purified PfATP6 supplemented with 1µg of total proteins of light membrane fraction of yeast expressing SERCA1a were loaded.

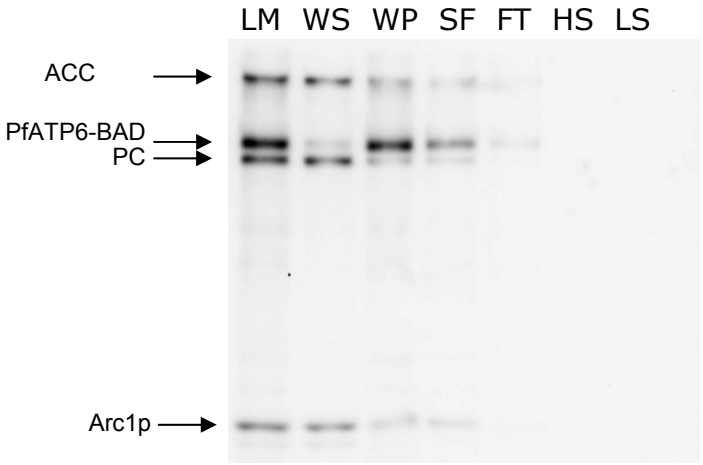

Fig. S3 Purification of PfATP6 on streptavidin Sepharose: prepurification and binding to the resin.
Western blot analysis with avidin peroxidase of the washing, the solubilization and the purification steps before thrombin cleavage of PfATP6.
0.5µL of each fraction were loaded (corresponding to 5 µg of total proteins in the LM lane, for example)
In order to remove soluble biotinylated proteins (ACC, Acetyl-CoA Carboxylase, 250kDa; PC, Pyruvate Carboxylase, 120kDa; Arc1p, Arc1p protein, 65kDa) light membranes were diluted in washing buffer at 10mg/mL (**LM**) and centrifuged. The resulting supernatant (**WS**) was discarded, the pellet was resuspended in solubilization buffer (**WP**) with the same volume as the LM fraction and centrifuged. The supernatant corresponding to the solubilized fraction (**SF**) was added to the resin and the flow through fraction (**FT**) was removed. The resin was then washed with high salt buffer (**HS**) and low salt buffer (**BS**).

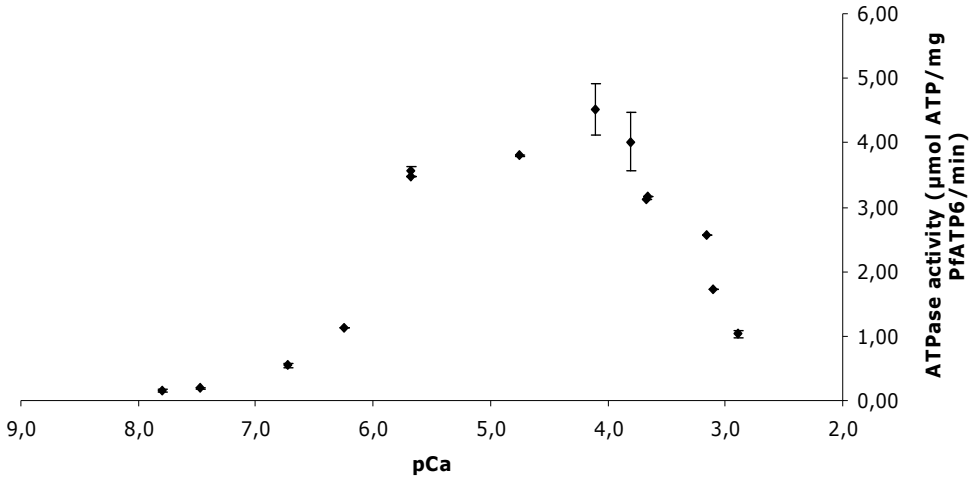

Fig. S4 ATPase activities of purified PfATP6 as a function of calcium concentrations.
Ca^{2+}-dependent ATPase activities (means and standard deviations) at 37°C of purified PfATP6 obtained from two different preparations. They were measured as described in SI Materials and Methods.

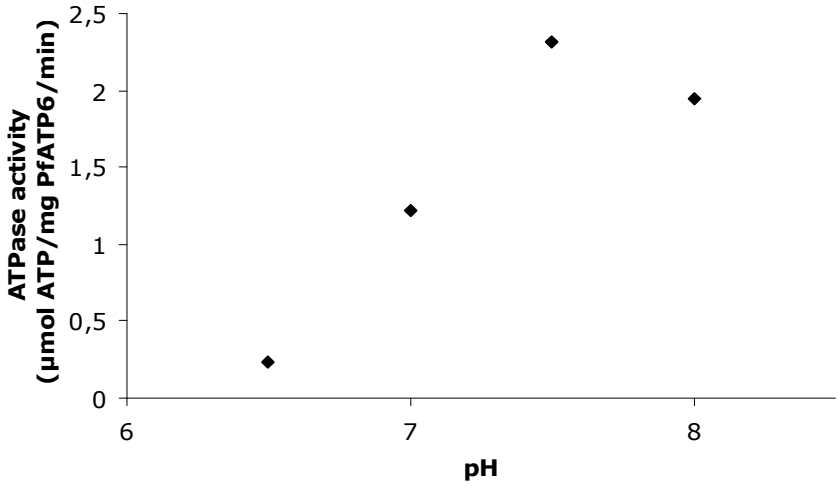

Fig. S5 ATPase activities of purified PfATP6 as a function of pH.
pH-dependent ATPase activities at 20°C of purified PfATP6. They were measured as described in SI Materials and Methods.

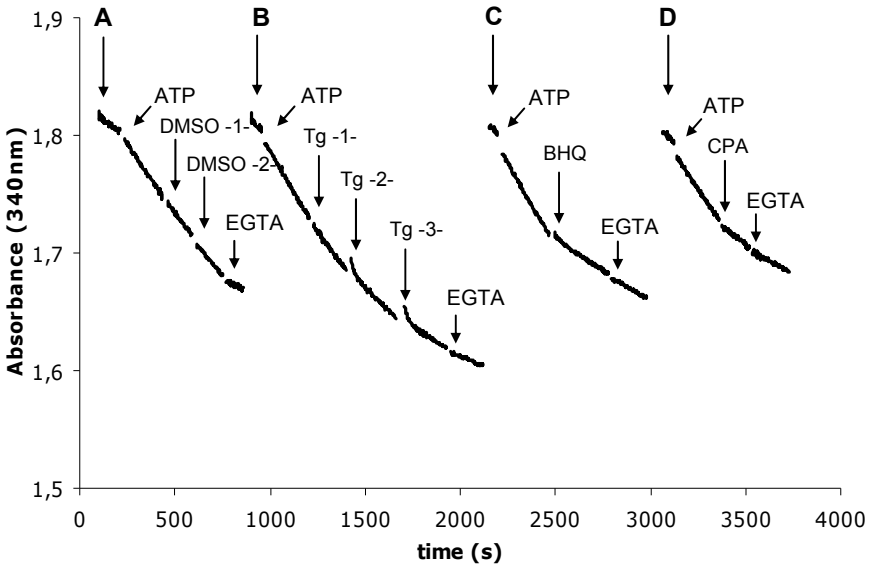

Fig. S6 Effect of inhibitors of SERCA type proteins on the ATPase activity of PfATP6
The reactions were performed with 1.5µg/mL of purified PfATP6 at 25°C in $C_{12}E_8$/DOPC (0.2/0.05 mg/mL). They were triggered by addition of 5mM ATP and stopped by the addition of 750µM EGTA. Inhibitors, diluted in DMSO, were added with 2µL of the corresponding mother solution.
First, the effect of DMSO on the activity of PfATP6 was monitored (**A**) after addition of 2µL (DMSO-1-) and 4µL (DMSO-2-) to PfATP6. Then, the inhibition of the enzyme by thapsigargin (**B**) (1.5µM, Tg-1 (final concentrations); 16.5µM, Tg-2- and 46.5µM, Tg-3-), 2, 5-Di(ter-butyl-1, 4-benzoquinone **(C)** (100µM, BHQ) and cyclopiazonic acid (**D**) (3µM, CPA) were tested.

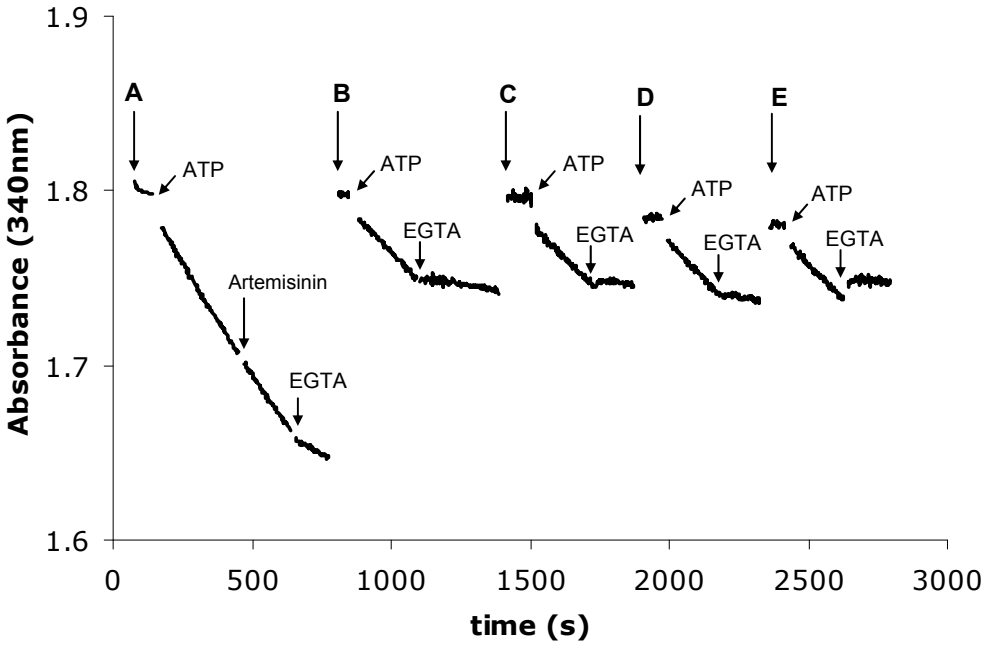

Fig. S7 Effect of artemisinin drugs on the ATPase activity of PfATP6.
The reactions were performed with 1.5µg/mL of purified PfATP6 at 25°C in $C_{12}E_8$/DOPC (0.2/0.05 mg/mL). They were triggered by addition of 5mM ATP and stopped by the addition of 750µM EGTA. Artemisinins were added with 2µL of a solution at 10mM prepared in DMSO. The effect of artemisinin was first tested by addition of 10µM (final concentrations) of this drug during the ATP hydrolysis of the enzyme (**A**). The effect of Fe^{2+} + DMSO was measured by addition of 10µM Fe^{2+} + 2µL DMSO to the protein before starting the reaction (**B**). Then, the effects of artemisinin drugs were tested by preincubation of the protein with 10µM Fe^{2+} + 10µM artemisinin (**C**), 10µM Fe^{2+} + 10µM artemisone (**D**), 10µM Fe^{2+} + 10µM artesunate (**E**) before starting the reaction. It could be noted that Fe^{2+} apparently reduces both the nonspecific and specific Ca^{2+} dependent activity.

Laboratoire des Protéines Membranaires ; Service de bioénergétique, biologie structurale et mécanismes ; Institut de Biologie et Technologie de Saclay, URA CNRS 2096 et LRA17V.
CEA de Saclay, 91191 Gif-Sur-Yvette

Résumé

Le puissant anti-paludéen, l'artémisinine a été décrit comme inhibiteur de l'activité ATPasique de PfATP6 après son expression dans des ovocytes de Xénope. PfATP6 est l'unique ATPase Ca^{2+} du réticulum endo/sarcoplasmique de *P. falciparum*, le parasite responsable du paludisme. Quand un acide aminé de SERCA1a de lapin (E255) est muté en son équivalent dans PfATP6 (L), l'activité de ce mutant exprimé en ovocyte de Xénope est inhibée en présence d'artémisinine. Après expression de ce mutant et de PfATP6 dans *S. cerevisiae* puis leur purification, nous avons constaté qu'aucune de ces deux protéines n'était sensible à l'artémisinine. En parallèle, nous montrons que PfATP6 purifiée est sensible aux principaux inhibiteurs de SERCA mais elle est moins sensible à la thapsigargine que ne l'est SERCA1a. Les résultats présentés ici suggèrent que le méchanisme d'action de l'artémisinine est complexe et ne peut pas être du à une interaction directe entre l'artémisinine et PfATP6. D'autre part, la purification de PfATP6 laisse entrevoir l'opportunité de mieux caractériser cette protéine voire même de développer de nouveaux anti-paludéens en recherchant des inhibiteurs de cette protéine.

Study of the mutant E255L of the rabbit Ca^{2+}-ATPase and of PfATP6, the Ca^{2+}-ATPase of *Plasmodium falciparum*

Heterologous expression in yeast (*S. cerevisiae), purification, characterization and inhibition assays by artemisinin, a powerful antimalaria*

The antimalarial drugs artemisinins have been described as inhibitors of the ATPase activity of PfATP6, the only sarcoplasmic/endoplasmic reticulum Ca^{2+}-ATPase (SERCA) of the parasite responsible for malaria, *Plasmodium falciparum*, after its expression in *Xenopus* laevis oocytes. Mutation of an amino acid residue in mammalian SERCA1 (E255) to the equivalent one predicted in PfATP6 (L) was reported to induce sensitivity to artemisinin in the oocyte system. However, after purification of PfATP6 and of mammalian SERCA1a E255L expressed in *Saccharomyces cerevisiae*, it is shown that artemisinins do not inhibit their ATPase activities whereas PfATP6 is somewhat less sensitive to thapsigargin than to rabbit SERCA1 and retains full sensitivity to SERCA1 inhibitors. The insensitivity of purified PfATP6 to artemisinins suggests that the mechanism of action of this class of drugs is complex and cannot be ascribed to direct inhibition of PfATP6. Furthermore, the successful purification of PfATP6 affords the opportunity to develop new antimalarials by screening for inhibitors against PfATP6.

Mots clés: PfATP6, ATPase-Ca^{2+}, protéines membranaires, expression hétérologue, purification, artémisinine, paludisme

Key words: PfATP6, Ca^{2+}-ATPase, membrane proteins, heterologous expression, purification, artemisinin, malaria

Laboratoire des Protéines Membranaires ; Service de bioénergétique, biologie structurale et mécanismes ; Institut de Biologie et Technologie de Saclay, URA CNRS 2096 et LRA17V.
CEA de Saclay, 91191 Gif-Sur-Yvette